AFFINITY-SELECTED HEPARAN SULFATE FOR THE EXPANSION OF ADULT HUMAN BONE MARROW-DERIVED MESENCHYMAL STEM CELLS

SAMPATH JEEWANTHA WIJESINGHE
(B.V.Sc, University of Peradeniya, Sri Lanka)
(M.Sc. (Animal Science), University of Peradeniya, Sri Lanka)

A THESIS SUBMITTED

FOR THE DEGREE OF DOCTOR OF PHILOSOPHY

NUS GRADUATE SCHOOL FOR INTEGRATIVE SCIENCES AND ENGINEERING

NATIONAL UNIVERSITY OF SINGAPORE

2013

DECLARATION

I hereby declare that the thesis is my original work and it has been written by me in its entirety. I have duly acknowledged all the sources of information which have been used in the thesis

This thesis has also not been submitted for any degree in any university previously.

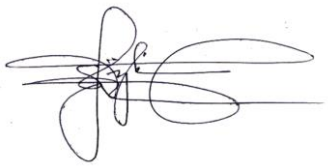

03.02.2015

SAMPATH JEEWANTHA WIJESINGHE

ACKNOWLEDGEMENT

I would like to express my heartfelt gratitude to my thesis supervisors, Professor Simon M. Cool, Professor Victor Nurcombe and Professor Kunchithapadam Swaminathan for their extreme patience, guidance and encouragement. They were not only mentors but also dear friends. First of all I have to thank Professors Simon and Victor for letting me join their vibrant, energetic lab in order to pursue my PhD. I thank Professor Simon for his enduring guidance, perseverance and support. I am also grateful for his constant challenging of my research outcomes and direction. He is a great mentor. I am so thankful to Professor Victor for his research perspectives and knowledge of the field. He is a terrific motivator and spent hours editing my thesis. Their collective advice and unsurpassed knowledge was key in this thesis reaching fruition. I am grateful to Prof. Swami for always being a kind, patient and inspiring advisor and motivating me to finish my thesis. I am deeply thankful to my thesis advisory committee members, namely, Professor James Hui and Professor Richard Boyd, for their support.

I would like to extend my heartfelt gratitude to all the current and past colleagues from the Glycotherapeutics group, Institute of Medical Biology, A*STAR, for their help and the great times that we shared. I would like say a warm thank you to Drs. Murali Sadasivam, Diah Bramono, Ling Ling, Bina Rai, Wang Chunming, Gajadhar Bhakta, Andrew Ekaputra, Harmeet Singh and Stephanie Koo, for sharing their time in research discussions and also as fabulous friends. I am also truly grateful to all research officers, Ms Yeong HuiQing, Ms Goh Ting Hwee, Ms Lin Tingxuan, Ms Zhuo Ying Jie, Ms. Jaslyn Lee, Ms Siti Shahera binte Anwar, Ms. Wennie Tan, Mr. Clement

Foong and, Mr. Tan Tuan Chun for being both colleagues and friends. I also like to thankful to my peers Mr. Jonathan Lee, Dr. Yap Yan Wen Lynn, Ms. Rebekah Margaret Samsonraj and Ms. Zophia Lim for the wonderful times that we shared, even during the most stressful days. I would like to make a special thank you for the assistance and guidance given to me by Dr. Murali Sadasivam in the isolation of HS8 variants, to Dr. Koo Chuay Yeng in the isolation of STRO-1 hMSCs, Dr. Diah Bramono in the isolation of HS variants and immunoblotting and Mr. Jonathan Lee with differential scanning fluorimetry. I am especially grateful to Rebekah Samsonraj for help in proofing this thesis and for administrative details during its submission. Similarly, I again thank Jonathan Lee, Yim Guo Rong Daniel and Wishva Hearth for help in submitting the thesis.

In addition, I would like to thank our collaborators at GlycoSyn, IRL (now Callaghan Innovation, Wellington, New Zealand) for their assistance with the disaccharide analysis of our HS variants and the Institute of Cell and Molecular Biology, A*STAR Histopathology Facility for their excellent help with chondrogenic pellet sectioning and analysis. Furthermore, I would like to take this opportunity to thank the Faculty of Integrative Sciences and Engineering (NGS) for providing me the NGS scholarship to pursue my PhD and all the staff for the wonderful support given to me throughout my studies. Furthermore I would like to thank all my friends that I met through NGS and at the Prince George Park Residencies.

I would not have contemplated this road if not for my parents and siblings; I would like to thank my family for their support and love. In addition, I would like to show my gratitude to my parent-in-laws for their

support and kindness during this stressful period in our lives. Last but not least, I am extremely thankful to my wife Dimuthu, daughter Aishwarya and son Damin for being with me during the good and difficult times of my PhD, and for continuously encouraging me to finish. This PhD is for you.

LIST OF PUBLICATIONS AND PRESENTATIONS

Wijesinghe SJ, Sadasivam M, Bramono D, Ling Ling[1], Rai B, Huiqing Yeong, Swaminathan K, Hinkley S, Bell T, Hui JH, Nurcombe[1], and Cool SM (2015) Affinity-selected heparan sulfate for the expansion of adult human bone marrow-derived mesenchymal stem cells (*Manuscript in preparation*)

Wijesinghe SJ, Ravindran G, Shenoy SP, Kumar P, Darwis DA, Bayat S, Chan WK (2009) Generation of Dopaminergic Neurons by Over-expression of NURR1 in Human Embryonic Stem Cells, Graduate student seminar, Chulalongakorn University, Thailand

TABLE OF CONTENTS

LIST OF TABLES

LIST OF FIGURES

ABBREVATIONS

°C	Degree Celsius
µl	Micro litre
3H-heparin	Tritiated heparin
^{3}H-thymidine	Tritiated heparin
Ab	Antibody
ADSCs	Adipose derived stem cells
Ahx	aminohexanoic acid
ANOVA	Analysis of variance
ATIII	antithrombin III
BMMNC	bone marrow mononuclear cells
BMP2	Bone Morphogenetic Protein-2
BrdU	5-bromo-2-deoxyuridine
BrdU-POD	5-bromo-2-deoxyuridine Fab fragments with peroxidase
BSA	Bovine serum albumin
Ca^{2+}	Calcium
CD105	Cluster of Differentiation 105
CD14	Cluster of Differentiation 14
CD19	Cluster of Differentiation 19
CD3	Cluster of Differentiation 3
CD34	Cluster of Differentiation 34
CD45	Cluster of Differentiation 45
CD49a	Cluster of Differentiation 49a
CD73	Cluster of Differentiation 73
CD90	Cluster of Differentiation 90

CE	capillary electrophoresis
CFU-F	Colony-forming units-fibroblastic
CG	cumulative growth the
Ci	Curie
CNS	Central Nervous System
CO_2	Carbon Dioxide
CS	Chondroitin sulfate
DI	Distilled water
DMEM-HG	Modified Eagle's medium-high glucose
DMEM-LG	Dulbecco's Modified Eagle's medium-low glucose
DMSO	Dimethylsulfoxide
DNA	deoxyribonucleic acid
DNA	Deoxyribonucleic acid
DNase 1	Deoxyribonuclease I
dp	degree of polymerization
DSF	Differential Scanning Fluorimetry
ECM	Extracellular matrix
EDTA	Ethylenediaminetetraacetic acid
EGF	Epidermal growth factor
ELISA	Enzyme-linked immunosorbent assay
ERK	Extracellular signal-regulated kinases
ESC	embryonic stem cell
FACS	Fluorescence activated cell sorting
FC	Flow cytometry
Fc	fragment of crystallization
FCS	Foetal calf serum

FGF-1	Fibroblast growth factor-1
FGF-2	Fibroblast growth factor-2
FGF-4	Fibroblast growth factor-4
FGF-7	Fibroblast growth factor-7
FGFR1	Fibroblast growth factor receptor-1
FGFR2	Fibroblast growth factor receptor-2
FGFR3	Fibroblast growth factor receptor-3
FGFR4	Fibroblast growth factor receptor-4
FGFs	Fibroblast growth factors
FITC	Fluorescein isothiocyanate
FRS2a	Fibroblast growth factor receptor substrate 2
FXa	Factor Xa
GAG	Glycosaminoglycan
GlcA	β-L-glucuronic acid
GlcNAc	2-deoxy-2-acetamido-α-D-glucopyranosyl
GlcNAc	2-deoxy-2-acetamido-α-D-glucopyranosyl
GlcNS	2-deoxy-2-sulfamido-α-D-glucopyranosyl
GlcNS (6S)	2-deoxy-2-sulfamido-α-D-glucopyranosyl-6-O-sulfate
GvHD	Graft versus host disease
h	Hour (s)
H_2O	water
H_3PO_4	Phosphoric acid
HA	Hyaluronic acid
HBD	heparin-binding domain (s)
HBGF	heparin-binding growth factors
HCl	Hydrogen chloride

HCT	Haemopoietic-cell transplantation
HGF	Hepatocyte growth factor
HHF	Hanks' Balanced Salt Solution Modified
HLA-DR	Human Leuukocyte antigen-DR
hMSCs	human mesenchymal stem cells
HPLC	High-performance liquid chromatography
HS	Heparan sulfate
HS	Heparan sulfate
$HS3^{+ve}$	Heparan sulfate variant with high BMP-2 binding affinity
$HS7^{+ve}$	Heparan sulfate variant with high $VEGF_{165}$ binding affinity
$HS8^{+ve}$	Heparan sulfate variant with high FGF-2 binding affinity
$HS8B^{+ve}$	Heparan sulfate variant with high FGF-2 binding affinity isolated with FGF-2-HBD Baird peptide
$HS8C^{+ve}$	Heparan sulfate variant with high FGF-2 binding affinity isolated with FGF-2-HBD Cardin peptide
$HS8G^{+ve}$	Heparan sulfate variant with high FGF-2 binding affinity isolated with FGF-2-HBD Gandhi peptide
$HS8^{-ve}$	Heparan sulfate variant with low FGF-2 binding affinity
HSPG	Heparan sulfate proteoglycan
HSpm	Heparan sulfate from porcine intestinal mucosa
IDO	indoleamine 2, 3-dioxygenase
IdoA	α-L-iduronic acid
IdoA (2S)	α-L-iduronic acid-2-O-sulfate
IgM	Immunoglobulin M
IgM	Immunoglobulin M
IL1	Interleukin 1

IL-4	Interleukin 4
IL-10	Interleukin 10
IMBR1	affinity purified polyclonal rabbit IgG
kDa	Kilodalton
KGF	Keratinocyte growth factor
Ki67	Antigen KI-67
KS	Keratan sulfate
LPS	Lipopolysaccharide
M	Molarity
M	Molarity
MACS	magnetic-activated cell sorting
mAU	milli-absorbance unit
mg/ml	milligram per milliliter
Mg^{2+}	Magnesium
min	Minute (s)
ml	Millilitre
MLD	Multilineage differentiation
Mrna	messenger ribonucleic acid
MSCs	Mesenchymal stem cells
Na_2HPO_4	Disodium hydrogen phosphate
NaAc	Sodium acetate
NaCl	Sodium chloride
NaOH	Sodium Hydroxide
NH_2	amidogen
nm	nanometer
NMR	Nuclear magnetic resonance

NO	nitric oxide
NOD-SCID	Non-obese diabetes- severe combined immunodeficiency
P	Passage
PBMC	peripheral blood mononuclear cell
PBS	Phosphate buffered saline
PBS	Phosphate buffered saline
PDGF-BB	platelet-derived growth factor-BB
PE	Phycoerythrin
PFA	paraformaldehyde
pH	decimal cologarithm of hydrogen
PNPP	p-nitrophenyl phosphate
rpm	Rounds per minute
RS	Rapidly self-renewing
SAB	standard assay buffer
SH2	Src Homology 2
SSEA-4	Stage-specific embryonic antigen-4
STRO-1	Stromal precursor antigen-1
$t_{1/2}$	Half-life
TBST	Tris-Buffered Saline and Tween 20
TFA	Trifluoroacetic acid
TGFβ3	Transforming growth factor beta 3
Tm	Temperature
TMB	3,3′,5,5′-Tetramethylbenzidine
TNFRI	Tumor necrosis factor alpha receptor type 1
TNF-α	Tumor necrosis factor alpha
TNFα	Tumor necrosis factor alpha

U	Unit
UA	Uronic acid
V	Volts
v/v	Volume per volume
VEGF	Vascular endothelial growth factor
Wnt3a	wingless-type MMTV integration site family, member 3A
α-MEM	α-modified Eagle's medium
λ_{ex}	Fluorescence excitation wavelength

ABSTRACT

Human mesenchymal stem cells (hMSCs) hold immense therapeutic potential in the field of tissue regeneration. The major factor delaying the wider exploitation of such cell-based therapies is the difficulty in generating sufficient cell numbers to meet the clinical demand. The low proportions of hMSCs within bone marrow are clearly hindering their widespread clinical adoption. Collectively, these issues negatively impact on the therapeutic potential of hMSC for regenerative medicine. Current *ex vivo* expansion strategies attempt to mimic the bone marrow microenvironment by utilizing extracellular matrix (ECM) substrates and exogenous applications of growth factors, but diminishing stemness under these conditions is a major deterrent. Notably, autocrine fibroblast growth factor 2 (FGF-2) has been shown to increase the multipotentiality of hMSCs. Therefore, enhancing the activity of FGF-2 produced endogenously by MSCs in culture presents as a worthy strategy.

As with many extracellular growth factors, the powerful stem cell mitogen FGF-2 depends for its activity on a heparan sulfate (HS) glycosaminoglycan sugar, that specifically cross-binds it to FGFR1. Our group has previously demonstrated that murine-derived HS variants from either embryonic neural progenitor cells or adult liver tissue are able to accelerate the growth of hMSCs without a significant loss of multipotentiality. However, to be of use for regenerative medicine, there is a need to scale-up the production of this HS, and prove it retains the properties of the original embryonic sugar.

Therefore this study was developed to address this major limitation. The strategy adopted was to isolate a bioactive HS sub-fraction by peptide-

affinity chromatography from a commercial source of HS. The rationale being that, this affinity-selected HS would mediate the activity of endogenous FGF-2 thereby acting to sustain the growth of hMSC without adversely affecting their multipotentiality.

To affinity isolate FGF-2-binding HS, ten customized peptides mimicking the heparan-binding domain of FGF-2 were trialed as a chromatographic substrate. Screening assays of FGF-2 binding affinity highlighted a particular HS variant (termed $HS8^{+ve}$) that could be isolated at scale from commercially available porcine mucosal HS (termed HS^{pm}). Moreover $HS8^{+ve}$ dose-dependently increased hMSC proliferation whilst maintaining the tri-lineage potential of the expanded cells. Application of $HS8^{+ve}$ also resulted in a higher efficiency of CFU-F formation. Compositional analysis by capillary electrophoresis revealed that $HS8^{+ve}$ contained an enrichment of trisulfated disaccharides with di-sulfated disaccharides (6O and NS) and a depletion of mono- and un-sulfated disaccharides compared with the starting HS^{pm} pool. This appeared critical for formation of the FGF-2-HS-FGFR1 ternary complex and downstream signal transduction, which required the HS to contain 2O-, 6O- and N-sulfation. In addition $HS8^{+ve}$ was devoid of anticoagulation activity and increased FGF-2 stability in culture. Moreover, hMSC growth induced by exogenous FGF-2 was further enhanced by addition of $HS8^{+ve}$, with FGF inhibition studies highlighting that $HS8^{+ve}$ actively promotes FGF-2-FGFR1 signaling.

This thesis describes the development a robust, highly scalable, simple and cost-effective affinity chromatography platform isolate a heparan sulfate variant ($HS8^{+ve}$) that can bind to endogenously produced FGF-2 and thereby

mediate hMSC proliferation. Further development of this particular HS strategy may yield benefits to the expansion and clinical use of hMSCs in regenerative medicine.

CHAPTER 1: LITERATURE REVIEW

1.1. Extra cellular matrix (ECM)

Generally, the ECM can be considered to consist of all the secreted molecules that are present outside the cells. In fact the ECM is a dynamic and complex environment with different physical and biochemical properties which gives architectural support for the tissues (Gattazzo *et al*., 2014; Maquart and Monboisse, 2014). During development, the embryo undergoes complex cell-cell and cell to-matrix interactions (Hynes, 2009; Zagris, 2000). It is these direct or indirect interactions with the surrounding extracellular matrix (ECM) that helps governs these cell-fate decisions (Hynes, 2009). The ECM, modulate the production, degradation, and remodelling of its components namely proteins, glycoproteins, collagens, glycosaminoglycans, proteoglycans and other macromolecules and thereby is involved in diverse functions such as the migration of cells, adhesion, proliferation and differentiation (Adams and Watt, 1993; Aumailley and Gayraud, 1998; Dutta and Dutta, 2010; Gattazzo *et al*., 2014; Hay, 1991; Lu *et al*., 2011; Page-McCaw *et al*., 2007; Timpl and Brown, 1994; Zagris, 2000). In addition, cells grown in tissue culture plates also depend on ECM components for their attachment, proliferation and differentiation (Evseenko *et al*., 2009; Hakala *et al*., 2009; Santiago *et al*., 2009).

Stem cells have an extensive ability to self-renew and to produce daughter cells and irrespective of their existence in adult tissue or in a culture dish, their stem cell fate is regulated by a combination of intrinsic and extrinsic mechanisms (Watt and Driskell, 2010; Watt and Huck, 2013). Transcription factors expressed by the cells govern the intrinsic mechanisms while the local microenvironment or the niche consisting of ECM, govern the

extrinsic mechanisms (Gattazzo *et al*., 2014; Watt and Huck, 2013). Two components distributed in the ECM which are important for embryonic and adult stem cell development (and an important conceptual part of this thesis) are the family of sulfated proteoglycans, and fibroblast growth factors (FGFs). The former comprise a large group of molecules which appear to modulate cell outgrowth in both positive and negative ways (Fernaud-Espinosa *et al*., 1994; Gandhi and Mancera, 2008; Ori *et al*., 2008) (Fernaud-Espinosa *et al*. 1994: Ori *et al*, 2008). The latter, the family of FGFs, are generically known as heparin-binding growth factors due to their affinity for heparin and heparan sulfate. In the embryonic mouse brain, a developmentally regulated, novel HSPG and FGF-2 have been colocalized (Ford *et al*. 1994) and are able to stimulate mitogenesis in neural precursor cells (Nurcombe *et al*. 1993). These discoveries helped stimulate the need for more information about the nature of the precise interaction between heparan sulfate proteoglycans, fibroblast growth factors, and the previously characterized high affinity transmembrane fibroblast growth factor receptors. The structure and function of these relationships underpin this thesis.

1.2. Heparan sulfate proteoglycans (HSPG)

1.2.1. Classification of Glycosaminoglycans (GAGs)

HSPGs are part of the major family of glycosaminoglycans (GAGs). They are linear, highly negatively charged, complex molecules with a wide range of molecular weight (10–100 kDa) (Gandhi and Mancera, 2008). These GAGs in aqueous solution are surrounded by a covering of water molecules, result in massive hydrodynamic volume in solution. Furthermore, they are

made up of repeating disaccharide units consist of uronic acid (D-glucuronic acid or its epimer L-iduronic acid) and an amino sugar (D-galactosamine or D-glucosamine). Therefore the GAGs differ depending on the sugar and the geometry of the glycosidic linkage between these units. They are categorized into two main types; sulfated and unsulfated. Notably hyaluronic acid (HA) is un-sulfated, while chondroitin sulfate (CS), keratin sulfate (KS), dermatan sulfate (DS) and heparan sulfate (HS) are the sulfated GAGs (Gandhi and Mancera, 2008; Ori *et al*., 2008). The non-sulfated HA which is synthesized without a core protein and is digested by enzymes at the cell surface directly into the extracellular space. It is often bound to HA-binding proteins and other proteoglycans (Delpech and Halavent, 1981; Delpech *et al*., 1991). In addition, HA is the major component in the synovial fluid lubricant within body joints (Itano, 2008). Furthermore it has been extensive used for wound healing, mostly being an excellent lubricant (Price *et al*., 2005; Weigel *et al*., 1986).

In contrast, sulfated GAGs secreted covalently attached to a core protein on the cell surface to yield the various species of proteoglycans as described above. The CS and DS contain galactosamine and called as galactosaminoglycans. The CS has a molecular mass of 5-50 kDa, and found particularly in cartilage, tendon, ligament and aorta (Clegg *et al*., 2006; Cummings and Etzler, 2009; Varki *et al*., 1998). On the other hand, DS is having a molecular weight of 15-40 kDa and is most common in skin and blood vessels (Trowbridge and Gallo, 2002; Varki *et al*., 1998). The KS can be found in cartilage and cornea with a molecular weight of 4-19 kDa (Cummings and Etzler, 2009; Varki *et al*., 1998). The other sulfated GAGs,

HSPGs consist of highly sulfated heparin and heparan sulfate (Ori *et al*., 2008).

1.2.2. Heparin and heparan sulfate

Heparin was identified in 1916 as a material extracted from dog liver which inhibit clotting of plasma *ex vivo* (Jorpes, 1959; McLean, 1916) while HS was discovered by Jorpes and Gardell in 1948 (Jorpes and Gardell, 1948). Whilst heparin is produced and stored in mast cells, HS is found in almost all animal tissues (Gandhi and Mancera, 2008; Ori *et al*., 2008). They are synthesized as covalent complexes with the GAG chains attached to core proteins to form HSPGs. Three families of HSPGs are named according to the type of proteins attached and include the transmembrane syndecans, the membrane bound glypicans and the ECM bound prelecan.

The biosynthetic pathway leading to HS and heparin formation has been reviewed by several groups (Bienkowski and Conrad, 1984; Kreuger and Kjellén, 2012; Lamanna *et al*., 2007; Lindahl *et al*., 1986; Ori *et al*., 2008). The steps in the biosynthesis of heparin and heparan sulfate are probably the same so at least in principle, all sequences found in heparin, which is highly substituted with sulfates, can be found in HS. In the case of DNA the biological information is coded as linear sequences in the molecules. In contrast, scientists are faced with a challenge in decoding the sulfation pattern and the dynamic nature of HS generation because of the non-template driven process (Lamanna *et al*., 2007). This process of HS occurs in Golgi, where multiple biosynthetic enzymes acts on the growing saccharide polymer, introducing modifications to the sugar backbone which do not go to

completion (Ori *et al*., 2008). There are 3 phases of HS synthesis that have been identified namely, chain initiation, polymerization and polymer modification. A linker tetrasaccharide attached to specific serine residues of newly translated core proteins in chain initiation step followed by addition of D-galactose residues. After that the polymerization of the heparin/HS chain occurs through alternate attachment of hexuronate and glucosamine residues in a non-branching polymer fashion. These are then subjected to the maturation process where epimerization and sulfation occur by sulfotransferases and an epimerase (Kreuger and Kjellén, 2012; Lamanna *et al*., 2007; Ori *et al*., 2008). However, epimerization and *N*-and *O*-sulfation reactions do not occur at all of the disaccharide units which results in a highly heterogeneous final product and an almost endless possibility of final products.

Heparin (7-20 kDa) and HS (10-70 kDa) are linear polysaccharides consisting of repeating uronic acid-(1→4)-D-glucosamine disaccharide subunits (Gandhi and Mancera, 2008). Uronic acid can either be D-glucouronic acid or L-iduronic acid. In addition, modifications at specific places give rise to different N-sulfated, O-sulfated and N-acetylated complex sequences (Ori *et al*., 2008). The most abundant disaccharide in heparin is IdoA(2S)-(1→ 4)-GlcNS(6S) therefore giving rise to a highly negative charge throughout the chain length, that affords heparin little to no selectivity in binding to proteins. Furthermore, heparin has a higher N-sulfation (> 80 %) as compared to HS (40-60 %) (Gandhi and Mancera, 2008). On the other hand, HS has the unsulfated GlcA-(1→4)-GlcNA disaccharide as the most common form giving rise to segregated blocks of unsulfated NA domains and blocks of

highly sulfated, heparin-like IdoA-(1→4)-GlcNS disaccharides (NS domain). The diversity of HS is due the different regions of sulfation along HS chains and different degree of sulfation on each of the disaccharide units (Ori *et al*., 2008). This diversity is responsible for the wide range of biological functions. HSPGs affect metabolism, transport, information transfer, cell adhesion, cell growth and differentiation, and support in all organ systems (Bishop *et al*., 2007; Gandhi and Mancera, 2008) by virtue of their attached HS-GAG chains.

1.3. Fibroblast growth factors (FGFs)

In 1939, the first experiments of FGF activity was described (Trowell and Willmer, 1939) and they derived their name because of the original assay used to identify the growth promoting activity on fibroblasts (Gospodarowicz, 1974).

The fibroblast growth factor family is comprised of 22 members in vertebrates with a molecular mass range from 17 to 34 kDa (Beenken and Mohammadi, 2009; Ornitz and Itoh, 2001; Powers *et al*., 2000; Steiling and Werner, 2003). Due to their isoelectric points (pI) of 9.6 and 5.6 the first two members of this family were originally known as basic FGF and acidic FGF respectively. Since the discovery of many other growth factors in the same family, the nomenclature has changed, and they are now numbered sequentially as discovered.

Their gene structure and core amino acid sequence of 120–130 amino acids are highly conserved in vertebrates (Beenken and Mohammadi, 2009; Ornitz and Itoh, 2001). They have numerous functions in developmental processes including brain patterning, branching morphogenesis and limb

development. In addition, they have mitogenic, cytoprotective and angiogenic properties in wound repair and even play a role in neuronal protection (Ornitz and Itoh, 2001; Powers *et al*., 2000; Steiling and Werner, 2003) (Beenken and Mohammadi, 2009).

Beenken and Mohammadi have shown that FGF consist of a core region organized in 12 anti-parallel β-strands (β1–β12), and on the either side are the amino and carboxyl terminals (Beenken and Mohammadi, 2009). The HS binding sites are contained in this β1–β2 loop as well as parts of regions located between β10 and β12. FGFs carry out their various functions through binding interactions that involve the four FGF receptors (FGFR 1-4). FGFRs are tyrosine kinase receptors with several notably isoforms (FGFR1b, FGFR1c, FGFR2b, FGFR2c, FGFR3b, FGFR3c and FGFR4). These receptors have temporal and tissue-specific expression patterns as well as specificity for FGF binding (Beenken and Mohammadi, 2009). FGF-1 and FGF-2 were the first two FGFs identified, with FGF-2 being the most relevant variant in relation to this thesis.

1.3.1. Fibroblast growth factor -2 (FGF-2)

FGF-2 was first identified in pituitary and brain extracts due to its ability to stimulate 3T3 cell proliferation in culture (Gospodarowicz, 1974). It is usually present in all organs, solid tissues, tumours and cultured cells (Baird, 1986; Gospodarowicz *et al*., 1987). It has been shown that most FGFs have amino terminal signal peptides and are readily secreted from cells (Miyamoto *et al*., 1993). On the other hand, FGF-2 along with FGF-1 and FGF-9 lack the secretory signal peptide (Miyamoto *et al*., 1993). Ornitz and

Itoh have mentioned that the methods of secretion of these FGFs are still not completely understood, however they can be found on the cell surface and in the ECM (Ornitz and Itoh, 2001). Steringer *et al* recently reviewed that FGF-2 been secreted independent of N-terminal signal recognition particle and rather by "unconventional Protein secretion" (Steringer *et al*., 2014). They further mentioned that FGF-2 is secreted from cells by direct translocation across plasma membranes (Schäfer *et al*., 2004; Steringer *et al*., 2014).

A variety of different FGF-2 mRNA transcripts, antisense transcripts and protein products have been identified in different tissues. Most of the variation arises from multiple initiation sites on the FGF-2 gene. For example, bovine pituitary FGF-2 is 146 amino acids long (Duchesne *et al*., 2012) whereas human placental FGF-2 consists of 157 amino acids (Sommer *et al.*, 1987) through the use of different initiation codons. FGF-2 consist of a core region organized in 12 anti-parallel β-strands (β1–β12) and the HS binding sites are contained in this β1–β2 loop as well as parts of regions located between β10 and β12 (Beenken and Mohammadi, 2009). There are two classic heparin-binding domains (HBD) in FGF-2, corresponding to amino acid residues 18-22 and 107-110 (Esch *et al*., 1985) although other regions have also been postulated to interact with this sugar (Baird *et al*., 1988). In fact, Ori and colleague recently claimed the identification of the third HBD (Ori *et al*., 2009).

FGF-2 carries out their various functions through binding interactions that involve the four FGF receptors (FGFR 1-4). Although, Dombrowski and colleagues have shown that FGFR1 signalling activity is rate limiting for self-renewal of hMSCs and thereby stimulates proliferation of hMSCs

(Dombrowski *et al*., 2013). FGFRs are receptor tyrosine kinases and receptor dimerization is needed for downstream signaling through ERK cascade. This uses a combination of bivalent ligand binding, direct receptor-receptor contacts, and the involvement of an accessory molecule (heparin/HS) (Lemmon and Schlessinger, 2010; Schlessinger, 2000; Schlessinger *et al*., 2000; Stauber *et al*., 2000). X-ray crystal structures of a 2:2:2 dimeric ternary complexes of FGF-2, fibroblast growth factor receptor-1 (FGFR1) and a heparin decasaccharide has been resolved and shown that each receptor molecule simultaneously contacts both FGF and heparin (Schlessinger *et al*., 2000). A more physiological model was proposed by Pellegrini *et al* who reported a crystal structure with the stoichiometric ratio 2:2:1 of FGFR2:FGF1:heparin decasaccharide where heparin simultaneously contacts both ligands in the dimer and both receptor molecules (Pellegrini *et al*., 2000).

In vivo administration of exogenous FGF-2 induces a variety of responses. The FGF-2 is well known for its angiogenic properties and the exogenous FGF-2 stimulates migration and proliferation of endothelial cells *in vivo* (Ware and Simons, 1997). In addition, it causes a rapid neovascularization in the cornea, kidney capsule, skin, and fibroplasia in the dermis (Davidson *et al*., 1985; Folkman and Klagsbrun, 1987; Hayek *et al*., 1987; Shing *et al*., 1985). Furthermore, FGF-2 plays a major role in controlling the growth of endothelial and smooth muscle cells (Lindner and Reidy, 1991). This further described the role of FGF-2 in inflammation; in response to asthma triggers FGF-2 enables airway smooth muscle cells to proliferate (Bossé and Rola-Pleszczynski, 2008).

In particular, of most interest to my thesis, FGF-2 has been shown to enhance the growth of mesenchymal stem cells (Auletta *et al*., 2011; Dombrowski *et al*., 2009; Ling *et al*., 2006; Sotiropoulou *et al*., 2006). In addition, Ng and colleagues have shown that FGF-2, TGFβ and PDGF signaling pathways are essential in hMSC proliferation (Ng *et al*., 2008). They have shown that in the presence of FGF-2 with TGFβ1 and PDGF BB in serum-free medium maintained hMSCs for 5 passages while in absence hMSCs showed a more flattened morphology. Furthermore, Rodrigues and colleagues in their review paper also highlighted the importance of FGF-2 as a mitogenic factor for MSC (Rodrigues *et al*., 2010). Moreover, Gharibi and Hughes have used several growth factors including FGF-2, PDGF BB, Wnt3a, IL-6 and EGF as medium supplements on MSC self-renewal and differentiation potential (Gharibi and Hughes, 2012). They have shown that out of all supplements FGF-2 has given the highest increase in MSC proliferation.

Szlachcic *et al* have mentioned that there are different strategies to improve the stability and the half-life of the protein drug efficiency (Szlachcic *et al*., 2011). These can be done by means of genetic and chemical modifications. Few studies have shown that introduction of single or multiple amino acid substitutions in the wild type FGF-1 sequence can affect its susceptibility to degradation and stability (Motomura *et al*., 2008; Szlachcic *et al*., 2011; Zakrzewska *et al*., 2005). Zakrzewska *et al* have shown that multiple mutants of FGF1 were able to significantly enhanced resistance to proteases and prolonged in vivo half-life, even up to ten-fold (Zakrzewska *et al*., 2005). Extensive manipulations of wild type sequence of FGF-1 can also

increase their half-life as described by Motomura *et al* (Motomura *et al.*, 2008). They have shown that the chimeric FGF1:FGF2 variant in which a segment of 43 residues from FGF2 was introduced into the FGF1 sequence, can be used as an agent to stimulate wound healing. In addition, Lee and Blaber also shown that functional half-life and mitogenic activity were greatly extended in FGF-1 after a single mutation of the Ala66 to Cys (Lee and Blaber, 2013). They further illustrate that this mutation recovered vestigial disulfide bond between absolutely conserved Cys residue of FGF family of proteins at position 83, and thereby will be useful in protein engineering strategy to improve the functional half-life of other FGF family members.

Besides amino acid sequence modifications, the covalent linkage of carbohydrate moieties or synthetic polymers also can increase the half-life of proteins. Beeken and Mohammadi have discussed the importance of administering growth factors for angiogenic stimulation; long-term presence and slow release in the tissue is important for maintenance of new vasculature. But the problem lies with the mean half-life of fibroblast growth factor 2 (FGF2) which is only about 7.6 hours in the body (Beenken and Mohammadi, 2009). This half-life can be extended when FGF-2 is co-administered with heparin (Beenken and Mohammadi, 2009; Bush *et al*., 2001). In addition, Caldwell *et al* using an ELISA assay, assessed the concentration of FGF-2 in growth media and shown that at 37 °C, FGF-2 levels dropped by over 80 % within the first 24 h (Caldwell *et al*., 2004). They also described that with the addition of heparin, this decline is significantly attenuated and prolonged the half-life of FGF-2. Furthermore, Uniewicz *et al* have successfully shown by

the differential scanning fluorimetry measurements, FGF-2 upon binding to heparin prevented its thermal degradation (Uniewicz *et al*., 2010).

1.4. HS-FGF interactions

The HSs regulate more than 400 extracellular proteins (Xu *et al*., 2012). HS as a key regulatory component in ECM, binds to FGF-2 and effects their pericellular matrix transport (Duchesne *et al*., 2012; Schmidt *et al*., 2006) which required for assembly and interaction with FGF receptors in signal transduction (Xu *et al*., 2012). Furthermore, Xu *et al* have mentioned key areas in the interaction specificity between HS and FGF-2 namely binding parameters, heparin binding domain (HBD) of FGFs, specific structures in the HSs and changes in secondary structure in FGFs upon HS binding (Xu *et al*., 2012).

Various studies have recognized common structural features in the heparin/HS binding sites of proteins (Gandhi and Mancera, 2008; Hileman *et al*., 1998; Ori *et al*., 2009). Cardin and Weintraub in 1989 made a first attempt to define heparin-binding domains (HBDs) after analyzing 21 heparin-binding proteins. They have looked at the sequences of basic regions of various heparin-binding proteins which were shown experimentally that bind to heparin. With respect to that heparin binding domains of Vitronectin, Apolipoproteins E and B -100 and Platelet Factor 4 were analysed and the organization of basic and non-basic residues were noted. Thereafter they have looked at the basic regions of other known heparin-binding proteins which were not experimentally shown to bind heparin. Afterwards the consensus sequences were determined and proposed that typical heparin-binding sites

have the sequence XBBXBX or XBBBXXBX, where B is a basic residue which is a positively charged amino acid (arginine, lysine and very occasionally histidine) and X is a non-basic residue (Cardin and Weintraub, 1989).

The next consensus sequence TXXBXXTBXXXTBB, was posited by Hileman *et al.* after comparing X-ray diffraction patterns and the NMR profiles of several proteins. In this sequence T defines a turn, B a basic amino acid (arginine or lysine) and X a non-basic residue (Hileman *et al*., 1998). In addition, Ori *et al* have described a method using the "protect and label" strategy with the basis of protecting against the chemical modification given by heparin/HS to the residues located in the heparin binding site (Ori *et al*., 2009). Therefore the once protected FGF-2 HBS can be identified by protein digestion and identified by MALDI-QTOF mass spectrometry. The differential scanning fluorimetry assay published by Uniewicz *et al* identified the preferences in various FGFs to different structural features of GAGs (Uniewicz *et al*., 2010).

Strong ionic interactions are obviously expected between GAGs and proteins, wherein the positively charged basic amino acids form ionic bonds with the abundant, negatively charged sulfate or carboxylate groups on the sugar chains. These bonds are particularly important in the NS domain regions of HS (Fromm *et al*., 1997a; Ori *et al*., 2009). In addition, there are other types of bonds contributing to such association, including van der Waals forces, hydrogen bonds and hydrophobic interactions. These bonds become more important for the interactions with more heterogeneous HS mixtures, where neutral amino acids are also required (Fromm *et al*., 1997a; Ori *et al*., 2009).

In considering FGF-2, glutamine and asparagine also play important roles by forming hydrogen bonds with the hydroxyl groups of the sugar (Thompson *et al*., 1994).

The numerous published studies so far have suggested several different peptide sequences as being the "key" heparin binding-domain of FGF-2; these have been compiled in Table 2.1. Here I have adopted a numbering system taking into the account the 288 aa which constitute the mature, secreted FGF-2 sequence.

Table 1.1. Putative heparin-binding domains within the FGF-2 sequence

	Residue/ Size	Sequence	Reference
1	**248-254/ 7aa**	^{248}YKRSRYT^{254} –paper Have to be ^{248}**YRSRKYT**^{254}	(Lee *et al.*, 2007)
2	**261-277/17aa**	^{261}KRTGQYKLGSKTGPGQK^{277}	
3	**260-277aa/18aa**	^{260}LKRTGQYKLGSKTGPGQK^{277}	(Hileman *et al.*, 1998)
4	**166-210/45aa**	^{165}YCKNGGFFLRIHPDGRVDGVREKSDPHIKLQLQAEERGVVSIKGV^{210}	(Baird *et al.*, 1988)
5	**235-262/ 28aa**	^{235}FFFERLESNNYNTYRSRKYTSWYVALKR^{262}	
6	**157-172/ 16aa**	^{157}GHFKDPKRLYCKNGGF^{172}	(Gandhi and Mancera, 2008)
7	**150-183/34aa**	^{150}GSGAFPPGHFKDPKRLYCKNGGFFLRIHPDGRVD^{183}	(Cardin and Weintraub, 1989; Esch *et al.*, 1985)
8	**185-194/ 10aa**	^{185}VREKSDPHIK^{194}	(Kinsella *et al.*, 1998)
9	**250-259/ 10aa**	^{250}SRKYTSWYVA^{259}	
10	**260-273/14aa**	^{260}LKRTGQYKLGSKTG^{273}	
11	**260-280/21aa**	^{260}LKRTGQYKLGSKTGPGQKAIL^{280}	(Ashikari-Hada *et al.*, 2004)
12	**168-277**	^{168}KNGGFFLRIHPDGRVDGVREKSDPHIKLQLQAEERGVVSIKGVCANRYLAMKEDGRLLASKCVTDECFFFERLESNNYNTYRSRKYTSWYVALKRTGQYKLGSKTGPGQK^{277}	(Thompson *et al.*, 1994) [Mentioned key aa in HBD]
13	**168-169,223,261-277-20aa**	^{168}KN^{169} ^{223}R ^{261}KRTGQYKLGSKTGPGQK^{277}	(Baird et al., 1988; Faham *et al.*, 1996b; Ori *et al.*, 2009; Thompson *et al.*, 1994)
14	**235-262/28aa**	^{235}FFFERLESNNYNTYRSRKYTSWYVALKR^{262}	

Disaccharide analyses of heparin have been published by various groups (Ampofo *et al*., 1991; Desai *et al*., 1993; Jandik *et al*., 1994; Karamanos *et al*., 1996; Ruiz-Calero *et al*., 1998; Scapol *et al*., 1996). As described, the key disaccharides of porcine intestinal mucosal heparin were DHexUA,2S-GlcNS,6S and DHexUA-GlcNS,6S, which indicated that trisulfated disaccharides (2O-, 6O- and N-sulfated) and disulfated disaccharides (6O- and N-sulfated) are major components for the binding to growth factors such as FGF-2. Various studies have presented data supporting the idea that HS's different capacity for proteins is due to differentially modified HS units. Lindahl's group in Sweden have shown that 3O-sulfated glucosamine, at a specific position in the antithrombin-binding sequence of heparin is essential for its anticoagulation effects (Lindahl *et al*., 1980).

Similarly, specific disaccharide sequences within HS GAGs chains support the signaling of the FGF family. The FGF1-binding affinity of HS is reduced in the absence of 6O-sulfate groups, indicating their importance for this interaction (Fromm *et al*., 1997b; Ishihara, 1994). Similarly, FGF4 requires both 2O- and 6O-sulfation for binding and signaling (Ashikari-Hada *et al*., 2009; Guimond *et al*., 1993; Ishihara, 1994). FGF-2 binding to HS requires 2O-sulfation (Faham *et al*., 1996a; Maccarana *et al*., 1993). Furthermore, in addition to the 2-O sulfation, 6-O-sulfation of N-sulfated glucosamine residues is required for the promotion of FGF-2 mitogenic activity (Pye *et al*., 1998). Lundin and colleagues have also supported this idea by showing that FGF-2 binding requires N and 2-O-sulfate groups, whereas stimulation of FGFR-1 and Erk2 kinases by FGF-2 also required the presence of 6O-sulfate groups (Lundin *et al*., 2000). Furthermore, they demonstrated

that 6O-desulfated heparin could inhibit FGF-2-induced angiogenesis in chick embryo chorioallantoic membranes. Thus, formation of the ternary complex of FGF-2-HS-FGFR1 critical for signal transduction requires 2O-, 6O- and N sulfation.

Furthermore, HS, in order to qualify as a coreceptor for the FGF/FGFR complex, must have sufficient length and the requisite disaccharide composition to couple both FGF-2 and FGFR1. The minimum oligosaccharide that can bind FGF-2 is a tetrasaccharide, as shown by optical NMR spectroscopy (Delehedde *et al*., 2002; Guglieri *et al*., 2008). In addition, an increasing gradient in affinity for FGF-2 was seen from tetrasaccharide to octasaccharide. However, according to Delehedde *et al.*, the oligosaccharides from tetrasaccharides to octasaccharides were less potent in their stimulation of the proliferation of rat mammary fibroblasts than deca- or longer -saccharides (Delehedde *et al*., 2002). In addition, a dodecasaccharide sequence has been proposed as the minimal requirement to promote receptor signaling by FGF-2 (Guimond *et al*., 1993). Thus an HS variant with the ability of binding to both FGF2 and FGFR1 will be critical in FGF-2 signal transduction.

1.5. Therapeutic uses of Mesenchymal stem cells (MSCs)

MSCs are defined as plastic-adherent fibroblast-like progenitor cells that can be directed to differentiate *in vitro* down the osteogenic, chondrogenic and adipogenic lineages at a minimum, as well as myogenic, and other lineages under certain conditions. More recently the term “multipotent mesenchymal stromal cells” was also coined to the acronym MSCs by the

International Society for Cytotherapy (Zulma *et al*., 2011). MSCs were first isolated from bone marrow by Friedenstein *et al* and reported as plastic adherent fibroblast cells (Friedenstein *et al*., 1976). Since then, MSCs have been discovered in various adult tissues (Ikehara, 2013; Si *et al*., 2011; Zulma *et al*., 2011), namely skeletal muscle (Williams *et al*., 1999), adipose tissue (Zuk *et al*., 2001), umbilical cord (Erices *et al*., 2000), synovium (De Bari *et al*., 2001), the circulatory system (Kuznetsov *et al*., 2001), dental pulp (Gronthos *et al*., 2000), amniotic fluid (Scherjon *et al*., 2003), fetal blood (Noort *et al*., 2002), lung (Fan *et al.*, 2005) and liver (Campagnoli *et al*., 2001).

The therapeutic potential of MSCs has long been suspected, and they have been used for many clinical applications, including soft tissue and bone tissue regeneration. Caplan and Correa in a recent review paper discussed the now standard view of MSCs: their multipotentiality, their means of tissue homing and integration, as well as the evolving view of their role as "cellular modulators" (Caplan and Correa, 2011). Most memorably, they likened the known trophic and immunomodulatory activities of MSCs, to them constituting an "injury drugstore". The MSCs have been widely used in tissue engineering pre-clinical models in various tissues such as bone, cartilage, tendon and connective tissue with promising results (Caplan, 2007). In addition, Humpreys and Bonventre, highlight the path to translating MSCs in-to the clinic (Humphreys and Bonventre, 2008) while Uccelli *et al* have described the possibility of forging new therapeutic approaches for MSCs (Uccelli *et al*., 2008).

1.5.1. MSCs as accelerators of wound healing

Wound healing is an intricate process that requires coordination between cells, growth factors and the ECM (Maxson *et al*., 2012). Maxson and colleagues posit that MSCs present at sites of injury coordinate healing by secreting growth factors and ECM substances and recruiting other cells to the trauma site. Non-healing chronic wounds have become a serious and increasing problem on a global scale (Jackson *et al*., 2012; Maxson *et al*., 2012). In the United States alone, 5-7 million cases of failure to heal have been reported, with current treatment methods ineffective for up to 50 % of these wounds (Hanson *et al*., 2010; Maxson *et al*., 2012; Mustoe *et al*., 2006).

Maxson *et al* propose that MSCs participate during the three phases of wound healing (Maxson *et al*., 2012). In the inflammatory phase MSCs regulate inflammation, produce IL-10 and IL-4 and suppress TNF production and T cell proliferation. By the proliferative phase, they produce growth factors like VEGF, PDGF, HGF and recruit keratinocytes, dermal fibroblasts and host stem cells. In the last remodeling stage, MSCs produce TGFβ3, KGF and regulate collagen deposition. The recruitment of host cells was further supported by Shin *et al* who showed that MSCs enhanced both normal and impaired wound healing (Shin and Peterson, 2013). Furthermore, Chen *et al* highlighted that paracrine factors secreted by MSCs recruit macrophages and endothelial cells to enhance wound healing (Chen *et al*., 2008). Moreover, following injury, MSCs are recruited to the injury site from their perivascular location and establish the regenerative microenvironment (Caplan, 2007; Caplan and Correa, 2011). Also, MSCs have been shown to alleviate bleomycin-induced tissue fibrosis and suppress inflammation while supporting

ECM remodeling (Wu *et al*., 2013). These collective properties highlight the increasing importance of MSCs for regenerative medicine, and underpins strategies to enhance their *ex vivo* growth prior to reimplantation.

1.5.2. MSCs in bone tissue engineering

Bone fractures most commonly occur due to trauma, surgical resection procedures and congenital defects. In most cases, normal healing progresses and the injury repairs itself. Unfortunately there are ~ 1 million cases of skeletal injuries per year that fail to heal, usually resulting from a large defect size coupled with other undesirable healing conditions (Chatterjea *et al*., 2010; Salgado *et al*., 2004). In such cases, bone-grafting strategies involving either autologous or allogenic bone are standard-of-care. Though autologous bone grafts are safe and relatively easy to access, patients must undergo an additional surgery that can be detrimental to their health. MSCs are being extensively trialed as alternatives to bone grafting in both autologous and allogeneic settings (Bueno and Glowacki, 2009; Chatterjea *et al.*, 2010). This cell based strategy is being trialed in the clinics for fracture nonunion, osteogenesis imperfecta and hypophospertasia (Undale *et al*., 2009), amongst others.

1.5.3. Immunomodulatory properties of MSCs

In recent years the immunosuppressive and anti-inflammatory effects of MSCs have received much attention. MSCs possess only slight or weak levels of immunogenicity, both because they express only low levels of major histocompatibility complex-I molecules (MHC-1) on their cell surfaces, and

because they have the ability to suppress the activation and proliferation of both T and B lymphocytes, and so modify the microenvironment of injured tissues by protecting damaged cells blood (Si *et al*., 2011; Zulma *et al*., 2011). This MSC-mediated immunosuppression, which has long been trialed for cases of severe graft-versus-host disease (GVHD) has a species variation in mechanism (Ren *et al*., 2009; Shi *et al*., 2010). MSCs in the cytokine-primed mouse model have their levels of activity mediated by nitric oxide (NO) whereas cytokine-primed human MSCs are controlled by indoleamine 2, 3-dioxygenase (IDO).

Haemopoietic-cell transplantation (HCT) is an intensive therapy used to treat haematological malignant diseases and its prevalence increases annually (Ferrara *et al*., 2009). The major complication of HCT is GvHD, an immunological disorder that affects mainly gastrointestinal tract, liver, skin, and lungs. According to Billingham, (1966, 1967), three conditions serve to trigger GvHD: 1) the graft must contain immunologically competent cells T lymphocytes, 2) the recipient must express tissue antigens that are not present in the transplant donor, and 3) the patient must be incapable of mounting an effective response to abolish the transplanted cells.

GvHD pathophysiology starts when myeloablative conditioning regimes are used to remove the host's defective bone marrow. The host's antigen-presenting cells become activated because certain cytokines (TNFα, IL1, LPS) are produced by the damaged tissues. Once the allogeneic HCT is performed, donor T cells get activated, thereby stimulating the release of more cytokines, leading to the cellular and inflammatory reactions that characterize GvHD. Non-haemopoietic stem cells such as MSCs seem to reduce allogeneic

T-cell responses due to their potent immunosuppressive capabilities, and often ameliorate the disorder (Le Blanc *et al*., 2008; Meuleman *et al*., 2009; Toubai *et al*., 2009).

1.5.4. Other clinical uses of hMSCs

In addition to MSC use in wound healing, bone tissue engineering and GvHD, their application to other areas of clinical interest has been investigated. Ikehara *et al* described hMSCs from bone marrow in various organ repair scenarios (Ikehara, 2013), including interstitial lung disease, acute and chronic kidney injuries (Morigi *et al*., 2004), myocardial infarctions in heart (Shabbir *et al*., 2009), acute liver injury (Dong *et al*., 2010), diabetes and acute pancreatitis (Lazebnik *et al*., 2011; Tu *et al*., 2012), brain and spinal cord injuries (Boido *et al*., 2012), inflammatory bowel disease (Castelo-Branco *et al*., 2012), bone repair (Chatterjea *et al*., 2010; Undale *et al*., 2009), arthritic diseases (Chen and Tuan, 2008) and limb ischaemia .

1.6. Is hMSC expansion needed for therapeutic purposes?

The potential of using cell and tissue based treatments for trauma and disease is immense, especially when conventional treatments fail (Rayment and Williams, 2010). Mesenchymal stem cells (MSCs) have been suggested to have significant therapeutic potential, and have already been trialed clinically for such purposes as tissue regeneration and to accelerate bone marrow transplant integration for some time. The major issue retarding the wider exploitation of human MSCs for cell-based therapies is the difficulty in generating sufficient cell numbers to meet the clinical demand. The low

proportions of hMSCs within bone marrow - they represent only 0.01 - 0.0001 % of the marrow mononuclear cell population - are clearly hindering their more widespread adoption. It has been established that bone marrow obtained from different aged donors, once placed into culture flasks, give rise to very different numbers of colony forming units-fibroblastic (CFU-Fs) (Caplan, 2009). Thus there is a relationship between donor age and hMSCs present in the nucleated marrow. A remarkable decrease in the proportion of hMSC-per-nucleated-marrow-cell has been observed, with a 10-fold decrease from birth to teens, and another 10-fold decrease from teens to old age. In addition, Caplan has pointed out that this proportional decrease correlates with the fracture healing rates in the young and in adults (Caplan, 2009). In contrast, the titres of haematopoietic stem cells in bone marrow, roughly one per 10^4 nucleated marrow cells, remain constant throughout the lifespan of an individual. Collectively, these issues negatively impact on the therapeutic potential of hMSC for regenerative medicine. In addition, most clinical trial needs hMSCs in very large quantities. Ringden *et al* have reported that 0.5-5x10^6/kg of MSCs needed for treatment of GvHD (Ringdén *et al*., 2006), while Phillipe *et al* have noted, for GvHD 3-8 x 10^8 per patient is required (Philippe *et al*., 2010). Therefore in order to obtain required quantities of hMSCs for clinical therapy we need *ex vivo* expansion. The product Prochymal, from Osiris Therapeutics which contains MSCs from healthy adult donors are now been used in phase III clinical trials with a dose of 2-8 x 10^6/kg for GvHD (Chen *et al*., 2013).

1.7. Current expansion methods of MSCs

In order to address this major question of the supply of hMSC, it was rapidly realized that *ex vivo* expansion was required in the same way that HSCs are treated. Thus, better mimicking of the bone marrow microenvironment is now a major research direction. It can be achieved in two broad ways: either growing hMSCs on properly constituted ECM substrates, or exogenous growth factor supplementation.

1.7.1. Expansion of MSCs with growth factors

Growth factors are known to influence cell proliferation. Ng and colleagues have shown that FGF-2, TGFβ and PDGF signaling pathways are essential in hMSC proliferation (Ng *et al*., 2008). They have shown that in the presence of FGF-2, TGFβ1 and PDGF BB hMSCs for 5 passages while in their absence hMSCs showed a more flattened morphology. In addition, Rodrigues and colleagues in their review paper described that several growth factors including TGFβ, FGF-2, FGF-4, VEGFA, PDGF BB, HGF, EGF and Wnt3a increase MSC proliferation (Rodrigues *et al*., 2010). Furthermore, Gharibi and Hughes have used several growth factors including FGF-2, PDGF BB, Wnt3a, IL-6 and EGF as medium supplements for MSC self-renewal and differentiation (Gharibi and Hughes, 2012). They have shown that out of all supplements FGF-2 resulted in the highest increase in MSC proliferation over passage 3 to 10. Therefore hMSC proliferation with FGF-2 supplementation can be used as guide to assess the relative effects of other agents on hMSC proliferation in a traditional monolayer system. Notably, increases in hMSCs numbers following FGF-2 supplementation has been widely reported (Auletta

et al., 2011; Dombrowski *et al*., 2009; Ling *et al*., 2006; Sotiropoulou *et al*., 2006).

Plastic adherence is a well described property of hMSCs: if cells are maintained and expanded in normal culture conditions they should adhere to plastic surface, and form mesenchymal stem cell colonies when plated at low densities (Friedenstein *et al*., 1976; Pochampally, 2008). Sotiropoulou and colleagues have isolated hMSCs with media supplemented with FGF-2 (Sotiropoulou *et al*., 2006). They also claimed that FGF-2 supplementation clearly affects isolation which resulted in vast numbers of cells, but the colony-forming ability of such cells does not differ significantly among the groups. Although, Martin and colleagues have reported that FGF-2 supplementation in isolation of hMSCs from BMMNCs significantly reduced the CFU-F efficiency compared to unsupplemented media (Martin *et al*., 1997). In addition, Fresciline *et al* claimed that rat MSC isolation from BMMNCs with FGF-2 supplemented media had decreased amounts of CFU-F efficiencies (Frescaline *et al*., 2012).

The MSCs grown with FGF-2 go on to generate greater and greater proportions of differentiated progenitors as compared to the unstimulated hMSCs in the control cultures (Gronthos *et al*., 1999; Walsh *et al*., 2000). The reduction in CD49, STRO-1, CD90, CD105 and HLA-DR in FGF-2 expanded cells as compared to controls were recently reported (Hagmann *et al*., 2013). In addition, Gharibi *et al* also supported the reduction in CD90 and CD105in FGF-2 expanded cells (Gharibi and Hughes, 2012).

In relation to multilineage differentiation, few groups have also reported that FGF-2 expanded cells have increased chondrogenic potential

(Hagmann *et al*., 2013; Tsutsumi *et al*., 2001). On the other hand, FGF-2 generated greater proportions of differentiated progenitors as compared to the unstimulated hMSCs in the control cultures (Gronthos *et al*., 1999; Walsh *et al*., 2000). In addition, Ling *et al.* have shown that the longer osteogenic cells are in contact with FGF-2, the less potential they have for osteogenic development (Ling *et al*., 2006). It needs to be kept in mind that others have claimed that MSCs grown with FGF-2 supplementation results in cells that do maintain their osteogenic development (Auletta *et al*., 2011; Gharibi and Hughes, 2012; Sotiropoulou *et al*., 2006). Supporting this, autocrine FGF-2 has also been shown to increases the multipotentiality of human adipose-derived MSCs (Rider *et al*., 2008). Endogenous growth factor activity also seems to modulate hMSC behaviour (Hudalla *et al*., 2011). As such, there remains a conflict in this area. In addition, FGF-2 grown hMSCs have shown to pocess potent immunosuppressive effect (Auletta *et al*., 2011; Sotiropoulou *et al*., 2006).

The question then becomes: is there a way of presenting hMSCs with the FGF-2 they need for expansion without simultaneously losing their capacity to differentiate from their multilineage potential?

1.7.2. Expansion of MSCs with ECM substrates

ECM substrates have been shown to increase both hMSC attachment and cumulative cell number (Grünert *et al*., 2007; Matsubara *et al*., 2004) but the resulting expanded cells appear to lose the requisite level of "stemness" for clinical usefulness (Cool and Nurcombe, 2005). On the other hand, Ang *et al* have mentioned that *in vivo* stem cell environment is physiologically crowded

as compared to *in vitro* culture practices (Ang *et al*., 2013). They have demonstrated that re-introducing macromolecular crowding (MMC) during chemically induced adipogenesis substantially enhanced the adipogenic differentiation potential of hMSCS (Ang *et al*., 2013). Furthermore they claim that the MMC significantly enhance the deposition of ECM. In addition, Dombrowski *et al* from our group has shown that embryonic HS can mediate the proliferation and differentiation of rat MSCs (Dombrowski *et al*., 2009).

Therefore, to answer the question in the previous sub chapter 1.7.1, sustaining the endogenous FGF-2 already secreted by MSCs through targeted HS fractions; the justification appeared reasonable as HS clearly regulates FGF signaling by direct molecular trimeric association with both FGFRs and FGFs (Pellegrini *et al*., 2000). The original data of Nurcombe *et al.* (1993) demonstrated that the activity of particular FGF isoforms for murine neural precursor cells was tightly regulated by HS and that this interaction is a requirement for the binding of FGF-2 to their receptors (Nurcombe *et al*., 1993). In addition, there was a significant difference in the binding of HS to FGFs such that at embryonic day 9, the HS produced within the neuroepithelium preferentially bound FGF-2, but by day 11, HS binding preference had shifted to FGF1. Furthermore, these unique HS forms mediated the binding of FGF-2 to specific receptors via an interaction with specific cell-surface receptors on the neural precursor cells (Brickman *et al*., 1995). In 1998, Brickman *et al* provided further structural support for these physiological findings by isolating and characterizing two separate HS pools from immortalized embryonic day 10 mouse neuroepithelial 2.3D cells, and proving they had quite distinct binding preferences (Brickman *et al*., 1998).

One pool was derived from cells in log growth phase, and showed an increase their ability to activate FGF-2, while the other pool, from the same cells but undergoing contact-inhibition and differentiation, had preference for the activation of FGF1. This led to the isolation and characterization of the embryonic HS preparation named HS2, which in turn was shown to be able to accelerate hMSC growth without significant loss of multipotentiality; cells grown in this mixture could in turn trigger increased bone formation in mice when they were transplanted *in vivo* (Helledie *et al*., 2011). As a direct development of this work, Murali *et al* looked into the liver in mice (Murali *et al*., 2011), an organ rich in stem cells. Liver is a highly regenerative tissue with high levels of FGF-2; I reasoned that it should contain high levels of activating HS. The HSs extracted from the livers of mice did indeed increase rates of hMSC expansion and osteogenic differentiation (Murali *et al*., 2011). These data suggested that the ECM component HS could selectively improve the growth of the hMSCs exposed to FGF-2 without adversely affecting their multipotentiality, notwithstanding that although liver is a better source of HS than embryonic mouse brain, the problem of scalability was not resolved.

1.7.3. Other expansion methods of MSCs

In addition to the two broad areas, other ways were also been investigated. One such method for ex vivo expansion for hMSCs is the forced expression human telomerase reverse transcriptase (hTERT) (Simonsen *et al*., 2002). But the immortalized hMSCs evolve into different types of tumor due to accumulated mutations (Burns *et al*., 2005). Others have replaced FCS in their protocols in expansion of hMSCs in order to eliminate the potential

source of xenogenic pathogens (Gottipamula *et al*., 2013; Hudson *et al*., 2010; Lange *et al*., 2007). Replacing FCS with human platelet lysates have shown that it alters some MSC relevant markers and decreased immunosuppression activity on T lymphocytes and Natural killer cells (Abdelrazik *et al*., 2011).

Furthermore the use of stirred microcarrier (MC) culture has been suggested as another method for supplying large volumes of hMSCs for clinics (Chen *et al*., 2013; Goh *et al*., 2013; Rafiq *et al*., 2013; Santos *et al*., 2011). Goh *et al.* have shown that a 12- to 16-fold enhancement in expansion of fetal MSCs can be effected by three-dimensional (3D) scaffold culturing as compared to the 4- to 6-fold expansion with traditional monolayer (MNL) cultures (Goh *et al*., 2013). Similar to these finding Rafiq *et al* have shown that hMSCs cultured at the litre-scale on microcarriers in a stirred-tank of 5 l bioreactor had a 6-fold increase with traditional monolayer (MNL) cultures while cells retained their multipotentiality (Rafiq *et al*., 2013). In addition, Santos *et al.* have shown 18-fold and 14-fold MSC expansion in bone marrow derived hMSCs and adipose derived hMSCs respectively in a microcarrier-based culture system under xeno-free conditions (Santos *et al*., 2011).

1.7.4. Adult stem cell therapy market.

Patent landscaping or patent mapping is a process where companies are able to identify relevant technology in particular technology space. Thereby, companies can verify the characteristics of each patent and identify the relationships among them to prevent any infringements. Further to the patent landscape of the adult stem cells, Syed and Evans in their recent review

described that beyond bone marrow transplantation there is a high near term prospects for mesenchymal stem cell derived stem cell therapies (Syed and Evans, 2013). They further mentioned that there are osteogenic products (Osteocel, Trinity and LiquidGen) already in the market which readily use MSCs to increase osteogenesis and decrease inflammation. In addition, MSC products like prochymal have already been approved in South Korea and Canada. Furthermore, they have summarized MSC products and their indications from companies like Aastrom, Gamida cell, Osiris and Mesoblast with near term approval as market products. Knowing the potential of this expanding market our group has patented methods of proliferating stem cells where the invention relate to expansion of hMSCs with the use of embryonic heparan sulfate (HS2) (Cool and Nurcombe, 2009). As a direct continuation of previous patent with embryonic heparan sulfate (HS2), another patent has been published by our laboratory as methods of culturing mesenchymal stem cells (Cool and Nurcombe, 2012). Investment in this sector is rapidly increasing due to the fact that the potential stem cell therapy market is expected to be around 8 billion by 2016 (Syed and Evans, 2013).

1.8 Affinity chromatography

Urh *et al* have described affinity chromatography as a powerful method which utilizes interaction between two molecules in order to purify a molecule from a mixture (Urh *et al*., 2009). They further mentioned that a thorough understanding of the target, ligand and the purification procedure is essential for success. On the other hand, fishing requires not only a fishing pole, but bait. A hook must have an appropriate bait attached at the end of the

fishing line of the pole to attract and catch a fish (Ward and Myers, 2007). The bait usually influences what you catch, as different fish are attracted to different type of fish bait. Managing bait type would seem to constitute a simple tool to influence the amount and composition of the fish catch (Alós *et al*., 2009), notwithstanding baited hooks can be also be re-used for catching fish.

Cain *et al.* have described an affinity purification and mass spectrometry method to analyze molecular interactions within elastic fibres which they termed "molecular fishing" (Cain *et al*., 2009). They confirmed the sensitivity and validity of their method by identifying known interactions with the bait proteins. They used "bait" proteins that were purified, tagged recombinant fragments, added them to cell cultures, and detected susceptible "prey" proteins.

We, the Glycotherapeutics group (IMB, A*STAR) have pioneered over several years an analogous affinity method that was sufficiently novel to allow patenting (#2009292236). With this technique our Glycotherapeutics group has built up a library of patent-protected heparan sulfates targeted to different, clinically relevant growth factors. Our platform resembles a relatively straightforward method of fishing (Fig. 1.1). Here we used an FGF-2-HBD peptide as the "bait" and pulled down the "prey" HS. Incorporation of the linker Ahx in the peptide design helped its free movement as it engaged candidate sugar chains in the HS mixture. In addition, the biotin's strong interaction with streptavidin maintained peptide fidelity, which enables continual usage of the peptide bound column in pull down assays of affinity chromatography.

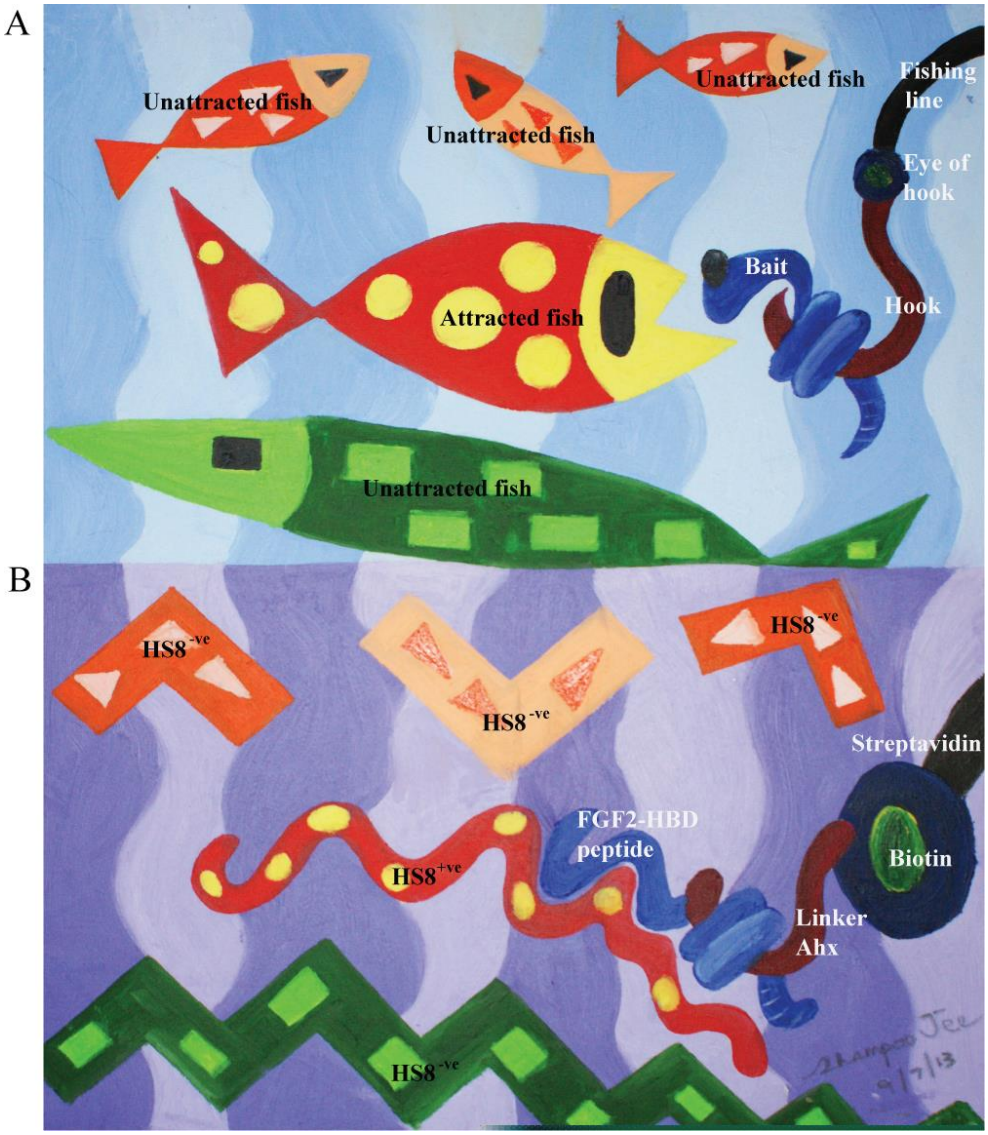

Figure 1.1. Molecular Fishing. An artistic rendering of our affinity chromatography technique platform that reinforces the concept of fishing. The FGF-2-HBD peptide as the "bait" protein pulls down the "prey" heparan sulfate, here termed as $HS8^{+ve}$.

1.9. Thesis outline

1.9.1. Motivation

We are now faced with an aging human population that is increasingly burdened by degenerative diseases. These illnesses are largely treated by surgery and drugs designed to mitigate symptoms. Given their role in maintaining and replenishing tissues, stem cells represent a potential means of

restoring tissue function and thereby treating the root cause of degenerative disease. The potential for hMSC therapy as an adult stem cell to contribute to this growing market are substantial.

The major drawback retarding the wider exploitation of hMSCs for cell-based therapies is the difficulty in generating sufficient cell numbers to meet the clinical demand, both real and potential. The low proportions of hMSCs within bone marrow - they represent only 0.01 - 0.0001% of the marrow mononuclear cell population - are clearly hindering their more widespread adoption (Caplan, 2009). In order to address this major question of the supply of hMSC, mimicking of the bone marrow microenvironment with ECM substrates (Grünert *et al*., 2007; Matsubara *et al*., 2004) and exogenous FGF-2 (Dombrowski *et al*., 2009; Ling *et al*., 2006; Sotiropoulou *et al*., 2006) were promising but the resulting expanded cells "stemness" was unpredictable (Auletta *et al*., 2011; Cool and Nurcombe, 2005; Gronthos *et al*., 1999; Sotiropoulou *et al*., 2006; Walsh *et al*., 2000). Although, autocrine FGF-2 has also been shown to increase the multipotentiality of human adipose-derived MSCs (Rider *et al*., 2008). Therefore, enhancing the endogenous FGF-2 already copiously secreted by MSCs through targeted HS fractions appeared reasonable as HS clearly regulates FGF signaling by direct molecular trimeric association with both FGFRs and FGFs (Pellegrini, 2001).

Previous work in our group had demonstrated the apparently remarkable properties of a neuroepithelially-derived HSPG that, although retaining its core protein identity, was able to switch its growth factor-potentiating abilities from FGF-2 to FGF-1 (Nurcombe *et al*., 1993). The group developed these findings by uncovering the structure compositions of

HS underpinning these (Brickman *et al*., 1995; Brickman *et al*., 1998):, showing they applied to bone (Jackson *et al*., 2002), and developing a rational platform for their scale-up (Murali *et al*., 2013) and showing they have therapeutic utility (Murali *et al*., 2013). In addition, this led to the isolation and characterization of the embryonic HS preparation named HS2, which in turn was shown to be able to accelerate hMSC growth without significant loss of multipotentiality; cells grown in this mixture could in turn trigger increased bone formation in mice when they were transplanted *in vivo* (Helledie *et al*., 2011). As a direct development of this work, Murali *et al* extracted HSs from the livers of mice which indeed increase rates of hMSC expansion and osteogenic differentiation (Murali *et al*., 2011). These data suggested that the ECM component HS could selectively improve the growth of the hMSCs exposed to FGF-2 without adversely affecting their multipotentiality, notwithstanding that although liver is a better source of HS than embryonic mouse brain, the problem of scalability was not resolved. Therefore, this thesis is aimed at resolving this scalability issue.

1.9.2. Specific Aims

As with many extracellular growth factors, maximum bioactivity of the powerful stem cell mitogen FGF-2 depends on the co-factor heparan sulfate glycosaminoglycan sugar. However, to fully realize the clinical potential of this important complexation event, sufficient HS GAG is required. Therefore the major aim of the thesis is to provide a scalable substance in the form of heparan sulfate that is capable of binding to FGF-2 without compromising its biological activity for scale up of naïve human mesenchymal stem cells within

a heterogeneous pool of adherent bone marrow cells. In development of this strategy, consideration was given to the key factors of simplicity, safety, scalability and efficacy. Thus the specific aims of this thesis are to:

1. Identifying the heparin binding domain of FGF-2 and to use this knowledge to synthesize FGF-2-HBD peptides in order to develop an affinity substrate capable of binding to unmodified FGF-2 based on its affinity to glycosaminoglycans.
2. Characterization of isolated heparan sulfate to determine its biological activity.
3. Evaluate the ability of isolated heparan sulfate to expand the hMSCs isolated from bone marrow, with a view to determining its clinical utility.

1.9.3. Hypothesis

An HS sub-fraction that mediates the bioactivity of FGF-2 can be isolated from a crude HS preparation by peptide-based affinity chromatography. When used as a culture supplement during the culture expansion of adult human mesenchymal stem cells (hMSC), this HS sub-fraction will bind and activate endogenously produced FGF-2 resulting in a maintenance of a naïve hMSC phenotype whilst prolonging the long-term culture potential of these cells.

1.9.4. Thesis Organization

This thesis is comprised of five chapters:

Chapter 1 presents a review of literature focusing on areas of extracellular matrix, proteoglycans, glycosaminoglycans, fibroblast growth factors (FGFs), FGF receptors (FGFRs), interactions of heparin/HS with FGF-2, mesenchymal stem cells (MSCs), the need to scale up of hMSC for therapeutic purposes, and current expansion methods for hMSCs. It will also describe the background, motivation, and objectives of this research.

Chapter 2 identifies the HBD of FGF-2 and used this knowledge to synthesize FGF-2-HBD peptides. It also describes the potential use of these peptides by means of ^{3}H heparin assay and GAG ELISA. These peptides were then used as "bait" in affinity chromatography in order to isolate the "prey" heparan sulfate.

Chapter 3 describes the characterization of isolated heparan sulfate to determine its capability of binding to unmodified FGF-2 without compromising its biological utility in expanding hMSCs. Various binding assays, including ELISA and heparin-sepharose competition were used to determine the binding affinity to full length FGF-2. Proliferation studies namely BrdU incorporation assay and GUAVA viacoiunt® assay were used to examine the effect of the isolated HS on hMSC proliferation. In addition, the HS's properties were further studied by anticoagulation assay and disaccharide analysis. Later in the chapter the effect of the HS variant on stability of FGF-2,

its synergistic activity with FGF-2, and inhibitor studies probe the mechanism involved.

Chapter 4 describes the application of the isolated HS substrate in expanding hMSCs isolated from bone marrow, with a view to determining its direct clinical utility.

Chapter 5 concludes with a summary of the findings of this study and recommendations for future research.

CHAPTER 2: ISOLATION

OF THE HS8 VARIANTS

2.1. Introduction

This initial study was developed to primarily address the issue of scalability; that is, to explore the possibility of isolating an HS variant not only with high binding affinity for FGF-2, but that potentiates the FGF-2-driven growth of hMSCs and which can ultimately be scaled with sufficient quality for future clinical use. This chapter describes such a strategy and further exemplifies the utility of a patent-protected (#2009292236) HS purification platform developed by the Glycotherapeutics group (IMB, A*STAR) (Murali *et al*., 2013). Importantly, the development of an affinity purified HS directed towards FGF-2 is a crucial extension of the exemplification of the platform first provided by the BMP-2 binding HS variant dubbed HS3 (Murali *et al*., 2013).

2.2. Materials and Methods

2.2.1. Preparation of FGF-2-HBD peptides

The first step was to identify a suitable FGF-2-HBD peptide that could be used to derivatize an affinity column. To achieve this, ten FGF-2-HBD peptides (12-20 mg, as depicted in Figure 2.1) were synthesized by GL Biochem (Shanghai) Ltd, Shanghai, China (peptides Sequence ID Nos. 1 and 2) and NTU-SBS Peptide Core Facility, Nanyang Technological University, Singapore (peptides sequence ID Nos. 3 to 10). As shown in Figure 2.1, biotinylation was performed at both the N-terminal (*) and the C-terminal (**) of the FGF-2-HBD peptides in attempts to attach the biotin sufficiently far away from any of the clusters of positively-charged, heparin-binding amino acids. A hydrophobic spacer/linker, aminohexanoic acid (Ahx), was included

(Fig. 2.2) between the biotin and the FGF-2-HBD peptide in order to provide free movement of the peptide when it was bound to the streptavidin column prior to the affinity chromatographic step. To facilitate C-terminal biotinylation, an additional lysine was included between the biotin and the Ahx (Fig. 2.2). In order to improve the screening, all ten FGF-2-HBD peptides were synthesized with a purity of > 95%, as verified via HPLC by the manufacturer. Once synthesized, the peptides were stored at -20 °C until required for screening assays or chromatography.

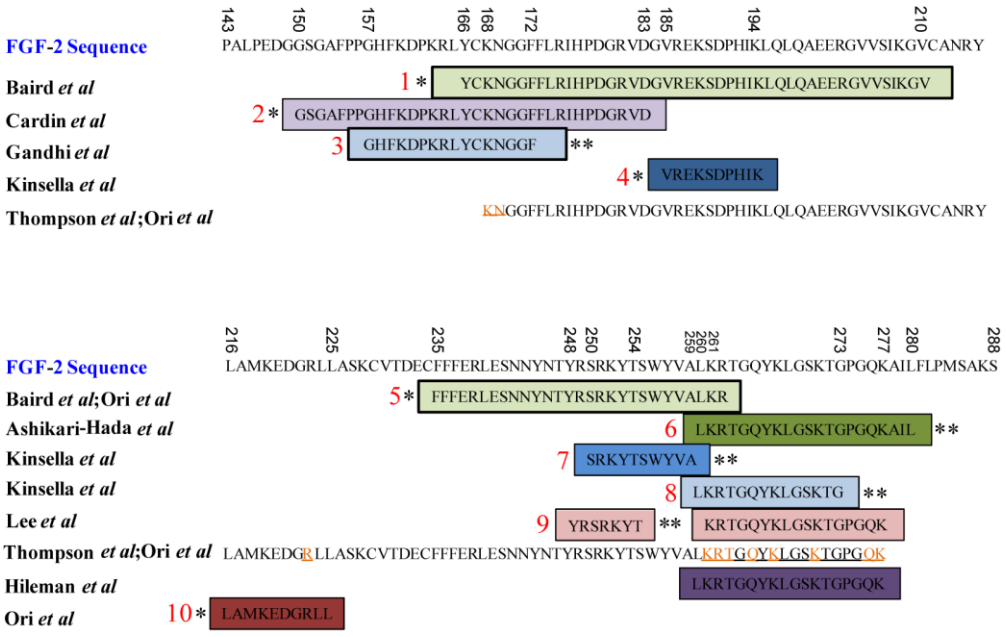

Figure 2.1. Illustration of overlapping peptides derived from the heparin-binding domain (HBD) of the FGF-2 sequence. Ten peptides were synthesized (sequence ID Nos. 1 to 10) with biotinylation at either at N-terminal (*) or at C-terminal (**).

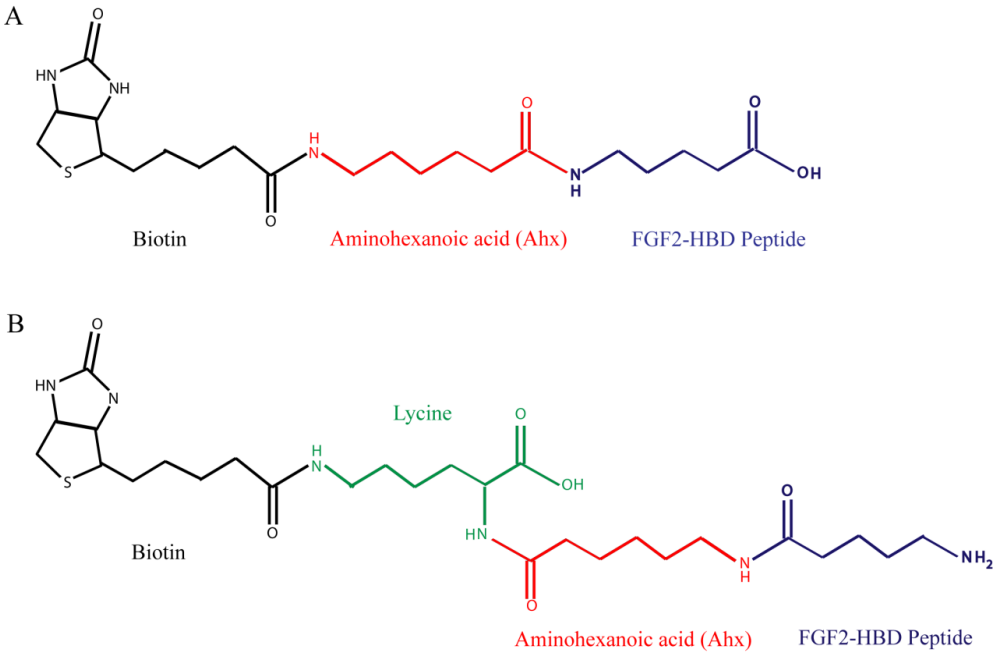

Figure 2.2. Illustration of FGF-2-HBD peptide modifications. (A) N-terminal biotinylation of FGF-2-HBD peptide, and (B) C-terminal biotinylation of FGF-2-HBD peptide.

2.2.2. Peptide binding assay with ^{3}H-heparin

To first confirm the binding ability of the synthesized FGF-2-HBD peptides for soluble heparin, before proceeding to subsequent experiments, a ^{3}H-heparin binding assay was employed, essentially as described by Baird *et al.* (Baird *et al.*, 1988). This assay was based on the immobilization of FGF-2-HBD peptides onto nitrocellulose membranes, and the ability of ^{3}H-heparin to bind to them.

Biotinylated FGF-2-HBD peptides were serially diluted in 2.5 µl of PBS (0, 4.66 x10^{-9}, 9.32x10^{-9}, 18.6x10^{-8} and 37.3x10^{-8} mol peptide) and individually spotted, in duplicate, onto uniform sheets of 0.2 µM nitrocellulose membranes (Biorad). The peptides were then air dried for 1 h at room temperature and heated to 80 °C with -10 psi in a vacuum oven (Thermo Fisher Scientific, USA) for 45 min. The membranes were then washed three

times with PBS. Thereafter 1 ml of 0.1 μCi of ^{3}H-heparin (Perkin Elmer) in 4 % BSA (Sigma Aldrich) was added to the membranes and incubated overnight (16 h) at room temperature with agitation (100 rpm). The next day, the membranes were washed four times with PBS and 1 ml of Ultima Gold scintillation cocktail (Perkin Elmer) added in a 5 ml scintillation vial (Perkin Elmer). The vial was analyzed in a liquid scintillation Tri-carb 2800TR counter (Perkin Elmer, Massachusetts, USA) for 2 min, twice. The counts-per-minute readings were averaged and plotted.

2.2.3. GAG ELISA – bound heparin and HS^{pm} and their ability to engage FGF-2-HBD peptides

To further validate the binding affinities of the synthesized FGF-2-HBD peptides for heparin, GAG ELISA (Glycosaminoglycan enzyme-linked immunosorbent Assay) was performed. A modified version this assay was used as described earlier by our group (Bramono *et al*., 2012; Murali *et al*., 2011). The GAG binding plates are produced by cold plasma polymerization where microtitre plate surfaces are coated with allyl amine (Mahoney *et al*., 2004; Marson *et al*., 2009). Heparin non-covalently immobilizes to these allyl amines by an electrostatic interaction without losing its ability to interact with proteins. The binding ability of each of the FGF-2-HBD peptides was then assessed via the biotinylated portion of the peptide, which yielded a colourimetric reaction as per the manufacturer's instructions (Fig. 2.3).

Wells were incubated overnight (16 h) at room temperature, protected from light, with 200 μl of a 5 μg/ml heparin solution in standard assay buffer (SAB:100 mM NaCl, 50 mM NaAc, (v/v) 0.2 % Tween 20, pH 7.2). Wells were then washed carefully with 250 μl of SAB three times, and blocked with

0.4 % (w/v) fish gelatin (Sigma Aldrich) in SAB (blocking buffer) for 1 h at 37 °C protected from light. The initial experiments were designed to optimize the concentrations of FGF-2-HBD peptides best suited to bind with the immobilized heparin (5 µg/ml) on the GAG-binding 96-well plates. Optimization was carried out with the FGF-2-HBD Gandhi (G) peptide in a range from 0 - 3200 nM in serial two-fold dilutions. The wells were washed with SAB thrice and FGF-2-HBD in blocking buffer at different optimized concentrations (0, 50, 100, 200 nM) was added into triplicate wells (200 µl each) to be incubated at 37 °C for further 2 h.

Wells were again washed thrice with SAB to remove unbound FGF-2-HBD peptides. Next, ExtrAvidin (200 µl of 220 ng/ml) (Sigma Aldrich) was added and incubated for another 30 min at 37 °C. Wells were finally washed with SAB (3 times) and 200 µl of development reagent SIGMA*FAST*™ p-Nitrophenyl phosphate (Sigma Aldrich) in DI water was added into the wells at room temperature for 40 min. Colourimetric absorbance was read at 405 nm with a Victor multiplate reader (Perkin Elmer, Massachusetts, USA).

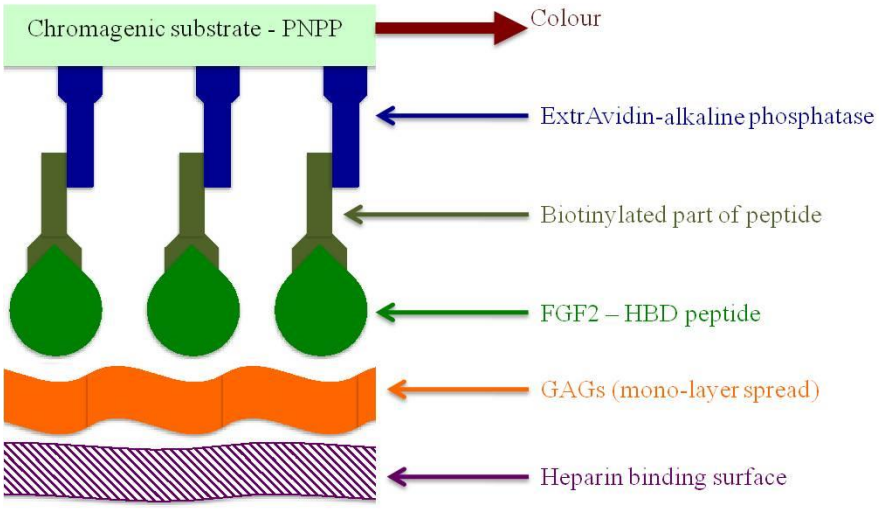

Figure 2.3. Diagram illustrating arrangement of the elements within the GAG-ELISA assay of heparin and FGF-2-HBD peptide binding.

The assay was repeated by replacing heparin in the initial step with porcine mucosal heparan sulfate (HS^{pm}) (Celsus Laboratories); the wells were incubated overnight (16 h) at room temperature protected from light with 200 µl of 5 µg/ml of HS^{pm} in standard assay buffer (SAB). HS^{pm} is a water-soluble, bulk-lyophilized fraction of crude heparin extracted from porcine mucosal tissue. This enabled a comparison between the binding affinities of the different FGF-2-HBD peptides for the starting HS^{pm}.

2.2.4. Affinity chromatography

Once the FGF-2 HBD peptides were synthesized, I pursued an experimental path our Glycotherapeutics group (IMB, A*STAR) has pioneered over several years (Murali *et al.*, 2013). FGF-2-binding HS fractions were isolated from a starting commercial source of porcine mucosal HS (HS^{pm}) (Celsus Laboratories, USA). Biotinylated FGF-2-HBD peptide was used as the capture ligand, and so needed to be derivatised to streptavidin

columns. This forms a very strong interaction that would require strong denaturing conditions for elution. This affinity chromatography platform (AKTA Purifier Core 10, GE Healthcare), which is under patent protection (#2009292236), was clearly able to separate HBD peptide-binding HS from unbound HS when a mixture of HS (HS^{pm}) was applied to the column (Fig. 2.4). Biotinylated FGF-2-HBD peptides, dissolved in low salt buffer (20 mM phosphate buffer, 150 mM NaCl, pH 7.2), were coupled to a 1 ml HiTrap streptavidin HP column (GE Healthcare) as monitored by the detection of unbound peptide at 215 nm in the flow-through. The peptides were applied at a concentration of 1 mg/ml to a total of 3 mg. To ensure each peptide was firmly bound to the column, a 1.5 M high salt buffer (20 mM phosphate buffer, 1.5 M NaCl) wash was performed. When no traces at 215 nm were detected, the column was equilibrated with low salt buffer and was considered ready for HS^{pm} loading.

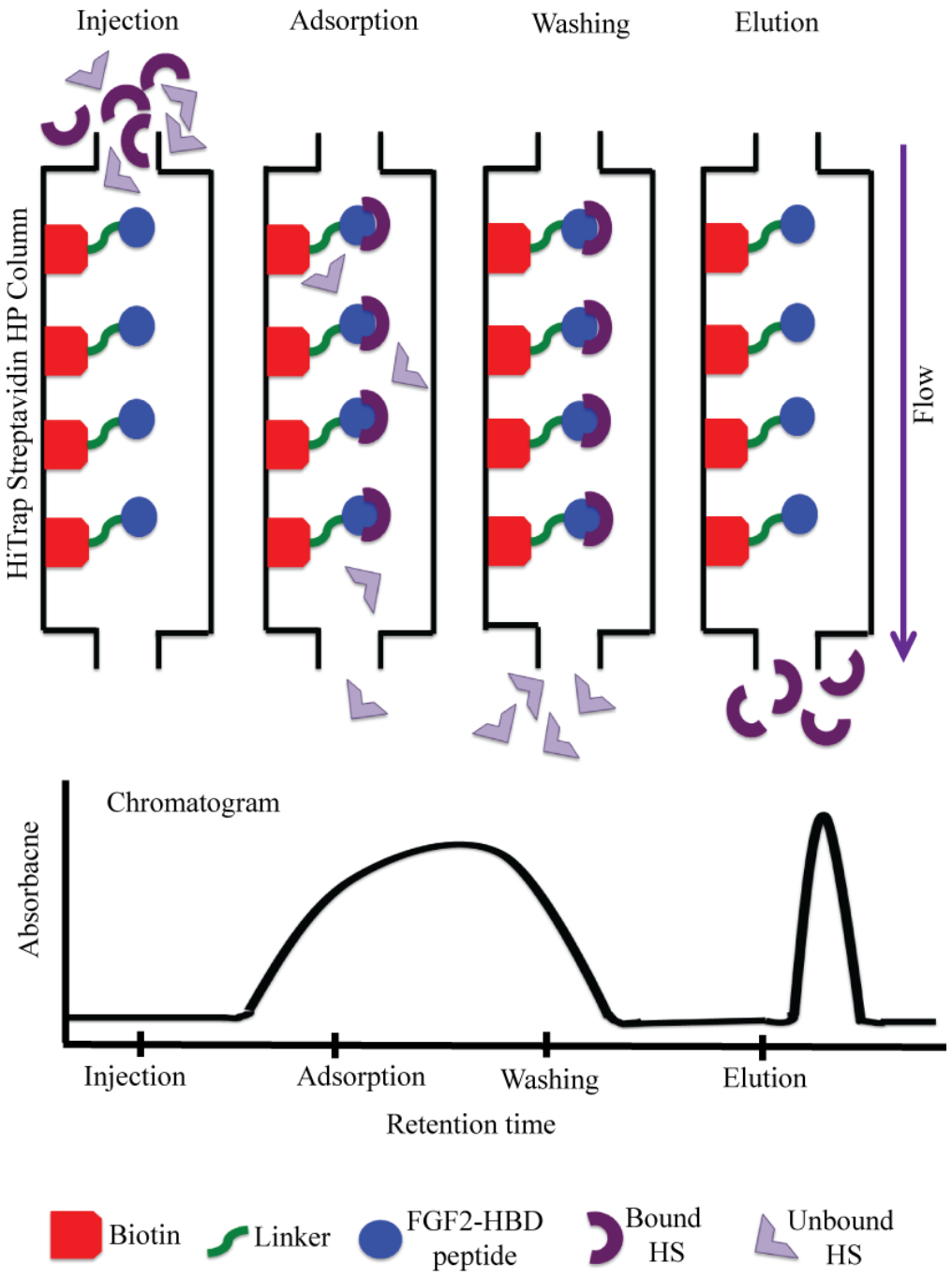

Figure 2.4. Diagram illustrating the affinity chromatography platform. Biotinylated FGF-2-HBD peptides were used as the capture ligand within streptavidin columns. This affinity platform was then able to separate FGF-2-HBD peptide-binding HS from unbound HS when a crude mixture of commercially available HS was applied.

Porcine mucosal HS (HS^{pm}) (Celsus Laboratories) was dissolved in low salt buffer (20 mM phosphate buffer, 150 mM NaCl, pH 7.2) at a concentration of 1 mg/ml. A total of either 100 mg or 400 mg HS^{pm} solution was loaded after a total of 40 or 160 separate injections, of 2.5 ml each, in

low-salt buffer at a flow rate of 0.2 ml/min, and the column washed with the same buffer until the baseline reached zero. The bound HS was eluted with a one-step gradient of 1.5 M high salt (20 mM phosphate buffer, 1.5 M NaCl), the bound and unbound variants collected (as monitored at A_{232} nm), and the column re-equilibrated with low-salt buffer. The eluent ($HS8^{+ve}$) and flow-through ($HS8^{-ve}$) peak samples were collected separately, freeze-dried, and stored at -20 °C.

Desalting, size-exchange chromatography was next exploited to separate the components of the eluent into two groups, so allowing for the purification of $HS8^{+ve}$ and $HS8^{-ve}$ variants away from the eluting NaCl. As shown in Figure 2.5, large molecular weight elements, such as HS, cannot enter the gel, and are so excluded from the gel bed, and thus elute before the small molecular weight ions (NaCl) which enter the pores freely, and thus take more time to elute. Both the $HS8^{+ve}$ and the $HS8^{-ve}$ variants were then separately dissolved in minimal amounts of HPLC grade water (Sigma Aldrich) until a clear solution was obtained, and the samples desalted once again on a HiPrep 26/10 desalting column (Amersham Biosciences) at a flow rate of 10 ml/min (AKTA Purifier, GE Healthcare). The HS variants were then collected, freeze-dried, and stored at – 20 °C.

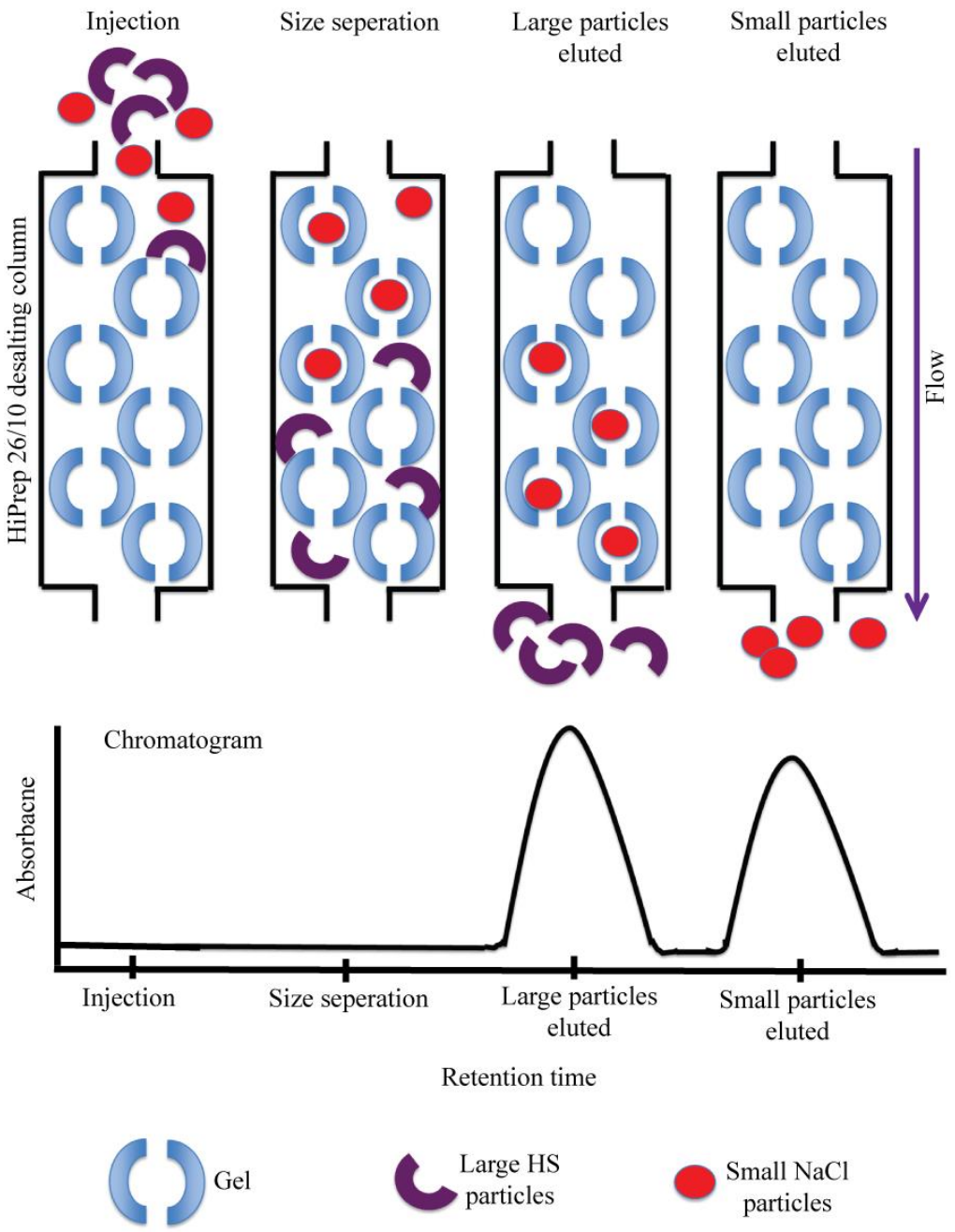

Figure 2.5. Diagram illustrating size exclusion chromatography platform. Large molecular weight components such as HS cannot enter the gel, and are thus excluded from the gel, so eluting first compared to the small molecular weight components (NaCl) which enter the pores freely and thus take more time to elute.

2.3. Results

2.3.1. Peptide binding assays with ^{3}H-heparin

Following the synthesis of the biotinylated FGF-2-HBD peptides (10 in total), their ability to bind to heparin needed to be confirmed. For this, a ^{3}H-heparin radioactivity-binding assay was performed. It was adapted from an assay originally published by Baird *et al.* where overlapping peptides derived from the primary structure of FGF-2 were synthesized and purified by solid-phase methodology, and gel permeation and ion exchange chromatography; they were then investigated as to their binding capacity for ^{3}H-heparin (Baird *et al*., 1988). Three peptides namely, FGF-2-HBD Baird(B) : Biotin-Ahx-YCKNGGFFLRIHPDGRVDGVREKSDPHIKL

QLQEERGVVSIKGV (Sequence ID No.1, Figure 2.1), FGF-2-HBD Cardin (C) - Biotin-Ahx-GSGAFPPGHFKDPKRLYCKNGGFFLRIHPDGRVD (Sequence ID No.2, Fig. 2.1) and FGF-2-HBD Gandhi (G): GHFKDPKRLYCKNGGF-Ahx-(K)Biotin (Sequence ID No.3, Fig. 2.1) were able to bind to ^{3}H-heparin in a concentration-dependent manner (Fig. 2.6). This suggested that these particular overlapping sequences of FGF-2, do indeed bind to heparin and were suitable for affinity chromatography. In addition, two other FGF-2-HBD peptides (Sequence ID Nos. 5 and 7, Fig. 2.1), were also able to bind to ^{3}H-heparin in a concentration-dependent manner (Fig. A1). These two peptides (Sequence ID Nos. 5 and 7, Fig. 2.1) however were not used for chromatography as they overlap the region that corresponds to the receptor-binding domain of FGF-2 (Plum *et al*., 2000), and would have been more likely to generate an artifact.

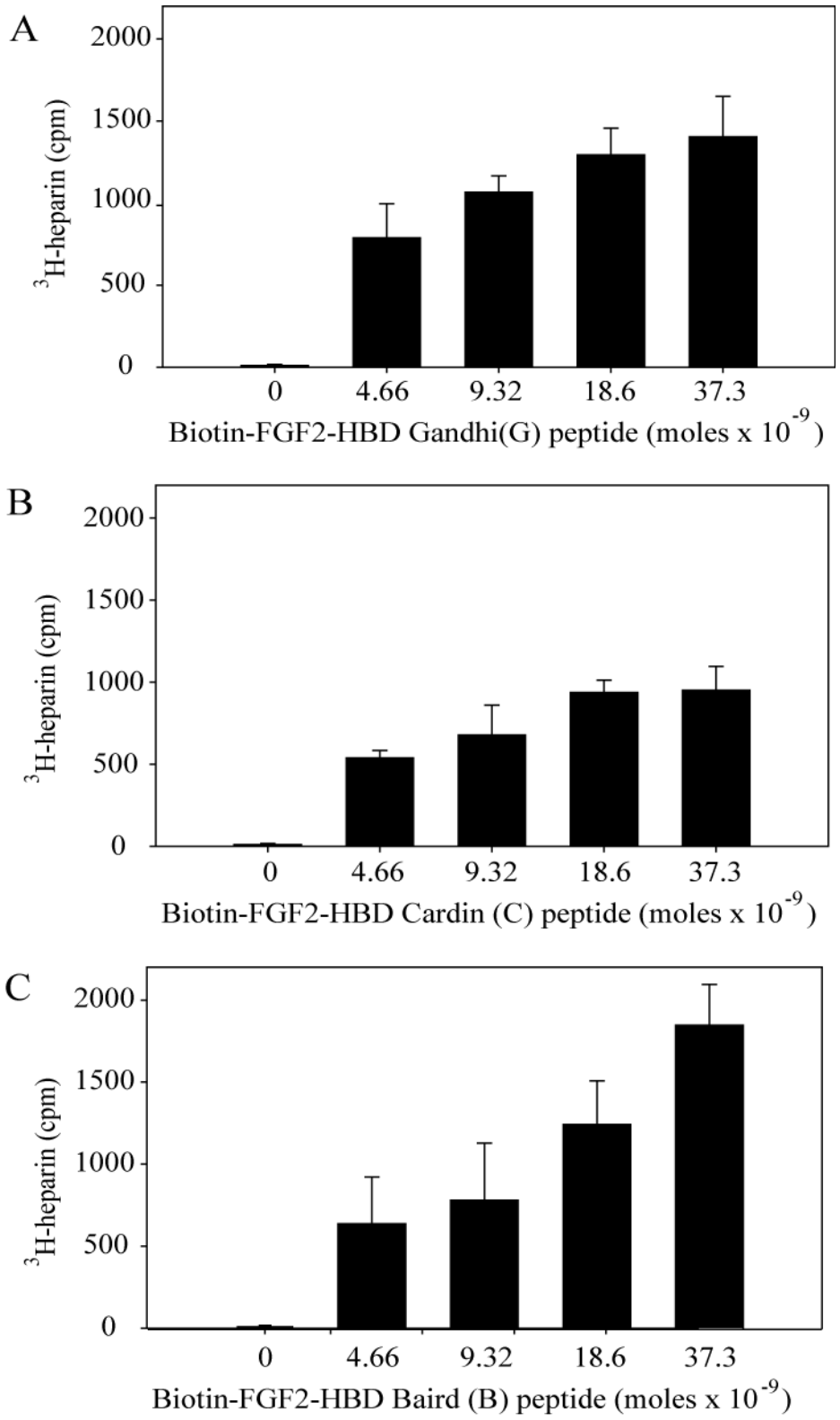

Figure 2.6. Binding of FGF-2-HBD to ^{3}H-heparin. FGF-2-HBD peptides (A) Gandhi-G, (B) Cardin-C and (C) Baird-B were spotted onto nitrocellulose membranes, air-dried and incubated with ^{3}H-heparin. Bound ^{3}H-heparin was determined by liquid scintillation as described.

2.3.2. GAG ELISA – FGF-2-HBD peptides

Further assessments of the synthesized FGF-2-HBD peptides, via their binding capacities for heparin, were conducted by GAG ELISA. The initial experiments were designed to optimize the concentrations of FGF-2-HBD peptides best suited to bind with coated (5 μg/ml) and immobilized heparin on GAG-binding 96-well plates following the manufacturer's recommendations (Iduron). Optimization was carried out with the FGF-2-HBD Gandhi (G) peptide in a range from 0 - 3200 nM in serial two-fold dilutions; from these experiments 0, 50, 100, and 200 nM concentrations were used for the rest of the study (Fig. 2.7).

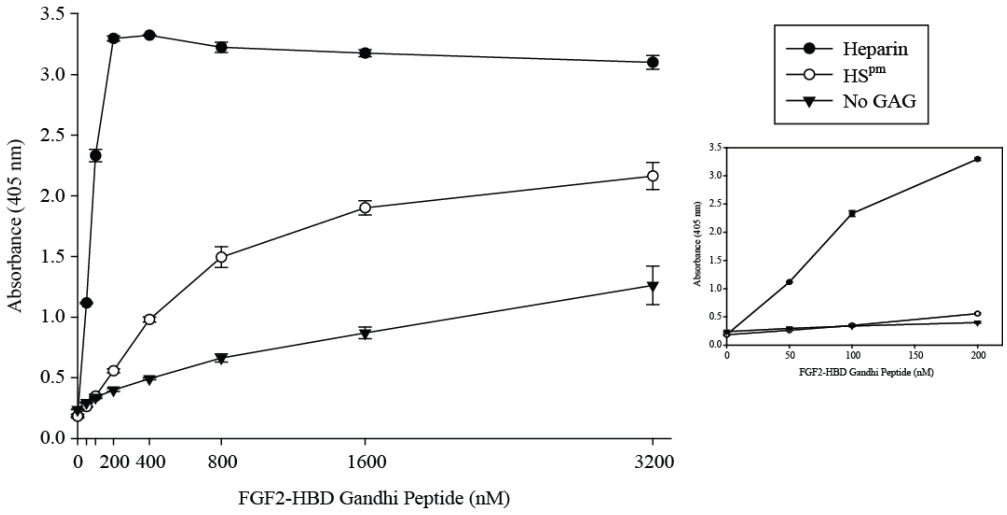

Figure 2.7. GAG ELISA – FGF-2 HBD peptide optimization. Optimization was carried out with the FGF-2-HBD Gandhi (G) peptide using a range from 0 - 3200 nM in serial two-fold dilutions. Thus 0, 50, 100, and 200 nM concentrations were used for the rest of the experiments.

After determining these optimal concentrations, a saturating heparin concentration (5 μg/ml) was coated overnight and the resulting surface investigated for its binding capacity for the different FGF-2-HBD peptides

(Fig. 2.8). The binding curves showed that, irrespective of FGF-2-HBD peptide, there was a dose-dependent increase in heparin binding with FGF-2-HBD Gandhi (G) clearly showing the highest capacity for the sugar. The lowest affinity for FGF-2 was shown by the FGF-2-HBD Baird (B) peptide, interestingly the longest peptide tested, whereas the FGF-2-HBD Cardin (C) peptide displayed an intermediate capacity for binding FGF-2. In addition, two other FGF-2-HBD peptides (Sequence ID Nos. 5 and 7, Fig. 2.1) were able to bind to heparin in a concentration-dependent manner, but were not subsequently used for chromatography, as previously explained (see Fig. A2). This further supported the results of the ^{3}H-heparin assay, and the combination of results enabled the narrowing down of the FGF-2-HBD peptides from the original ten (Fig. 2.1) to just three.

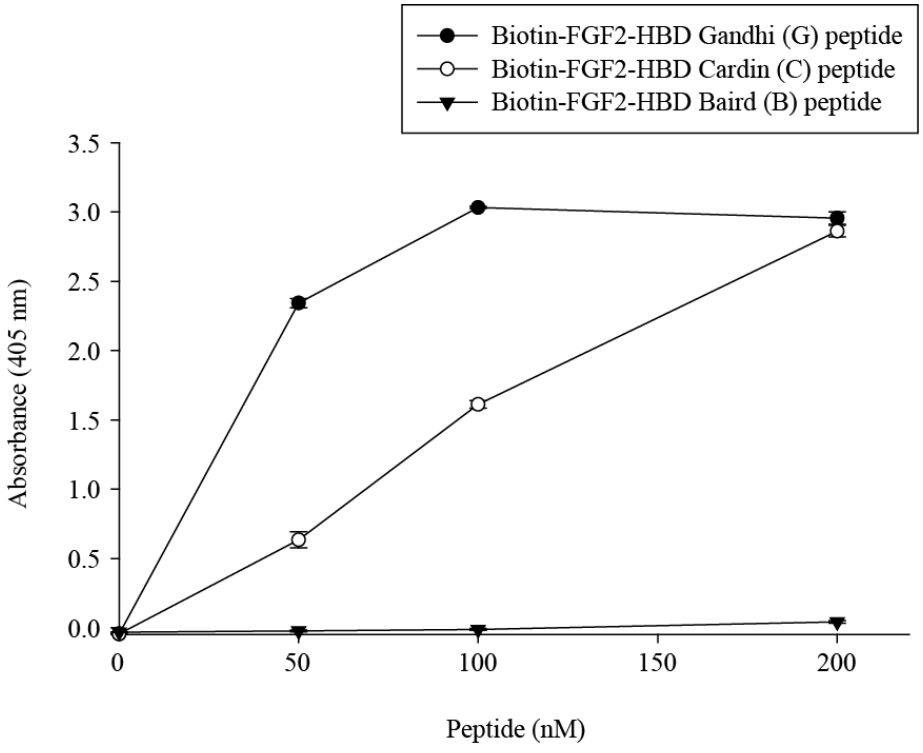

Figure 2.8. Binding capacities of FGF-2-HBDs for heparin. Heparin was immobilized onto the GAG-binding 96-well plates (Iduron) by electrostatic interaction, which did not affect their protein binding capabilities. The Gandhi-G, Cardin-C and Baird-B FGF-2-HBD peptides had their binding ability for immobilized heparin assessed by dint of their biotinylated portion yielding a colourimetric reaction.

Finally, the binding affinity of the three FGF-2-HBD peptides for HS^{pm}, the commercially available source of heparan sulfate (Celsus Laboratories, USA) was tested. It was necessary to confirm that these peptides were indeed able to bind to HS^{pm}, as they were to be used to harvest active HS fractions in the chromatographic steps. As shown in Figure 2.9, all three peptides gave rise to a dose-dependent increase in heparin binding. The binding affinities of these peptides for HS^{pm} were similar to the binding affinities to heparin, wherein FGF-2-HBD-Gandhi (G) > FGF-2-HBD-Cardin (C) > FGF-2-HBD-Baird (B). With these results a strong foundation was laid down for the isolation of higher affinity HS from crude HS^{pm}.

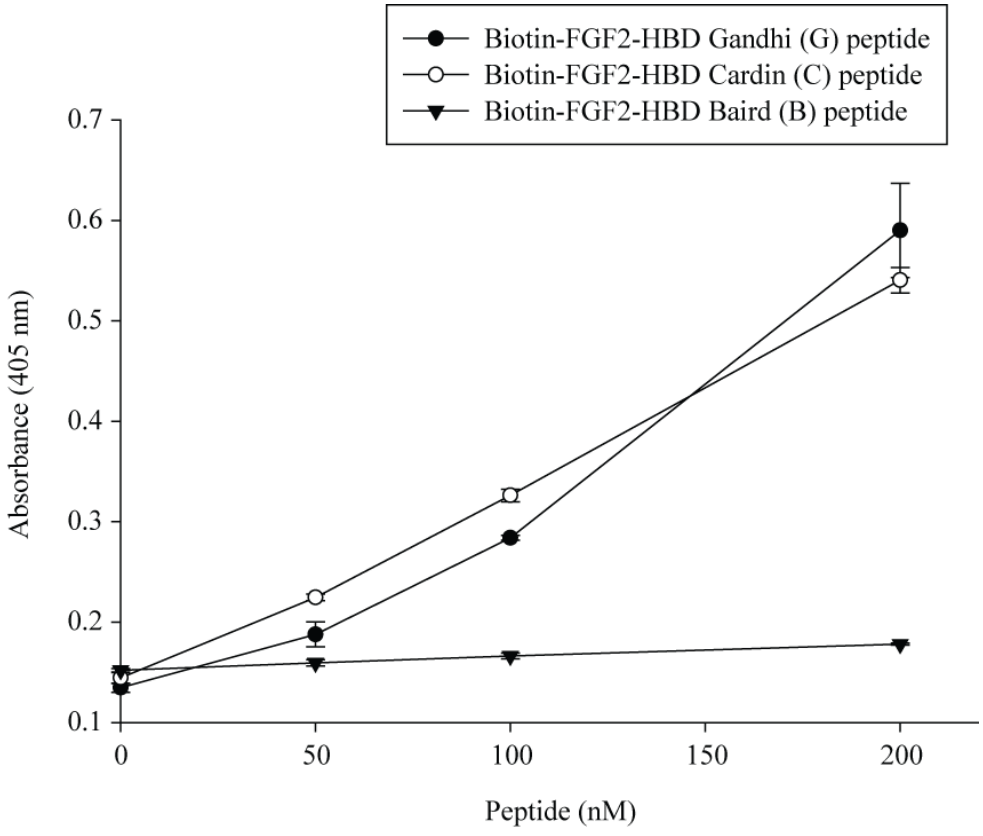

Figure 2.9. Binding ability of FGF-2-HBD to HS^{pm}. HS^{pm} was immobilized onto the GAG-binding 96-well plates (Iduron) by electrostatic interaction in such a way that its protein-binding capabilities were not affected. The binding capacity of FGF-2-HBD peptides Gandhi-G, Cardin-**C and Baird-B,** for immobilized heparin was assessed via the biotinylated portion of the FGF-2-HBD peptides, and yielded a measurable colourimetric reaction.

2.3.3. Affinity chromatography

2.3.3.1. Affinity chromatography – HS8G

As the peptides were able to bind both heparin and HS^{pm}, they were used to derivatise streptavidin columns for affinity chromatography. The FGF-2-HBD Gandhi (G) peptide was tested first. The column was saturated with biotin-peptide 1 ml each (1 mg/ml), up to 3 ml in total, until excess peptide (pink trace) was observed in the flow-through at 215 nm (Figs. 2.10 and 2.11). To check the binding affinity between the immobilized streptavidin and the biotinylated peptides, the column was challenged by washing with a 1.5 M high salt buffer (brown trace, Fig. 2.11). No peptide eluted off the column, indicating that the columns were saturated with strongly bound peptides that would not dissociate during the later elution of HS variants. The column was equilibrated with low salt buffer in readiness for loading of the commercially available HS^{pm} sugar.

Next the column was loaded with increasing amounts of HS^{pm} (2, 2.5 and 3 mg) in order to determine the optimum amount of HS^{pm} to be used (Figs. 2.12 and 2.13). The fractionated HS was dubbed HS8 (and was given the variant name HS8G). The HS that did not bind to the peptide (red trace) was designated as the $HS8G^{-ve}$ variant. Bound variants were eluted from the column using a one-step 1.5 M NaCl elution (brown trace), and collected as the $HS8G^{+ve}$ variant (red trace). The height of the $HS8G^{+ve}$ variant curve increased with increasing amount of HS^{pm} injected to the column, wherein 2.5 mg of HS^{pm} triggered a 240 mAU peak and 3 mg triggered a 245 mAU peak. Although the peak of $HS8G^{+ve}$ increased slightly from 2.5 mg to 3 mg of HS^{pm} injected, the $HS8G^{-ve}$ curve started to get broader, indicating that the

streptavidin column was saturating. In addition, this indicated that the unbound HS8G^{+ve} was present in the flow-through after 3 mg of HS^{pm} loading. Hence, 2.5 mg of HS^{pm} was selected to be injected for each cycle of HS8G isolation. After running for 160 separate cycles of HS8G variant isolation, the NaCl was removed by a desalting step using HiPrep 26/10 desalting columns (Fig. 2.14). From 400 mg of starting HS^{pm}, 36.2 mg (9.05 %) of HS8G^{+ve} and 173.3 mg (43.33 %) of HS8G^{-ve} were isolated; the rest of the weight was constituted by NaCl.

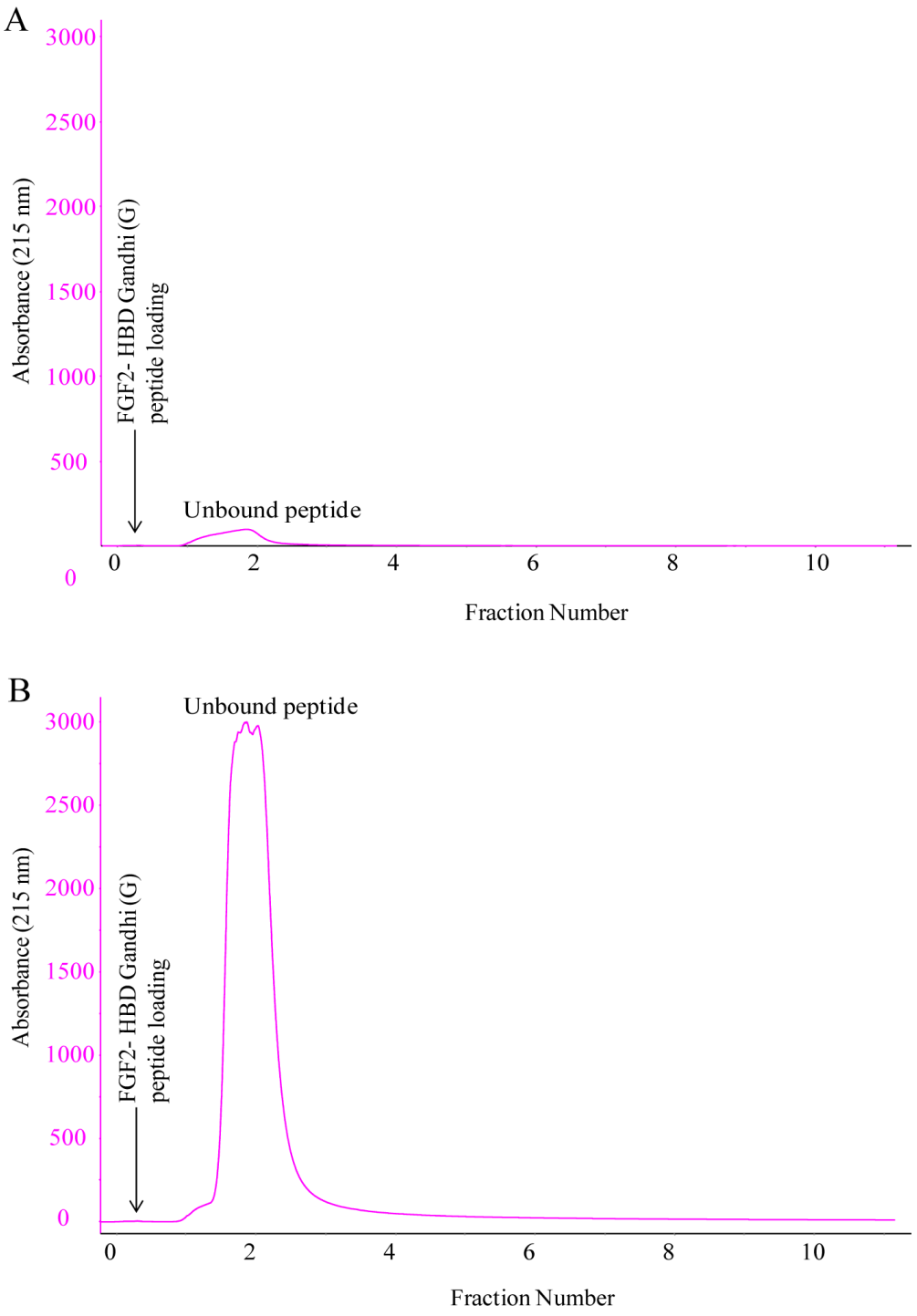

Figure 2.10. Biotinylated FGF-2-HBD Gandhi (G) peptide coupling. (A) A first 1 mg and (B) a second 1 mg of peptide were loaded into the streptavidin column and excess peptide flowing out of the column was monitored at 215 nm.

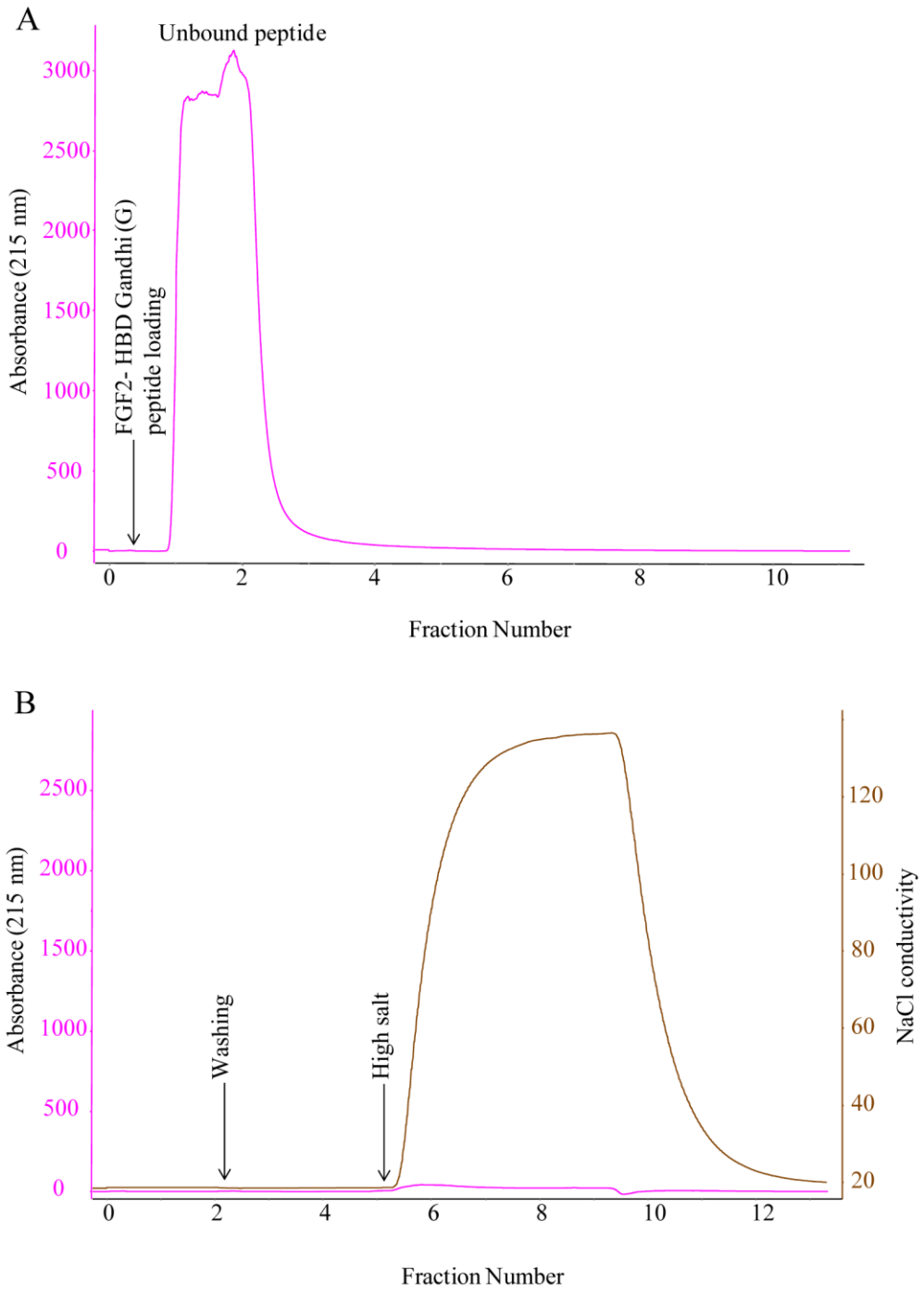

Figure 2.11. Biotinylated FGF-2-HBD Gandhi (G) peptide coupling and challenge with high salt buffer. (A) The third 1 mg of peptide was loaded into the streptavidin column and excess peptide that flowed out of the column was monitored at 215 nm. (B) Columns were washed with 1.5 M high salt buffer to ensure peptide is tightly bound to the column.

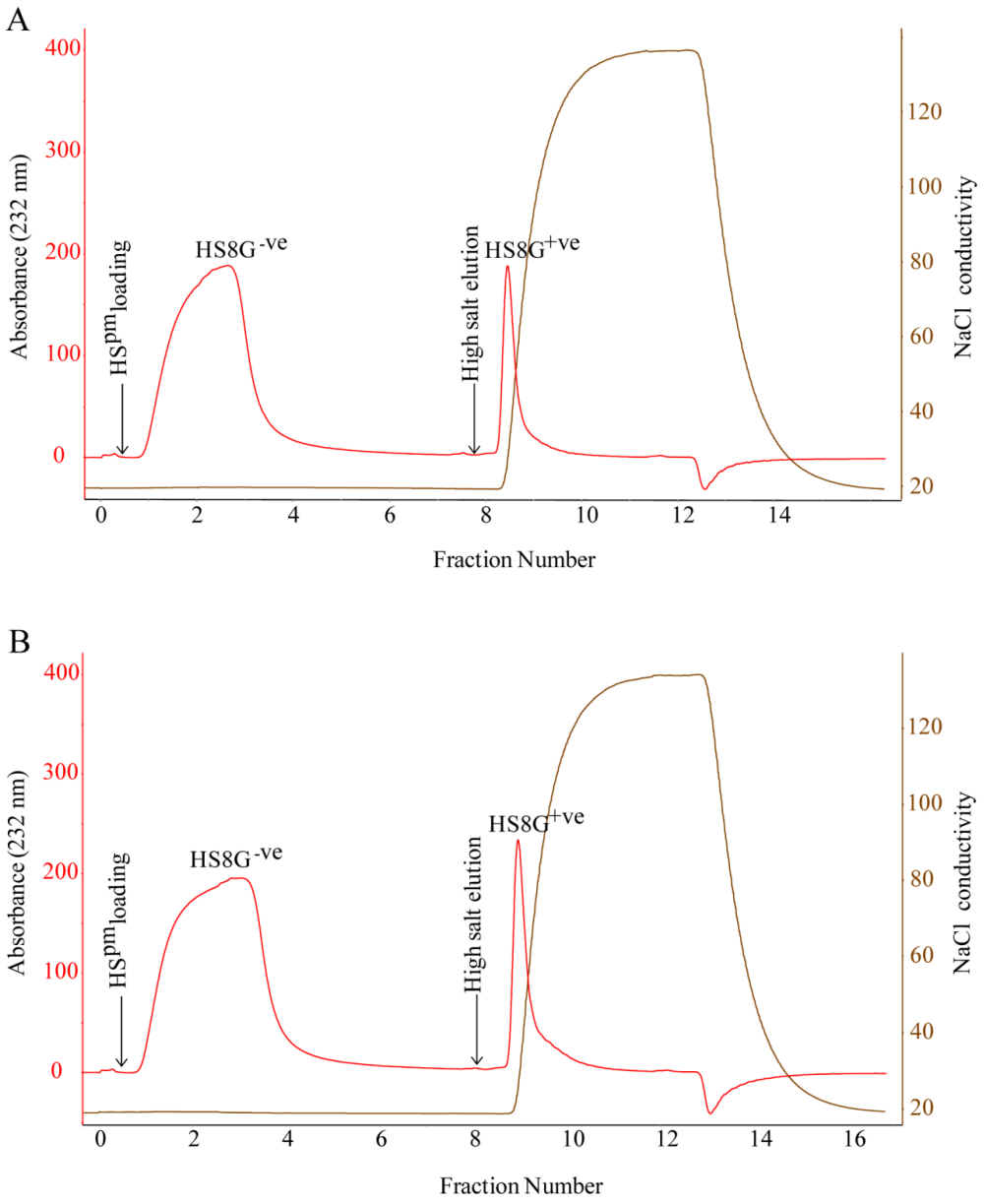

Figure 2.12. Chromatograms depicting HS8G^{+ve} isolation. HS8G^{+ve} variant was isolated from the starting (A) 2 mg and (B) 2.5 mg of HS^{pm} mixture using streptavidin column pre-bound with FGF-2-HBD Gandhi (G) peptide. A high salt wash (1.5 M) (brown trace) released the HS8G^{+ve} variant (red trace) and was collected.

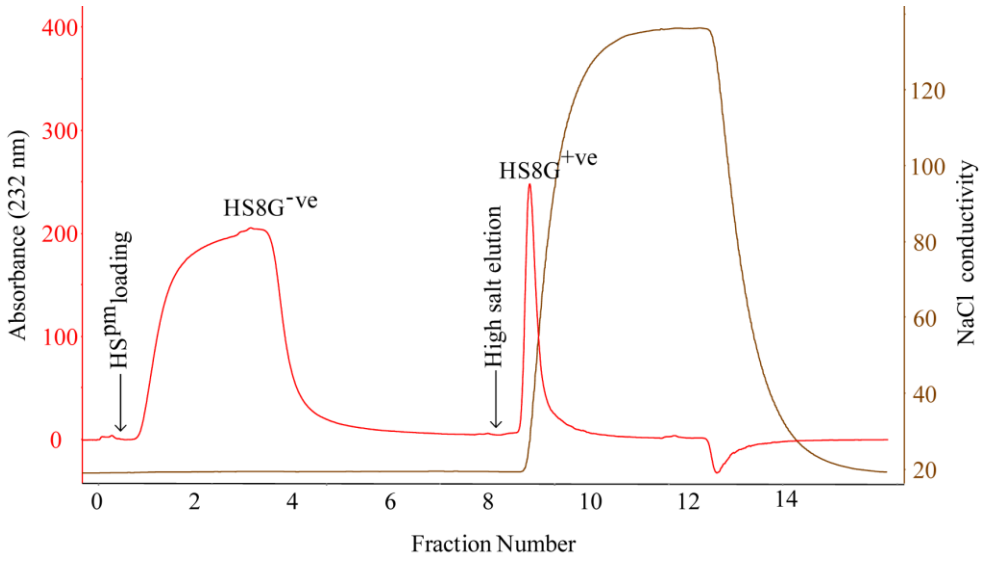

Figure 2.13. Chromatogram depicting HS8G^{+ve} isolation. HS8G^{+ve} variant was isolated from the starting 3mg of HS^{pm} mixture using streptavidin columns pre-bound with FGF-2-HBD Gandhi (G) peptide. A high salt wash (1.5 M) (brown trace) released the HS8G^{+ve} variant (red trace) and was collected.

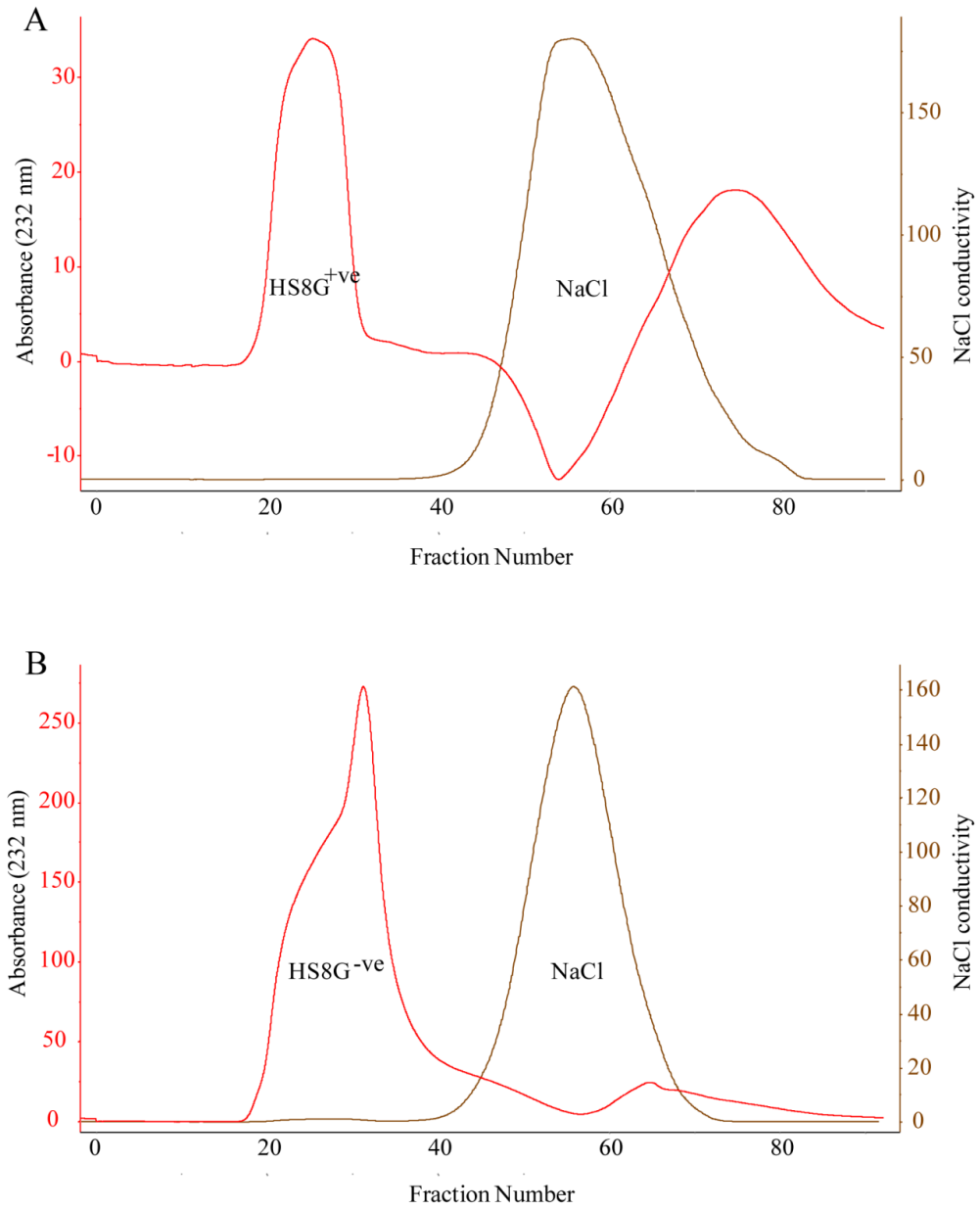

Figure 2.14. Elution profile of desalted HS8G variants. The high molecular weight HS eluted first, while NaCl eluted later. (A) Elution profile of HS8G^{+ve} variant (B) Elution profile of the HS8G^{-ve} variant.

2.3.3.2. Affinity chromatography – HS8C

Next, the FGF-2-HBD Cardin (C) peptide was used to isolate HS8 variants from the commercial HS^{pm} source; the isolated variant was dubbed HS8C. Similar to the isolation of HS8G, steptavidin columns were first saturated with biotin-peptide 1 ml each (1 mg/ml), up to 3 ml, in total until excess peptide (pink trace) was observed in the flow-through at 215 nm; the column was challenged with 1.5 M high salt buffer (brown trace) and it was confirmed that the peptide was strongly bound to the column (Figs. 2.15 and 2.16). Then the column was loaded with increasing amounts of HS^{pm} (2, 2.5 and 3 mg). For the $HS8C^{+ve}$ curves, 2.5 mg of HS^{pm} yielded a 160 mAU peak, and with 3 mg HS^{pm}, a 165 mAU peak was observed (Figs. 2.17 and 2.18). As above with HS8G, 2.5 mg of HS^{pm} was selected as the optimum amount to be injected for each cycle of HS8C isolation. After 40 cycles of isolation, a desalting step (Fig. 2.19) was carried out to separate HS8C variants from NaCl. A yield of 5.06 mg (5.06 %) of $HS8C^{+ve}$ and 67 mg (67 %) of $HS8C^{-ve}$ were isolated from 100 mg of starting HS^{pm}.

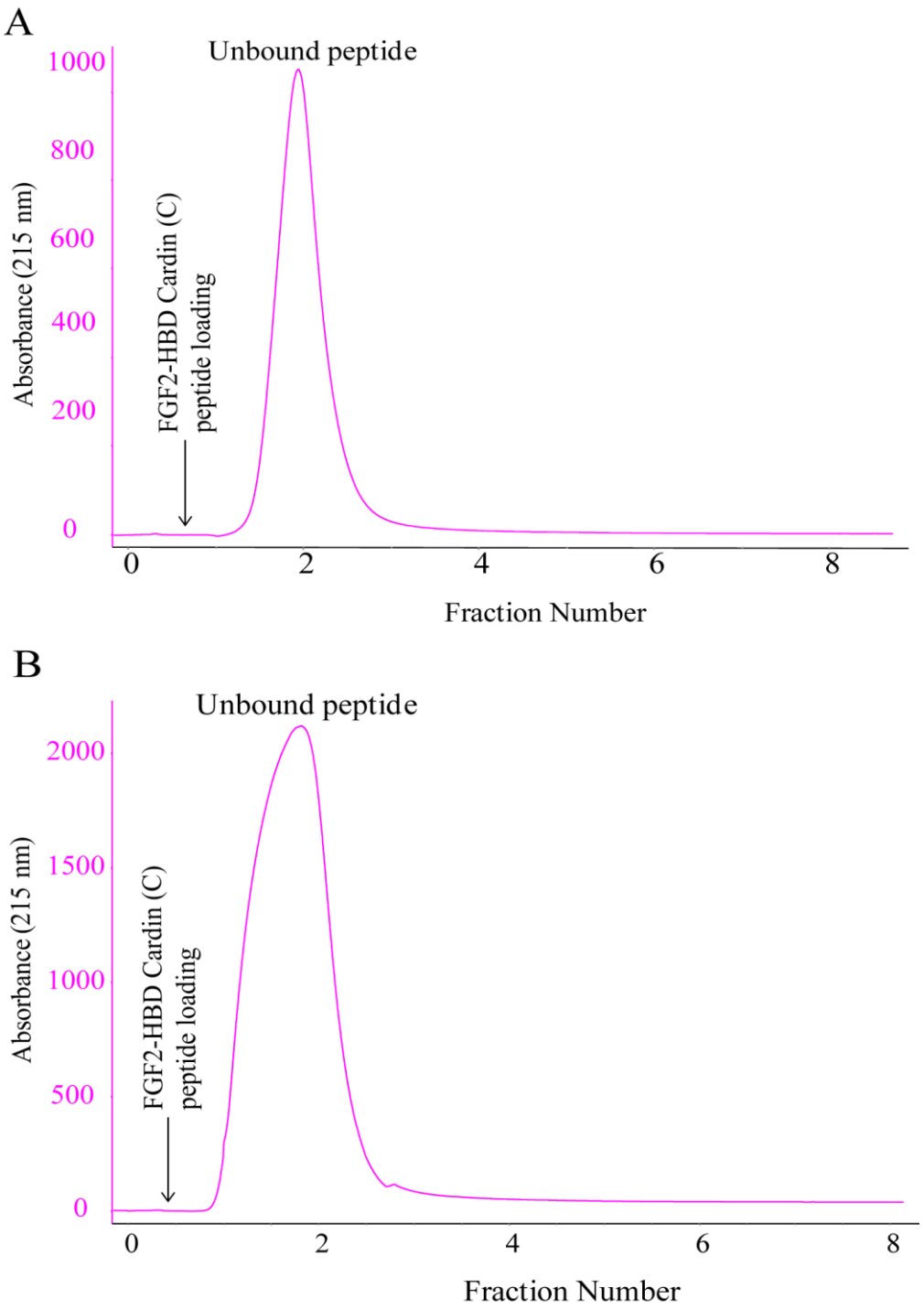

Figure 2.15. Biotinylated FGF-2-HBD Cardin (C) peptide coupling. (A) A first 1 mg and (B) a second 1 mg of peptide were loaded into the streptavidin column and excess peptide that flowed out of the column was monitored at 215 nm.

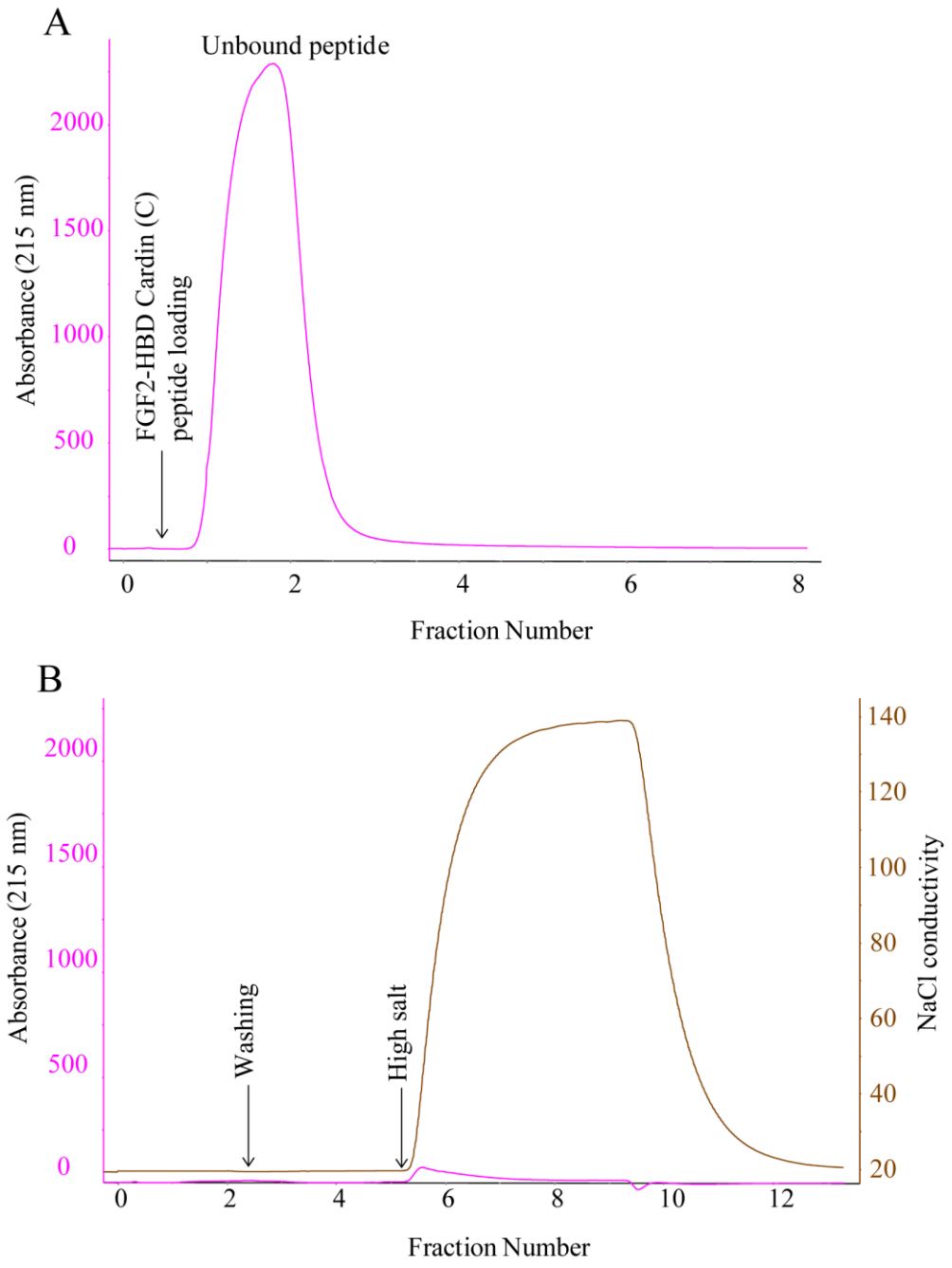

Figure 2.16. Biotinylated FGF-2-HBD Cardin (C) peptide coupling and challenge with high salt buffer. (A) A third 1 mg of peptide was loaded into the streptavidin column and excess peptide that flowed out of the column was monitored at 215 nm. (B) The column was washed with 1.5 M high salt buffer to ensure peptide was tightly bound to the column.

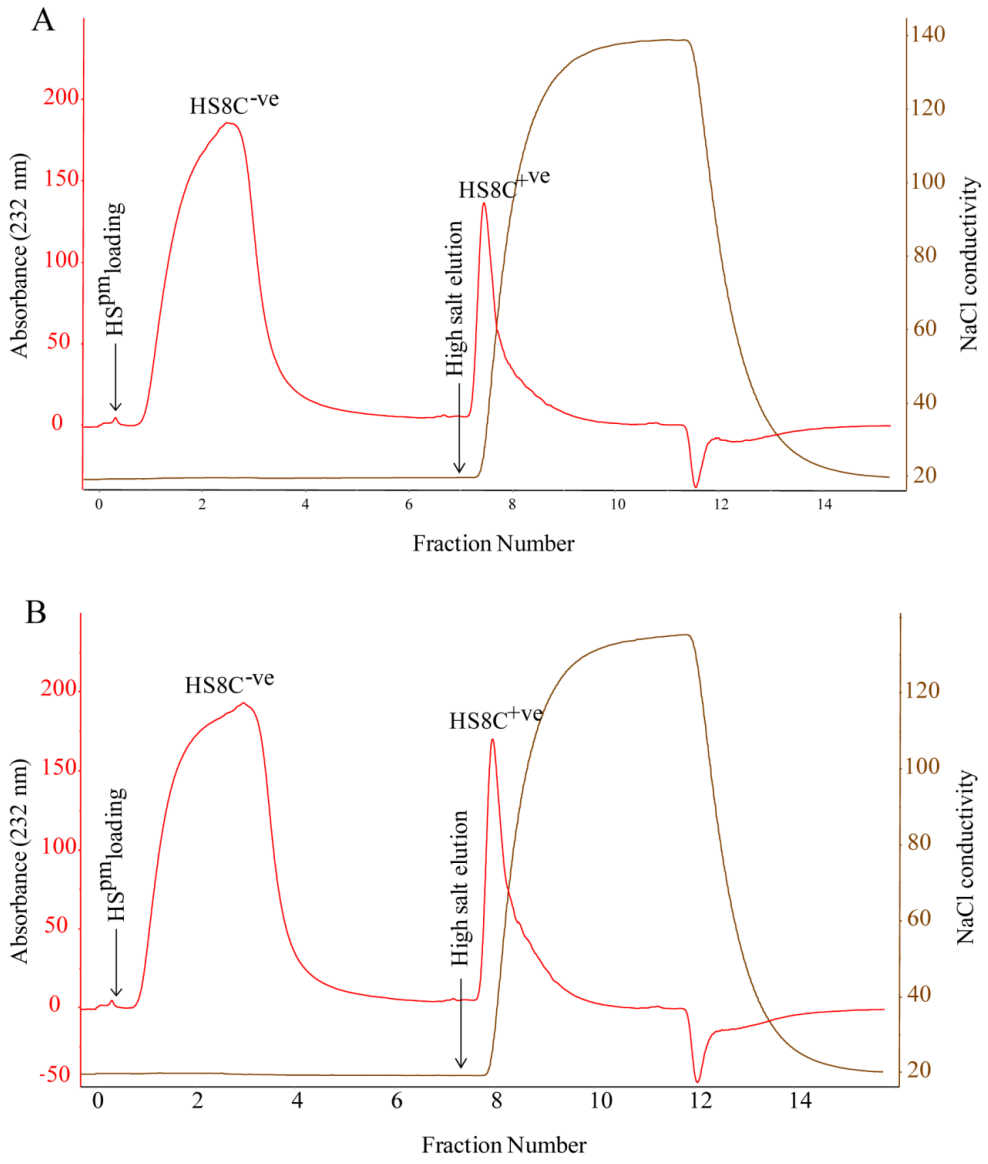

Figure 2.17. Chromatograms depicting HS8C^{+ve} isolation. The HS8C^{+ve} variant was isolated from the starting (A) 2 mg and (B) 2.5 mg of HS^{pm} mixture using streptavidin column pre-bound with FGF-2-HBD Cardin (C) peptide. A high salt wash (1.5 M) (brown trace) released the HS8C^{+ve} variant (red trace) and was collected.

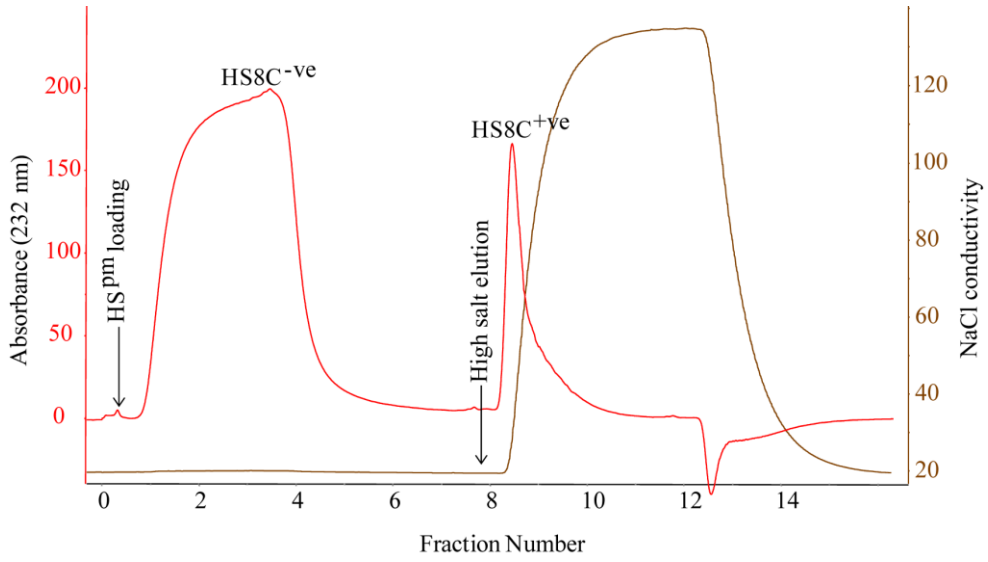

Figure 2.18. Chromatogram depicting HS8C^{+ve} isolation. HS8C^{+ve} variant was isolated from the starting 3 mg of HS^{pm} mixture using streptavidin column pre-bound with FGF-2-HBD Cardin (C) peptide. A high salt wash (1.5 M) (brown trace) released the HS8C^{+ve} variant (red trace) and was collected.

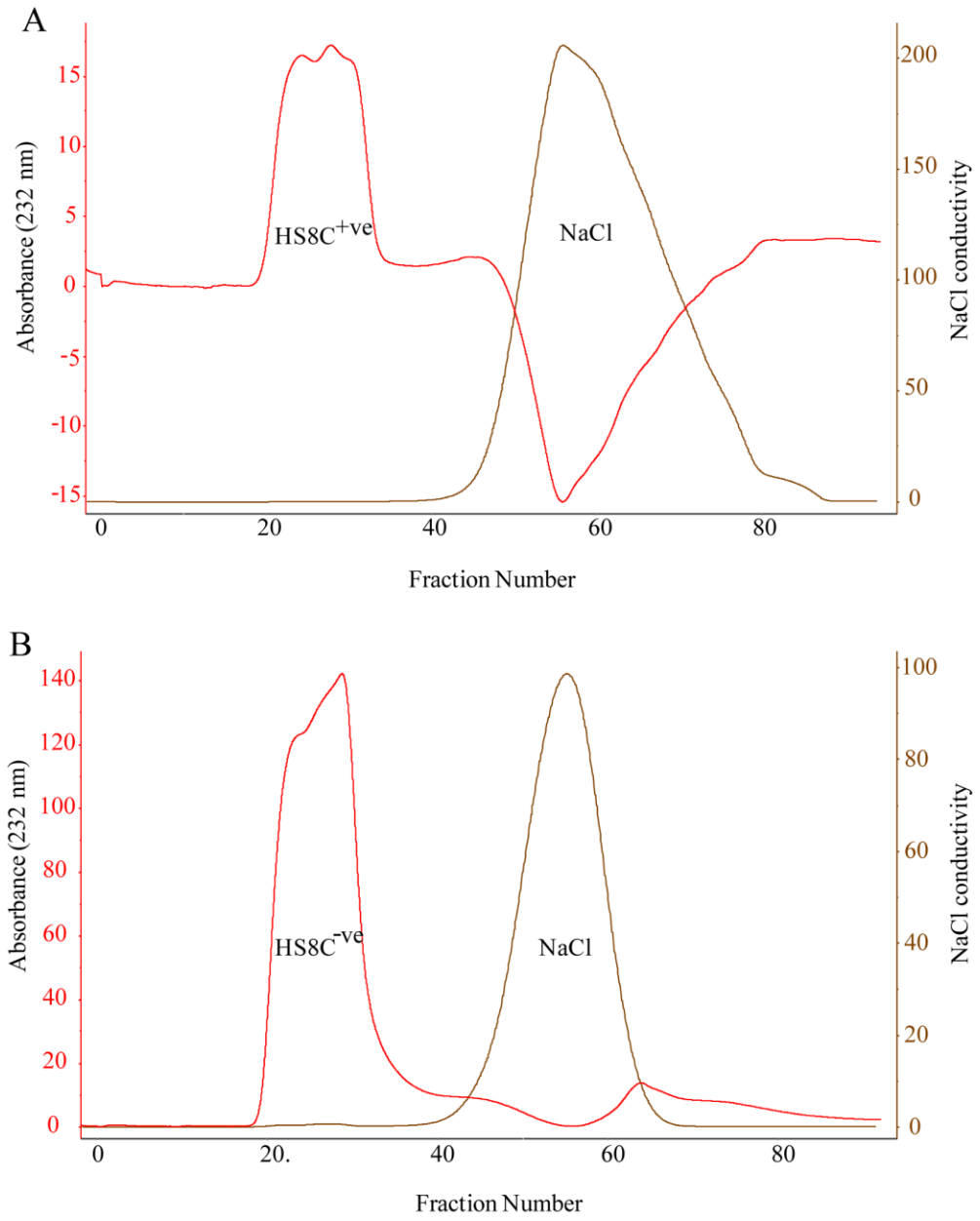

Figure 2.19. Elution profile of desalted HS8C variants. The high molecular weight HS eluted first, while the NaCl eluted later. (A) Elution profile of the HS8C^{+ve} variant (B) Elution profile of the HS8C^{-ve} variant.

2.3.3.3. Affinity chromatography – HS8B

The FGF-2-HBD Baird (B) peptide was used to isolate HS8 variants from the HS^{pm} mixture and the isolated variant was dubbed HS8B. Similar to the isolation of HS8G, the steptavidin column was first saturated with biotin-peptide 1 ml each (1 mg/ml) up to 3 ml in total until excess peptide (pink trace) was observed in the flow-through at 215 nm, whereafter the column with the peptide bound was challenged with 1.5 M high salt buffer (brown trace) (Figs. 2.20 and 2.21). No peptide was eluted off the column, confirming the strong interaction of biotinylated peptide with the streptavidin column. The column was equilibrated with low salt buffer then loaded with increasing amounts of HS^{pm} (2, 2.5 and 3 mg) while observing the peak height of the $HS8B^{+ve}$ curve. A peak of 70 mAU arose from 2.5 mg of HS^{pm} loaded and a peak of 65 mAU with 3 mg HS^{pm} (Figs. 2.22 and 2.23). As above with HS8G, 2.5 mg of HS^{pm} was selected as the optimum amount to be injected for each cycle of HS8B isolation. After 40 cycles of HS8B isolation and a desalting step (Fig. 2.24), 100 mg of starting HS^{pm} yielded 2.24 mg (2.2.4%) of $HS8B^{+ve}$ and 68 mg (68 %) of $HS8B^{-ve}$.

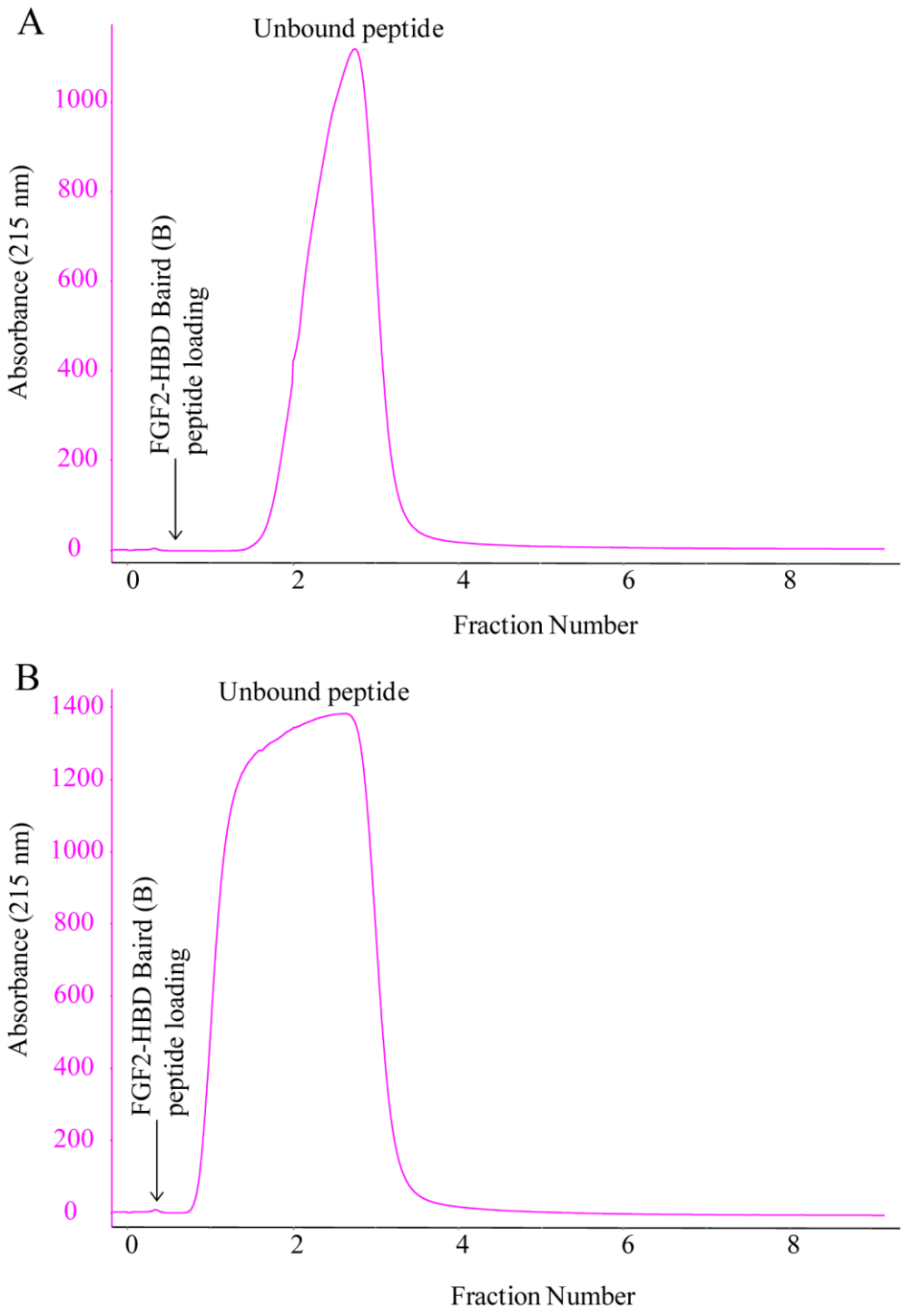

Figure 2.20. Biotinylated FGF-2-HBD Baird (B) peptide coupling. (A) A first 1 mg and (B) a second 1 mg of peptide were loaded into the streptavidin column and excess peptide that flowed out of the column was monitored at 215 nm.

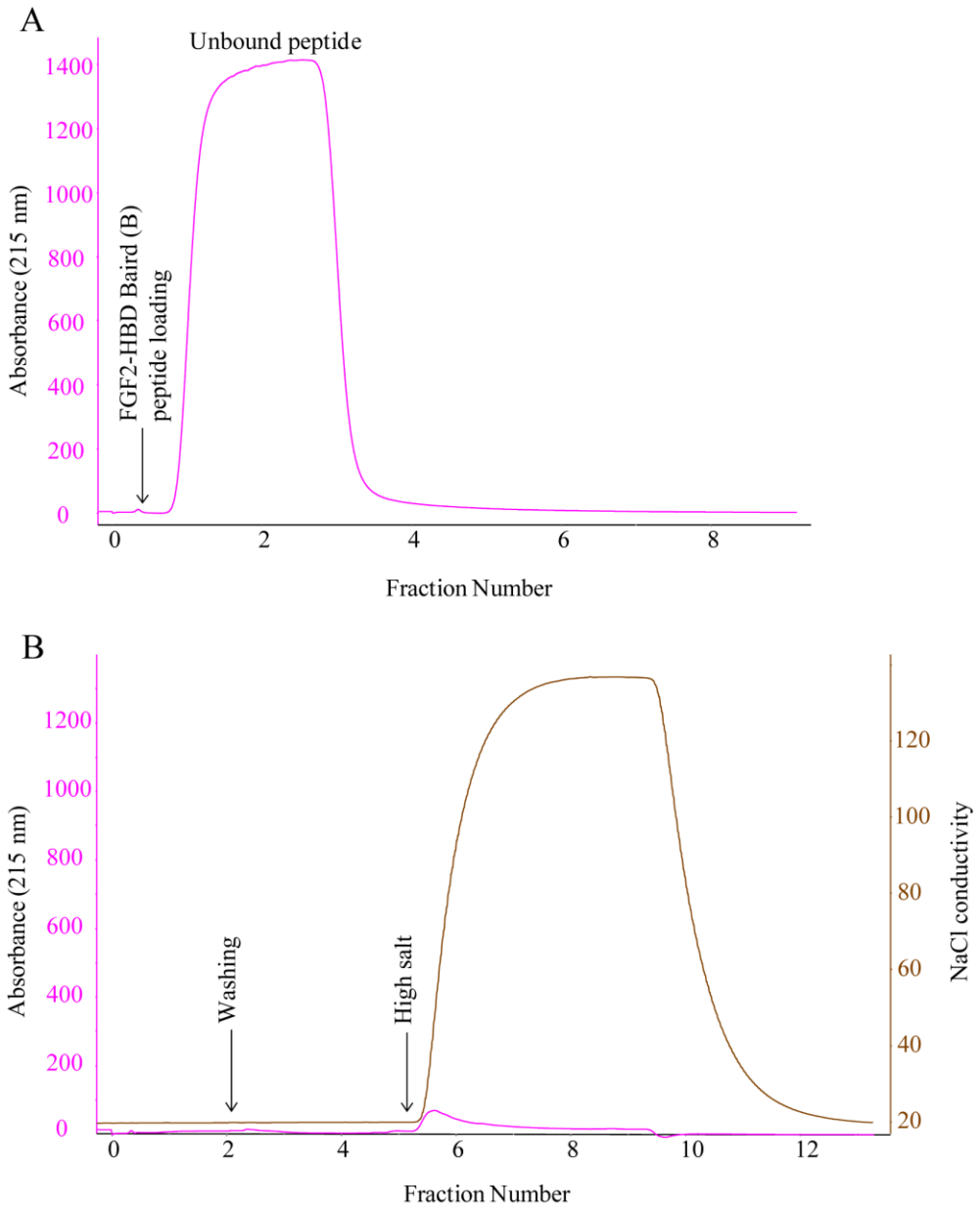

Figure 2.21. Biotinylated FGF-2-HBD Baird (B) peptide coupling and challenge with high salt buffer. (A) A third 1 mg of peptide was loaded into the streptavidin column and excess peptide that flowed out of the column was monitored at 215 nm. (B) The column was washed with 1.5 M high salt buffer to ensure peptide was tightly bound to the column.

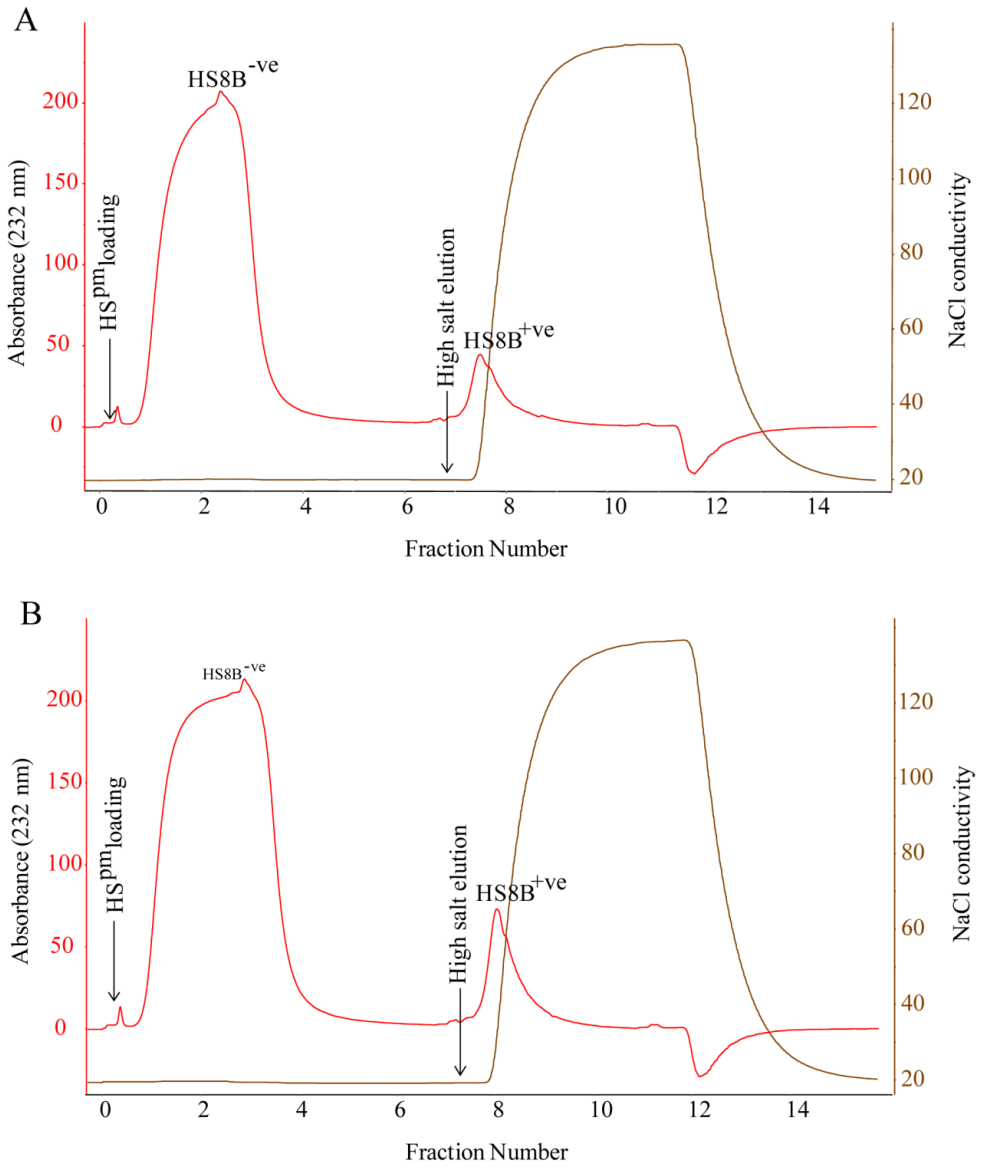

Figure 2.22. Chromatograms depicting HS8B+ve isolation. The HS8B^{+ve} variant was isolated from the starting (A) 2 mg and (B) 2.5 mg of HS^{pm} mixture using streptavidin column pre-bound with FGF-2-HBD Baird (B) peptide. A high salt wash (1.5 M) (brown trace) released the HS8B^{+ve} variant (red trace) and was collected.

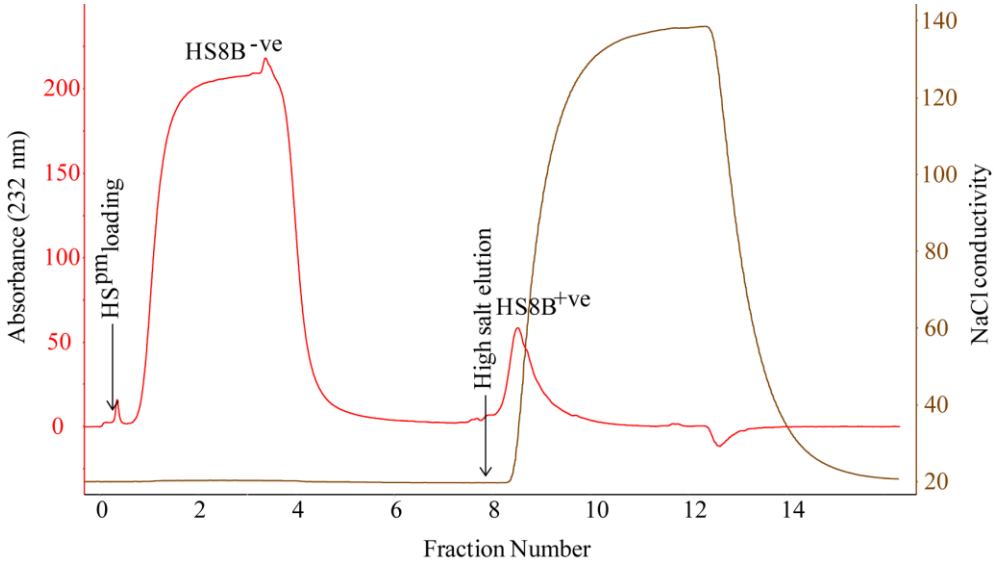

Figure 2.23. Chromatogram depicting HS8B^{+ve} isolation. HS8B^{+ve} variant was isolated from the starting 3 mg of HS^{pm} mixture using streptavidin columns pre-bound with FGF-2-HBD Baird (B) peptide. A high salt wash (1.5 M) (brown trace) released the HS8B^{+ve} variant (red trace) and was collected.

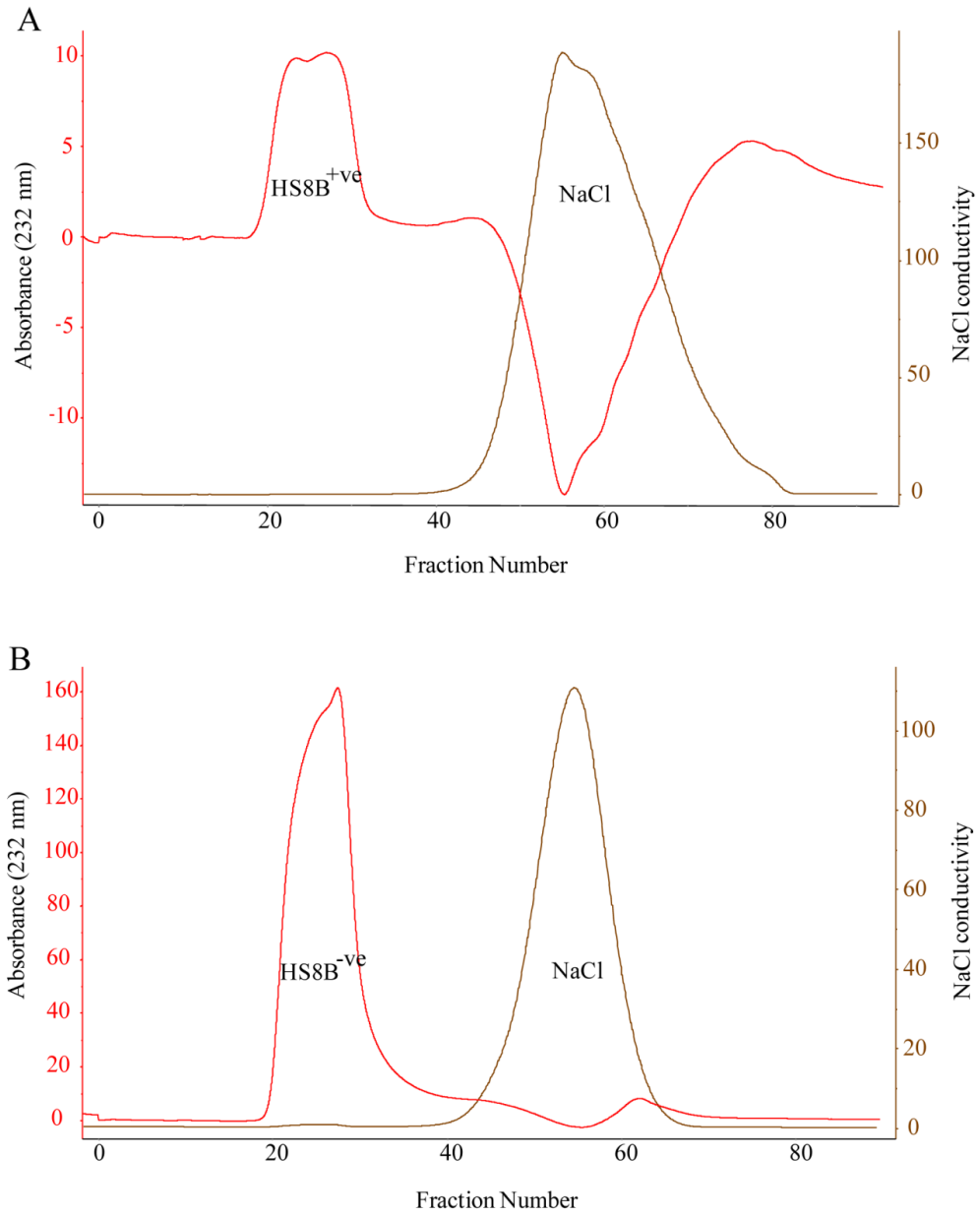

Figure 2.24. Elution profile of desalted HS8B variants. The high molecular weight HS eluted first, while NaCl eluted after. (A) Elution profile of HS8B^{+ve} variant (B) Elution profile of the HS8B^{-ve} variant.

2.4. Discussion

In the past, affinity separated heparin variants have been isolated not using peptides, but rather using native protein. For example, Barzu *et al.* used oligosaccharides generated from nitrous acid depolymerisation of standard heparin and separated them by affinity chromatography on Sepharose-immobilised FGF1 (Bârzu *et al*., 1989). Furthermore, Brickman *et al.* used FGF-2-coupled Sepharose packed into small columns to isolate HS chains with high affinity for FGF-2 (Brickman *et al*., 1995). Moreover, heparin variants of high affinity for fibronectin (Falcone and Salisbury, 1988), heparin co-factor II (Kim and Linhardt, 1989; Sinniger *et al*., 1993) and anti-thrombin III (Höök *et al*., 1976; Scully *et al*., 1988; Sinniger *et al*., 1993) have been isolated using native proteins as the bait in affinity chromatography approaches. Although promising results were noted, usage of full length proteins is prohibitively costly and such columns cannot be re-used. McCaffrey *et al*. demonstrated the heparin-binding capacity of transforming growth factor-βl (TGF-βl) using synthetic peptides derived from various regions of TGF-βl, and isolated two sugar variants (with high and low TGF-β1 binding affinity) from heparin mixtures (McCaffrey *et al*., 1992). However, a major problem is that heparin was used as the starting material, which is clearly not suitable for clinical applications because of its inherent anticoagulant activity and capacity for non-specific binding.

The isolation of HS described here consisted of several steps, including affinity chromatography. The first involved the identification of suitable FGF-2-HBD peptides from the candidates already described in the available literature for the derivatisation of affinity columns. Next, the candidate HBD

peptides were engineered in such a way that a hydrophobic spacer was attached, so that biotinylation at both N-terminal or C-terminal was possible. Prior to the exploitation of these peptides in the affinity column, their FGF-2 binding capabilities were confirmed by means of ^{3}H-heparin and GAG ELISA association assays. Thereafter, the solid phase affinity chromatography platform was constructed, wherein streptavidin columns saturated with the FGF-2-HBD biotinylated peptides, rather than full length proteins as earlier described, (Bârzu *et al*., 1989; Brickman *et al*., 1995) were exposed to raw HS preparations. In comparison to McCaffrey *et al.*, commercially available porcine intestinal mucosal HS was used instead of heparin to start the fractionation, an affinity method sufficiently novel to allow patenting (#2009292236) (McCaffrey *et al*., 1992; Murali *et al*., 2013). Using such approaches and techniques, our Glycotherapeutics group has built up a library of patent-protected heparan sulfates targeted to a variety of clinically relevant growth factors. Thus the platform resembles a relatively straightforward method of sugar ligand "fishing", as described in the literature review (Fig. 1.1). Here the FGF-2-HBD peptide was the "bait", and proved able to pull down the "prey", an HS sugar subfraction thereafter dubbed HS8^{+ve}. Incorporation of the linker Ahx in the peptide design helped its free movement and better allowed it to engage susceptible, complementary sugar chains (Fig. 2.2 and 1.1) from the mixture of HS^{pm} starting material. In addition, the biotin's strong interaction with streptavidin maintained peptide fidelity, and the same column could be used for more than 40 extraction cycles without loss of selective capacity (Figs. 2.2 and 1.1). As described by our collaborators at GlycoSyn, (now the Ferrier Institute, Victoria University of Wellington, New

Zealand), in referring to a similar scale-up process of for the BMP-2 binding HS variant dubbed HS3 (Murali *et al*., 2013), 20 ml column lifetimes can be most accurately evaluated through affinity chromatography performance following one month storage (in 20 % aqueous ethanol with 20 mM phosphate buffer at 4 °C) of the affinity column. They have shown that under otherwise identical conditions, the peak area of the retained HS is > 90 % of that seen in a fresh column. Here, the 1 ml streptavidin derivatised columns were used within 2-3 days of synthesis for the pull-down assays.

In addition, as indicated by the analysis of the pooled HS3 sample, our collaborators were able to determine the sodium chloride levels, not previously possible due to insufficient material. The desalting was almost to purity, albeit not 100% efficient using the HiPrep column. The HiPrep 26/10 column packed with Sephadex G-25 Fine does a group separation of a sample into high molecular weight substances, which are excluded from the gel and thus elute first, from low molecular weight substances that enter the pores freely and thus elute later (Amersham Biosciences). As per the manufacturer's advice, the HiPrep 26/10 column can separate proteins/peptides larger than 5000 g/mol from molecules with a molecular weight less than 1000 g/mol. The molecular weight of the eluting NaCl is 58.44 g/mol and the linear, sulfated glycosaminoglycans have both real and apparent molecular masses that typically range from 10 to 100 kDa (Gandhi and Mancera, 2008). Thus the HiPrep 26/10 was an appropriate medium with which to gently separate NaCl from the HS. Subsequent findings by our collaborators, and the difficulties of salt contamination of final product, could theoretically be solved by one of two means. A second pass through the desalting column would be

the simplest, if least elegant solution, albeit some loss of sugar, due to its extraordinarily high charge density, could be anticipated. Alternatively, dialysis could be employed along with in-process (conductivity) testing to confirm salt removal. The latter would allow partial concentration of the HS8 solution prior to freeze-drying which would have the advantage of yielding smaller, more manageable volumes from which the HS8 product is isolated. All-in-all, although complete salt removal is difficult, and has always been through the history of heparin/HS preparation, the use of repeated desalting on such columns as the HiPrep 26/10, or via dialysis, could overcome these problems without compromising specific activity.

This chapter describes how ten initial custom-made FGF-2-HBD peptides were narrowed down to just three candidates by filtering them through ^{3}H-heparin and GAG ELISA assays. These were then used in affinity chromatography to three HS8 variants: HS8G, HS8C and HS8B. The next aim was to select the best of these HS8 variants to be developed further. For that reason the yield of each variant after affinity chromatography was carefully checked. As shown in the Table 2.2, the isolation of $HS8G^{+ve}$ yielded the highest yield extraction percentage (9.05 %) of the $HS8^{+ve}$ eluates. In comparison, $HS8B^{+ve}$ isolation yielded the lowest percentage extraction (2.24 %) from the starting HS^{pm} mixture (while HS8C was intermediate at 5.06 %). The yields corresponded to the $HS8^{+ve}$ peak heights, where $HS8B^{+ve}$ had the lowest, and HS8C height was middling at 160 mAU. Interestingly, there was a relationship between the binding efficiencies of peptides for heparin and HS^{pm} in the GAG ELISA assay, and the final yield (Figs. 2.7 and 2.8 and Table 2.1). FGF-2-HBD Gandhi (G) had the highest binding efficiency, and consequently

the highest yield: ~ 9 %. FGF-2-HBD Baird (B) had the weakest binding and the least yield (~ 2 %). The intermediate level of $HS8C^{+ve}$ yield also correlated to the peptide binding performance towards heparin and HS^{pm}. This constitutes a remarkable consistency, presaging the intrinsic reliability of the method. In addition, another relationship was observed between the length of the synthesized peptide and the yield. $HS8G^{+ve}$ had the highest yield, but with the least length of the FF-HBD peptide; in contrast, $HS8B^{+ve}$, with the lowest yield, was the longest FGF-2-HBD peptide. Finally, it can be noted that the $HS8G^{+ve}$ yield (~ 9 %) was comparable to other HS variants with affinity directed towards other growth factor proteins isolated (often ~ 10-12 %) by our laboratory.

Table 2.1. $HS8^{+ve}$ variant elution curve heights and extracted percentages

	$HS8^{+ve}$ elution curve height with 2.5 mg of HS^{pm} loading (mAU)	Percentage extracted from Starting HS^{pm} mixture
$HS8G^{+ve}$	240	9.05
$HS8C^{+ve}$	160	5.06
$HS8B^{+ve}$	70	2.24

2.5. Summary

This chapter serves to establish a reliable means of reproducibly synthesising an HS variant with relative affinity for FGF-2. Once synthesized, the peptide could be stored in a -20 °C freezer until required for affinity chromatography. Despite this precaution, observations made during bulk HS3 synthesis have noted degradation of at least one peptide from a purity of 88.86 % to 71.37 % after storage for 5 months. A contributing factor to this degradation may be high levels of residual TFA, present as a result of HPLC purification. Given this information I instituted a process where the peptide was prepared “on demand” and not held in storage for any significant amount of time. Scale-up of affinity chromatography was attempted based on equal linear velocity of solvent through the packed bed. However due to the low pressure rating of the polypropylene columns, a reduced flow rate (50 % of the scale-equivalent rate) was mandatory. Thus scale-up must be monitored carefully, and should take into account the maximal gel bed volume.

Nevertheless, these data indicate that HS8G isolation was the most rewarding, particularly in respect of % yield. The next aim was to examine the biological activities of each of the HS8 variants separately before to be able to come to a final conclusion. Thus the next chapter explores each isolated HS8 variant’s FGF-2-binding ability via GAG ELISA and as well as the effects on hMSC proliferation.

CHAPTER 3: CHARACTERIZATION OF THE HS8 VARIANTS

3.1 Introduction

The previous chapter described a method to create a scalable means for isolating HS variants with increased binding affinity for FGF-2. In this chapter, a range of biochemical assays are described that were employed to determine the relationship between HS affinity for FGF-2 and subsequent bioactivity.

It was first important to determine which one of the 3 $HS8^{+ve}$ variants ($HS8G^{+ve}$, $HS8C^{+ve}$ and $HS8B^{+ve}$), isolated by affinity chromatography, could drive best the actions attributable to FGF-2. This was done by a combination of GAG ELISA binding assays and hMSC short-term proliferation assays. In particular, the binding assays were conducted to confirm the ability of this purified $HS8^{+ve}$ to bind FGF-2, compared to the non-binding $HS8^{-ve}$ and starting HS^{pm} material. Two different hMSC preparations were used: those selected through plastic-adherence and those selected by virtue of their STRO-1 expression. Additional binding assays, together with the assessment of unwanted anti-coagulant properties, the disaccharide composition and as well as differential scanning fluorimetry were also performed. Thereafter any synergistic effect of HS8 on FGF-2 was monitored by means of proliferation assays and cell signaling studies. Finally, the means by which the HS8 variants mediated the action of FGF-2 were studied by the blocking of FGF signaling with specific antibodies. The results of the studies allowed the selection of the most active of the 3 variants for further study.

3.2 Material and Methods

3.2.1. GAG ELISA

To first investigate the binding affinities of each HS variant (heparin control, HS^{pm}, $HS8^{+ve}$ and $HS8^{-ve}$) for FGF-2, and other heparin-binding domain proteins, GAG ELISA was performed. This assay has been well described by our laboratory for other HS isolates (Bramono *et al*., 2012; Murali *et al*., 2011; Murali *et al*., 2013; Wang *et al*., 2014). HS variants were immobilized onto specifically prepared glycosaminoglycan-binding 96-well plates (Iduron) by electrostatic interaction in a way that does not substantially affect their protein-binding capabilities. Binding abilities were assessed by sandwich antibodies, which yield a colourimetric reaction as per the manufacturer's guidelines (Fig. 3.1)

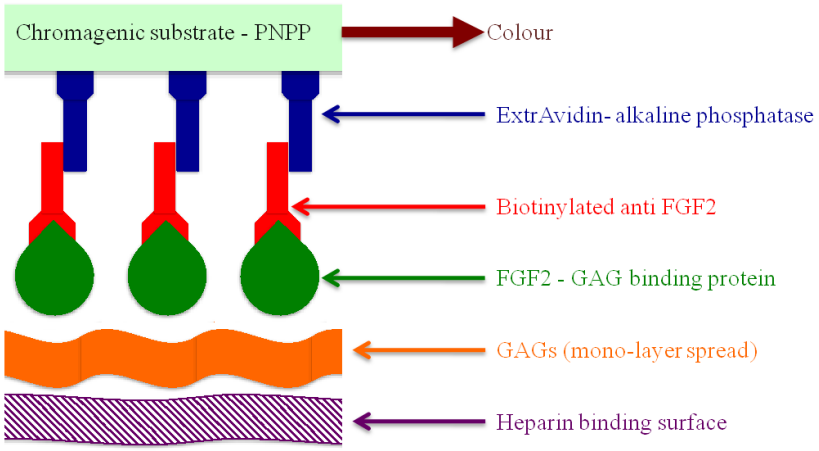

Figure 3.1. Diagram illustrating the GAG ELISA assay for HS8 variants and FGF-2.

Wells were incubated overnight (16 h) at room temperature protected from light with 200 µl of 2.5, 5, 10 µg/ml GAGs in standard assay buffer

(SAB: 100 mM NaCl, 50 mM NaAc, (v/v) 0.2 % Tween 20, pH 7.2). In initial optimization experiments to determine the concentration which saturates the plate surface, all the three concentrations of GAGs were used to coat the GAG-binding plates. After optimizatio, 5 µg/ml of each GAG was used. Wells were then washed carefully with 250 µl of SAB three times and blocked with 0.4 % (w/v) fish gelatin (Sigma Aldrich) in SAB (blocking buffer) for 1 h at 37 °C protected from light. Then wells were washed with SAB three times and FGF-2 (R&D Systems) in blocking buffer at different concentrations (0, 25, 50, 100 ng/ml equivalent to 0, 0.781, 1.56, 3.125 nM) was added (200 µl each) into the wells and incubated at 37 °C for 2 h. Wells were again washed three times with SAB and 200 µl of biotinylated anti-FGF-2 (250 ng/ml) R&D Systems) added into the wells and incubated at 37 °C for 1 h. Next, wells were washed with SAB (3 times) to remove unbound antibody and ExtrAvidin (200 µl of 220 ng/ml) (Sigma Aldrich) added and incubated for 30 min at 37 °C. Wells were finally washed with SAB (3 times) and 200 µl of development reagent SIGMA*FAST*™ p-nitrophenyl phosphate (Sigma Aldrich) in DI water added into the wells to be incubated at room temperature for 40 min. Colourimetric absorbance was read at 405 nm with a Victor multiplate reader (Perkin Elmer, Massachusetts, USA).

To investigate the affinity of binding of above HS8 variants to other heparin-binding proteins such as BMP-2, PDGF-BB, VEGF, FGF-1, FGF-7 (0, 0.781, 1.56, 3.125 nM) (R&D Systems) in comparison to the FGF-2, GAG ELISA assay was also performed. Here different proteins, other than FGF-2, were incubated with corresponding biotinylated antibodies (250 ng/ml; R&D Systems) to identify the bound proteins.

This assay was also used to investigate the binding affinities of each $HS8^{+ve}$ variant ($HS8G^{+ve}$, $HS8C^{+ve}$ and $HS8B^{+ve}$) to FGF-2. The wells were incubated overnight (16 h) at room temperature protected from light with 200 µl of 5 µg/ml different HS8 variants in SAB and the assay conducted as above.

3.2.2. Isolation and characterization of human mesenchymal stem cells

The human mesenchymal stem cells (hMSCs) used here were isolated from the Poietics® bone marrow mononuclear cells (BMMNCs) of young healthy adult human donors (Lonza, USA) aged between 18 and 45. The Poietics® BMMNCs were employed in two different ways to isolate human mesenchymal stem cells: plastic adherence and magnetic-activated cell sorting (MACS).

3.2.2.1. Isolation of hMSCs by adherence

The precursors of non-hematopoietic tissues in the bone marrow, essentially the MSCs, were initially referred to as plastic-adherent cells or colony forming-unit fibroblasts in the literature (Colter *et al*., 2000; Friedenstein *et al*., 1976). I adopted the plastic adherence method for isolation of hMSCs established by Friedenstein *et al* (Friedenstein *et al*., 1976).

3.2.2.1.1. Thawing of Poietics® bone marrow mononuclear cells

The Poietics® bone marrow mononuclear cells were initially thawed as per the manufacturer's specifications. The pre-warmed basal media consisting

of Dulbecco's Modified Eagle's medium-low glucose (DMEM-LG 1000 mg/l) supplemented with 10 % fetal calf serum (FCS), 50 units/ml penicillin and 50 µg/ml streptomycin and 2 mM L-glutamine with DNase 1 (20 u/ml) (Roche) was used to quickly thaw the vial of $2x10^8$ frozen mononuclear cells (Lonza, Product No. 2M-125A, Lot No. 0F4312B from 20 year old male Hispanic) in a 37 °C water bath. The outside of the vial was wiped with 70 % ethanol and the cells were aseptically transferred to a 50 ml conical tube. The vial was rinsed with another 1 ml of medium that was added drop-wise to the cells with gentle swirling. Then a further 2 ml of culture medium was added drop-wise to the cells, with gentle swirling after each addition of several drops of medium. Next, the volume of the tube was brought to 45 ml by adding 1 ml to 2 ml volumes of medium drop-wise, while gently swirling. Then the cell suspension was centrifuged for 15 min at 200 g at room temperature. The supernatant was removed without disturbing the cell pellet and gently resuspended in 30 ml of medium with gentle swirling. The cell suspension was centrifuged for 15 min at 200 g at room temperature. The supernatant was removed and the pellet was gently resuspended in 10 ml of culture medium. The cells were incubated for 1 h in a humidified incubator at 37 °C with 5 % CO_2 and counted before seeding.

3.2.2.1.2. Isolation of hMSCs by adherence

The bone marrow mononuclear cells ($1x10^7$) were then seeded into T175 flasks (Nunc) in hMSC basal media (Dulbecco's Modified Eagle's medium-low glucose (DMEM-LG 1000 mg/l) supplemented with 10 % FCS, 50 units/ml penicillin and 50 µg/ml streptomycin) and the cells allowed to

adhere for 5 days before the first media change. The cells were cultured in basal medium with a media replacement every 3 days. Cells were detached with 0.125 % trypsin/Versene (pH 7.0) upon reaching 75–80 % confluence and then washed once in basal medium before being re-plated at a density of 3000 cells/cm^2. All cultures were maintained under humidified atmosphere at 37 °C with 5% CO_2.

3.2.2.2. Isolation of STRO1^{+ve} human mesenchymal stem cells by magnetic activated cell sorting (MACS)

The use of MACS allowed the fractional purification of the bone marrow mononuclear cell population and the processing of large numbers of bone marrow mononuclear cells without compromising overall stem cell yield. The STRO-1^{+ve} cells were isolated from BMMNCs by magnetic-activated cell sorting (MACS) as per the method described by Gronthos *et al* (Gronthos and Zannettino, 2008; Gronthos *et al*., 1999; Gronthos *et al*., 2003).

3.2.2.2.1. Thawing of Poietics® bone marrow mononuclear cells for STRO-1 isolation

As for the isolation of hMSCs by plastic adherence, the Poietics® bone marrow mononuclear cells were thawed as per manufacturer's specifications. The pre-warmed basal media, consisting of α-modified Eagle's medium (α-MEM) supplemented with 20 % FCS, 100 µM L-ascorbate-2-phosphate, 50 units/ml penicillin and 50 µg/ml streptomycin and 2 mM L-glutamine with DNase 1 (20 u/ml) (Roche), was used to quickly thaw the vials of $2x10^8$

frozen mononuclear cells (Lonza, Product No. 2M-125A, Lot No. 091295A, from male Hispanic 21 y old) in a 37 °C water bath. The next steps were identical to the steps followed in the isolation of hMSCs by adherence discussed above.

3.2.2.2.2. Isolation of STRO1^{+ve} hMSCs by MACS

The isolation procedure follows the method described by Gronthos *et al* (Gronthos and Zannettino, 2008; Gronthos *et al*., 1999; Gronthos *et al*., 2003). After incubation for 1 h in a humidified incubator at 37 °C with 5% CO_2, the BMMNCs were resuspended in 0.5 ml of blocking buffer (HHF supplemented with 5% (v/v) normal human serum) and further incubated on ice for 30 min to reduce the possibility of Fc receptor-mediated-binding of antibodies. BMMNCs were pelleted by centrifugation at 400 *g* at 4 °C for 10 min and resuspended in 500 µl of STRO-1 supernatant per 5 x 10^7 BMMNCs and incubated on ice for 60 min with occasional, gentle mixing. Then the BMMNCs were washed twice in HHF wash buffer and resuspended in 0.5 ml of HHF containing biotinylated goat anti-mouse I (µ-chain specific) at a 1/50 dilution and incubated at 4 °C for 45 min. Next the BMMNCs were washed again three times in HHF and resuspended in 450 µl of MACS buffer (Ca^{2+} and Mg^{2+}-free PBS supplemented with 1 % BSA in PBS, 5mM EDTA and 0.01 % sodium azide) to which 50 µl of streptavidin microbeads were added (10 µl of microbeads/10^7 cells in 90 µl MACS buffer). The mixture was incubated on ice for 15 min. After one wash in ice-cold MACS buffer, a small aliquot of cells was removed for flow cytometric analysis (pre-sample). The remaining cells were then placed onto a mini MACS column (column capacity

of 10^8 cells, Miltenyi Biotec, MS). The STRO-1^{-ve} cells (negative fraction) are not retained within the column and passed through into a fresh 2 ml polypropylene tube, under gravity into the effluent, while the STRO-1^{+ve} cells remained attached to the magnetised matrix. The column was washed 3 times with 0.5 ml MACS buffer to remove any nonspecifically-bound STRO-1^{-ve} cells, which were collected in a fresh 2 ml polypropylene tube. The STRO-1^{+ve} cells (positive fraction) were recovered by flushing the column with MACS buffer into a fresh 2-mL polypropylene tube after withdrawing the column from the magnetic field. The STRO-1^{+ve} cells were then counted and processed for two-color FACS. Small samples (0.5–1.0 x 10^5 cells) from each of the pre-MACS, STRO-1^{-ve} and STRO-1^{+ve} fractions were removed into separate 2 ml polypropylene tubes containing 0.2 ml of streptavidin-FITC conjugate (1/50 in dilution). The cell samples were then incubated for an additional 5 min on ice to enable assessment of the enrichment procedure. A sample of (1.0 x10^5 cells) unlabeled pre-MACS cells served as a negative control. These samples were washed twice in HHF, fixed in FACS Fix solution and subsequently analyzed by flow cytometry to assess purity and recovery.

The partially purified STRO-1^{+ve} BMMNCs were passaged 2-4 times. Cells were seeded at a density of 0.5-1.0 x 10^4 per cm^2 initially, in a medium containing α-MEM supplemented with 10 % FCS, 100 µM L-ascorbate-2-phosphate, 50 units/ml penicillin and 50 µg/ml streptomycin and 2 mM L-glutamine at 37 °C in 5% CO_2. Cells were detached with 0.125 % trypsin/versene (pH 7.0) upon reaching 75–80 % confluence and re-plated at a

density of 3000 cells/cm^2 in later passages. All cultures were maintained under humidified atmosphere at 37 °C with 5% CO_2.

3.2.2.3. Cryopreservation and thawing of hMSCs

Cells were cryopreseved in FCS (Hyclone, Thermo Scientific) containing 10 % (v/v) dimethyl sulfoxide (DMSO, Sigma Aldrich). Cells were detached with 0.125 % trypsin/Versene (pH 7.0) upon reaching 75–80 % confluence and collected for cryopreservation. The cell pellet was resuspended at a concentration of 2 $x10^6$ cells per ml in FCS and maintained on ice. An equal volume of freeze mix (20 % DMSO in cold FCS) was then added gradually while gently mixing the cells to give a final concentration of 1 x 10^6 cells per ml in 10 % DMSO/FCS. One-milliliter aliquots were then distributed into 1.8 ml cryoampoules (Nalgene) pre-cooled on ice, then frozen at a rate of -1 °C per min using a “Mr. Frosty” cryopreservation container (Nalgene) and placed in a -80 °C freezer overnight. The frozen vials were then transferred to liquid nitrogen for long-term storage at -196 °C.

Recovery of the frozen stocks was achieved by rapid thawing the cells in a 37 °C water bath. Once thawed, the cells were resuspended in pre-warmed hMSC culture media in a 15 ml Falcon tube. This preparation was centrifuged at 300 g for 5 min to remove DMSO/FCS. The cell pellet was resuspended in appropriate culture media and plated for expansion.

3.2.3. Characterization of hMSCs

hMSCs possess substantial therapeutic potential and have been intensively studied. Dominici *et al.* have remarked about the major issues in

comparing and contrasting study outcomes, as different researchers use different methods of isolation and expansion, and different approaches in characterizing the cells. They went on to highlight that the Mesenchymal and Tissue Stem Cell Committee of the International Society for Cellular Therapy have proposed a minimal criteria to define hMSCs (Dominici *et al.*, 2006). Firstly, MSCs must be plastic-adherent when maintained in standard culture conditions; must be positive for certain surface markers while negative for certain surface markers; and retain the capacity to differentiate into osteoblasts, adipocytes and chondroblasts *in vitro*. Thus the first task was to determine whether the plastic adherent and STRO-1^{+ve} hMSCs met these minimal criteria.

3.2.3.1. Colony-forming units-fibroblastic (CFU-F) Assay

Plastic adherence is a well-described property of hMSCs; if cells are maintained and expanded in normal culture conditions they should adhere to the plastic surface and form mesenchymal stem cell colonies when plated at low densities (Friedenstein *et al*., 1976; Pochampally, 2008). Hence the next step was to perform CFU-F assays to determine the CFU-F capacities of isolated and expanded hMSCs were consistent with the laboratory's previously published work (Rider *et al*., 2008). The hMSCs were seeded at a seeding density of 150 cells per 100 x 15 mm Petri dish (Nunc) in triplicates in 10 ml of culture basal media. The cells were cultured for 14 days in standard culture conditions as described earlier with a medium change at day 7. At day 14, cultures were terminated and stained with crystal violet (Sigma-Aldrich) to visualize the colonies. The media was removed and the cells carefully washed

twice with PBS. Then each 10 ml/dish received 0.5% crystal violet in 100 % methanol and was incubated for 30 min at room temperature. Excess stain was washed once each with PBS and, and the plates were dried. The colonies were counted when they were greater than 50 cells in size and not in contact with another colony. The CFU-F efficiency was calculated as a percentage of colonies formed against the number of cells seeded.

3.2.3.2. Flow cytometry analysis for surface markers

Flow cytometric analysis of hMSCs (gated at 1% of the isotype control) was performed to determine whether they fulfill the minimal criteria to conform to the definition of multipotent MSCs (Dominici *et al*., 2006). It needed to be demonstrated that the hMSCs used in this study were positive for the surface markers CD73, CD90, CD105, and negative for CD14, CD19, CD34, CD45, HLA-DR, when compared to isotype-matched controls IgG1, IgG1κ and IgG2bκ. All the antibodies for flow cytometry were conjugated with either PE or FITC (BD Biosciences, USA) and details of the antibodies and their corresponding isotypes are provided in the Appendix B.

The hMSCs were detached with 0.125 % trypsin/versene upon reaching 75–80 % confluence and then washed once with PBS before being used for flow cytometry. Cells ($1x10^5$) were aliquoted into 600 µl Eppendorf tubes and blocked for 1 h on ice with 200 µl of blocking buffer (PBS, 5% FCS, 1% BSA and 10 % human serum). Cells were spun down for 2 min at 4000 rpm and washed thrice with PBS. Next the cells were resuspended in 100 µl of staining buffer (PBS, 2 % FCS, 0.02 % sodium azide) with pre-diluted respective antibodies and incubated for 1 h on ice. Again cells were pelleted

by centrifugation at 4000 rpm for 2 min and washed 3 times with PBS. Cells were resuspended in 150 µl of staining buffer and analyzed on a BD FACS Array™ Bioanalyzer with FlowJo software (Tree Star, Inc.).

3.2.3.3. Multi-lineage differentiation

In order to verify the multipotentiality of hMSCs, the cells were treated to differentiate into either adipogenic, osteogenic, or chondrogenic lineages as previously described by Rider *et al* (Rider *et al*., 2008). The hMSCs were detached with 0.125 % trypsin/Versene upon reaching 75–80% confluence and then washed once in maintenance medium before being used for differentiation assays.

3.2.3.3.1. Osteogenic differentiation

For osteogenesis, hMSCs were seeded at 3,000 cells per cm^2 in basal medium (Dulbecco's Modified Eagle's medium-low glucose (DMEM-LG 1000 mg/l) supplemented with 10% FCS, 50 units/ml penicillin and 50 µg/ml streptomycin and 2 mM L-glutamine) in 6-well, 12-well and 24-well plates for 24 h in a humidified atmosphere at 37 °C with 5% CO_2. The next day the medium was changed either to osteogenic medium (maintenance medium, 10 nM dexamethasone, 25 µg/ml ascorbic acid, and 10 mM β-glycerophosphate) or fresh basal medium. Cells were then maintained for up to 28 days, with a medium change every 3 days. After 28 days, the cells were stained with Alizarin Red S for calcium and with von Kossa staining method for calcium phosphate.

3.2.3.3.2. Alizarin Red Staining

The media were removed from the cells and washed three times with PBS. Then the cells were fixed in 4 % paraformaldehyde (PFA) for 10 min in the fume hood, and carefully washed three times with double distilled water. Next the cells were incubated in 0.1 % solution of Alizarin Red S (Sigma-Aldrich, USA) for 30 min with gentle shaking (100 rpm). The excess stain was rinsed with distilled water three times and the stained calcific depositions were scanned and analyzed.

3.2.3.3.3. von Kossa staining

The cells were carefully washed and fixed as described earlier for the Alizarin Red staining. Then the cells were incubated in 1 % silver nitrate solution for 45 min under ultra-violet illumination and then rinsed with ultra-pure water three times. The plates were then treated with 5 % sodium thiosulphate for 2 min and washed twice with ultra-pure water. Cells with brownish-black calcium phosphate depositions were scanned and analyzed.

3.2.3.3.4. Adipogenic differentiation

For adipogenesis, cells were seeded at 18,000 cells per cm^2 in maintenance media (Dulbecco's Modified Eagle's medium-low glucose (DMEM-LG 1000 mg/l) supplemented with 10 % FCS, 50 units/ml penicillin and 50 µg/ml streptomycin and 2 mM L-glutamine) in 6-well, 12-well and 24-well plates for 24 h in a humidified atmosphere at 37 °C with 5% CO_2. The cells were cultured till 100 % confluence (for 2 days) in a humidified

atmosphere at 37 °C with 5% CO_2. The medium was removed, and cells were washed once in PBS before the addition of adipogenic maintenance medium (90 % Dulbecco's Modified Eagle's medium-high glucose (DMEM-HG 4500 mg/l) supplemented with 10 % FCS, 50 units/ml penicillin and 50 µg/ml streptomycin and 2 mM L-glutamine) or adipogenic medium (adipogenic maintenance media with 10 µg/ml insulin, 115 µg/ml methyl-isobutylxanthine, 1 µM dexamethasone, and 20 µM indomethacin). Cells were then maintained for up to 28 days, with a medium change every 3 days. After 28 days, the cells were stained with Oil Red O (Sigma-Aldrich, USA) to visualize the lipid droplets.

3.2.3.3.5. Oil Red O staining

The media were removed from the cells and washed three times with PBS. Then the cell were fixed in 4 % paraformaldehyde (PFA) for 1 h, and carefully washed once with double distilled water. Then the cells were incubated with 0.36 % Oil Red O solution for 1 h. Next cells were washed twice with 60 % 2-propanol followed by 5 washes with water. The stained lipid droplets were scanned and analyzed.

3.2.3.3.6. Chondrogenic differentiation

For chondrogenesis, cells were counted and resuspended at $5x10^5$ cells per milliliter in chondrogenic medium (Cambrex chondrogenic single aliquots) with or without 10 ng/ml TGFβ3 (R&D Systems), and then 500 µl aliquots were put into 15 ml Falcon tubes. The cells were pelleted with centrifugation

at 150 *g* at room temperature for 10 min and incubated for 2 days in a Falcon tube (loosened cap) in a humidified atmosphere at 37 °C with 5% CO_2. After 2 days, the pellets attained loose round shapes and the pellets were cultured for 28 days with a medium change every 3 days. After 28 days, the cells were stained with Alcian blue (Sigma-Aldrich, USA) to visualize glycosaminoglycans.

3.2.3.3.7. Alcian blue staining

The chondrogenic pellet sectioning and Alcian blue staining was carried out at the Histopathology Facility of Institute of Cell and Molecular Biology, A*STAR, Singapore. Media were aspirated and the pellets washed with PBS twice. They were then fixed in 4 % paraformaldehyde (PFA) overnight in 4 °C with slow shaking. The pellets were embedded in paraffin using plastic cassette systems and sectioned into 5 µm thick sections, using a standard bench-top rotary microtome. The paraffin sections were first deparaffinised by washing in the following order; 3 min washes in xylene for 3 times, 2 min washes in 100 % ethanol 3 times, 2 min in 95 % ethanol once, 2 min in 80 % ethanol once, 2 min in 70 % ethanol once and 5 min in deionised water once. Next the sections were incubated with 1 % Alcian blue solution (pH 1.0) for 30 min at room temperature. Then the sections were washed with 0.1 M HCl for 3 min to remove excess stain. Lastly the sections were dehydrated by washing with solutions used to deparaffinise but in reverse order; 5 min in deionised water once, 2 min in 70 % ethanol once, 2 min in 80 % ethanol once, 2 min in 95 % ethanol once, 2 min washes in 100 % ethanol 3 times and 3 min washes in Xylene 3 times. Then the slides were mounted in

Neomount. Micrographs of the chondrogenic pellet sections were taken and analyzed.

3.2.4. Cell Proliferation Assays (Short-term growth)

Next the effect of HS variants on hMSC proliferation when used as a "stand-alone" media supplement were investigated. The hMSC proliferation assays were conducted by two means, namely BrdU incorporation assay and the GUAVA Viacount® assay. The BrdU incorporation assay is a colourimetric immunoassay based on the measurement of BrdU incorporation during the DNA synthesis, a non-radioactive alternative to the ^{3}H-thymidine incorporation assay. The GUAVA Viacount® assay uses a mixture of two DNA binding dyes to provide sensitive, accurate detection of viable, apoptotic, and dead cells.

3.2.4.1. BrdU incorporation proliferation assay

A BrdU incorporation proliferation assay (Cell Proliferation ELISA, BrdU (Colorimetric) Roche) was conducted to establish the effect of HS variants on hMSC proliferation. BrdU is incorporated in place of thymidine into the DNA of proliferating cells and followed with an ELISA assay which detects the subsequent substrate colour development that directly correlates to the amount of DNA synthesis and thereby to the number of proliferating cells in the respective microcultures. Here the dose-responses of hMSCs to HS variants were monitored by BrdU incorporation over 36 h according to manufacturer's specifications. The cells were seeded at a density of 5000 cells

per well in 96 well plate (Nunc) with 190 µl of culture media per well. The cells were incubated in a humidified atmosphere of 37 °C and 5 % CO_2 for 6 h. Afterwards, different doses (0.3125, 0.625, 1.25, 2.5, 5, 10 of FGF-2 (ng/ml) and GAGs (µg/ml) of treatments in 10 µl of media were added to designated wells as in the experimental layout. Then the cells were further incubated for another 36 h in the usual humidified environment. Each well was added with 20 µl of 100 µM BrdU labeling solution (5-bromo-2-deoxyuridine) to achieve final concentration of 10 µM BrdU and incubated for another 2 h. The labeling medium was removed by tapping off the plate on clean C-fold towels and the cells were fixed for 30 min at 15-25 °C by adding 200 µl of FixDenat fixative solution to each well. The FixDenat solution was removed thoroughly by flicking and tapping. Then 100 µl of anti-BrdU-POD working solution (monoclonal antibody from mouse-mouse hybrid cells (clone BMG 6H8) conjugated with peroxidase) was added per well and incubated for 90 min at 15-25 °C. The antibody conjugate was removed by flicking and the wells were rinsed thrice with 250 µl of washing solution (1x PBS) per well. Following the last wash and removal of the washing solution by tapping, 100 µl TMB substrate solution (tetrmethyl-benzide) was added to each well and incubated for 30 min at 15-25 °C. Finally the optical density was determined within 30 min, using a Bechmark Plus Spectophometer (Bio-Rad) set to 370 nm with a wavelength correction made by subtracting the readings at 492 nm. All samples were measured in triplicate. The fold increase in proliferation of hMSCs in relation to different treatments was calculated against the controls.

In addition, this assay was used to determine the dose-responses of hMSCs to $HS8^{+ve}$ variants namely $HS8G^{+ve}$, $HS8C^{+ve}$ and $HS8B^{+ve}$. The HS8

variants were used at 0.3125, 0.625, 1.25, 2.5, 5, 10 µg/ml and the assay conducted as above.

3.2.4.2. GUAVA Viacount® assay

The GUAVA Viacount assay exploiting the Guava EasyCyte™ Plus System/CytoSoft™ software (Millipore™) was performed to monitor dose-responses of hMSCs to HS variants over 6 days according to manufacturer's specifications. The Viacount flex reagent (Millipore) uses two DNA binding dyes. One membrane-permeant dye stains all nucleated cells while another membrane-impermeant dye stains only damaged cells thus indicating apoptotic and dying cells. These stained cells were then detected within a microcapillary flow cytometry platform.

The cells were seeded at a density of 3000 cells/cm^2 in 24 well plates (Nunc) with 500 µl of culture media. The cells were incubated in humidified atmosphere of 37 °C and 5 % CO_2 for 16 h overnight allowing cells to be attached to the plate. Next day, different doses (0.156, 0.3125, 0.625, 1.25, 2.5, 5, 10 (ng/ml) of FGF-2 and GAGs (µg/ml) as treatments in 500 µl of fresh media were added to designated wells as in the experimental layout. Then the cells were further incubated for another 6 days in the usual humidified environment. The media was changed either every 2 days or every 3 days. Cells were harvested at designated time points (day 2, day 4 and day 6) with 100 µl of 0.125 % trypsin/Versene (pH 7.0±0.3) and neutralized with 100 µl of media (day 2) or 300 µl of media (day 4 and 6). The Viacount flex reagent was added to the cell suspension (1 µl for 200 µl of media) and incubated for

10 min. Finally these stained cells were detected by the microcapillary flow cytometry platform of the EasyCyte™ Plus System and analyzed by EasyCyte™ Plus System (Millipore). All samples were measured in triplicate. The fold increase in proliferation of hMSCs in relation to different treatments was calculated against the controls.

In addition, this assay was used to determine the dose-responses of hMSCs to HS8 variants namely HS8G, HS8C and HS8B. The HS8 variants were dosed at 2.5 µg/ml and the assay was conducted as above.

3.2.5. Heparin-Agarose bead competition assay

Heparin-Sepharose bead competition assays were performed to further investigate the binding affinity of each desalted HS variant (heparin, HS^{pm}, $HS8^{+ve}$ and $HS8^{-ve}$) for FGF-2 according to Ono *et al* (Ono *et al*., 1999). In addition, the comparative ability of each HS variant to compete with highly sulfated heparin was also investigated. The reasoning was that an HS variant with strong affinity for FGF-2 should compete against the affinity of FGF-2 for heparin. The assay was done at room temperature. First a "master mix" of bead slurry was prepared to reduce error. Equal amounts of (20 µl) of heparin-Agarose beads Type 1 (Sigma Aldrich) and polyacrylamide gel (Biogel P-30, Biorad) were mixed and used for each reaction. The total volumes required for all the reactions were calculated and brought together to form the "master mix" where the height of the suspension was marked for later resuspension. The bead suspension was washed 3 times with 1 ml of 1 % BSA (Sigma Aldrich) in PBS. Between the washes the beads were spun down at 2000 rpm for 1 min initially and later allowed to settle to the bottom of the tube for 1

min. After the last wash, beads were left to settle and resuspended back to the original height using the initial marked height. From the master mix, aliquots (40 µl) of bead slurry were separated into individual 1.5 ml Eppendorf tubes for binding experiments.

Protein optimization was first carried out with the intension of optimizing the amount of FGF-2 needed to achieve sub-optimal binding to beads. Varying concentrations of FGF-2 (0, 5, 10, 20, 40, 80 ng/ml) in 100 µl volume were added in triplicates to the 40 µl of beads and incubated for 30 min under constant rotation. The beads were spun down at 2000 rpm for 1 min, allowed to settle for 1min, and washed twice each, with 1 ml of 1 % BSA (Sigma Aldrich) in PBS and with 1 ml of 0.02 % Tween20 (Sigma Aldrich) in PBS. Excess wash buffer was removed from the last wash. To each tube, 100 µl of biotinylated anti-FGF-2 (R&D Systems) prepared in 1 % BSA in PBS (using the FGF-2 conjugate – Part no: 890657 from the FGF-2 Quantikine ELISA kit – R&D Systems Catalog #: DFB50, 1-in-10 dilution) was added and incubated at room temperature for 1 h with constant rotation. The beads were washed again as previously described and 100 µl of TMB substrate (R&D Systems) (using the TMB substrate – Parts #: 895000 and 895001 from the FGF-2 Quantikine ELISA kit - R&D Systems Catalog #: DFB50, 1-in-10 dilution) was added and the mixture incubated for 30 min at room temperature under constant rotation to develop the colour. The reaction was stopped at 30 min by adding 50 µl of 2 M H_2SO_4. Beads were centrifuged at 2000 rpm for 1 min and allowed to settle to the bottom of the tube for 1 min. Subsequently 100 µl of the supernatant was removed and added into 96-well plates (Nunc) to be read at 450 nm.

Results were plotted and sub-optimal concentrations of FGF-2 (10 ng/ml) used for the subsequent competition assay. The competition was carried out with the objective of investigating the binding affinities of the GAGs to FGF-2, as well as how much they can compete with heparin in binding to FGF-2. Different concentrations (0, 5, 50 and 100 µg) of GAGs were pre-incubated with FGF-2 (10 ng/ml) in 100 µl in triplicates for 30 min with constant rotation. Assays were continued after this step similar to the FGF-2 optimization, in being washed with 40 µl of bead slurry as previously prepared, was added to each reaction mixture and incubated for a further 30 min under constant rotation. Results were expressed as "percentage bound" by normalizing to readings from control (uncompleted) beads.

Immunoblotting was performed to confirm the results from the competition assay. Here the competition was performed and the beads were washed as above. Then the beads were boiled at 95 °C for 5 min with 30 µl of 2x Laemmli buffer (Sigma Aldrich). Next the beads were centrifuged at 2000 rpm for 1 min and 20 µl of the supernatant was loaded into each lane of Novex 4-12 % Bis-Tris SDS PAGE gels, 15 well (Invitrogen, Catalog # NP0323BOX). The gel was run at 150 V for 1 h in 1x MOPS buffer and transferred to nitrocellulose membranes and run at 100 V for 90 min in 1x transfer buffer. Next the nitrocellulose membranes were stained with Ponceau S solution (Sigma Aldrich) and cut into strips according to the size of the protein of interest. Membrane was blocked in 5 % BSA (Sigma Aldrich) in TBST for 1 h at room temperature with slow shaking (100 rpm). The membrane was then probed with the human FGF basic biotinylated primary antibody (R & D Systems, Catalog #: BAF 233) (1:2000) in 5 % BSA at room

temperature for 1 h. Afterwards, membranes were washed with TBST 3 times for 5 min each. Then, the membrane was probed with 1- drop streptavidin peroxidase (Invitrogen, Catalog no: 50-242Z) in 1 ml of PBS and incubated for 15 min at room temperature with slow shaking (100 rpm). Membranes were finally washed 3 times with TBST for 5 min each and exposed to LumiGLO ReserveTM chemiluminescent substrate (Kirkegaard & Perry Laboratories) to visualize the bands on X-ray films.

3.2.6. Capillary electrophoresis –disaccharide analysis

To investigate the different molar percentages of each disaccharide present in HS^{pm} and $HS8^{+ve}$, capillary electrophoresis (CE) was performed. CE is a sensitive technique to determine the composition of HS by separating the samples based on charge and molecular weight (Lamari *et al*., 2001). The disaccharide analysis was performed with the assistance of GlycoSyn, IRL, (now The Ferrier Institute, Victoria University of Wellington, New Zealand).

Twelve disaccharide standards, derived from the digestion of high-grade porcine heparin by bacterial heparinases and a synthetic derivative of a non-naturally occurring disulfated disaccharide (ΔUA,2S-GlcNCOEt,6S) (as an internal standard) were used in this assay (Iduron Ltd, Manchester, UK). Capillary electrophoresis (CE) analysis was completed on an Agilent3D CE (Agilent Technologies, Waldbronn, Germany) instrument using uncoated fused silica capillary tubes (75 mm ID, 64.5 cm total and 56 cm effective length, Polymicro Technologies, Phoenix, AZ, Part # TSP075375). Heparin lyase I (Heparitinase, EC 4.2.2.8, also known as heparitinase I), heparin lyase II (heparitinase II, no EC number assigned) and heparin lyase III (heparinase,

EC 4.2.2.7, also known as heparitinase III) and keratin sulfate (KS) were obtained from Seikagaku Corporation, Japan. The enzymes, supplied as lyophilized powders (0.1 U/vial), were dissolved in 0.1 % BSA to five solutions containing 0.5 mU/µl. Aliquots (5 µl; 2.5mU) were frozen (-80 °C) until needed.

3.2.6.1. Digestion of HS preparations with heparan lyase enzymes

HS preparations (1 mg) were each dissolved in 500 ml of sodium acetate buffer (100 mM containing 10 mM calcium acetate, pH 7.0) and 2.5 mU each of the 3 enzymes added. The samples were incubated at 37 °C overnight (24 h) with gentle inversion (9 rpm) of the tubes. A further 2.5 mU each of the 3 enzymes was added to the samples which were incubated at 37 °C for a further 48 h with gentle inversion (9 rpm) of the tubes. Digests were halted by heating (100 °C, 5 min) and then lyophilized. The digests were resuspended in 500 µl water and an aliquot (50 µl) taken for analysis by CE.

3.2.6.2. Capillary electrophoresis (CE)

The capillary electrophoresis operating buffer was made by adding an aqueous solution of 20 mM H_3PO_4 to a solution of 20 mM $Na_2HPO_4.12H_2O$ to give pH 3.5. The column wash was 100 mM NaOH (diluted from 50 % w/w NaOH). The operating buffer and the column wash were both filtered using a Millipore filter unit fitted with 0.2 µm cellulose acetate membrane filters (47mm ø; Schleicher and Schuell, Dassel, Germany).

Stock solutions of the 12 disaccharide standards were prepared by dissolving the disaccharides in water (1 mg/ml). To determine the calibration

curves for the standards, a mix containing all twelve standards was prepared. The stock solution of the 12 standard mix contained 10 µg/100µl of each disaccharide and a dilution series containing 10, 5, 2.5, 1.25, 0.625, 0.3125 µg/100 µl was prepared; including 2.5 µg of internal standard (ΔUA,2S-GlcNCOEt,6S). The digests of HS were diluted (50 (ΔUA,2S-GlcNCOEt,6S)l/ml) with water and the same internal standard was added (2.5 µg) to each sample. This internal standard was added because of its distinct migration time from the Δ-disaccharide standards and thus could be utilized for the determination of each disaccharide unit from its relative migrational shift. The solutions were freeze-dried and re-suspended in water (1 ml). The samples were filtered using PTFE hydrophilic disposable syringe filter units (0.2 µm; 13mm ø; Advantec, Toyo Roshi Kaisha, Ltd., Japan).

The analysis was performed using an Agilent^{3D}CE (Agilent Technologies, Waldbronn, Germany) instrument on an uncoated fused silica capillary tube (75 µm ID, 64.5 cm total and 56 cm effective length, Polymicro Technologies, Phoenix, AZ, Part Number TSP075375) at 25^{0}C using 20 mM operating buffer with a capillary voltage of 30 kV. The samples were introduced to the capillary tube using hydrodynamic injection (50 mbar x 12 sec) at the cathodic (reverse polarity) end to generate the electropherogram. Before each run, the capillary was flushed with 100 mM NaOH (2 min), with water (2 min) and pre-conditioned with operating buffer (5 min). A buffer replenishment system replaced the buffer in the inlet and outlet tubes to ensure consistent volumes, pH and ionic strength were maintained. Water only blanks were run at the beginning, middle and end of the sample sequence. Absorbance was monitored at 232 nm. All data was stored in a Chemstore

database and was subsequently retrieved and re-processed using ChamStation software. The area-under the-peak was then measured and compared to a standard curve to derive the concentrations. Molar percentages of each sample were then calculated from the molecular weight of each standard.

3.2.7. Anti-coagulation assay

HS variants (Heparin, HS^{pm}, $HS8^{+ve}$ and $HS8^{-ve}$) were assessed for their effect on antithrombin III activity. If any fragment should show such activity, it would be useless as a prospective therapy. The assay was performed using the COATEST Heparin kit (Chromogenix) according to Bramono *et al.* where the absorbance values were represented as the relative inhibition of excess Factor Xa activity when compared to the treatment group containing no GAG (Bramono *et al*., 2012).

All assay reagents were downscaled for 96-well plates based on the recommended protocol from COATEST Heparin kit (Chromogenix, Catalog #: 25553963). HS variants were diluted in kit buffer added with human plasma and antithrombin to produce 0.3125, 0.625, 1.25 and 2.5 µg/ml of GAG solution through serial dilution. The wells were added with 50 µl of sample or positive control and incubated for 3 min at 37 °C. Then 25 µl of Factor Xa was added, mixed and incubated for 30 sec at 37 °C. The wells were supplemented with 50 µl of chromogenic substrate S-2222, mixed and incubated for exactly 3 min at 37 °C. Next 75 µl of 20 % acetic acid was added and mixed. The wells containing 50 µl of prepared blank were added with 75 µl of 20 % acetic acid and 75 µl of water. Colourimetric absorbance was read at 405 nm with a Victor multiplate reader (Perkin Elmer,

Massachusetts, USA). The blank readings were subtracted from the samples and positive control and sample readings were normalized to the positive control.

3.2.8. FGF-2 stability assay – Quantikine

It was next necessary to test whether $HS8^{+ve}$ could stabilize FGF-2. FGF-2 is known to be highly unstable, with its integrity dependent on the solvent used to dissolve it. In addition, Caldwell *et al* (Caldwell *et al*., 2004) have shown that heparin is known to stabilize FGF-2 from degradation in culture media by quantikine assay for FGF-2 from R&D systems. To investigate HS variants (Heparin, HS^{pm}, $HS8^{+ve}$ and $HS8^{-ve}$) stabilization of FGF-2, solid phase sandwich ELISA was performed similar to Caldwell *et al* (Caldwell *et al*., 2004).

FGF-2 at 2.5 ng/ml was incubated alone or in the presence of 2.5 µg/ml of GAGs (Heparin, HS^{pm}, $HS8^{+ve}$ and $HS8^{-ve}$) with 1 ml of hMSC culture media (DMEM with 10mg/l glucose, 10 % FCS, 1 % Pen/Strep, 2 mM L-glutamine) in 1.5 ml Eppendorf tubes in triplicates in a humidified incubator at 37 °C with 5 % CO_2. The media (150 µl) was collected at indicated time points (0 h, 24 h, 48 h and 72 h) and stored at -80 °C. Samples were analyzed avoiding repeated freeze-thaw cycles.

The FGF-2 standard was reconstituted as recommended with calibrator diluent RD5-14 to produce a stock solution of 640 pg/ml. After the standard was mixed with gentle agitation for 15 min 0, 10, 20, 40, 80, 160, 320, 640 pg/ml standard solutions were made through serial dilution. All reagents and working standards were brought to room temperature and all standards,

samples and controls were assayed in duplicates. Firstly, each well of the microplate strips was added with 100 µl of assay diluent RD1-43. Afterwards, 100 µl of standard, control, or sample was added per well and the microplate covered with the adhesive strip and incubated for 2 h at room temperature. Each well was aspirated and washed, repeating the process three times for a total of four washes using 400 µl of wash buffer (dilute 20 ml of wash buffer concentrate in 500 ml of deionized or distilled water) per well. After the last wash the microplate was inverted and blot dried against clean paper towels to remove liquids completely. Then 200 µl of FGF-2 conjugate was added to each well, covered with the adhesive strip and incubated for 2 h at room temperature. Wells were aspirated and washed as earlier. Then 200 µl of substrate solution (colour reagents A and B mixed in equal volumes) was added to each well and incubated for 30 min at room temperature while protecting from light. Next 50 µl of stop solution was added to each well while observing any colour change from blue to yellow. Finally the optical density was determined within 30 min, using a Bechmark Plus Spectophometer (Bio-Rad) set to 450 nm with a wavelength correction made by subtracting the readings at 540 nm. Optical density readings of the standards were used to plot the standard curve. The best-fit line was determined by regression analysis and the equation yielded used to determine the FGF-2 concentrations of the samples.

3.2.9. Differential Scanning Fluorimetry (DSF)

Differential Scanning Fluorimetry (DSF) assays were performed to further investigate the thermal stability of FGF-2 by HS variants (Heparin,

HS^{pm}, $HS8^{+ve}$ and $HS8^{-ve}$) according to Uniewicz *et al* (Uniewicz *et al*., 2010). As described previously by Niesen *et al* (Niesen *et al*., 2007), this experiment employs a ABI PRISM® 7500 PCR machine (Applied Biosystems) and a Sypro Orange dye (Invitrogen). This dye binds and detects the exposed core residues of denatured proteins when the samples are subjected to a heating cycle (Uniewicz *et al*., 2010).

Heparin and HS variants (20 % v/v), FGF-2 stock solutions (R & D Systems) (40 % v/v), and Dulbecco's phosphate-buffered saline without CaCl2/MgCl2 (Gibco) (30 % v/v) were added to a Fast Optical 96 Well Reaction Plate (Applied Biosystems) maintained on ice. Freshly prepared water-based dilutions of Sypro Orange 5000 (Invitrogen) were added as 10 % v/v. Each sample was assayed in triplicate. The final volume of the reaction mixture was 10 µl. After sealing with an Optical Adhesive Film (Applied Biosystems), the plate was gently vortexed for 300 rpm for 1 min and directly analyzed in the real-time polymerase chain reaction (RT-PCR) instrument. The heating cycle comprised a 120 sec prewarming step at 31 °C and a subsequent gradient between 32 and 81 °C in 99 steps of 20 sec, each of 0.5 °C ramp. Data were collected using the calibration setting for TAMRA dye detection (λ_{ex} 560 nm; λ_{em} 582 nm) installed on the instrument.

Initially the experiment was performed only with FGF-2 without the heparin and HS variants. This was done in order to find out the optimum protein concentration for later experiments. FGF-2 at the concentrations of 2.5, 5, 7.5 and 10 µM were used. Next, a gradient of heparin (Sigma) concentrations (2.5, 5, 10 and 20 µM) were used with the optimum FGF-2 (10 µM) in order to calculate the optimum heparin versus FGF-2 concentration.

Heparin and HS variants are comprised of pools of different oligosaccharides and therefore the molarity is difficult to define. Hence the concentration range expressed in μg/ml was selected to compare their stabilization effects. Thus, the effective concentration of heparin was chosen (for instance, 160 μg/ml corresponding to ~10 μM), and all other HS variants were used at the same w/v ratio (160 μg/ml).

The data were analyzed using the Origin Pro 8 software by application of an exponential correlation function approximation of the first derivative for each melting curve as described earlier (Uniewicz *et al*., 2010). The average of triplicate samples was used to calculate distinct melting curves and the highest values were used to calculate the mean Tm (melting temperature). After the Tm values were measured the data were normalized to compare between the stabilization effects of FGF-2 by HS variants relative to heparin. Firstly, the difference between the Tm of the FGF-2 in PBS (Tm^{FGF-2}) and the Tm of the FGF-2 in the presence of the HS variants (Tm^{HS}) were calculated as below.

$$Tm^{HS} - Tm^{FGF2} \longrightarrow \text{equation (1)}$$

Next, the difference between Tm^{FGF-2} and Tm of the FGF-2 in the presence of the heparin ($Tm^{Heparin}$) were calculated using the formula given below.

$$Tm^{Heparin} - Tm^{FGF2} \longrightarrow \text{equation (2)}$$

The relative stabilization potency, was calculated using

$$\frac{(1)}{(2)} \quad \frac{Tm^{HS} - Tm^{FGF2}}{Tm^{Heparin} - Tm^{FGF2}} \longrightarrow \text{equation (3)}$$

Two independent experiments in triplicate were analyzed and the final Tm is the mean of all obtained values.

3.2.10. Synergistic effect of HS8 variants on FGF-2

Heparan sulfate regulates FGF signaling by direct molecular association with FGFRs (Pellegrini, 2001). Therefore the higher binding affinity $HS8^{+ve}$ should greatly potentiate the FGF signaling by assembling the trimeric signaling structure on cell surface. Any synergistic effect of $HS8^{+ve}$ on FGF-2 and how it effects hMSC proliferation should be readily detectable.

3.2.10.1. Proliferation assay – GUAVA viacount®

This assay was performed as described earlier. The cells were seeded at a density of 3000 cells/cm^2 in 24 well plates (Nunc) with 500 µl of culture media (DMEM-LG 1000 mg/l supplemented with 10 % FCS, 50 units/ml penicillin and 50 µg/ml streptomycin and 2 mM L-glutamine). The cells were incubated in humidified atmosphere of 37 °C and 5% CO_2 for 16 h overnight allowing the cells to be attached to the plate. Next day, FGF-2 (0.156 ng/ml and 2.5 ng/ml) alone or FGF-2 (0.156 ng/ml) with various concentrations of HS variants (0.156, 0.3125, 0.625, 1.25, 2.5, 5, 10 µg/ml) in 500 µl of fresh media were added to designated wells as in the experimental layout. Then the cells were further incubated for another 4 days in the usual humidified environment with a fresh media changed after 2 days. Cells were harvested with 100 µl of 0.125% trypsin/Versene (pH 7.0±0.3) and neutralized with 300 µl of media. The Viacount flex reagent (Millipore) was added to the cell suspension (1 µl for 200 µl of media) and incubated for 10 min at room temperature. Finally these stained cells were detected by the microcapillary flow cytometry platform of the EasyCyte™ Plus System and analyzed by EasyCyte™ Plus System (Millipore). All samples were measured in triplicate.

3.2.10.2. Cell signaling assays - immunoblotting

Immunoblotting was performed to confirm the results of synergistic effect of $HS8^{+ve}$ and FGF-2 on hMSC proliferation. The cells were seeded (10,000 cells/cm^2) on 6-well plates (Nunc) with 2 ml/well of maintenance media (DMEM-LG 1000 mg/l supplemented with 10 % FCS, 50 units/ml penicillin and 50 µg/ml streptomycin and 2 mM L-glutamine). Cells were allowed to adhere to the plastic surface for 16 h in humidified atmosphere. The following day when the plate was 50 % confluent, maintenance media was removed and the cells were washed once with PBS. Then 2 ml of serum-free media (DMEM-LG 1000 mg/l supplemented with 0.2 % FCS, 50 units/ml penicillin and 50 µg/ml streptomycin and 2 mM L-glutamine) was added to each well and further incubated for 2 days. After 48 h of serum starvation the required amounts of GAGs (2.5 µg/ml) and/or FGF-2 (0.156 ng/ml), dissolved appropriately in serum-free media, was added at 10 µl/well. The cells were harvested in 100 µl/well with 1.5 X laemmli buffer (Sigma Aldrich) at different time points (30 min, 6 h and 24 h). The cell lysates were heated for 5 min at 95 °C and stored at -20 °C. Samples were freeze-thawed only once and 20 µl/well of sample was loaded into each lane of Novex 4-12 % Bis-Tris SDS PAGE gel, 10 well (Invitrogen). The gel was run at 180 V for 50 min with 1x MOPS buffer. Then the resolved protein bands were transferred to nitrocellulose membrane at 100 V for 90 min in 1x transfer buffer. Next the nitrocellulose membranes were stained with Ponceau S solution (Sigma Aldrich) and cut into strips according to the size of the protein of interest. The membranes were then blocked in either 5 % BSA (Sigma Aldrich) or 5 % non-fat dry milk (Anlene) in TBST for 30 min to 1h at room temperature with slow

shaking (100 rpm). Primary antibodies of recommended dilutions (phospho-FRS2a (Cell Signaling, 1:1000 in 5% BSA), phospho-ERK1/2 (Cell Signaling, 1:2000 in 5% BSA), total ERK1/2 (Cell Signaling, 1:1000 in 5% BSA) and actin (Millipore, 1:8000 in 5% milk)) were then incubated overnight at 4 °C with slow shaking (100 rpm). The blots were then washed three times with TBST for 5 min each. Secondary antibodies of recommended dilutions (goat anti mouse (Jackson ImmunoResearch, 1:10000) and goat anti rabbit (Jackson ImmunoResearch, 1:10000) either in 5% milk or 5% BSA) were then incubated for 1 to 2 h at room temperature with slow shaking (100 rpm). Membranes were finally washed 3 times with TBST for 5 min each and exposed to LumiGLO ReserveTM chemiluminescent substrate (Kirkegaard & Perry Laboratories) to visualize the bands on X-ray films. In case of reblotting, the membranes were stripped by incubating with Restore western blot stripping buffer (thermo Scientific) at room temperature for 10 min. Blots were then washed 3 times with TBST for 5 min each. Thereafter, membranes were re-blocked and immunolabeled as desired.

3.2.11. HS8 can mediate the action of FGF-2

The final part of this chapter is dedicated to determining how $HS8^{+ve}$ might be mediating the action of FGF-2. Heparan sulfate is a coreceptor for the FGF/FGFR complex and FGFR1 is a high affinity receptor for FGF-2 binding (Chellaiah *et al.*, 1999; Dombrowski *et al.*, 2009; Pellegrini, 2001). FGF-2 inhibition via a neutralizing antibody (R & D Systems), was employed, as well as FGF receptor inhibitors, either the neutralizing antibody IMBR1

(Ling *et al*., 2006) or the chemical inhibitor SU5402 (Calbiochem, Millipore) respectively, in the following studies.

The three assays, FGF-2 neutralization, SU5402 and IMBR1, utilized the hMSC proliferation assays (BrdU and GUAVA Viacount®) described earlier. Briefly, in the BrdU incorporation proliferation assay, 5000 cells/well were seeded into 96-well plates (Nunc) with 190 µl of culture media and incubated for 6 h. Different treatments were added to the existing media with 10 µl of media and further incubated for another 36 h. Then the substrate colour development that directly correlates to the amount of DNA synthesis yielded the number of proliferating cells in the respective microcultures.

For the GUAVA Viacount® assay, 3000 cells/cm^2 were seeded in 24-well plates (Nunc) with 500 µl of culture media and incubated 16 h. Then different treatments were added in 500 µl of fresh media and further incubated for another 4 days with a fresh media changed after 2 days. Stained cells with viacount flex reagent (Millipore) were detected by the microcapillary flow cytometry platform of the EasyCyte™ Plus System and analyzed by EasyCyte™ Plus System (Millipore).

3.2.11.1. FGF-2 neutralizing antibody assay

FGF-2 neutralization (R & D Systems) was effected with affinity purified polyclonal goat IgGs. The basis of this assay relies on the antibody (Ab) neutralization of FGF-2 activity, thereby inhibiting hMSC proliferation induced by FGF-2 and $HS8^{+ve}$ media supplements. In the proliferation assay cells were cultured with FGF-2 (2.5 ng/ml) and $HS8^{+ve}$ 2.5 µg/ml with or

without FGF-2 neutralizing Ab (2 µg/ml). Cells cultured with media alone or with FGF-2 neutralizing Ab (2 µg/ml) served as controls.

3.2.11.2. SU5402 Assay

SU5402 (Calbiochem, Millipore), a chemical inhibitor of FGF receptor activity was also used. In proliferation assays, cells were cultured with FGF-2 (2.5 ng/ml) and $HS8^{+ve}$ 2.5 µg/ml with or without two doses of SU5402 (10 and 25 µM) in DMSO. Cells cultured with media alone or with two doses of SU5402 (10 and 25 µM) in DMSO served as controls.

3.2.11.3. IMBR1 Assay

In this assay I used IMBR1, an affinity purified polyclonal rabbit IgG against the peptide sequence SSSEEKETDNTKPNR located between the 1^{st} and 2^{nd} Ig loop of FGFR (Ling *et al*., 2006). This strategy relies on inhibition of FGF-2 signaling by inhibit FGFR1 signaling using IMBR1. Hence IMBR1 inhibition of hMSC proliferation usually induced by FGF-2 and $HS8^{+ve}$ media supplements was monitored in this assay. In the proliferation assay, cells were cultured with FGF-2 (2.5 ng/ml) and $HS8^{+ve}$ 2.5 µg/ml with or without two doses of IMBR1 (1:2000 and 1:1000). Cells cultured with media alone or with two doses of IMBR1 (1:2000 and 1:1000) served as controls.

3.2.12. Statistical analysis

All data values are reported as the mean ± standard deviation (SD) taken from triplicate experiments. Where appropriate, mean differences between samples were analyzed using SPSS statistics software (IBM, USA)

by performing an exploratory data analysis and homogeneity of variance test, followed by ANOVA and Tukey's or Games–Howell posthoc testing. Statistical significance was defined as >0.05. Graphs were plotted and data transformed using Sigma plot software (Systat software Inc, USA) and Adobe illustrator (Adobe, USA).

3.3. Results

3.3.1. GAG ELISA – HS8G variants and FGF-2

In the previous chapter the isolation and purification of a novel FGF-2-binding HS from a commercially available porcine mucosal heparan sulfate source (Celsus Laboratories) suitable for scale up and which can be readily upgraded for use in the clinic was described. Custom-made peptide fragments were utilized and were successful in isolating three prospective HS8 variants. Here the HS variants' binding ability for bioactive, full length FGF-2, employing a GAG-ELISA binding assay was first investigated. The GAG binding plates are manufactured by cold plasma polymerization where microtitre plate surfaces are coated with allyl amine (Mahoney *et al*., 2004; Marson *et al*., 2009). The GAGs thereby non-covalently immobilize to these allyl amines without hindering their ability to interact with proteins. The initial experiments were designed to optimize the concentrations of GAGs (heparin, HS^{pm}, HSG^{8+ve} and $HS8G^{-ve}$) required to completely saturate the GAG plate surface.

Three concentrations of GAGs, namely 2.5, 5 and 10 μg/ml, were used to coat the wells and their FGF-2 binding ability investigated (Fig. 3.2). Even with the various heparin concentrations, similar FGF-2 binding was observed (Fig. 3.2A). For the HS^{pm} coatings, a dose-dependent increase in FGF-2 binding was observed, albeit the increase in FGF-2 binding was less significant between 5 μg/ml and 10 μg/ml HS^{pm} (Fig. 3.2B). Similar trends were also observed with the $HS8G^{+ve}$ and $HS8G^{-ve}$ variants (Fig. 3.2 C and D). As significant differences were not observed between the 5 and 10 μg/ml for

any of the GAGs, the 5 µg/ml concentration was adopted generally as it was sufficient to completely saturate the wells with sugar.

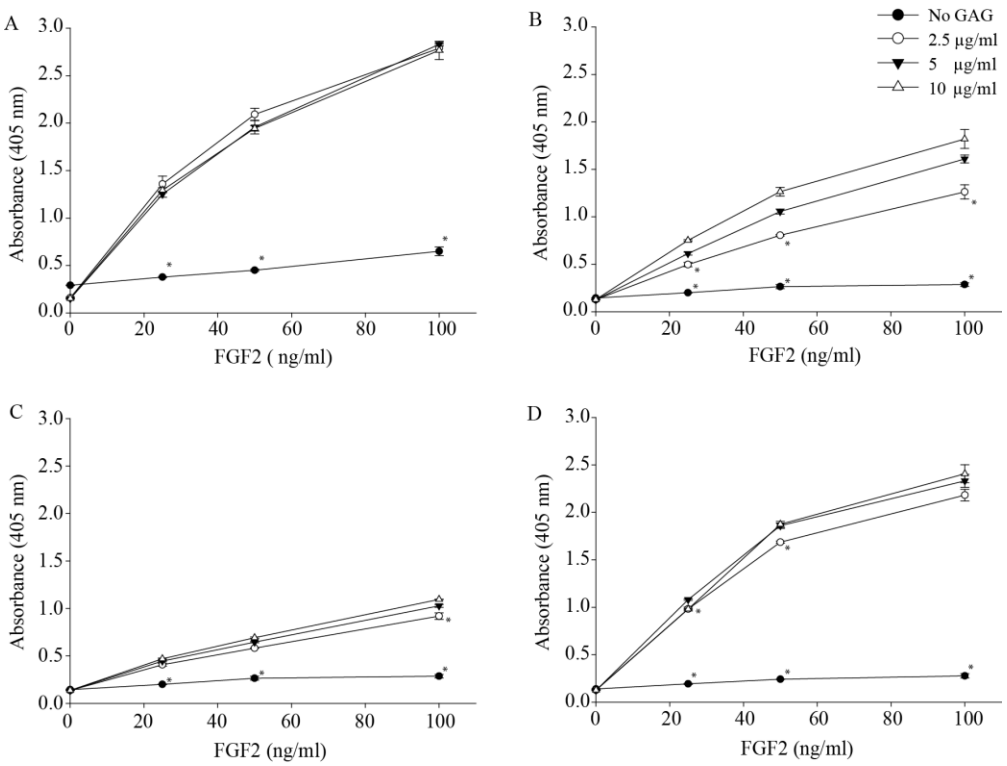

Figure 3.2. Determination of saturating amounts of GAGs for the GAG ELISA. Different concentrations (2.5, 5, 10 µg/ml) of (A) heparin, (B) HS^{pm}, (C) $HS8G^{-ve}$ and (D) $HS8G^{+ve}$ were coated onto the wells and FGF-2 binding ability were analyzed with GAG binding plates (Iduron). The 5 µg/ml dose was selected for all HS species as no significant difference observed at either 5 or 10 µg/ml. Uncoated wells (No GAG) served as the negative control. Significant difference is represented as * when compared to 10 µg/ml GAG at equivalent dose ($p<0.05$).

HS8G^{+ve} was next investigated for its relative specificity for FGF-2 as compared to heparin, HS^{pm} and HS8G^{-ve} (Fig. 3.3). Irrespective of GAG, there was a dose-dependent increase in FGF-2 binding as shown by the respective binding curves. HS8G^{+ve} variants had a significantly higher affinity for FGF-2, almost as good as the heparin positive control. In addition, HS8G^{+ve} binding to FGF-2 was significantly better than either the crude unfractionated HS^{pm} starting material or the flow through HS8G^{-ve}. HS8G^{-ve} showed the weakest binding, as expected, while HS^{pm} showed only a moderate binding to FGF-2, again as predicted.

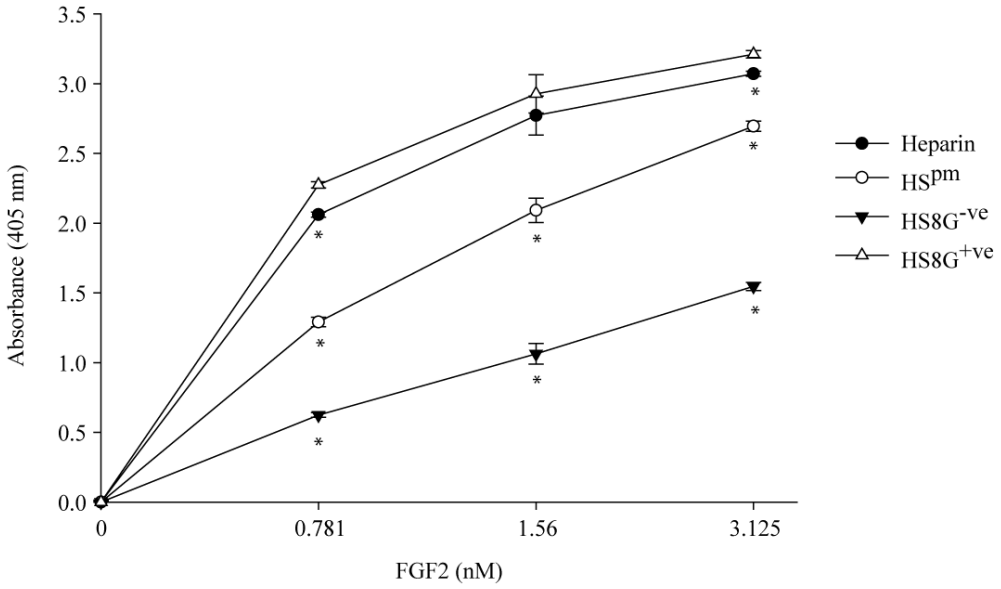

Figure 3.3. Binding profile of various GAGs to FGF-2. Heparin, HS^{pm}, HS8G^{+ve} and HS8G^{-ve} were coated (5 µg/ml) onto the wells and their binding ability for different concentrations of FGF-2 (0, 0.781, 1.56 and 3.125 nM) analyzed on GAG binding plates (Iduron). HS8G^{+ve} variants had a significantly higher affinity for FGF-2 almost as good as the heparin positive control, and significantly better than the raw starting material HS^{pm} and the flow-through HS8G^{-ve}. Significant difference is represented as * when compared to HS8G^{+ve} at equivalent dose ($p<0.05$).

To understand more fully how selective the HS fractions were for FGF-2, I next examined the extent of their binding, and HS^{pm} and $HS8G^{-ve}$ binding, to other heparin-binding growth factors (HBGFs), namely BMP-2, FGF-1, FGF-7, PDGF-BB and VEGF (Fig. 3.4). The binding curves revealed that irrespective of GAG, there was a significant difference in the individual binding of BMP-2, FGF-1 and FGF-2 as compared to individual binding of FGF-7, PDGF BB and VEGF at all the doses tested. Considering the binding of each GAG to BMP-2, FGF-1 and FGF-2, the $HS8G^{-ve}$ fraction had a decreasing order of binding of $HS8G^{-ve}$, such that BMP-2 > FGF-2 > FGF-1. The HS^{pm} and $HS8^{+ve}$ fractions bound to them in the decreasing order of HS^{pm} and $HS8^{+ve}$, such that FGF-2 > BMP-2 > FGF-1. By taking into account the

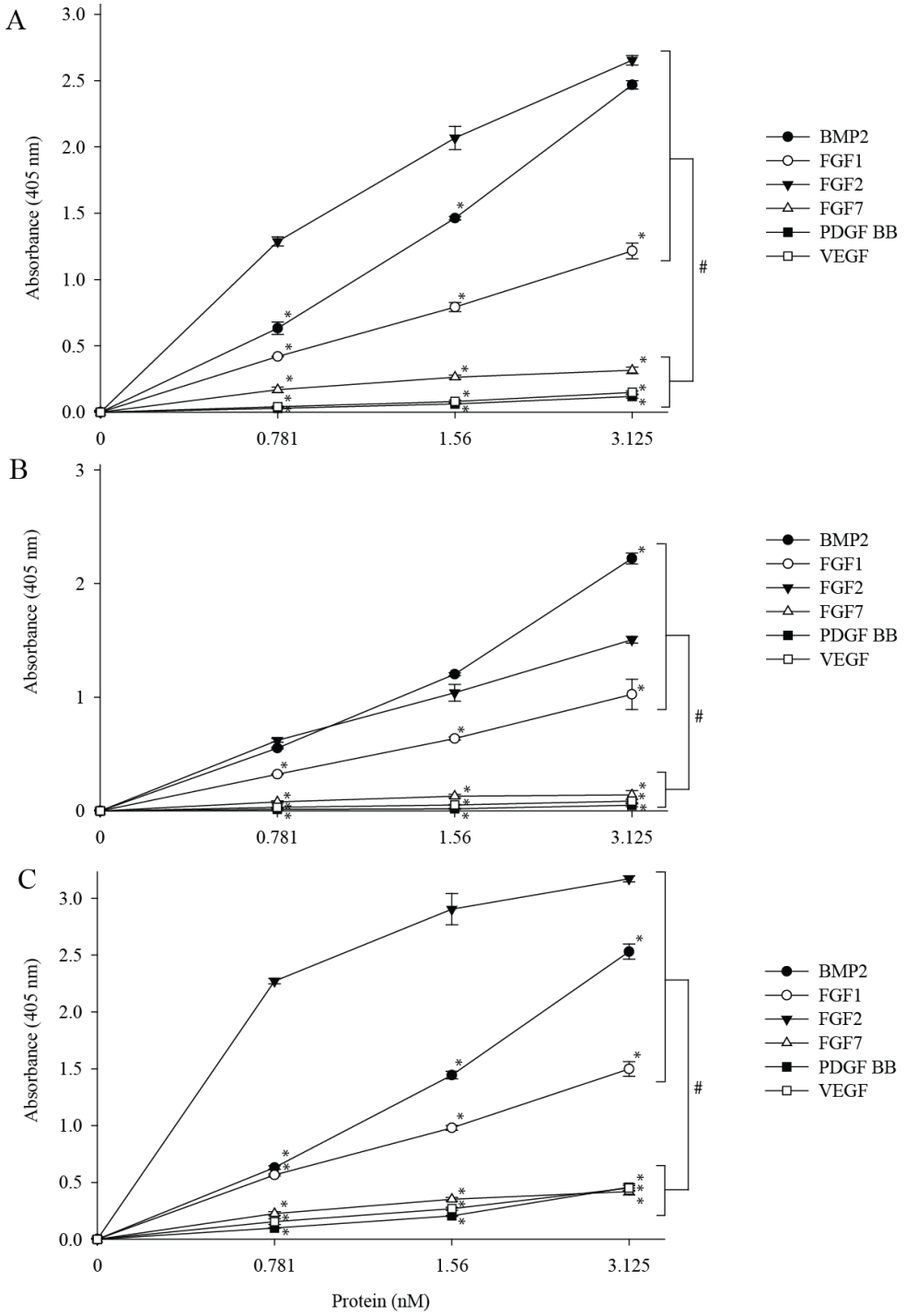

Figure 3.4. Binding profile of GAGs to heparin-binding growth factors (HBGFs). Comparative ability of immobilized (A) HS^{pm}, (B) $HS8G^{-ve}$ and (C) $HS8G^{+ve}$ (5 µg/ml) binding to BMP-2, FGF1, FGF-2, FGF7, PDGF-BB and VEGF (0, 0.781, 1.56 and 3.125 nM) were analyzed with GAG binding plates (Iduron). The HS^{pm} preferentially binds to FGF-2 (Fig. 3.4A) while $HS8G^{-ve}$ had a preference in binding to BMP2 over all of the other HBGFs (Fig. 3.4B). The $HS8G^{+ve}$ fraction preferentially binds to FGF-2 (Fig. 3.4C) similar to HS^{pm} but with almost two-fold greater preference for FGF-2 over other HBGFs when compared to HS^{pm}. Significant difference is designated as * when compared to FGF-2 binding at equivalent dose ($p<0.05$) and $^{\#}$ when each of BMP-2, FGF-1 and FGF-2 was compared to each of FGF-7, PDGF BB and VEGF at all the doses tested ($p<0.05$).

difference in absorbance (405 nm) in binding between FGF-2 and BMP-2 at the lowest, but supraphysiological dose of 0.781 nM, $HS8^{+ve}$ (1.64) had a ~ 2.5-fold higher difference than HS^{pm} (0.66) and ~ 16-fold higher difference than $HS8^{-ve}$ (0.09). Similarly, between FGF-2 and FGF-1, $HS8^{+ve}$ (1.76) had a ~ 2-fold higher difference than HS^{pm} (0.87) and ~ 5.5 fold higher difference than $HS8^{-ve}$ (0.30). These data suggest that $HS8^{+ve}$ is more selective for FGF-2 over other HBGFs when compared to HS^{pm} and $HS8^{-ve}$.

The various $HS8^{+ve}$ variants' binding affinity to FGF-2 as compared to HS^{pm} (Fig. 3.5). All $HS8^{+ve}$ variants, that is, HS8 Gandhi ($HS8G^{+ve}$), HS8 Cardin ($HS8C^{+ve}$) and HS8 Baird ($HS8B^{+ve}$), dose-dependently had increases in their binding ability for FGF-2 without any significant difference. All of them individually had significantly higher binding for FGF-2 than crude HS^{pm}. This assay further validates our affinity chromatography platform for the isolation of HS variants that bind with high affinity to FGF-2, $HS8G^{+ve}$, $HS8C^{+ve}$ and $HS8B^{+ve}$ had comparable binding affinities for FGF-2.

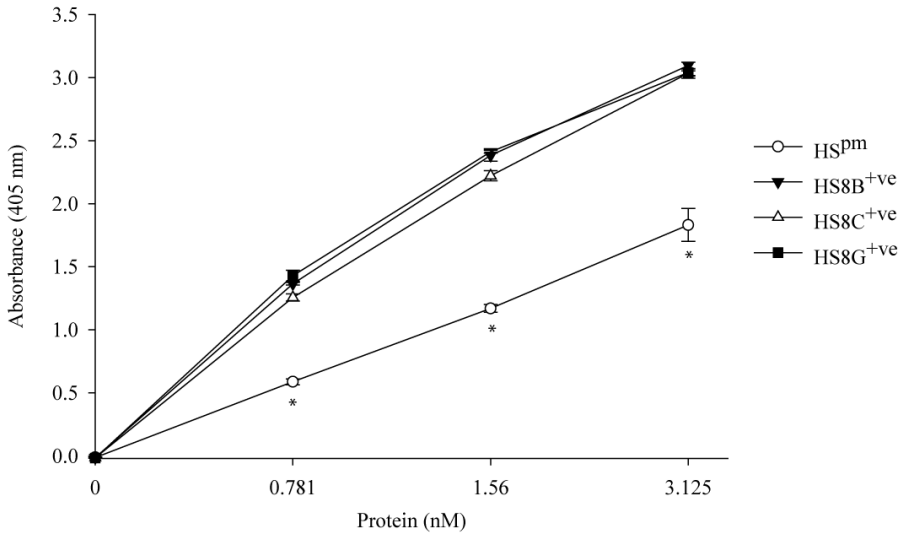

Figure 3.5. Binding profile of various HS8^{+ve} variants to FGF-2. HS8^{+ve} variants (HS8G^{+ve}, HS8C^{+ve} and HS8B^{+ve}) and HS^{pm} were coated (5 µg/ml) onto wells surfaces and their binding preferences for different concentrations of FGF-2 (0, 0.781, 1.56 and 3.125 nM) analyzed via GAG binding plates (Iduron). All HS8^{+ve} variants had similar binding affinities for FGF-2, and all were significantly higher than HS^{pm}. Significant difference is represented as * when compared to each HS8^{+ve} variant at equivalent dose ($p<0.05$).

3.3.2. Proliferation studies of hMSCs with HS variants

3.3.2.1. Isolation and characterization of hMSCs

The hMSCs that were used in the short-term proliferation studies were isolated from the Poietics® bone marrow mononuclear cells of young healthy adult human donors. Isolation was done by two means: plastic adherence and magnetic-activated cell sorting (MACS) as described. After successful isolation, and prior to the proliferation studies, the hMSCs (at passage 3) were subjected to a series of tests in order to determine whether they conformed to the minimal criteria for mesenchymal stem cells according to the International Society for Cellular Therapy (Dominici *et al*., 2006).

As hMSCs must demonstrate adherence, and form colonies when passaged under normal culture conditions, both hMSC types were first

subjected to CFU-F assay. It was confirmed that both hMSC types were capable of forming colonies after adhering to tissue culture plastic, as revealed by the crystal violet staining (Fig. 3.6 A and 3.7 A). The STRO-1^+ hMSCs had a higher CFU-F efficiency rate (48.4±3.15) than that of the plastic adherent hMSCs (31.5±1.37). Furthermore, single-color flow cytometry analysis revealed that the hMSCs were positive for the MSC-related markers CD73, CD90, CD105 (> 99% positive) while negative for haematopoeitic markers (< 2% positive) of CD14, CD19, CD34, CD45 and HLA-DR (Fig. 3.6 B and 3.7 B). There weren't any differences in either hMSCs cell types in relation to their positive and negative MSC-related markers. Thus it can be concluded that other cell types were not contaminating the hMSCs. Finally, hMSCs were directed to trilineage differentiation, and, after culturing *in vitro* for 28 days, the hMSCs readily differentiated into osteoblasts, adipocytes, and chondroblasts. This was confirmed by positive staining with Alizarin Red, von Kossa, Oil Red O, and Alcian blue respectively (Figures 3.6 C and 3.7 C). The STRO-1^+ hMSCs displayed qualitatively slightly higher rates of osteogenesis compared to plastic adherent hMSCs, albeit adipogenesis and chondrogenesis rates were lacking any such differences. Collectively, the data confirmed both hMSC types met the criteria stated above and were suitable for the proliferation studies.

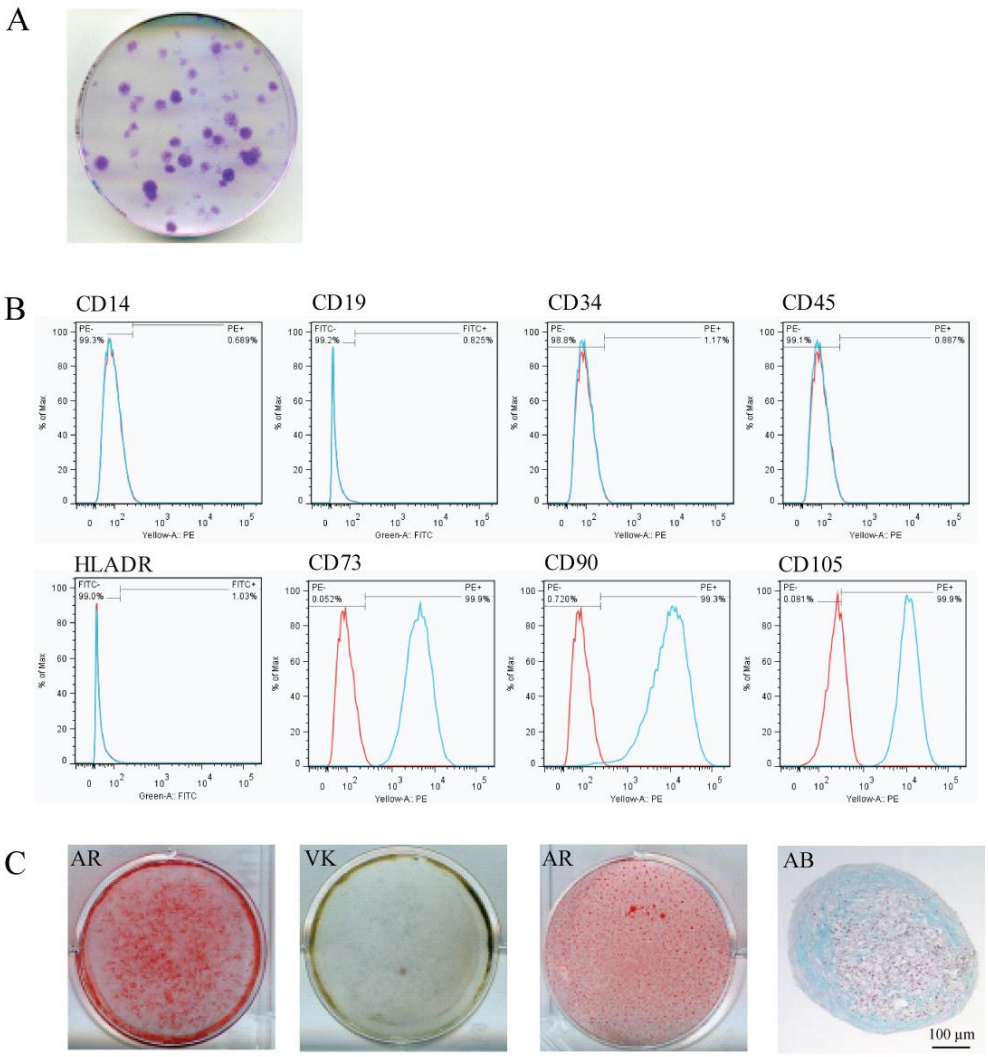

Figure 3.6. Characterization of plastic adherent human mesenchymal stem cells. (A) Colonies of adherent cells formed when passaging hMSCs (P3) were seeded on to tissue culture plastic as depicted by crystal violet staining (B) Single-color flow cytometry as represented by phycoerythrin (PE) and Fluorescein isothiocyanate (**FITC**) histograms were performed on passage 3 hMSCs after examination for the expression of surface markers CD73, CD90, CD105, CD14, CD19, CD34, CD45 and HLA-DR. The hMSCs expressed the MSC-related markers CD73, CD90, CD105 at significantly high levels (> 99% positive) while lacking the expression of haematopoeitic markers (< 2% positive) of CD14, CD19, CD34, CD45 and HLA-DR indicating that the hMSCs are not confounded by other cells. Red lines represent isotype IgG controls gated at 1 % and blue lines represent surface markers under study. (C) Passage 3 hMSCs were subjected to osteogenic, adipogenic, or chondrogenic *in vitro* differentiation to for 28 days. Mineralization in osteogenic cultures stained positively with Alizarin Red (AR) and von Kossa (VK). The lipid droplets in adipogenic cultures and glycosaminoglycans in sections of the chondrocyte pellets were detected by Oil Red O (OR) and Alcian blue (AB) staining respectively.

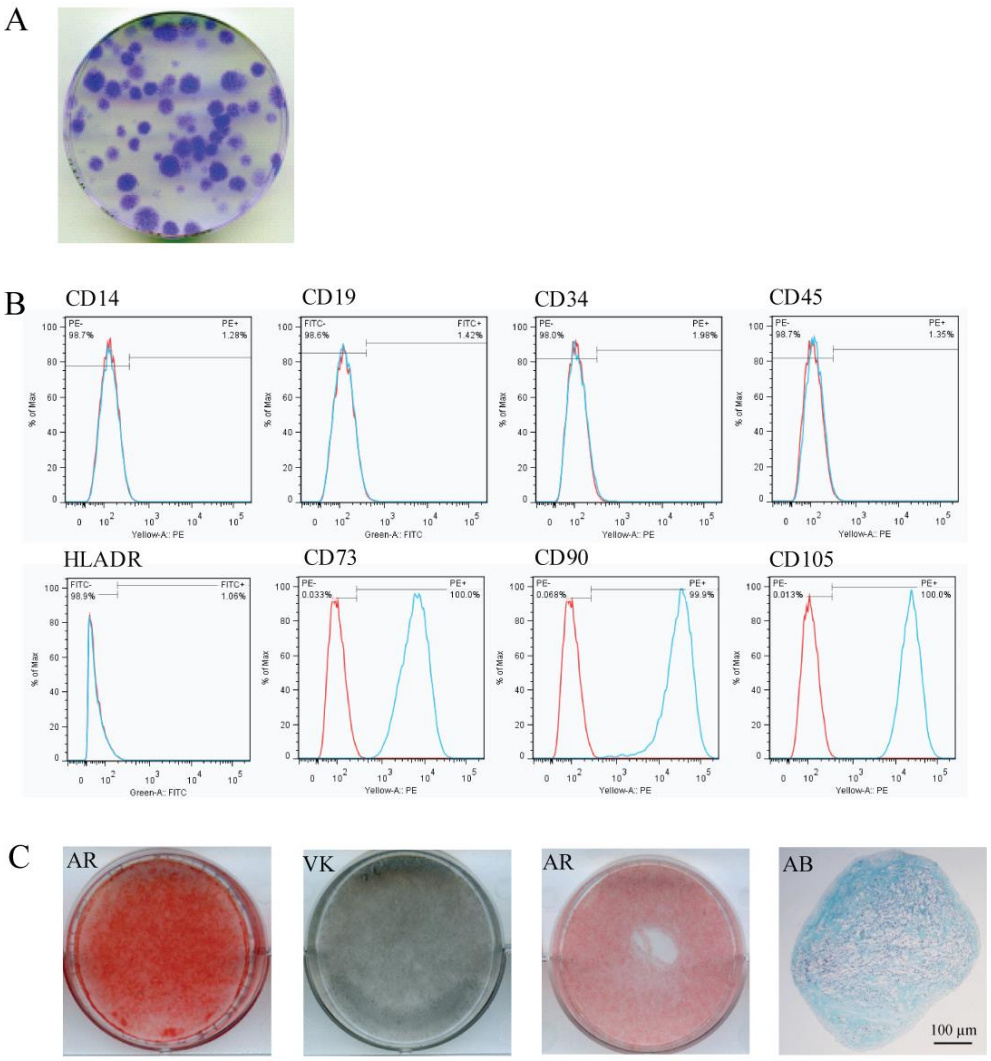

Figure 3.7. Characterization of STRO-1 isolated human mesenchymal stem cells. (A) Colonies of adherent cells formed when passaging hMSCs (P3) were seeded on to tissue culture plastic as depicted by crystal violet staining (B) Single-color flow cytometry as represented by phycoerythrin (PE) and Fluorescein isothiocyanate (**FITC**) histograms was performed on passage 3 hMSCs examining the expression of surface markers CD73, CD90, CD105, CD14, CD19, CD34, CD45 and HLA-DR. The hMSCs expressed the MSC-related markers CD73, CD90, CD105 at significantly high levels (> 99% positive) while lacking the expression of haematopoeitic markers (< 2% positive) of CD14, CD19, CD34, CD45 and HLA-DR indicating that the hMSCs are not confounded by other cells. Red lines represent isotype IgG controls gated at 1 % and blue lines represent surface markers under study. (C) Passage 3 hMSCs were subjected to osteogenic, adipogenic, or chondrogenic *in vitro* differentiation to for 28 days. Mineralization in osteogenic cultures stained positively with Alizarin Red (AR) and von Kossa (VK). The lipid droplets in adipogenic cultures and glycosaminoglycans in sections of the chondrocyte pellets were detected by Oil Red O (OR) and Alcian blue (AB) staining respectively.

3.3.2.2. HS8G^{+ve} enhances hMSC proliferation; BrdU incorporation assay

Having established that HS8^{+ve} variants generally have a higher affinity for FGF-2, next it was necessary to determine whether the HS variants have the ability to drive hMSC proliferation. For this, both preparations of hMSCs were again utilised. First a BrdU incorporation proliferation assay was employed, where BrdU incorporates in place of thymidine into the DNA of proliferating cells and is measured photometrically using TMB substrate.

Passage 4-6 cells were seeded at a density of 5000/cm^2 and cultured for 36 h with different HS variants added to maintenance media as stand-alone media supplements. After 2 h exposure to BrdU, cell proliferation was measured photometrically. Irrespective of GAGs, for both preparations, hMSC proliferation showed an upward trend with low doses, peaked with intermediate doses and a slight reduction with higher doses of HS variants (Fig. 3.8). For almost all the doses proliferation was equal or better than unsupplemented control cells in maintenance media. HS8^{-ve} yielded the least induction of fold increase absorption (maximum ~ 1.2-fold) while HS^{pm} had an intermediary effect on proliferation (maximum ~ 1.2-1.3 fold). In contrast, HS8G^{+ve} had the highest effect on hMSC proliferation, with a maximum fold-increase of 1.5 – 1.6-fold. The statistical testing by one-way ANOVA of plastic adherent cells revealed that, the fold-increase in absorption with HS8^{+ve} at concentrations of 1.25, 2.5, 5 and 10 µg/ml were significantly greater than the controls. In addition, in STRO-1$^+$ cells exposed to HS8^{+ve}, the significance was evident at concentrations of 0.625, 1.25, 2.5, 5 and 10 µg/ml. The fold-increases for plastic adherent and STRO-1 hMSCs with media supplemented with of HS^{pm} and HS8^{-ve} were not significantly different from the

unsupplemented control at any of the concentrations tested. The effect of HS8G^{+ve} on hMSC proliferation was consistent with its higher affinity to FGF-2.

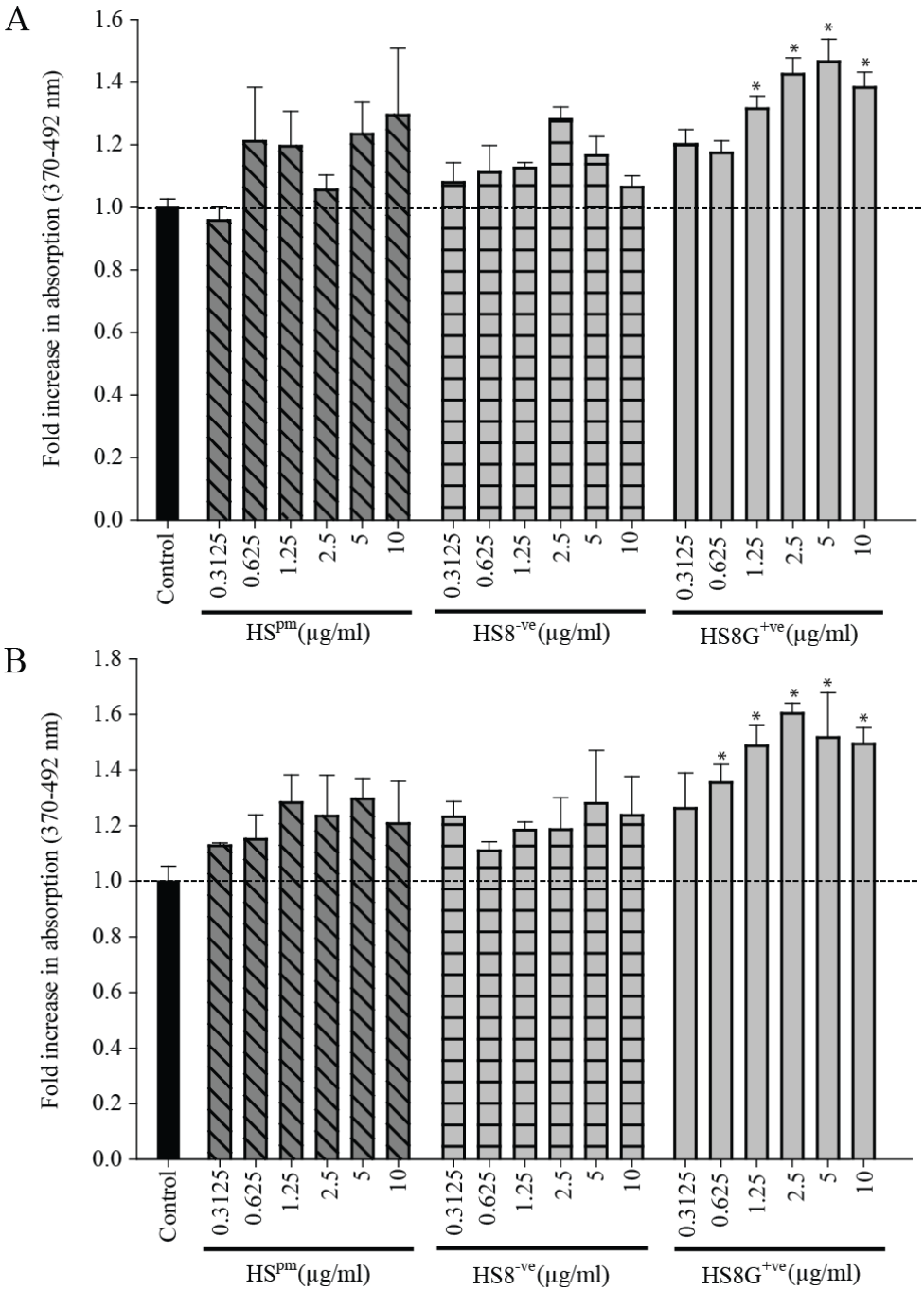

Figure 3.8. HS8G^{+ve} enhances hMSC proliferation. Cells were seeded at 5000/well in 96-well plates and cultured for 36 h with different doses of the HS variants (0, 0.156, 0.3125, 0.625, 1.25, 2.5, 5 and 10 µg/ml) as stand-alone media supplements. BrdU incorporation into the DNA of proliferating cells was measured photometrically using TMB substrate. The graphs show the dose responses of (A) plastic adherent hMSCs (B) STRO-1 hMSCs in the presence of unfractionated HS^{pm}, HS8^{-ve} and HS8G^{+ve}. Significant difference is represented as * when compared to control (0 µg/ml GAG) ($p<0.05$).

3.3.2.3. HS8G^{+ve} enhances hMSC proliferation; GUAVA Viacount® assay

BrdU assays provide a snap-shot of proliferation; the next investigation of cell proliferation utilized the GUAVA Viacount® assay. Cells were seeded at 3000 cells/cm^2 in 24-well plates and incubated for 6 days with or without the HS8G^{+ve} fraction. The existing media was changed once every 2 or 3 days with fresh media with or without HS8G^{+ve}. Counts of viable cells at periodic intervals were obtained after staining with the Viacount flex reagent and detected by microcapillary flow cytometry (Guava EasyCyte™ Plus System/CytoSoft™ software).

Irrespective of the media change interval (note the 3 day media change data on Fig. 3.10), and the day of the viability count, hMSCs showed the same trends of proliferation as with BrdU (Fig. 3.9). The hMSCs showed an upward trend in proliferation as shown by the fold-increase in viable cell counts with low doses, peaked with 2.5 µg/ml doses and displayed a slight reduction with higher doses of HS8G^{+ve}. The cell proliferation with 2-day media changes was higher than with media changes at 3-day intervals (Fig. 3.10). The effect of 2.5 µg/ml HS8G^{+ve} variant was evident even at day 2 (~ 1.15-fold) where the hMSCs have reached around ~ 40 % confluence by day 2, and the maximum effect (~ 1.4-fold) which was significantly higher than the controls, seen by day 4 when the cells reached ~ 80 % confluence (Fig. 3.9 A and B). Even though hMSCs were 100 % confluent by the 6th day, they still showed an increase in proliferation with the HS8G^{+ve} fraction.

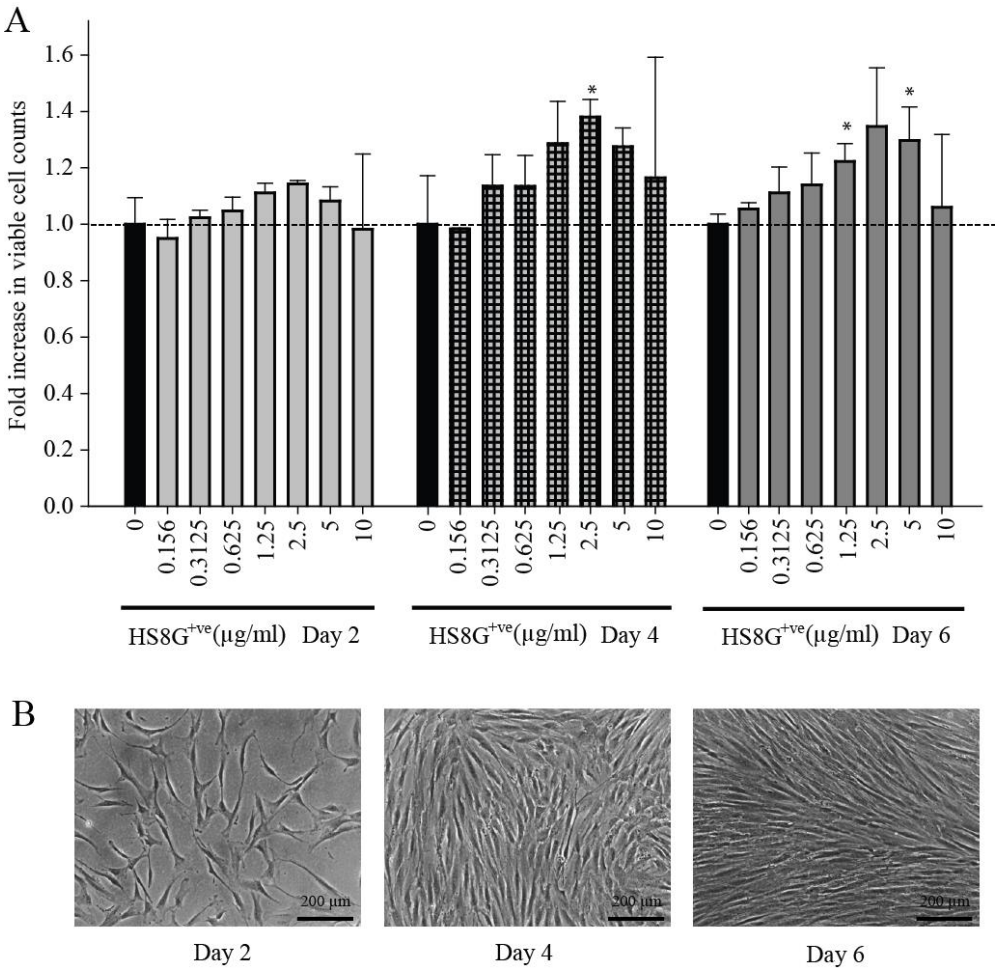

Figure 3.9. HS8G^{+ve} enhances plastic adherent hMSCs proliferation. Cells were seeded at 3000/cm^2 in 24-well plates and cultured for 6 days with HS8G^{+ve} at different doses (0, 0.156, 0.3125, 0.625, 1.25, 2.5, 5 and 10 µg/ml) as stand-alone media supplement with media change every 2 days. The cells were stained with Viacount flex reagent (Millipore) and viable cells detected by the microcapillary flow cytometry platform of Guava EasyCyte™ Plus System/CytoSoft™ software (Millipore™). (A) The graph shows the dose-dependent fold increase in viable cell counts of plastic adherent hMSCs to HS8G^{+ve} at every 2 days of culture. (B) Phase-contrast photomicrographs of plastic adherent hMSCs cultured with 2.5 µg/ml HS8G^{+ve} variant. Bar represents 200 um. Significant difference is represented as * when compared to the control at equivalent day of cell count (0 µg/ml GAG) ($p<0.05$).

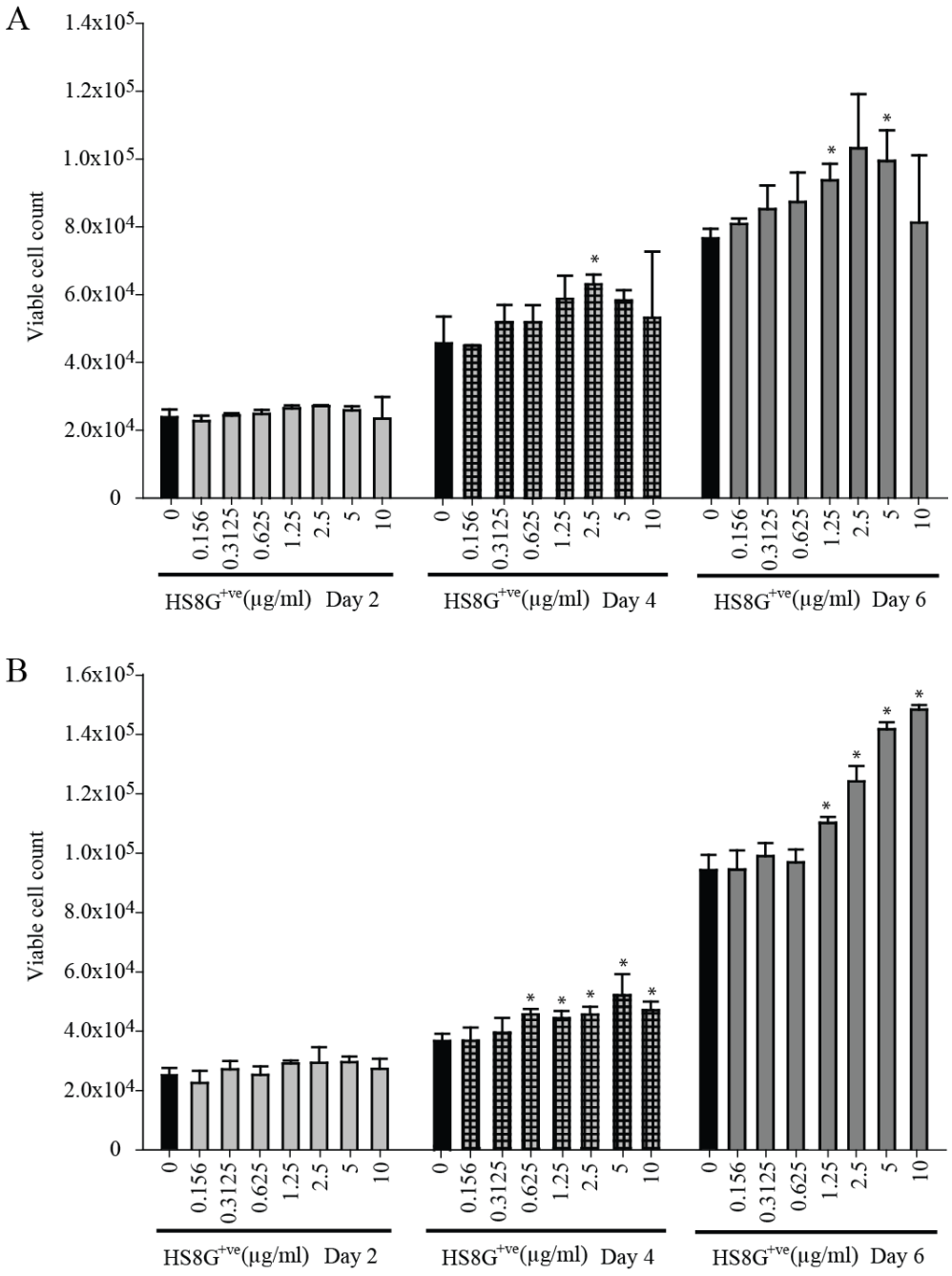

Figure 3.10. HS8G^{+ve} enhances plastic adherent hMSCs proliferation at different media change intervals. Cells were seeded at 3000/cm^2 in 24-well plates and cultured for 6 days with HS8G^{+ve} at different doses (0, 0.156, 0.3125, 0.625, 1.25, 2.5, 5 and 10 µg/ml) as stand-alone media supplement with media change every 2 and 3 days. The cells were stained with Viacount flex reagent (Millipore) and viable cells detected by the microcapillary flow cytometry platform of Guava EasyCyte™ Plus System/CytoSoft^{TM} software (Millipore^{TM}). The graph shows the dose-dependent increase in viable cell counts of plastic adherent hMSCs to HS8G^{+ve} at (A) every 2 days and at (B) every 3 days of culture. Significant difference is represented as * when compared to the control at equivalent day of cell count (0 µg/ml GAG) ($p<0.05$).

STRO-1^{+} hMSCs were also cultured for 4 days with or without HS8G^{+ve} (Fig. 3.11). Similar to the proliferation with plastic adherent hMSCs, the HS8G^{+ve} fraction at 2.5 µg/ml showed the highest fold stimulus of STRO-1 cell viability (~ 1.5-fold) which was significantly higher than the control.

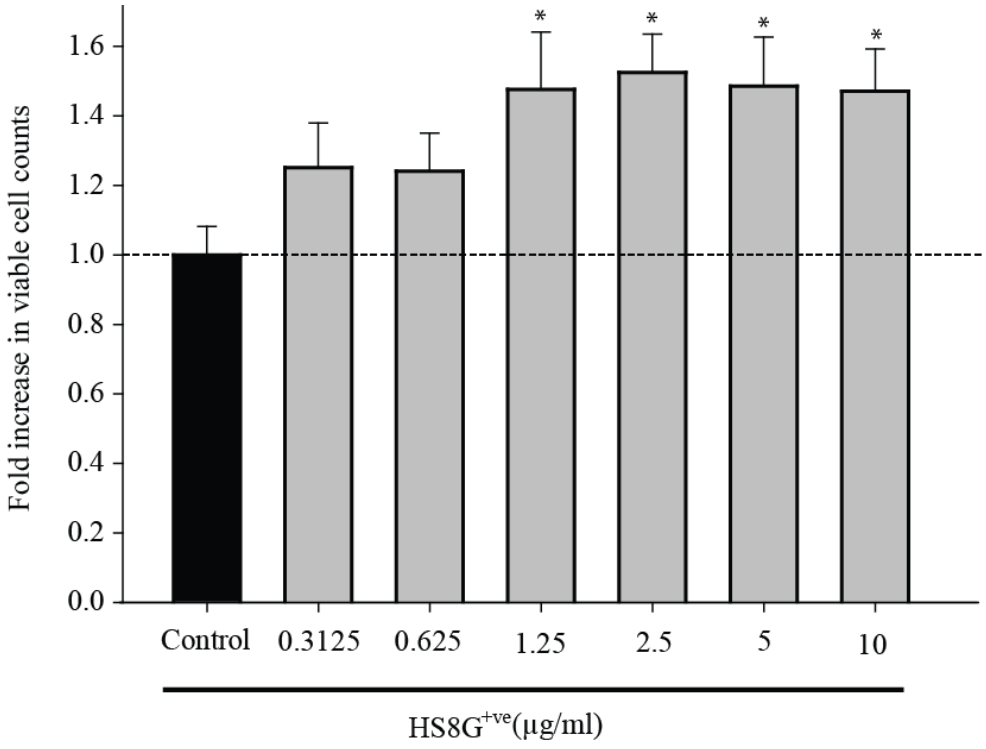

Figure 3.11. HS8G^{+ve} enhances STRO-1 hMSC proliferation. Cells were seeded at 3000/cm^2 in 24-well plates and cultured for 4 days with HS8G^{+ve} at different doses (0, 0.156, 0.3125, 0.625, 1.25, 2.5, 5 and 10 µg/ml) as stand-alone media supplement with media change at every 2 days. The cells were stained with Viacount flex reagent (Millipore) and viable cells detected by the microcapillary flow cytometry platform of Guava EasyCyte™ Plus System/CytoSoft™ software (Millipore™). The graph shows the dose-dependent fold increase in viable cell counts of STRO-1 hMSCs to HS8G^{+ve} after 4 days of culture. Significant difference is represented as * when compared to the control (0 µg/ml GAG) ($p<0.05$).

3.3.2.4 HS8G^{+ve}, HS8C^{+ve} and HS8B^{+ve} has similar effect on hMSCs proliferation

As confirmed by the GAG ELISA assay all the HS8^{+ve} fractions, HS8 Gandhi (HS8G^{+ve}), HS8 Cardin (HS8C^{+ve}) and HS8 Baird (HS8B^{+ve}), dose-dependently increased their binding capacity for FGF-2. Hence, next the various HS8^{+ve} variants effect on hMSC proliferation were examined by means of BrdU incorporation (Fig. 3.12) and GUAVA Viacount® proliferation assays (Fig. 3.13). The BrdU incorporation assay over 36 h showed a similar cell proliferation for all three HS8^{+ve} fractions (Fig. 3.12). The statistical testing of one-way ANOVA in plastic adherent cells revealed that, the fold-increase in absorption with HS8G^{+ve} at concentrations of 1.25, 2.5, 5 and 10 µg/ml were significantly greater than the controls. In addition, with HS8C^{+ve} the significance was evident at concentrations of 0.3125, 0.625, 1.25, 2.5, 5 and 10 µg/ml and with HS8B^{+ve} the significance was evident at concentrations of 0.625, 1.25, 2.5, 5 and 10 µg/ml. Furthermore, with GUAVA, where cells were cultured for 4 days with 2.5 µg/ml of any of the three HS8^{+ve} fractions, each showed similar fold-increases in their viable cell count, without any significant difference between them (Fig. 3.13).

These data confirmed that the three HS8^{+ve} fractions (HS8G, HS8C and HS8B) are able to stimulate similar levels of biological activity. As seen in chapter 2, HS8G^{+ve} fractions had the highest yield after isolation by affinity chromatography (table 2.1). Thus, henceforth through this thesis, all subsequent experiments were performed with the HS8G^{+ve} fraction, which will hereafter be referenced as the HS8^{+ve} fraction variant.

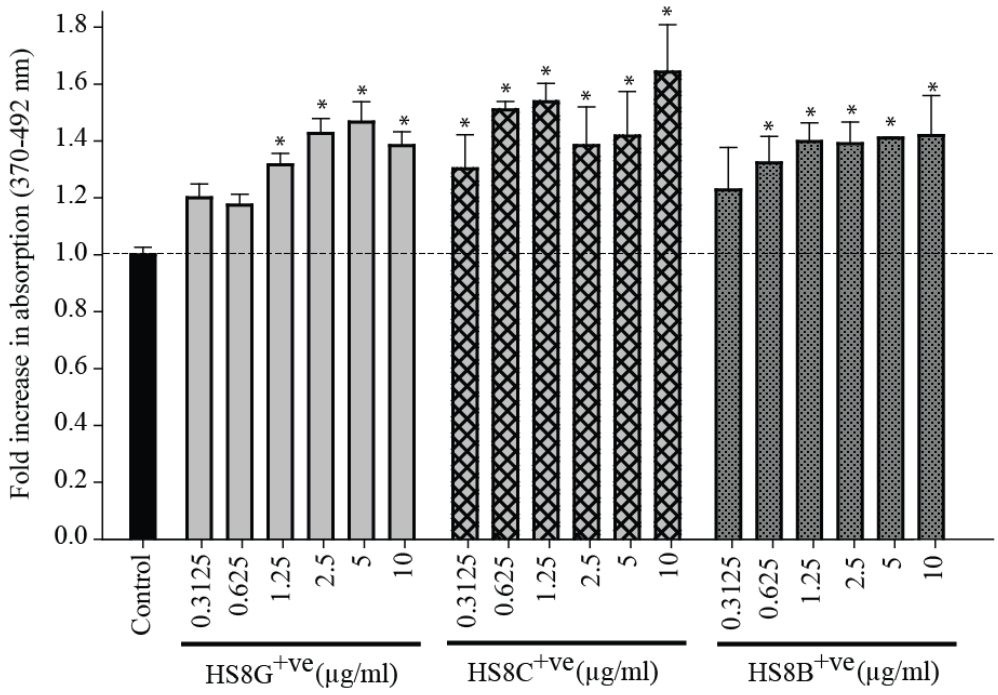

Figure 3.12. HS8G^{+ve}, HS8C^{+ve} and HS8B^{+ve} have similar effects on hMSC proliferation. Cells were seeded at 5000/well in 96-well plates and cultured for 36 h with different HS8^{+ve} fractions (HS8G^{+ve}, HS8C^{+ve} and HS8B^{+ve}) at different doses (0, 0.3125, 0.625, 1.25, 2.5, 5 and 10 µg/ml) as stand-alone media supplements. BrdU incorporated in place of thymidine into the DNA of proliferating cells was measured photometrically using TMB substrate. The graph shows the dose-responses of plastic adherent hMSCs in the presence of different HS8^{+ve} fractions. Significant difference is represented as * when compared to control (0 µg/ml GAG) ($p<0.05$).

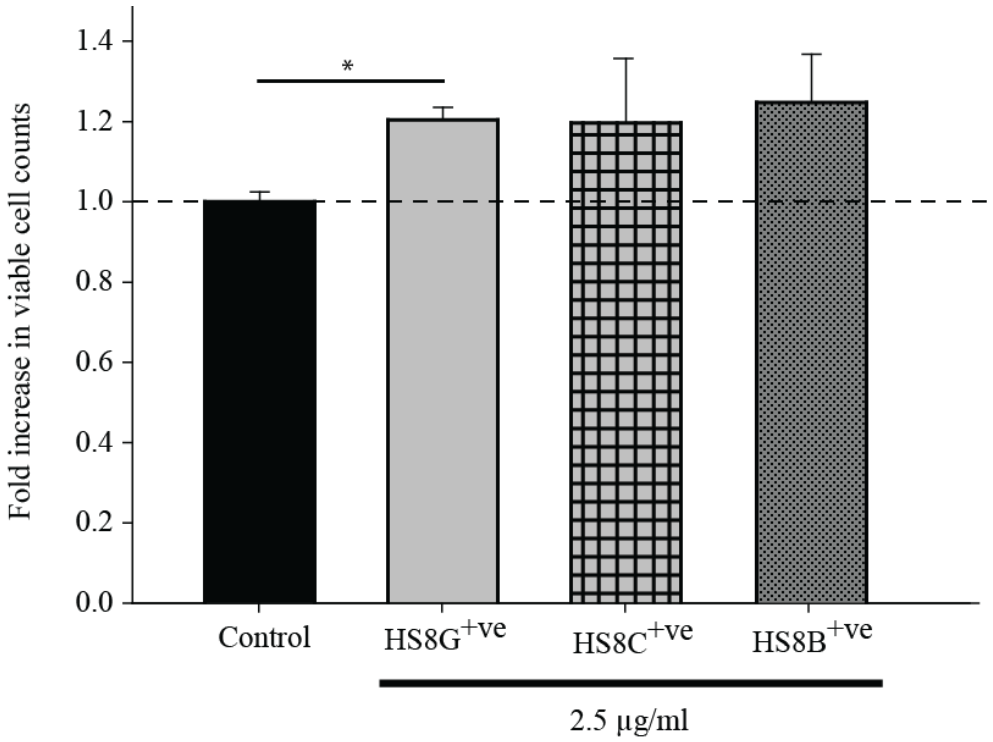

Figure 3.13. . HS8G+ve, HS8C+ve and HS8B+ve have similar effects on hMSC proliferation. Cells were seeded at 3000/cm^2 in 24-well plates and cultured for 4 days with 2.5 µg/ml of three HS8^{+ve} variants (HS8G^{+ve}, HS8C^{+ve} and HS8B^{+ve}) as stand-alone media supplement with media change every 2 days. The cells were stained with Viacount flex reagent (Millipore) and viable cells detected by the microcapillary flow cytometry platform of Guava EasyCyte™ Plus System/CytoSoft^{TM} software (Millipore^{TM}). The graph shows the proliferation of plastic adherent hMSCs over 4 days in the presence of HS8G^{+ve}, HS8C^{+ve} and HS8B^{+ve}. A similar fold increase in viable cell counts were observed with each of the variant tested. Significant difference is represented as * when compared to 2.5 µg/ml of HS8G^{+ve} variant ($p<0.05$).

3.3.2.5. HS8^{+ve} expands more hMSCs than other GAGs preparations

Lastly, while still exploiting short-term proliferation assays, it was necessary to confirm whether HS8^{+ve} had greater effects on cell proliferation than either crude HS^{pm} or flow-through HS8^{-ve} (Fig. 3.14). Irrespective of HS fraction, hMSCs proliferated in similar manner, an upward trend with low doses, peaking with intermediate doses and a slight reduction with higher doses. However, the fold-increase in viable cell counts with HS8^{+ve} at concentrations of 1.25 and 2.5 µg/ml were significantly greater than the controls. The fold-increases for cells with media supplemented with of HS^{pm}

and HS8^{-ve} were not significantly different from the unsupplemented control at any of the concentrations tested. The highest fold-increase (~ 1.4-fold) was shown by HS8^{+ve} at 2.5 µg/ml. Crude HS^{pm} and HS8^{-ve} had their greatest fold-increase at the 1.25 µg/ml concentration (~ 1.1-fold). In statistical testing by one-way ANOVA, the HS8^{+ve} stimulus was significantly greater than for HS^{pm}. Therefore, for the long-term proliferation assays that will be described in Chapter 4,I was able to optimize the concentrations for each HS fraction (HS8^{+ve} at 2.5 µg/ml, HS^{pm} and HS8^{-ve} at 1.25 µg/ml).

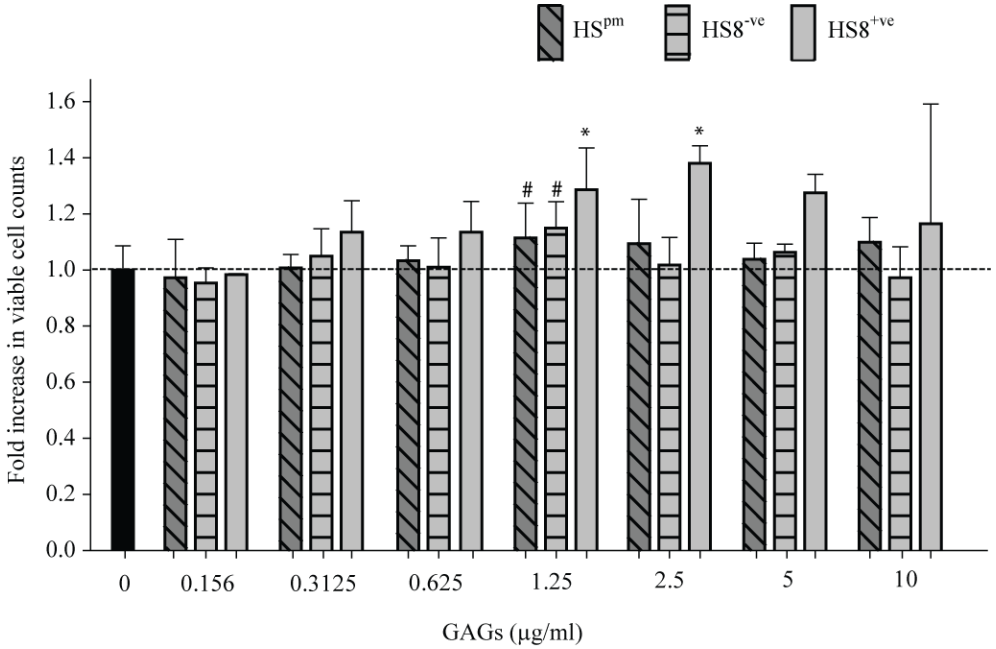

Figure 3.14. HS8^{+ve} expands more hMSCs compared to other GAGs. Cells were seeded at 3000/cm^2 in 24-well plates and cultured for 4 days with HS^{pm}, HS8^{-ve} and HS8G^{+ve} at different doses (0, 0.156, 0.3125, 0.625, 1.25, 2.5, 5 and 10 µg/ml) as stand-alone media supplement with media change every 2 days. The cells were stained with Viacount flex reagent (Millipore) and viable cells detected by the microcapillary flow cytometry platform of Guava EasyCyte™ Plus System/CytoSoft™ software (Millipore™). The graph shows the dose dependent fold-increase in viable cell counts of plastic adherent hMSCs to HS8^{+ve} at 4 days of culture. Significant difference is represented as * when compared to control (0 µg/ml GAG) ($p<0.05$) and $^{\#}$ when compared to 2.5 µg/ml of HS8^{+ve} dose ($p<0.05$).

3.3.3. Heparin-Sepharose bead competition assay

Heparin-Sepharose bead competition assays were performed to further explore the relative affinity of HS variants for FGF-2. This assay measures the ability of each HS variant to competitively inhibit the relatively strong binding of FGF-2 to heparin. In the case of a successful challenge one would expect lower FGF-2 binding to the heparin beads at the end of the assay, indicating that the particular HS fraction binds to FGF-2 with a higher affinity.

First it was necessary to establish an optimal working concentration of FGF-2. Various FGF-2 concentrations (0-80 ng/ml) were used and their binding to heparin beads detected by ELISA. The FGF-2 saturation curve revealed that FGF-2 binds to heparin in concentration-dependent manner, with maximal binding occurring at 40 ng/ml of FGF-2 (Fig. 3.15A). A sub-optimal FGF-2 concentration (10 ng/ml) which was statistically significant when compared to the maximal binding of FGF-2 to heparin (40 ng/ml), chosen to forestall false positive results from non-specific binding, was selected from the saturation curve and from the immunoblots (Fig. 3.15 A and B).

In the subsequent competition assay I used 10 ng/ ml of FGF-2 as the control, and its absorbance was used as the 100 % "FGF-2 bound" to the beads. FGF-2 was pre-incubated with soluble heparin (as a positive control), HS^{pm}, $HS8^{-ve}$ and $HS8^{+ve}$ each (5, 50 and 100 μg) and the results normalized to the absorbance of 100 % FGF-2-bound beads. The values were plotted as % bound to beads relative to this 100 % level (Fig. 3.16A). The HS fractions that more specifically bound to FGF-2 would competitively inhibit the binding of the FGF-2 to the heparin beads. The soluble heparin control (100 μg), being

the most negatively charged variant, could almost completely inhibit FGF-2 binding (down to only ~ 8 % binding) to the heparin beads.

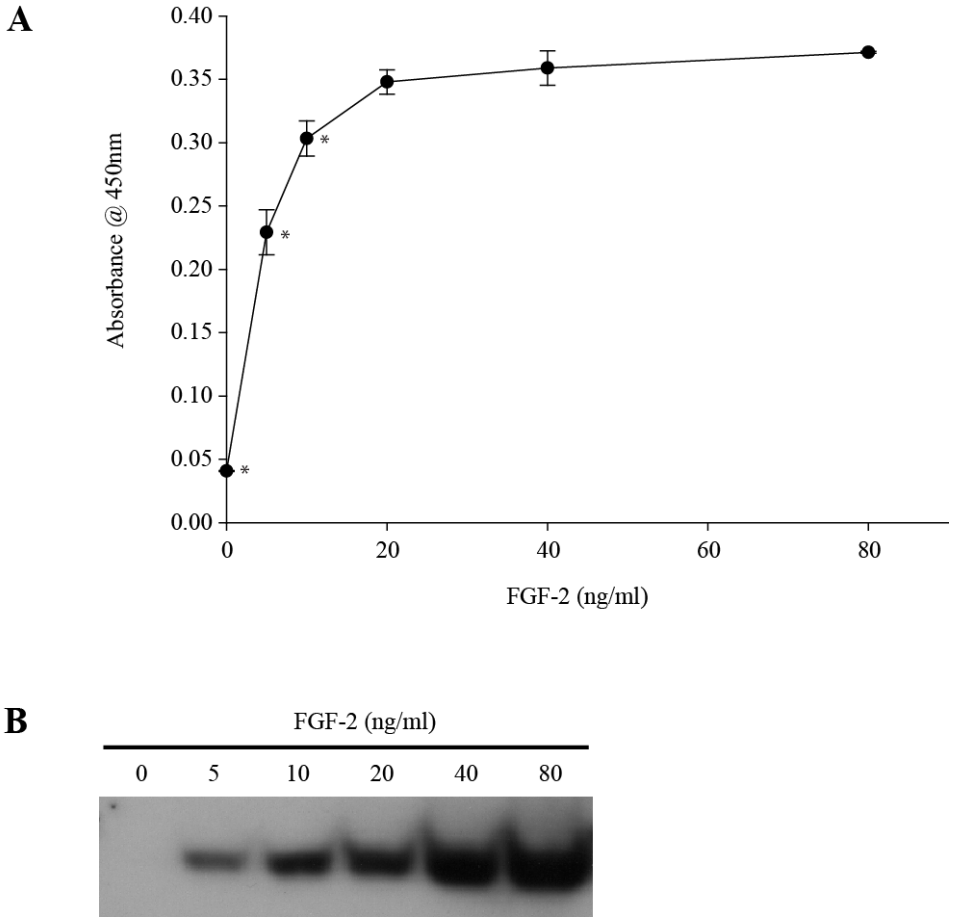

Figure 3.15. FGF-2 binding profile on heparin beads. (A) Beads were incubated with different amounts of FGF-2 (0, 10, 20,40 and 80 ng/ml), at sub-optimal binding levels. To prevent non-specific binding, to prevent false positive results, 10 ng/ml of FGF-2 was used for all subsequent competition assay. (B) Immunoblot images of FGF-2 incubation with heparin beads. Significant difference is represented as * when compared to maximal binding of FGF-2 to heparin (40 ng/ml) ($p<0.05$).

The $HS8^{-ve}$ fraction had the weakest binding affinity for FGF-2, as shown by the high proportion of "compatibility". Increasing amounts of $HS8^{-ve}$, even at 100 μg, could only partially inhibit the interactions between FGF-2 and the beads, with a substantially higher amount (~ 55 %) remaining bound to the beads. Intermediate binding affinity to FGF-2 was shown by HS^{pm}, where, with 100 μg, ~ 51 % was still bound to the beads. In contrast, with increasing amounts of $HS8^{+ve}$, a concentration-dependent inhibition of FGF-2 binding to the beads was observed, in a manner not significantly different to the positive heparin control (~ 10 % bound at 100 μg of $HS8^{+ve}$). This clearly indicated that HS^{pm} and $HS8^{-ve}$ have much less competitive binding affinity for FGF-2 as compared to the heparin and the $HS8^{+ve}$. The findings followed our prediction that the binding affinity of $HS8^{+ve}$ for FGF-2 should be the greater, and that unfractionated HS^{pm}, which still contains a proportion of $HS8^{+ve}$, should have an intermediate binding capacity, and that the denuded $HS8^{-ve}$ should have relatively little competitive capacity. The band intensities of the immunoblotting results also revealed the same descending order of binding to FGF-2; heparin > $HS8^{+ve}$ > HS^{pm} > $HS8^{-ve}$ (Fig. 3.16B). Collectively this assay further validated the GAG-ELISA results and thus our affinity chromatography platform approach for purifying better targeted HS fractions to FGF-2 from the starting HS^{pm} mixture.

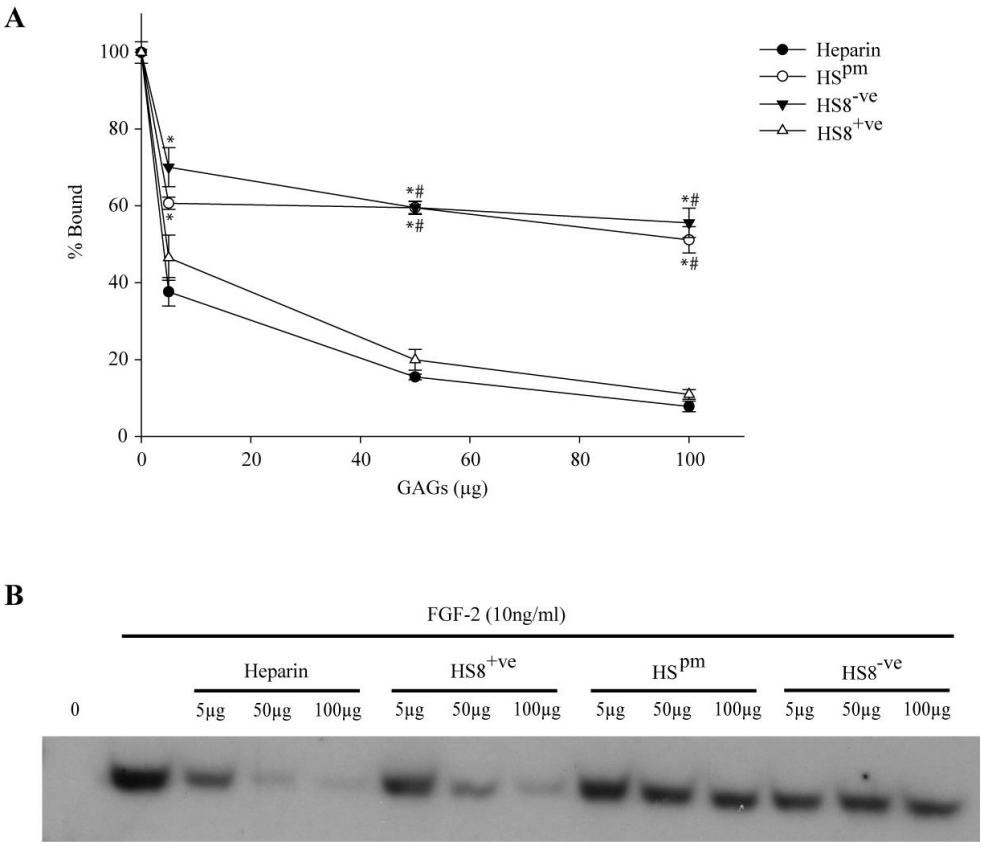

Figure 3.16. Inhibitory effects of HS variants on the binding of FGF-2 to heparin beads. (A) The competition assay was performed with exogenous soluble heparin (as a positive control), and the other HS fractions. Soluble heparin binds to most avidly to FGF-2, followed by $HS8^{+ve}$, HS^{pm} and $HS8^{-ve}$. (B) Immunoblot images of the FGF-2 left on the beads after competition. Significant difference is represented as * when compared to soluble heparin (positive control) at equivalent dose ($p<0.05$) and $^{\#}$ when compared to $HS8^{+ve}$ at equivalent dose ($p<0.05$).

3.3.4. Capillary Electrophoresis (CE)

Capillary electrophoresis (CE) is a sensitive and powerful technique for the separation of individual heparin disaccharides based on size and charge in a small electrolyte-filled capillary. This method was used to further analyze crude HS^{pm} and $HS8^{+ve}$ with the assistance of our collaborators at GlycoSyn, IRL (now Callaghan Innovation, Wellington, New Zealand).

Eleven of the 12 disaccharides in the standard mix were separated while the 12^{th} disaccharide, ΔUA-GlcN, did not migrate under the conditions used (Fig. 3.17), notwithstanding this disaccharide has not been reported to occur naturally in heparan sulfates. The R^2 values for the standard calibration curves ranged between 0.99 and 1.0. The heparin lyase I, II and III digests of HS^{pm} and $HS8^{+ve}$ were injected and out of the 11 disaccharides separated from the standard mix, only eight were detected in the HS digests. They were ΔUA-GlcNAc without any sulfation, mono-sulfates; ΔUA-GlcNS containing only N-sulfation, ΔUA-GlcNAc,6S containing only 6-O-sulfation, ΔUA2S-GlcNAc containing only 2-O-sulfation, di-sulfates; ΔUA-GlcNS,6S containing 6-O- and N-sulfation, ΔUA,2S-GlcNS containing 2-O- and N-sulfation, ΔUA2S-GlcNAc,6S containing 2-O- and 6-O-sulfation and tri-sulfates; and ΔUA,2S-GlcNS,6S containing 2-O-, 6-O- and N-sulfation.

The disaccharide composition of each digested HS variant is shown in Table 3.1. The HS^{pm} digests revealed a larger complement of ΔUA-GlcNAc (37 %) and ΔUA-GlcNS (25 %), ΔUA-GlcNAc,6S (10 %), ΔUA2S-GlcNAc (10 %) that corresponds to a combination of mono- and un-sulfated disaccharides. It has a decreased proportion (16 % in total) of disulfated disaccharide (ΔUA-GlcNAc,6S, ΔUA-GlcNS,6S and ΔUA2S-GlcNAc,6S)

and only a small proportion (7 %) of trisulfated disaccharide (ΔUA,2S-GlcNS,6S). The distinctive feature of the

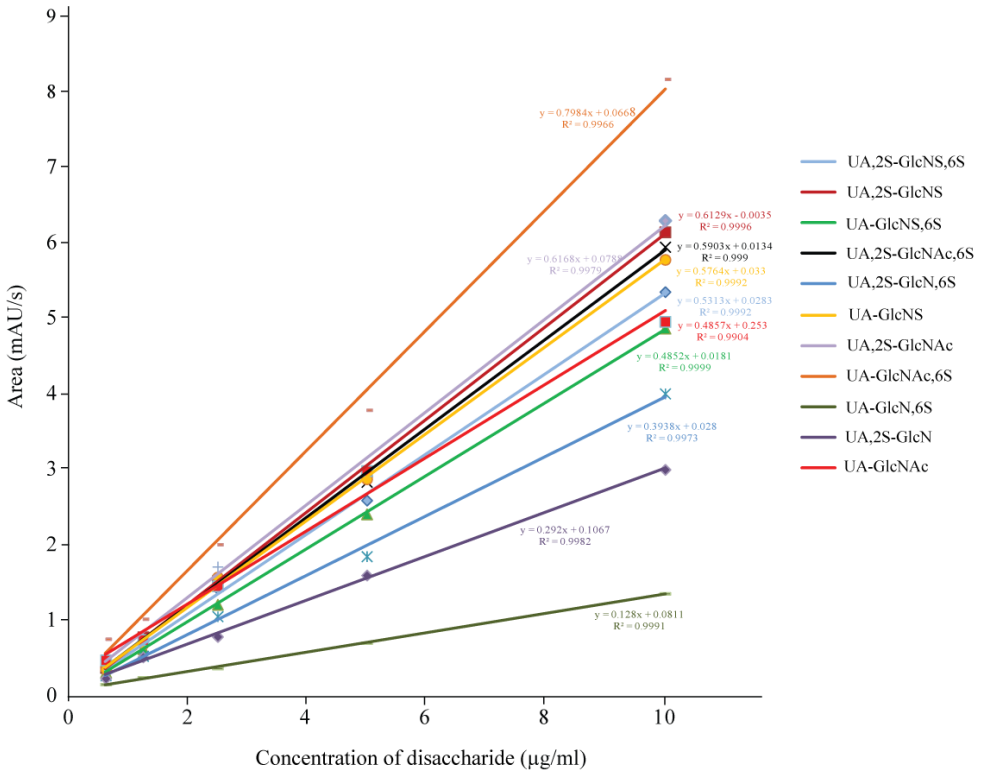

Figure 3.17. Δ-disaccharide standard curve. Different dilutions of each standard (Iduron) were separated by CE, the area-under-the curve determined and standard curves plotted.

Table 3.1. Disaccharide composition of HS^{pm} and $HS8^{+ve}$

Disaccharides	Normalized weight % disaccharide	
	HS^{pm}	$HS8^{+ve}$
DHexUA,2S-GlcNS,6S	7.4	12.7
DHexUA,2S-GlcNS	5.6	7.2
DHexUA-GlcNS,6S	9.3	15.5
DHexUA,2S-GlcNAc,6S	4.3	6.5
DHexUA-GlcNS	25.2	15.7
DHexUA,2S-GlcNAc	0.8	1
DHexUA-GlcNAc,6S	10.1	8.9
DHexUA-GlcNAc	37.3	32.6

disaccharide analysis of $HS8^{+ve}$ is the relative enrichment of the trisulfated disaccharide (increased from 7 % to 13 %), the depletion of mono- and un-sulfated disaccharide (ΔUA-GlcNAc reduced from 37 % to 32 % and ΔUA-GlcNS reduced from 25 % to 15 %) compared with HS^{pm}. In addition, there was a clear increase from 9 % to 16 % in the di-sulfated disaccharide ΔUA-GlcNS,6S as compared to HS^{pm}.

The assays served to confirm that the differing biological activities of the HS fractions were subserved through sugar chains with different compositions.

3.3.5. Anti-coagulation assay: $HS8^{+ve}$ has no anti-coagulant activity

In the reactive phase of fracture healing, the formation of a haematoma plays an important role in the initiation of bone healing. Hence it made sense

to determine the anticoagulation activity of the HS8 variants, to confirm their suitability for use in fracture healing situations. Obviously HS fractions that prevent coagulation would be of little clinical use in regenerative medicine. The relative anti-coagulant activity of each HS variant was analyzed after complexing with antithrombin (Fig. 3.18).

In this assay pre-incubated antithrombin (AT) was combined with each HS variant together with excess Factor Xa (FXa). If the AT is activated during the pre-incubation after binding to HS variants, it leads to inactivation of FXa. Only the uninhibited FXa can cleave the chromogenic substrate S-2222 and release a chromophore (Fig. 3.17). Heparin, the supreme example of an anti-coagulant, activated AT, resulting in the inhibition of FXa even at the lowest concentration tested. It also showed a dose-dependent inhibition of FXa ($P<0.05$). In contrast, with HS^{pm}, $HS8^{-ve}$ and $HS8^{+ve}$ I observed only a slight reduction in inhibition of FXa. In the presence of HS^{pm} at a concentration of 2.5 μg/ml, FXa activity was significantly reduced, whereas $HS8^{-ve}$ and $HS8^{+ve}$ did not significantly activate antithrombin at any of the doses tested.

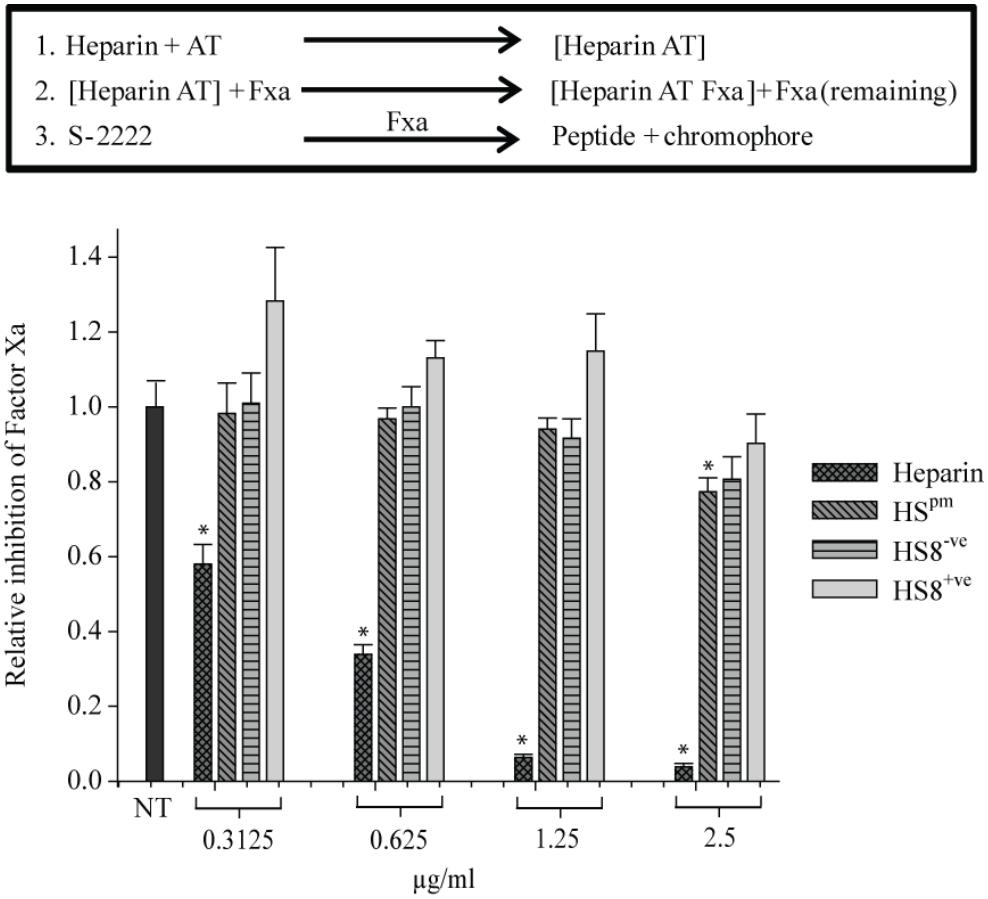

Figure 3.18. HS8^{+ve} has minimal anti-coagulant activity compared to heparin. At the indicated concentration, HS variants were pre-incubated with antithrombin (AT) before the addition of excess factor Xa (FXa). Any FXa that was not inhibited by AT was measured photometrically using chromogenic substrate S-2222. Relative inhibition was measured by normalizing the values to that of the treatment group containing no GAG (NT). Significant difference ($p<0.05$) is represented as * when compared to the treatment group containing no GAG.

3.3.6. Quantikine FGF-2 stability assay: $HS8^{+ve}$ prolonged FGF-2 stability

FGF-2 is highly unstable, with its viability dependent on the solvent used to dissolve it. Heparin is known to stabilize FGF-2 at an optimum culture temperature of 37 °C (Caldwell *et al*., 2004). The next test was whether $HS8^{+ve}$ could stabilize FGF-2. Therefore in this assay the stabilizing effects of HS^{pm}, $HS8^{+ve}$ and $HS8^{-ve}$ on FGF-2 was investigated against a heparin positive control.

The amount of exogenously added FGF-2 detectable in media subsequently decreased to a very marked degree over a 3-day test period (Fig. 3.19). FGF-2 levels dropped to 13 % within the first 24 h, and by 72 h, only 1.8 % was detectable in the culture media. As documented earlier in the presence of heparin, 74% of the FGF-2 could be detected after 24 h and 60 % after 72 h. All the other HS fractions tested were able to stabilize FGF-2 at intermediate levels as compared to heparin. When considering the three HS fractions in particular, $HS8^{-ve}$ showed the weakest levels of stabilization, where only 17 % of FGF-2 was detectable at the end of the 72 h incubation period. HS^{pm} stabilization of FGF-2 was at an intermediate level, with 56 % detectable after 24 h and 21 % after 72 h. The highest levels of stabilization of FGF-2 were offered by $HS8^{+ve}$, where 59 % of the growth factor could be detected after 24 h and 31 % after 72 h. By taking into account the initial and final amounts of FGF-2 present in solution after 48 h, the apparent half-life of FGF-2 ($t_{1/2} \approx 10$ h) was improved ~ 4-fold in the presence of $HS8^{+ve}$ ($t_{1/2} \approx 41$ h).

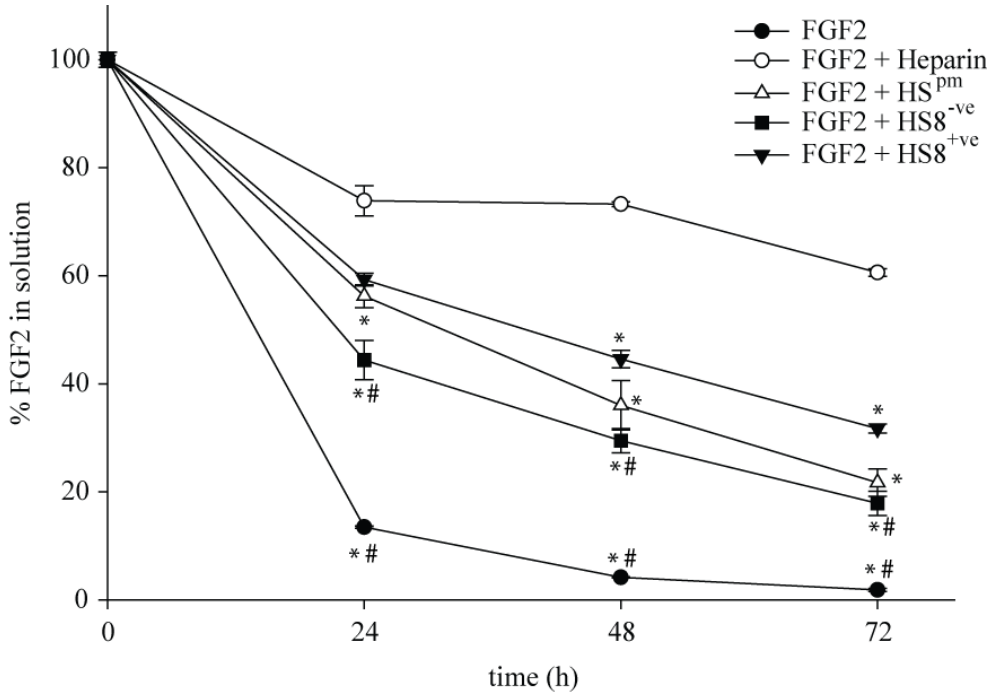

Figure 3.19. HS8^{+ve} prolongs FGF-2 stability. FGF-2 (2.5 ng/ml) was incubated alone or in the presence of 2.5 µg/ml of GAGs (Heparin, HS^{pm}, HS8^{+ve} and HS8^{-ve}) in 1 ml of hMSC culture media at 37^{0}C with 5% CO_2. Samples were collected at 0, 24, 48 and 72 h and analyzed by solid phase sandwich ELISA (R & D Systems). Significant difference is represented as * when compared to soluble heparin (positive control) at equivalent dose ($p<0.05$) and $^{\#}$ when compared to HS8^{+ve} at equivalent dose ($p<0.05$).

3.3.7. Differential Scanning Fluorimetry (DSF): HS8^{+ve} stabilize FGF-2 against thermal denaturation

FGF-2 is highly unstable and heparin is known to stabilize FGF-2 from thermal denaturation (Prestrelski *et al*., 1992; Vemuri *et al*., 1994). DSF can be used to measure protein-sugar interactions by means of a sensitive dye, Sypro Orange (Uniewicz *et al*., 2010). This dye binds and detects the exposed core residues of denatured proteins when the protein samples are subjected to a heating cycle. Hence I sought to determine the possibility of using DSF to measure the HS (heparin, HS^{pm}, HS8^{+ve} and HS8^{-ve}) variants' ability to stabilize FGF-2. First I needed to determine an optimal working concentration of FGF-2; various FGF-2 concentrations (2.5, 5, 7.5 and 10 µM) were used to

examine the thermal effect on FGF-2 (Fig. 3.20). The denaturation curves revealed that greater fluorescence was evident, in a concentration-dependent manner, compared to the negative control; the best signal was achieved when I used 10 μM of FGF-2 (Fig. 3.20A). The first derivatives of the denaturation curves were plotted, where the maxima defined the Tm of FGF-2 as 57.5 °C (Fig. 3.20B and Table 3.2).

Next, the optimal concentration of 10 μM of FGF-2 was used as the constant baseline and tested against a range of heparin concentrations (2.5, 5, 10 and 20 μM) (Table 3.3). The denaturation curves show that a stabilizing effect is apparent from 2.5 μM heparin (heparin-FGF-2 molar ratio 1:4), and that the stability increased with increasing concentrations of heparin (Fig. 3.21A). The plotted first derivatives of the denaturation curves showed an increasing Tm of FGF-2 with the increasing amounts of heparin used (Fig. 3.21B and Table 3.3). Hence DSF clearly showed that heparin has a concentration-dependent effect on FGF-2 stability, and can offer a means of comparison for the other HS fractions.

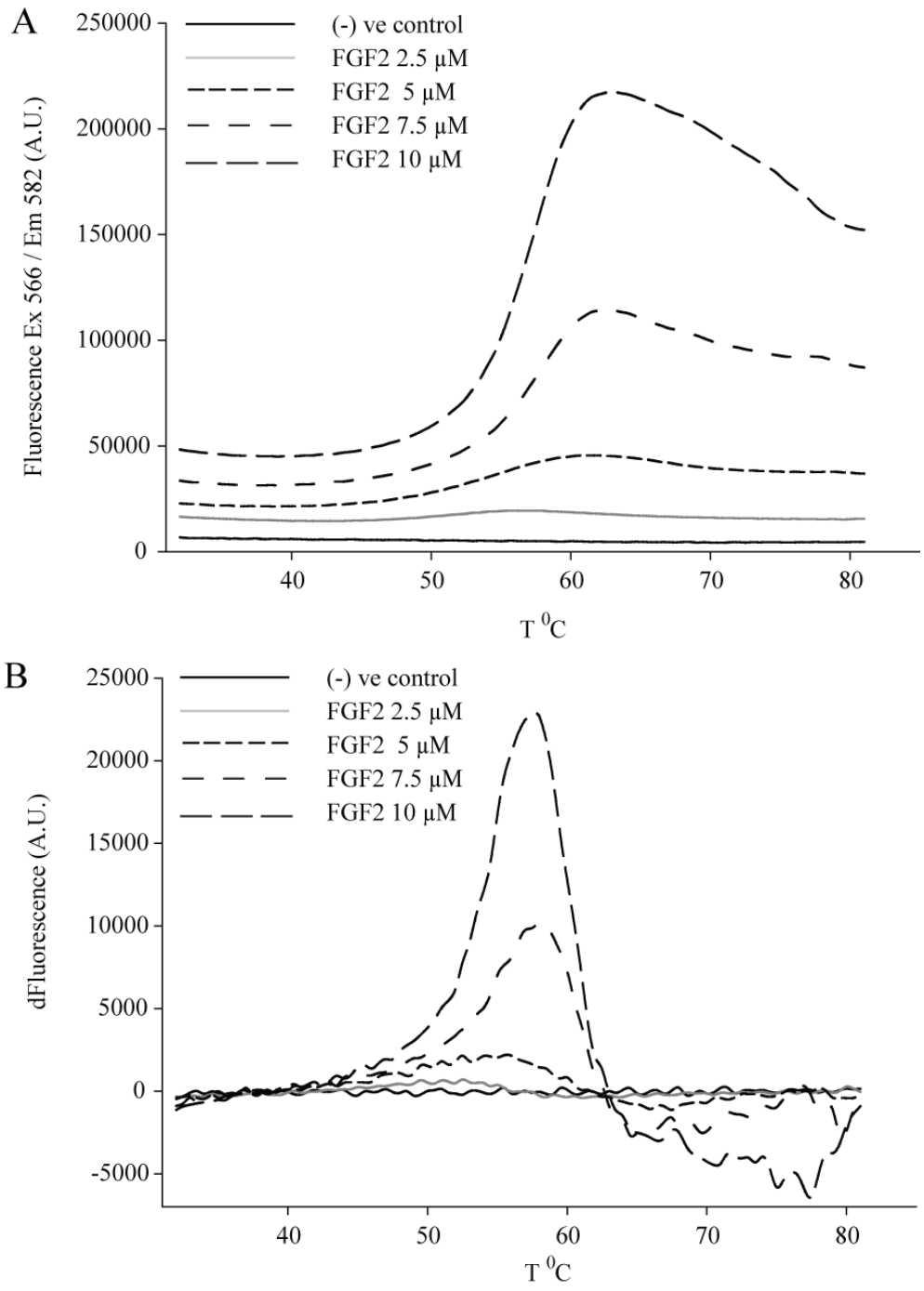

Figure 3.20. Thermal effect on FGF-2. (A) Melting curve profile of different concentrations of FGF-2 (2.5, 5, 7.5 and 10 µM) (B) The first derivatives of each melting curve where each maximum of the first derivative indicates the Tm (melting temperature)

Table 3.2. Concentrations of FGF-2 assayed and their corresponding mean Tm values, calculated from triplicate determinations.

FGF2 concentration		
μg/ml	μM	Tm ^{0}C
40	2.5	-
80	5	-
120	7.5	58
160	10	57.5

My aim was to find out whether the different HS variants have differing stabilization effects corresponding to their different binding affinities to FGF-2. The molar ratio of 1:1 of FGF-2:heparin was chosen for this experiment because of the medium-to-high stabilization effect seen, which in turn corresponded to the results of Uniewicz *et al* (Uniewicz *et al*., 2010). For the HS variants, the same concentration (160 μg/ml) was employed. The collected data were analyzed as detailed earlier and normalized to reveal the ability of each compound to stabilize FGF-2 relative to heparin (Fig. 3.22). The least thermal stabilizing affect was shown by $HS8^{-ve}$ and the greatest by $HS8^{+ve}$ as compared to heparin. In addition, HS^{pm} afforded an intermediate level of thermal stability of FGF-2. The stabilizing affect shown by $HS8^{+ve}$ was significantly higher than HS^{pm} and $HS8^{-ve}$. The previous GAG ELISA and heparin-Sepharose bead competition assays established that the HS variants affinity for FGF-2 is in the descending order of $HS8^{+ve} > HS^{pm} > HS8^{-ve}$. This was also evident in this assay, where among the HS variants tested, $HS8^{+ve}$ possessed the highest affinity for FGF-2 and correspondingly displayed the highest thermal stability for FGF-2.

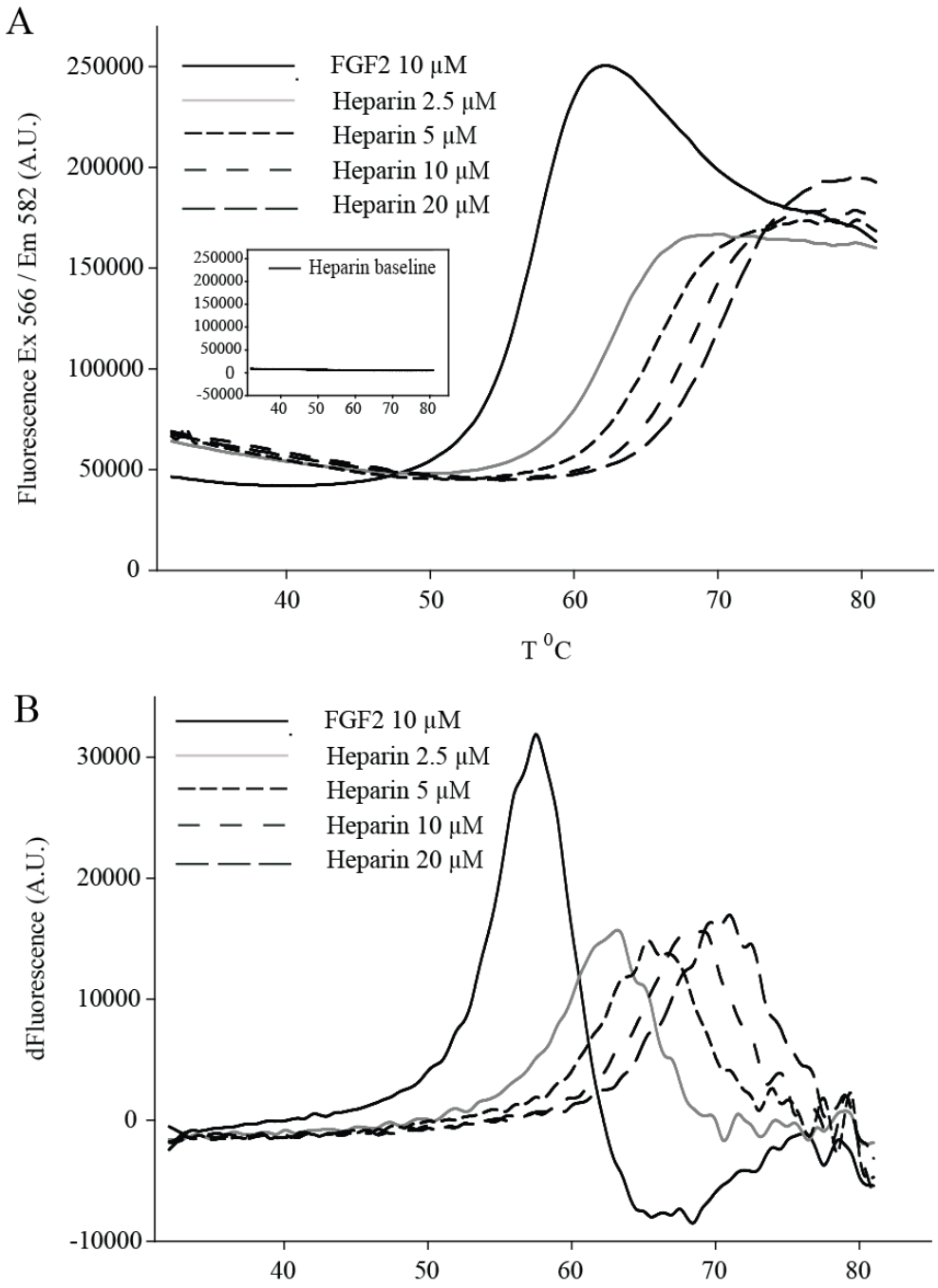

Figure 3.21. Heparin effect on thermal stabilization of FGF-2. (A) Melting curves of 10 µM FGF-2 in the presence of different concentrations of heparin (0, 2.5, 5, 10 and 20 µM). (B) The first derivatives of each melting curve; maximum indicates the Tm.

Table 3.3: Ratios of assayed concentrations of FGF-2 and heparin with their corresponding mean Tm values, calculated from triplicate determinations

FGF2 concentration		
µg/ml	µM	Tm ^{0}C
160	10	57.5

Heparin concentration			
µg/ml	µM	Molar ratio	Tm ^{0}C
40	2.5	0.25	63
80	5	0.5	65.5
160	10	1	68
320	20	2	71

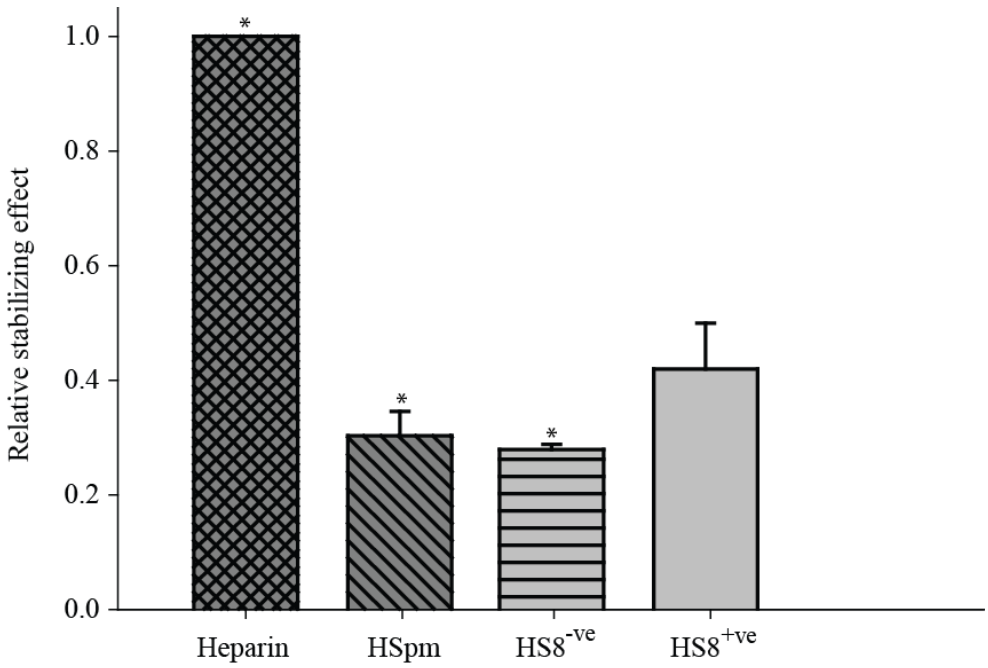

Figure 3.22. Relative thermostabilizing effect of HS variants on FGF-2 calculated according to equation (3) as compared to heparin. Results are the mean ± SD of two repeats after normalization.). Significant difference is represented as * when compared to $HS8^{+ve}$ ($p<0.05$).

3.3.8. Synergistic effect of $HS8^{+ve}$ and FGF-2 on hMSCs proliferation

As there was a statistically significant increase in hMSC proliferation when cells were cultured for 4 days with $HS8^{+ve}$ (1.25 and 2.5 µg/ml), it was used as a media supplement. Of course, FGF-2, as a media supplement, also increased hMSC growth (Fig. 3.23). The highest fold-increase in viable cell counts with statistical significance was triggered with 2.5 ng/ml of FGF-2.

Next, the proliferation response of hMSCs with a combination of an HS variant (either HS^{pm}, $HS8^{-ve}$ and $HS8^{+ve}$) was examined together with FGF-2. The cells were seeded at 3000 cells/cm^2 in 24-well plates and incubated for 4 days with suboptimal doses of FGF-2 (0.156 ng/ml) with or without increasing doses of each HS variant (0, 0.156, 0.3125, 0.625, 1.25, 2.5, 5 and 10 µg/ml) and the additive effect on FGF-2 mediated proliferation monitored (Fig. 3.24). Cells cultured in maintenance media (baseline control) supplemented with 2.5 ng/ml of FGF-2 served as positive control. FGF-2, even at a sub-optimal dose (0.156 ng/ml) increased hMSC proliferation by ~ 1.3-fold. The crude HS^{pm} and the flow-through $HS8^{-ve}$, even with increasing concentrations, were unable to increase cell proliferation beyond this 1.3-fold point. In contrast, $HS8^{+ve}$, even with only 0.3125 µg/ml added, together with 0.156 ng/ml of FGF-2, markedly increased the cell proliferation (~ 1.7-fold). This fold-increase in cell number was similar to the cell proliferation with 2.5 ng/ml of FGF-2 (~1-6 - 1.7-fold). Thus, I was able to reach the maximum fold-increase in hMSC proliferation with 16-times less FGF-2 (from 2.5 to 0.156 ng/ml) combined with 8-times less $HS8^{+ve}$ (from 2.5 to 0.3125 µg/ml). In addition, $HS8^{+ve}$ was also able to bind and increase the stability of FGF-2

under the culture conditions, as previously shown by binding assays and stability assays.

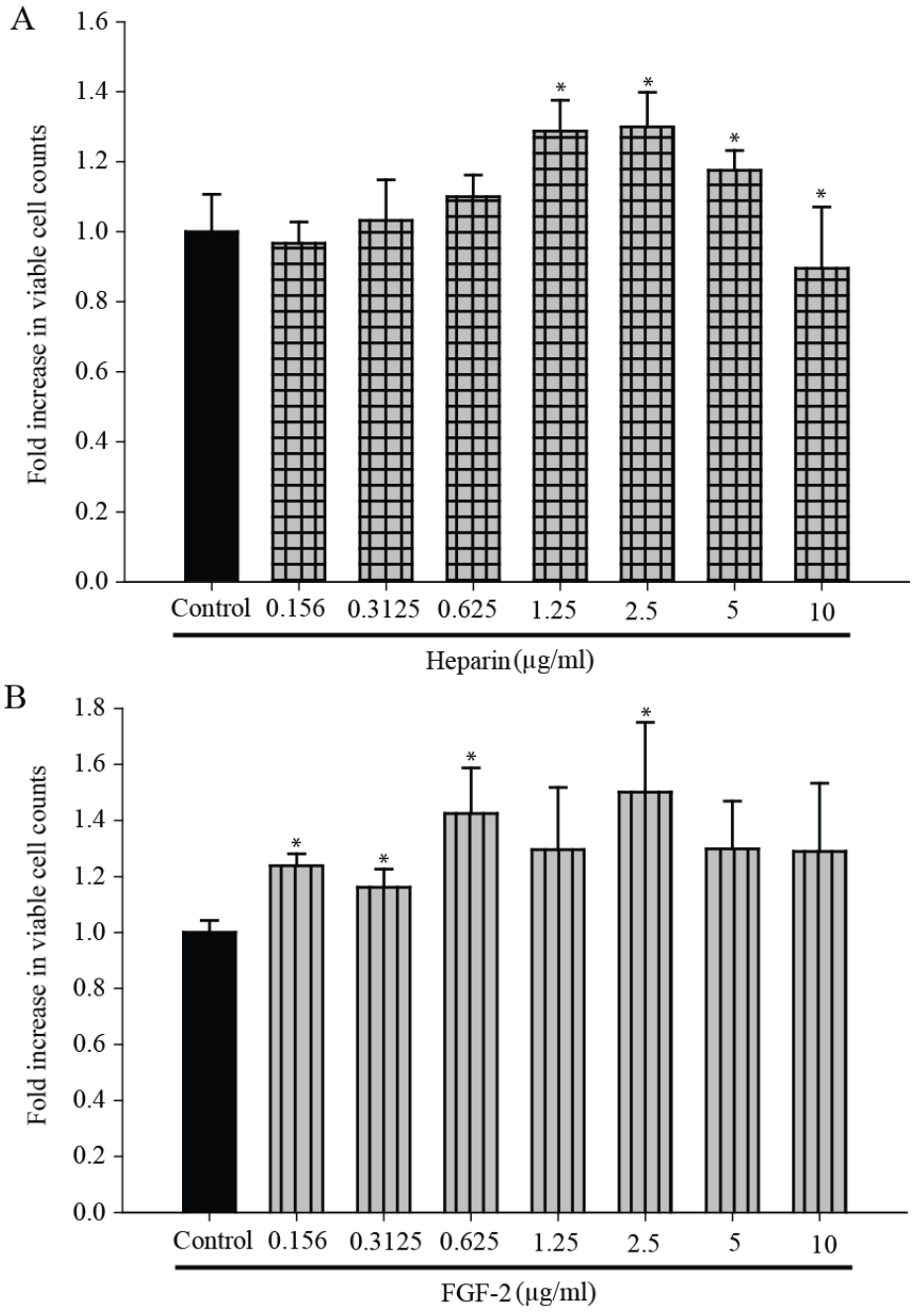

Figure 3.23. Heparin and FGF-2 (Positive controls) enhances plastic adherent hMSC proliferation. Cells were seeded at 3000/cm^2 in 24-well plates and cultured for 4 days with Heparin and FGF-2 at different doses (0, 0.156, 0.3125, 0.625, 1.25, 2.5, 5 and 10 µg/ml) as stand-alone media supplement with media change every 2 days. The cells were stained with Viacount flex reagent (Millipore) and viable cells detected by the microcapillary flow cytometry platform of Guava EasyCyte™ Plus System/CytoSoft™ software (Millipore™). The graph shows the dose dependent fold-increase in viable cell counts of plastic adherent hMSCs to (A) heparin and (B) FGF-2 at 4 days of culture. Significant difference is represented as * when compared to control (0 µg/ml GAG) ($p<0.05$).

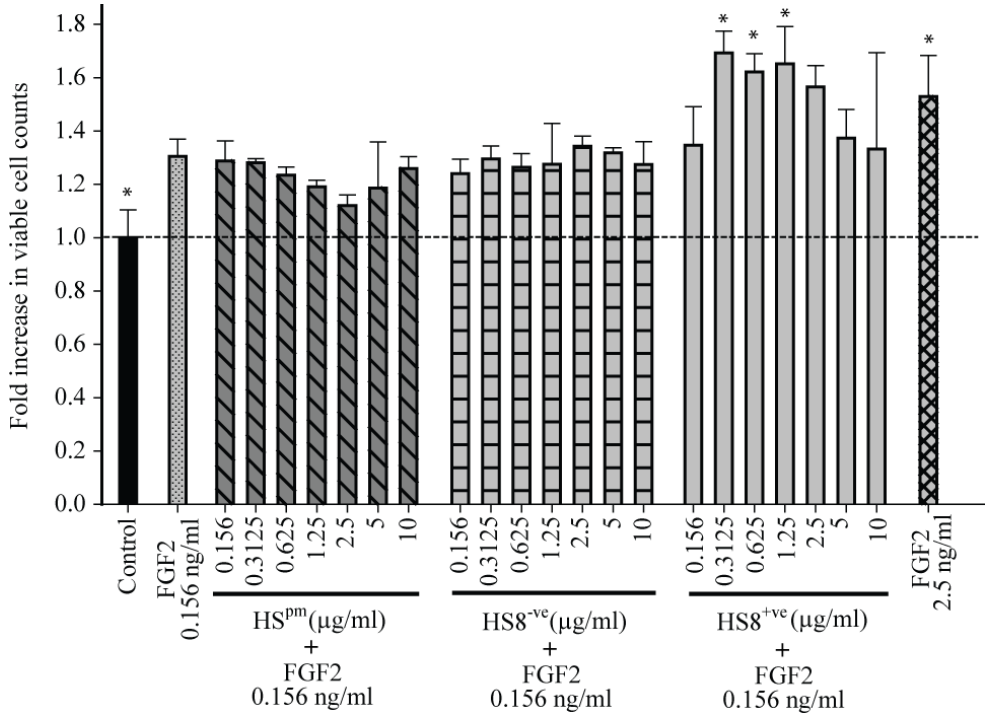

Figure 3.24. HS8^{+ve} enhances FGF-2-mediated MSC growth. Cells were seeded at 3000/cm^2 in 24-well plates and cultured for 4 days with HS^{pm}, HS8^{-ve} and HS8^{+ve} at different doses (0, 0.156, 0.3125, 0.625, 1.25, 2.5, 5 and 10 µg/ml) with or without FGF-2 (0.156 ng/ml) with media change at every 2 days. Cells cultured in maintenance media and with 2.5 ng/ml of FGF-2 served as baseline control and positive control respectively. The cells were stained with Viacount flex reagent (Millipore) and viable cells detected by the Guava EasyCyte™ Plus microcapillary flow cytometry platform and System/CytoSoft™ software (Millipore™). The graph shows the dose-dependent fold-increase in viable cell counts of plastic adherent hMSCs with varying doses of HS variants with a fixed dose of FGF-2. Significant difference is represented as * when compared to 0.156 ng/ml FGF-2 ($p<0.05$).

Immunoblotting was performed to confirm the results of additive effect of HS8^{+ve} and FGF-2 on hMSC proliferation as shown by viability assays.

As discussed in the introduction, activation of the ERK cascade is required for FGF-induced mitogenesis. Thus, it was necessary verify that HS8^{+ve} in the presence of FGF-2 could induce ERK activation in low serum conditions. Here, cells were seeded (10,000 cells/cm^2) on 6-well plates (Nunc) and allowed to adhere to the plastic surface for 16 h in a humidified atmosphere. After 48 h of serum starvation cells were stimulated with GAGs (2.5 µg/ml) and/or FGF-2 (0.156 ng/ml) and monitored for FRS2a

phosphorylation and ERK1/2 phosphorylation after 30 min, 6 h and 24 h post stimulation. Although a marked increase with lower doses of $HS8^{+ve}$ (0.3125 µg/ml; Fig. 3.25), was seen, in this experiment I used the 2.5 µg/ml GAG dose to mimic the scenario wherein I added HS variants as stand-alone media supplements.

FGF-2 rapidly elevated both FRS2a phosphorylation and ERK1/2 phosphorylation from 30 min after the treatment and sustained it until 6 h, after which the signal started to decline over 24 h (Fig. 3.25). When $HS8^{+ve}$ was present, the levels of FRS2a and ERK1/2 phosphorylation were higher than with stimulation through FGF-2 alone at 30 min and 6 h. In addition, $HS8^{+ve}$ with FGF-2 managed to sustain signaling even at 24 h after which the cells in FGF-2 alone showed reduced levels phosphorylation levels of FRS2a and ERK 1/2. I next examined whether $HS8^{+ve}$-mediated FGF-2 signaling was superior to the other HS variants. Here heparin used as a positive control. As expected, the highly negative charged heparin sustained FRS2a and ERK1/2 phosphorylation to 24 h, similar to $HS8^{+ve}$ (Fig. 3.26), albeit that the levels of FRS2a and ERK1/2 phosphorylation at 24 h with HS^{pm} and $HS8^{-ve}$ were lower than of $HS8^{+ve}$. My results thus confirmed the additive effect of $HS8^{+ve}$ and FGF-2 seen in the GUAVA Viacount® assay.

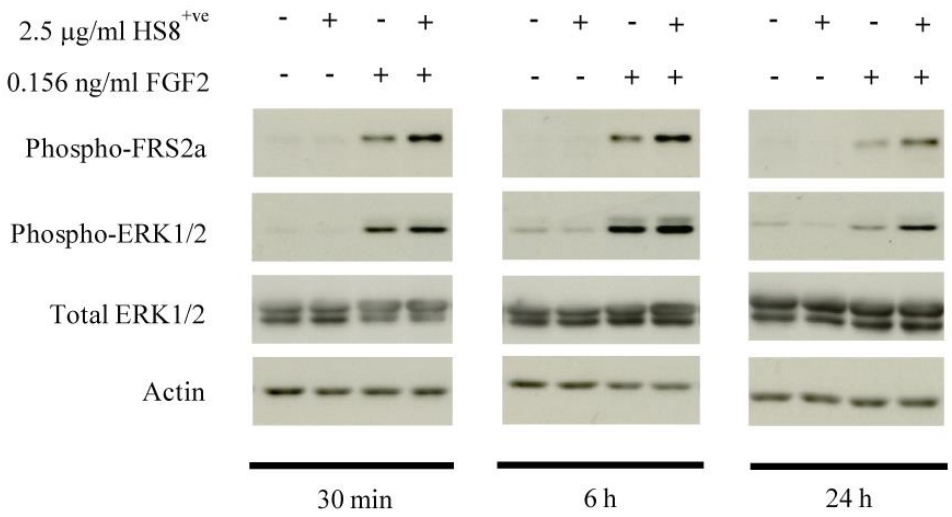

Figure 3.25. HS8^{+ve} sustains FGF-2 signaling. The cells were seeded (10,000 cells/cm^2) on 6-well plates and were allowed to adhere to the plastic surface for 16 h. The cells were then serum starved for 48 h. Immunoblots showing FRS2a phosphorylation and ERK1/2 and phosphorylation at 30 min, 6 h and 24 h post stimulation with FGF-2 (0.156 ng/ml) with or without HS8^{+ve} (2.5 µg/ml).

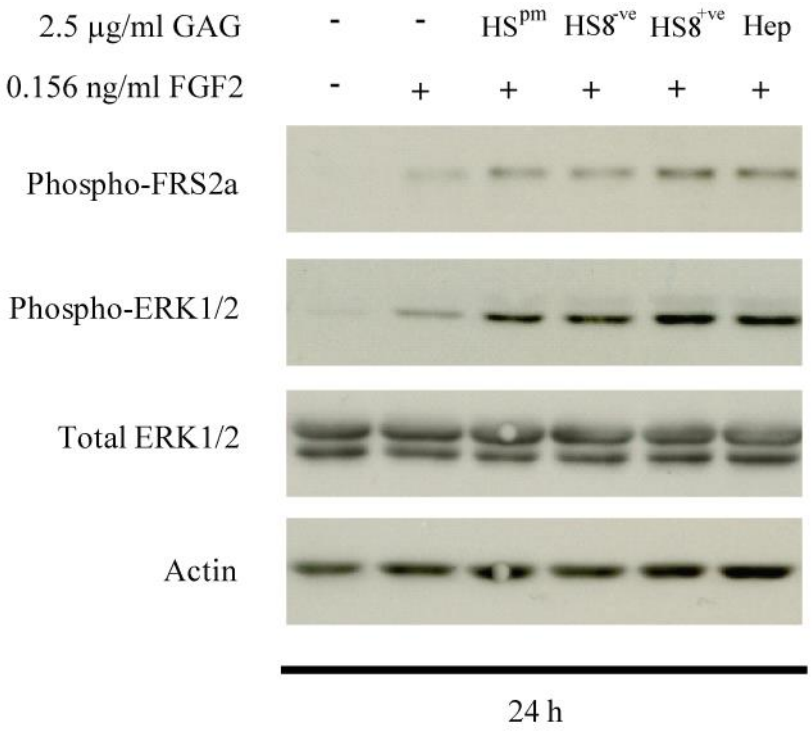

Figure 3.26. HS8^{+ve} sustains FGF-2 signaling as compared to HS^{pm} and HS8^{-ve}. The cells were seeded (10,000 cells/cm^2) on 6-well plates and were allowed to adhere to the plastic surface for 16 h. Afterwards cells were serum starved for 48 h. Immunoblots showing FRS2a phosphorylation and ERK1/2 phosphorylation at 24 h post stimulation with FGF-2 (0.156 ng/ml) with or without GAGs (2.5 µg/ml).

3.3.9. $HS8^{+ve}$ enhance hMSC proliferation via FGF-2-FGFR signaling.

HS is a coreceptor for the FGF/FGFR complex, and FGFR1 is a high affinity receptor for FGF-2 binding (Chellaiah *et al.*, 1999; Dombrowski *et al*., 2009; Pellegrini, 2001). Inhibitor studies were next used to show that the mechanism for triggering the proliferation by the $HS8^{+ve}$ involved FGF-2. First it was necessary to inhibit the FGF-2 in the culture media with a neutralizing antibody (Ab; R & D Systems). The presence of the FGF-2-neutralizing Abs had a clear inhibitory effect on the basal growth of hMSCs (Fig. 3.27). $HS8^{+ve}$ (2.5 µg/ml) and FGF-2 (2.5 ng/ml) significantly increase hMSC proliferation while the FGF-2 neutralizing antibody significantly prevented $HS8^{+ve}$ and FGF-2 induced proliferation as revealed by BrdU incorporation and GUAVA Viacount® assays (Fig. 3.27). This blocking of fold-increases in viable cell counts in $HS8^{+ve}$ and FGF-2 grown cells was similar to the controls as evident in the GUAVA Viacount® assay. Similarly, in the BrdU incorporation assay prevention of fold-increases in absorbance with $HS8^{+ve}$ was similar to the control but with FGF-2 it was significantly dissimilar. This may be due to BrdU constituting only a snap shot of proliferation and the amount of FGF-2 neutralizing antibody might not have been sufficient to neutralize the amount of FGF-2 in culture at the examined time point.

This further strengthens the hypothesis that $HS8^{+ve}$ increases hMSC proliferation via FGF-2, as previously indicated by the additive effect of $HS8^{+ve}$ and FGF-2 (Figs. 3.24 and 3.25).

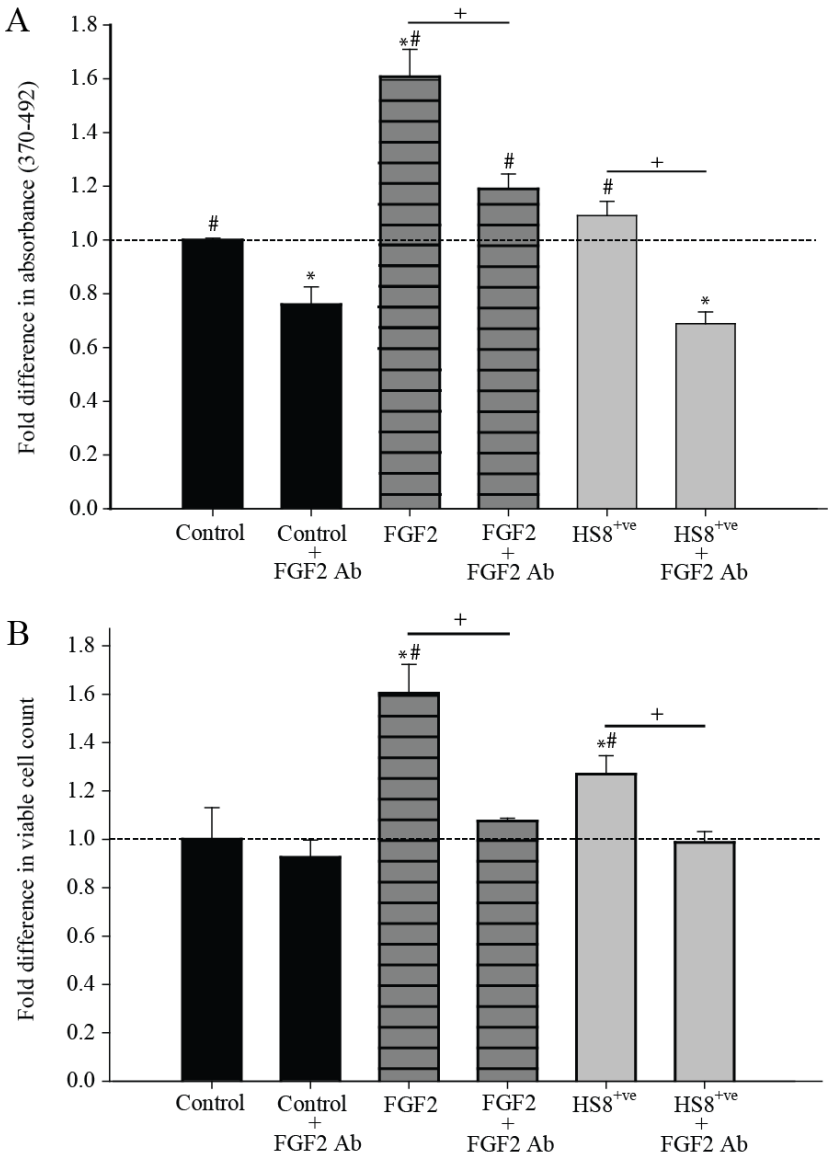

Figure 3.27. FGF-2-neutralizing antibody reduces the hMSC proliferation. The cells were cultured with FGF-2 (2.5 ng/ml) and $HS8^{+ve}$ 2.5 µg/ml with or without FGF-2 neutralizing Ab (2 µg/ml) (R & D Systems). Cells cultured with media with or without FGF-2 neutralizing Ab (2 µg/ml) served as controls. The graphs show the inhibition of the hMSC growth usually induced by FGF-2 and $HS8^{+ve}$ supplementation (A) BrdU incorporation assay (Roche) (B) GUAVA Viacount® assay (Millipore). In BrdU incorporation assay cells were seeded at 5000/well in 96 well plates, cultured for 36 h and BrdU incorporation into DNA of proliferating cells was measured photometrically using TMB substrate. In GUAVA Viacount® assay cells were seeded at 3000/cm^2 in 24 well plates, cultured for 4 days, stained with Viacount flex reagent and viable cells detected by Guava EasyCyte™ Plus System/CytoSoft™ software. Significant difference is represented as * when compared to control, # when compared to control with FGF-2 neutralizing Ab (2 µg/ml) and + when significant among respective bars ($p<0.05$).

It was next necessary to verify the importance of FGFR signaling for hMSC proliferation under $HS8^{+ve}$ stimulation. Two forms of FGFR1 inhibition were used: either the chemical inhibitor SU5402 (Calbiochem, Millipore) or the neutralizing antibody IMBR1 (Ling *et al*., 2006). Clearly, if the $HS8^{+ve}$ variant was involved in the direct binding of FGF-2 to FGFR1, the effect on proliferation should be blocked by FGFR1 inhibitors as compared to the controls. Pulsing SU5402 at two different doses (10 and 25 µM) had a statistically significant dose-dependent inhibitory effect on the basal growth of hMSCs (Fig. 3.28). $HS8^{+ve}$ (2.5 µg/ml) and FGF-2 (2.5 ng/ml) significantly increase hMSC proliferation; SU5402 successfully prevented $HS8^{+ve}$/FGF-2-induced proliferation as evident in the GUAVA Viacount® assay. This prevention of fold-increases in viable cell counts in $HS8^{+ve}$ and FGF-2 exposed cells was significantly similar to the controls. Similarly, in the BrdU incorporation assay prevention of fold-increases in absorbance with $HS8^{+ve}$ was similar to the control but with FGF-2 and SU5402 (10 µM) it was significantly dissimilar. This may be due to BrdU is providing only a snap shot of proliferation and that the amount of SU5402 was not sufficient to inhibit the FGFR1 activation by the amount of FGF-2 in culture at that time point.

Almost identical results were seen with the FGFR1-neutralizing antibody IMBR1 with few exceptions. The difference in absorbance (BrdU assay) with FGF-2 and IMBR1 (1:1000 and 1:2000) and the difference in fold increase (GUAVA assay) with IMBR1 (1:2000) were significantly dissimilar when compared with equivalent control groups (Fig. 3.29). This may be due to both doses of IMBR1 in BrdU assay and the lower dose in GUAVA assay were not sufficient in inhibiting the potent FGF-2's effect on FGFR1

activation as compared to controls. Nevertheless, these results indicated that the mechanism involved in triggering the proliferation by the HS8^{+ve} was indeed via FGF-2-FGFR1 signaling.

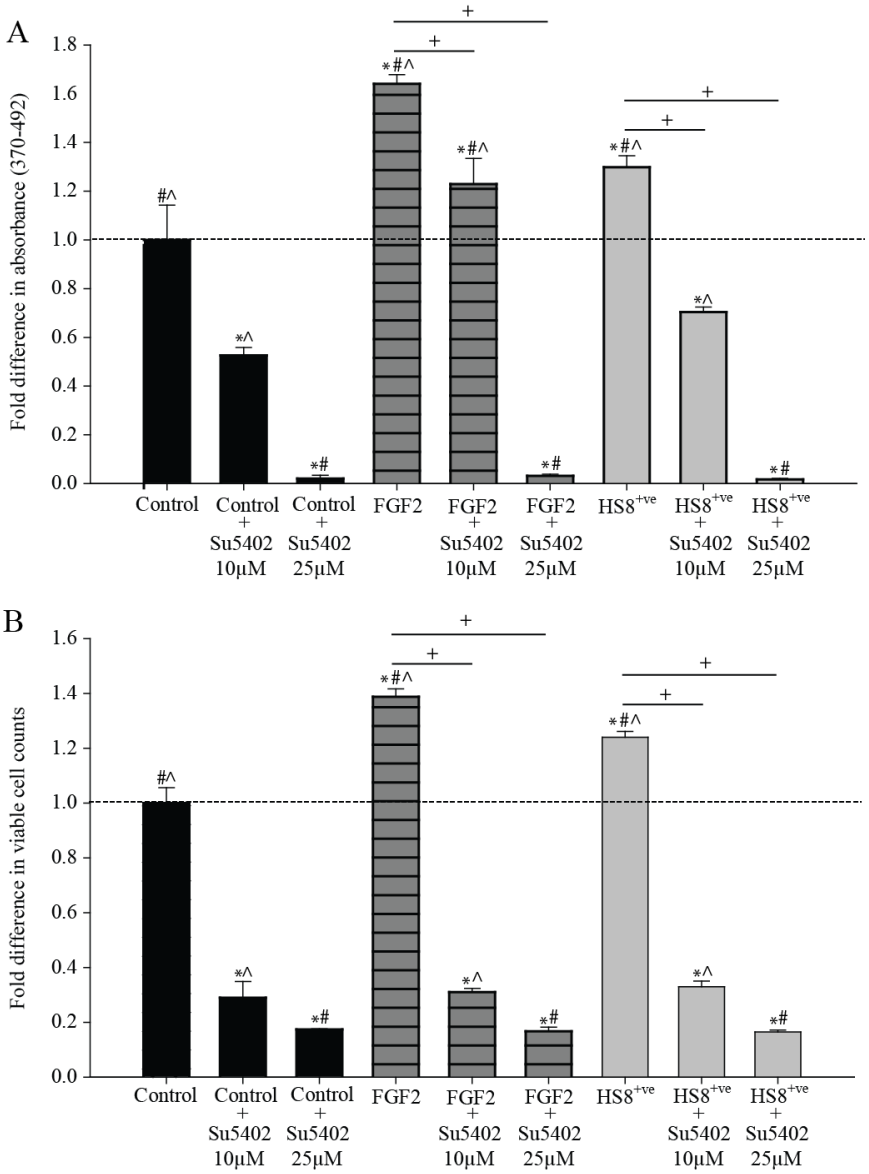

Figure 3.28. SU5402 inhibits hMSC proliferation. Cells were cultured with FGF-2 (2.5 ng/ml) and HS8^{+ve} 2.5 µg/ml with or without SU5402 (10 and 25 µM) in DMSO (Calbiochem, Millipore). Cells cultured with media alone with or without SU5402 (10 and 25 µM) in DMSO served as controls. The graphs show the inhibition of hMSC growth usually induced by FGF-2 and HS8^{+ve} media supplements (A) BrdU incorporation assay (Roche) (B) GUAVA Viacount® assay (Millipore). In BrdU incorporation assay cells were seeded at 5000/well in 96 well plates, cultured for 36 h and BrdU incorporation into DNA of proliferating cells was measured photometrically using TMB substrate. In GUAVA Viacount® assay cells were seeded at 3000/cm^2 in 24 well plates, cultured for 4 days, stained with Viacount flex reagent and viable cells were detected by Guava EasyCyte™ Plus System/CytoSoft™ software. Significant difference is represented as * when compared to control, $^{\#}$ when compared to control with SU5402 (10 µM), ^ control with SU5402 (25 µM) and $^{+}$ when significant among respective bars ($p<0.05$).

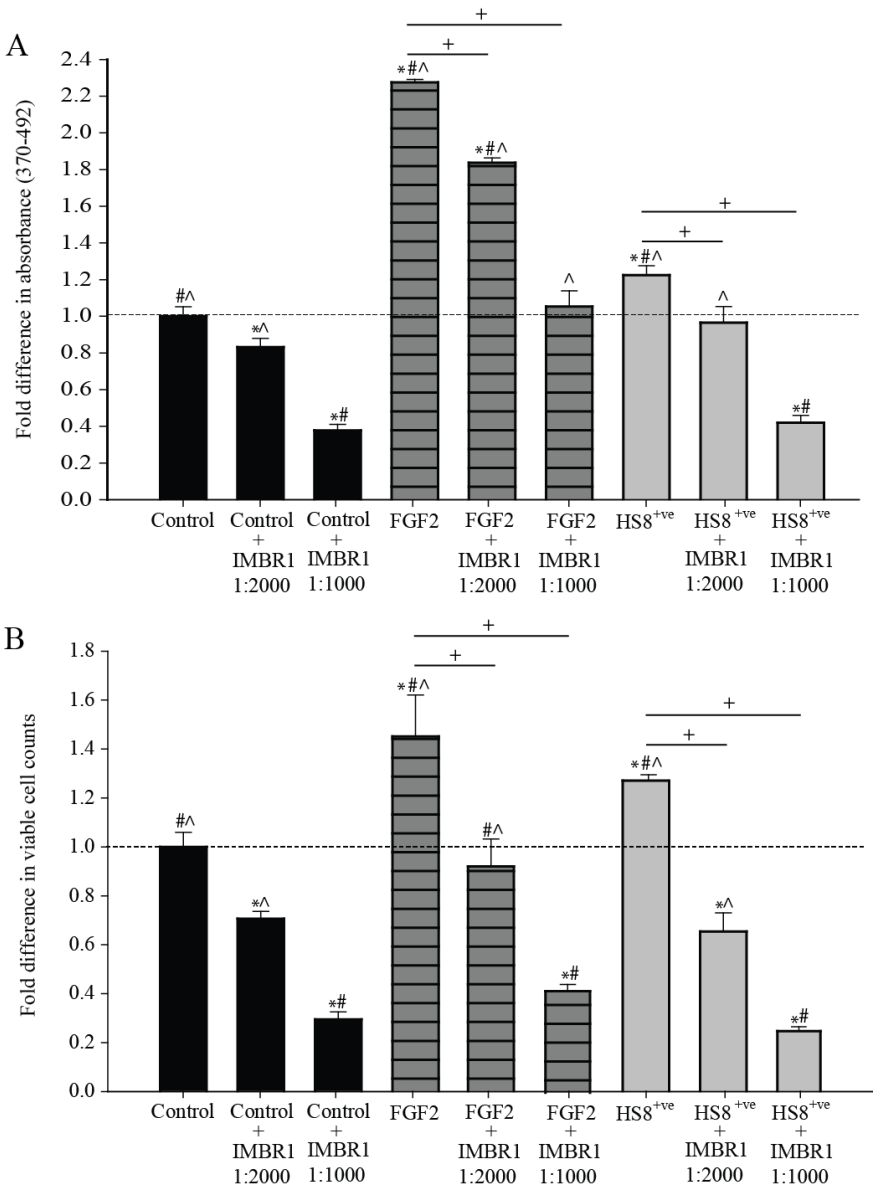

Figure 3.29. IMBR1 inhibits hMSC proliferation. The cells were cultured with FGF-2 (2.5 ng/ml) and HS8^{+ve} 2.5 µg/ml with or without IMBR1 (1:2000 and 1:1000) (Ling *et al*., 2006). Cells cultured with media alone with or without IMBR1 (1:2000 and 1:1000) served as controls. The graphs show the inhibition of hMSCs growth usually induced by FGF-2 and HS8^{+ve} media supplements (A) BrdU incorporation assay (Roche) (B) GUAVA Viacount® assay (Millipore). In BrdU incorporation assay cells were seeded at 5000/well in 96-well plates, cultured for 36 h and BrdU incorporation into DNA of proliferating cells was measured photometrically using TMB substrate. In GUAVA Viacount® assay cells were seeded at 3000/cm^2 in 24 well plates, cultured for 4 days, stained with Viacount flex reagent and viable cells were detected by Guava EasyCyte™ Plus System/CytoSoft™ software. Significant difference is represented as * when compared to control, $^{\#}$ when compared to control with IMBR1 (1:2000), ^ control with IMBR1 (1:1000) and $^{+}$ when significant among respective bars ($p<0.05$).

3.3.10. $HS8^{+ve}$ binds both FGF-2 and FGFR1

In order to act as a coreceptor for the FGF/FGFR complex, an HS chain must have sufficient length to couple both FGF-2 and FGFR1 within one, or at most two sulfated domains. To explore the importance of length, hMSCs were cultured for 4 days with both full-length heparin, and a smaller heparin fragment, of d.p. (degree of polymerization) 10 (dp10) at different doses (0, 0.156, 0.3125, 0.625, 1.25, 2.5, 5 and 10 µg/ml) with or without FGF-2 (0.156 ng/ml), and the additive effect on FGF-2-mediated proliferation monitored (Fig. 3.30). As noted above, the highly negatively charged heparin, even at 0.156 µg/ml, together with FGF-2, increased cell proliferation considerably more than with FGF-2 alone at an otherwise sub-optimal dose (0.156 ng/ml). The cell proliferation with 0.625 µg/ml heparin and 0.156 ng/ml of FGF-2 was similar to the cell proliferation with 2.5 ng/ml of FGF-2. These data were similar to the additive effect of $HS8^{+ve}$ on FGF-2-mediated hMSC proliferation (Fig. 3.24). In contrast, the dp10 fragment at increasing concentrations was unable to increase cell proliferation beyond the 1.3-fold point when FGF-2 was at sub-optimal concentrations. Furthermore, a dose-dependent antagonistic effect was shown by dp10 on FGF-2-mediated cell growth. This might have been because dp10 was binding to FGF-2 but lacked the length to cross-bind to FGFR1 and mediate cell proliferation.

As $HS8^{+ve}$ clearly enhances FGF-2 mediated cell growth, it can concluded that $HS8^{+ve}$ has a length exceeding dp10.

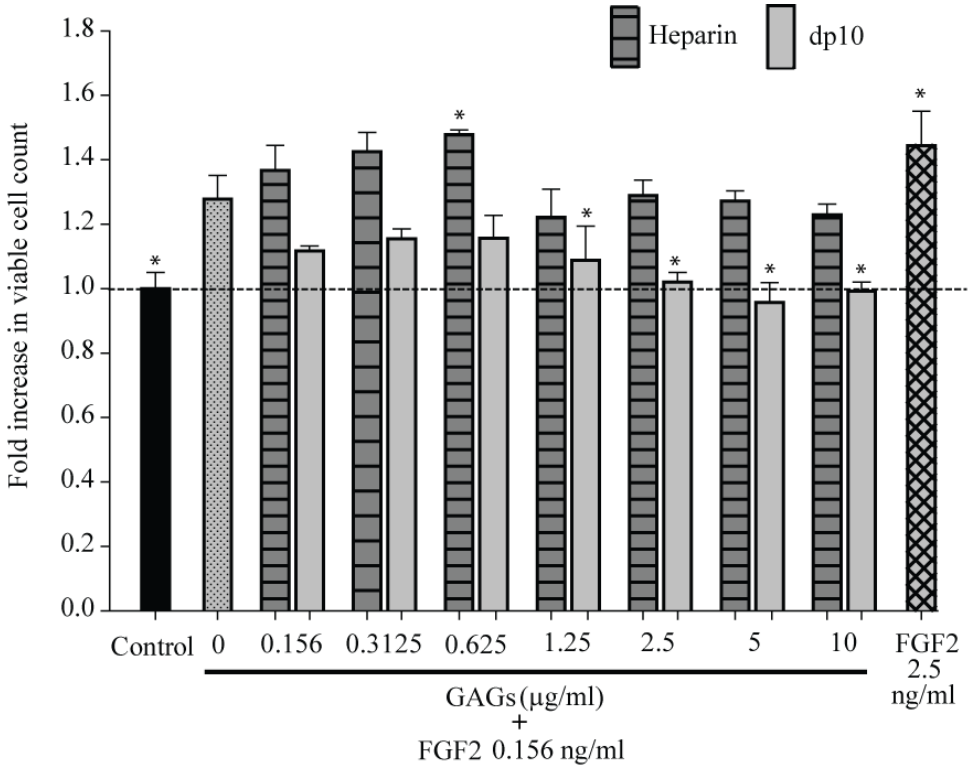

Figure 3.30. Full-length heparin enhances FGF-2 mediated MSC growth, but not dp10 heparin. Cells were seeded at 3000/cm^2 in 24-well plates and cultured for 4 days with heparin and dp10 at different doses (0, 0.156, 0.3125, 0.625, 1.25, 2.5, 5 and 10 µg/ml) with or without FGF-2 (0.156 ng/ml) with media change at every 2 days. Cells cultured in maintenance media and with 2.5 ng/ml of FGF-2 served as baseline control and positive control respectively. The cells were stained with Viacount flex reagent (Millipore) and viable cells detected by the microcapillary flow cytometry platform of Guava EasyCyte™ Plus System/CytoSoft™ software (Millipore™). The graph shows the dose-dependent fold-increase in viable cell counts of plastic adherent hMSCs in varying doses of heparin and dp10 with a fixed, suboptimal dose of FGF-2. Significant difference is represented as * when compared to 0.156 ng/ml FGF-2 ($p<0.05$).

3.4. Discussion

Glycosaminoglycans (GAGs), large, unbranched, yet complex carbohydrate molecules, constitute an important structural and functional compartment of the extracellular matrix ((ECM) (Gandhi and Mancera, 2008). The role of HS becomes particularly important during phases of tissue building, in the embryo, and during phases of tissue regeneration in the adult. Like all GAGs, HS is a polymer of repeating disaccharide units (Ori *et al*., 2009). It binds and regulates a wide variety of proteins, now thought to be over 400, and participates in many biological processes; in the stereotypical example, HS regulates the FGF signaling by direct molecular association with FGFRs to nucleate a trimeric complex (Pellegrini, 2001). In Chapter 2, the possibility of fine tuning and enhancing the endogenous FGF-2 activity of MSCs through judicious use of targeted HS was examined. The successful isolation of a highly scalable HS fraction variant with higher binding affinity for FGF-2 was performed. A full range of biochemical assays was then deployed to examine the suitability of such an HS for the putative expansion of hMSCs.

In order to effectively exploit GAGs in tissue engineering, there is an essential need to understand the interactions between GAGs and proteins. Therefore the assays utilised should allow sufficient attachment of GAGs to a surface without hindering their binding properties to proteins. Marson and colleagues have discussed the limitations of covalent coupling of GAGs to bovine serum albumin and binding of biotinylated GAGs to immobilized proteins as methods to adhere GAGs to plastic surfaces (Mahoney *et al*., 2004; Marson *et al*., 2009). To overcome those limitations they have described a

way, by means of cold plasma polymerization whereby microtitre plate surfaces are coated with allyl amine (Mahoney *et al*., 2004; Marson *et al*., 2009). The GAGs thereby non-covalently immobilized to these allyl amines without hindering their ability to interact with proteins. The binding capacity of purified $HS8^{+ve}$, non-binding $HS8^{-ve}$ and starting material HS^{pm} for FGF-2 was compared using GAG-ELISA and heparin-Sepharose beads competition assays in chapters 3.3.1 and 3.3.3. In addition, the binding specificity of $HS8^{+ve}$ was compared with other heparan-binding proteins. The results confirmed that $HS8^{+ve}$ binds FGF-2 with greater relative specificity as compared to HS^{pm} and $HS8^{-ve}$. These results further validated our affinity chromatography platform for the isolation of HS variants that $HS8^{+ve}$ bind with high affinity to FGF-2 similar to other HS variants isolated by our group for BMP-2 and $VEGF_{165}$ (Murali *et al*., 2013; Wang *et al*., 2014).

Next two types of hMSCs, plastic adherent and STRO-1-positive, in short-term proliferation studies were used to examine the suitability of $HS8^{+ve}$ for expanding hMSCs compared to HS^{pm} and $HS8^{-ve}$. These data also showed that, $HS8^{+ve}$ statistically increased cell proliferation (~ 1.4-1.5) compared to HS^{pm} and $HS8^{-ve}$ (Figs. 3.8, 3.9, 3.11 and 3.14). The hMSC proliferation by $HS8^{+ve}$ was comparable to published results that utilised embryonic form of heparan sulfate (HS2) which specifically binds FGF-2 (Helledie *et al*., 2011). Helledie and colleagues have shown this HS2 increased the proliferation of sub-confluent hMSCs over a 6-day period by ~ 65% (Helledie *et al*., 2011). In addition, the fold increase in proliferation of hMSCs with $HS8^{+ve}$ was similar to that of heparin (positive control) while FGF-2 supplementation (other positive) yielded higher cell proliferation of ~ 1.6 (Fig. 3.23). Furthermore,

such assays were used to narrow down to an $HS8^{+ve}$ variant from three starting preparations ($HS8G^{+ve}$, $HS8C^{+ve}$ and $HS8B^{+ve}$) (Figs. 3.12 and 3.13). $HS8G^{+ve}$ was selected since it gave me the better yield as described in chapter 2.4. Murali *et al.* have already described the isolation of an affinity-selected HS with relative specificity for BMP2 (with this platform) and successful employed it to trigger *in vivo* bone repair (Murali *et al*., 2013). Similarly, Wang *et al*. also described an affinity-isolated heparan sulfate glycotherapeutic ($HS7^{+ve}$) that binds to, and enhances the bioactivity of, $VEGF_{165}$ (Wang *et al*., 2014).

Wang and colleagues have recently mentioned that subtle variations in disaccharide sequence, chain length and biosynthesis give rise to specific HS variants with unique characteristics of bindings to different growth factors (Murali *et al*., 2011; Murali *et al*., 2013; Nurcombe *et al*., 2007; Wang *et al*., 2014). Therefore the compositional make up of $HS8^{+ve}$ is an important aspect for the future if we are to design synthetic equivalents with even greater affinity for FGF-2. The sensitive and powerful technique of capillary electrophoresis (CE) revealed major differences between starting HS^{pm} and $HS8^{+ve}$. $HS8^{+ve}$ was enriched for trisulfated disaccharides and was relatively depleted in mono- and un-sulfated disaccharide as compared with HS^{pm}. In addition, there was a clear increase in di-sulfated disaccharides, particularly ΔUA-GlcNS,6S. Similarly, Murali *et al*., and Wang *et al*., have described that the heparan sulfates pulled down from BMP-2-HBD ($HS3^{+ve}$) and VEGF-HBD ($HS7^{+ve}$) peptide affinity columns have higher amounts of trisulfated disaccharide species and enriched with ΔUA-GlcNS,6S disulfide species as compared to the starting mixture HS^{pm} (Murali *et al*., 2013; Wang *et al*.,

2014). A closer look across these three HS variants revealed that DHexUA,2S-GlcNS,6S was highest (15 %) with $HS3^{+ve}$ and lowest with (11 %) with $HS7^{+ve}$ while $HS8^{+ve}$ had an intermediary level (13 %). On the other hand DHexUA-GlcNS,6S was highest (15 %) with $HS7^{+ve}$ and lowest with (11 %) with $HS3^{+ve}$ while $HS8^{+ve}$ again had an intermediary level (13 %).

Disaccharide analyses of heparin have been published by various groups (Ampofo *et al*., 1991; Desai *et al*., 1993; Jandik *et al*., 1994; Karamanos *et al*., 1996; Ruiz-Calero *et al*., 1998; Scapol *et al*., 1996). As described, the key disaccharides of porcine intestinal mucosal heparin were DHexUA,2S-GlcNS,6S and DHexUA-GlcNS,6S, which indicated that trisulfated disaccharides (2O-, 6O- and N-sulfated) and disulfated disaccharides (6O- and N-sulfated) are major components for the binding to growth factors such as FGF-2. Our data clearly suggests that an increase in trisulfated disaccharides and 6O- and N-sulfated disaccharides is indeed very important for HS binding to FGF-2. Furthermore, lack of enrichment of unsulfated and monosulfated (NS) compared to HS^{pm} suggests that neither disaccharide by itself is sufficient for FGF-2 binding. Heparin has very low levels of unsulfated and monosulfated (NS) disaccharides. I posit that the levels of disaccharides that are different to those levels in heparin and as well as other two HS variants namely ($HS3^{+ve}$ and $HS7^{+ve}$) may be the reason that $HS8^{+ve}$ has a relative affinity for FGF-2 over the other heparin binding growth factors, notwithstanding the final arbiter are the actual disaccharide sequences within N-sulfated domains greater than dp 10 in length. A dodecasaccharide, whose sequence has been proposed as the minimal requirement to promote receptor signaling by FGF-2 (Guimond *et al*., 1993), was the reason that only

heparin dp 10 was utilized here to gain an insight of the length of $HS8^{+ve}$. Usually the linear, sulfated glycosaminoglycans have molecular masses that typically range from 10 to 100 kDa (Gandhi and Mancera, 2008). In addition, the chain length of HS is also important in giving rise to HS variants with unique characteristics of bindings to different growth factors. Therefore, the exploration of the length and the MW of $HS8^{+ve}$ was recommended as future research as described by Murali *et al.* (Murali *et al*., 2011) . This provided new data and the data on the composition of $HS8^{+ve}$ in chapter 3.4.4 will be beneficial in artificial synthesis of $HS8^{+ve}$.

Various studies have presented data supporting the idea that HS's varying capacity for proteins is due to differentially modified HS units. Lindahl's group in Sweden have shown that 3O-sulfated glucosamine, at a specific position in the antithrombin-binding sequence of heparin is essential for its anticoagulation effects (Lindahl *et al*., 1980). Heparin's anticoagulation activity was clearly highlighted by the data shown in chapter 3.3.5. In contrast, the $HS8^{+ve}$ fraction did not show any significant anticoagulation activity, suggesting that it is devoid of 3O-sulfation. HS^{pm} did trigger a slight anticoagulation activity at higher doses, implying that it may contain some lesser amount of 3O-sulfation.

Similarly, specific disaccharide sequences within HS GAGs chains support the signaling of the FGF family. The FGF1-binding affinity of HS is reduced in the absence of 6O-sulfate groups, indicating their importance for this interaction (Fromm *et al*., 1997b; Ishihara, 1994). Similarly, FGF4 requires both 2O- and 6O-sulfation for binding and signaling (Ashikari-Hada *et al*., 2009; Guimond *et al*., 1993; Ishihara, 1994). FGF-2 binding to HS

requires 2O-sulfation (Faham *et al*., 1996a; Maccarana *et al*., 1993). Furthermore, in addition to the 2-O sulfation, 6-O-sulfation of N-sulfated glucosamine residues is required for the promotion of FGF-2 mitogenic activity (Pye *et al*., 1998). Lundin and colleagues have also supported this idea by showing that FGF-2 binding requires N and 2-O-sulfate groups, whereas stimulation of FGFR-1 and Erk2 kinases by FGF-2 also required the presence of 6O-sulfate groups (Lundin *et al*., 2000). Furthermore, they demonstrated that 6O-desulfated heparin could inhibit FGF-2-induced angiogenesis in chick embryo chorioallantoic membranes. Thus, formation of the ternary complex of FGF-2-HS-FGFR1 critical for signal transduction requires 2O-, 6O- and N sulfation. Hence, the levels of these required sulfated disaccharides in $HS8^{+ve}$ might have been somewhat optimised for FGF-2 binding and signal propagation by the platform. This further validates our affinity chromatography approach as a promising technique for isolating FGF-2-binding HS forms from a heterogeneous HS mixture.

Stabilization of FGF-2 by HS variants in culture conditions is important for the enhancement of endogenous growth factor activity. The stability of FGF-2 afforded by heparin (as also shown by my results in chapter 3.3.6) was comparable to published results that utilised quantikine assays (Caldwell *et al*., 2004). The affinity purified $HS8^{+ve}$ increased the $T_{1/2}$ of FGF-2 by 4-fold, which was significantly higher than that afforded by either HS^{pm} or $HS8^{-ve}$. The thermal stability of FGF protein is known to be a determinant factor for human embryonic stem cell (ESC) self-renewal, differentiation, and reprogramming (Chen *et al*., 2012). These researchers have shown it is the thermal instability of FGF1, rather than receptor specificity that leads to

failure in ESC maintenance. These results obviously suggest that the thermal stability of FGF-2 under culture conditions is important for prolonged hMSC growth. I have shown by the differential scanning fluorimetry assay that the thermal stability of FGF-2 is increased by $HS8^{+ve}$ compared to HS^{pm} and HS^{-ve}. Although $HS8^{+ve}$ did not afford the same level of thermal stabilization as heparin, this may be due to rare structures, such as heparin's 3O-sulfation, or the simple fact of extra sulfation that allow for a stronger interaction (Xu *et al*., 2012). In addition, others have shown the importance of FGF-2–heparin interactions for the protection of the growth factor from denaturation and proteolytic digestion (Gospodarowicz and Cheng, 1986). Therefore, $HS8^{+ve}$, with its higher binding ability for FGF-2, might well perform in a similar manner.

The additive effect of $HS8^{+ve}$ and FGF-2 were monitored by both proliferation assays and cell signaling studies. $HS8^{+ve}$, but not HS^{pm} or $HS8^{-ve}$, increased the FGF-2-mediated cell growth (Fig. 3.24). In addition, highly sulfated heparin when used as a positive control also increased the FGF-2-mediated cell growth similar to that of $HS8^{+ve}$ (Figs. 3.24 and 3.30).

Heparan sulfate is a coreceptor for the FGF/FGFR complex and FGFR1 is a high affinity receptor for FGF-2 binding (Chellaiah *et al.*, 1999; Dombrowski *et al*., 2009; Pellegrini, 2001). X-ray crystal structures of the trimeric complex have shown two main models. One, with a stoichiometric ratio 2:2:2 of FGFR2:FGF1:heparin decasaccharide (Schlessinger, 2000; Turnbull *et al*., 1992) and the other with a stoichiometric ratio 2:2:1 of FGFR2:FGF1:heparin decasaccharide (Pellegrini, 2001). Both receptors in the FGF-2 dual receptor system must be present for FGF-2 to trigger a

proliferative response (Delehedde *et al*., 2002). Therefore the inhibitor studies that I exemplified clearly demonstrated that the mechanism involved in triggering the proliferation by the $HS8^{+ve}$ was consistent with FGF-2-FGFR1 signaling. In accordance with the inhibitor studies detailed here, Dombrowski *et al* also observed similar results when they used HS isolated from mouse embryonic tissue and FGF2 on rat MSCs (rMSCs) (Dombrowski *et al*., 2009). They have clearly shown that the inhibition of FGFR1 with either a neutralizing antibody (IMBR1) or the chemical inhibitor SU5402 prevented HS and FGF-2-induced proliferation similar to that of basal growth of rMSCs. They also claim that according to their results, the embryonic HS directs FGF-2 signaling in rMSCs preferentially through FGFR1.

Furthermore, HS, in order to qualify as a coreceptor for the FGF/FGFR complex, must have sufficient length and the requisite disaccharide compositions within its binding sites to couple both FGF-2 and FGFR1. The minimum oligosaccharide that can bind FGF-2 is a tetrasaccharide, as shown by optical NMR spectroscopy (Delehedde *et al*., 2002; Guglieri *et al*., 2008). In addition, an increasing gradient in affinity for FGF-2 was seen from tetrasaccharide to octasaccharide. However, according to Delehedde *et al.*, the oligosaccharides from tetrasaccharides to octasaccharides were less potent in their stimulation of the proliferation of rat mammary fibroblasts than deca- or longer -saccharides (Delehedde *et al*., 2002). In addition, a dodecasaccharide sequence has been proposed as the minimal requirement to promote receptor signaling by FGF-2 (Guimond *et al*., 1993), notwithstanding I have observed in chapter 3.3.10 that heparin oligosaccharides of dp 10 were not sufficient to enhance the FGF-2-mediated hMSC proliferation. Recently Dombrowski and

colleagues have shown that FGFR1 signalling activity is rate limiting for self-renewal of hMSCs and thereby stimulates proliferation of hMSCs (Dombrowski *et al*., 2013). This is achieved by several mechanisms by inhibiting the cyclin-dependent kinase inhibitors $p21^{Waf1}$ and $p27^{Kip1}$. Together with our group's data that the $HS8^{+ve}$ variant displays maximum, plateau binding to FGFR1 protein in GAG-ELISA assays, I conclude that $HS8^{+ve}$ is highly likely to have a relatively specific binding site for FGFR1.

3.5. Summary

The aim of this chapter was to test the $HS8^{+ve}$ variants isolated in the previous chapter by means of a wide range of biochemical assays. The binding studies revealed that $HS8^{+ve}$ had a higher binding specificity for FGF-2 than starting material HS^{pm} and non-binding $HS8^{-ve}$. Also $HS8^{+ve}$ bound to FGF-2 with a greater propensity than other heparin-binding growth factors. Proliferation studies showed that $HS8^{+ve}$ statistically increased the cell proliferation compared to HS^{pm} and $HS8^{-ve}$. Furthermore, the above assays were useful in narrowing down to one $HS8^{+ve}$ variant, $HS8G^{+ve,}$ out of the three prospective variants.

The compositional make up of $HS8^{+ve}$ revealed an enrichment of trisulfated disaccharide with di-sulfated disaccharide (6O and NS) and a depletion of mono- and un-sulfated disaccharide compared with HS^{pm}. This appeared critical for the formation of the FGF-2-HS-FGFR ternary complex and downstream signal transduction, which required 2O-, 6O- and N-sulfation. In addition, $HS8^{+ve}$ was devoid of anticoagulation activity.

The affinity purified $HS8^{+ve}$ increased FGF-2 stability compared to HS^{pm} and $HS8^{-ve}$ in culture conditions. The additive effect of $HS8^{+ve}$ and FGF-2 were monitored by proliferation assays and cell signaling studies, which revealed its enhanced effects on FGF-2-mediated hMSC growth. Inhibitor studies showed the mechanism involved in triggering the proliferation by the $HS8^{+ve}$ was indeed via FGF-2-FGFR1 signaling. The mechanism by which $HS8^{+ve}$ mediate its action is proposed in an abstract art piece (Fig. 3.32). Thus I have developed a robust, highly scalable, simple and cost-effective process to identify a ligand that can bind to both endogenous FGF-2 and FGFR1 and thereby better control FGF-2-mediated hMSC proliferation.

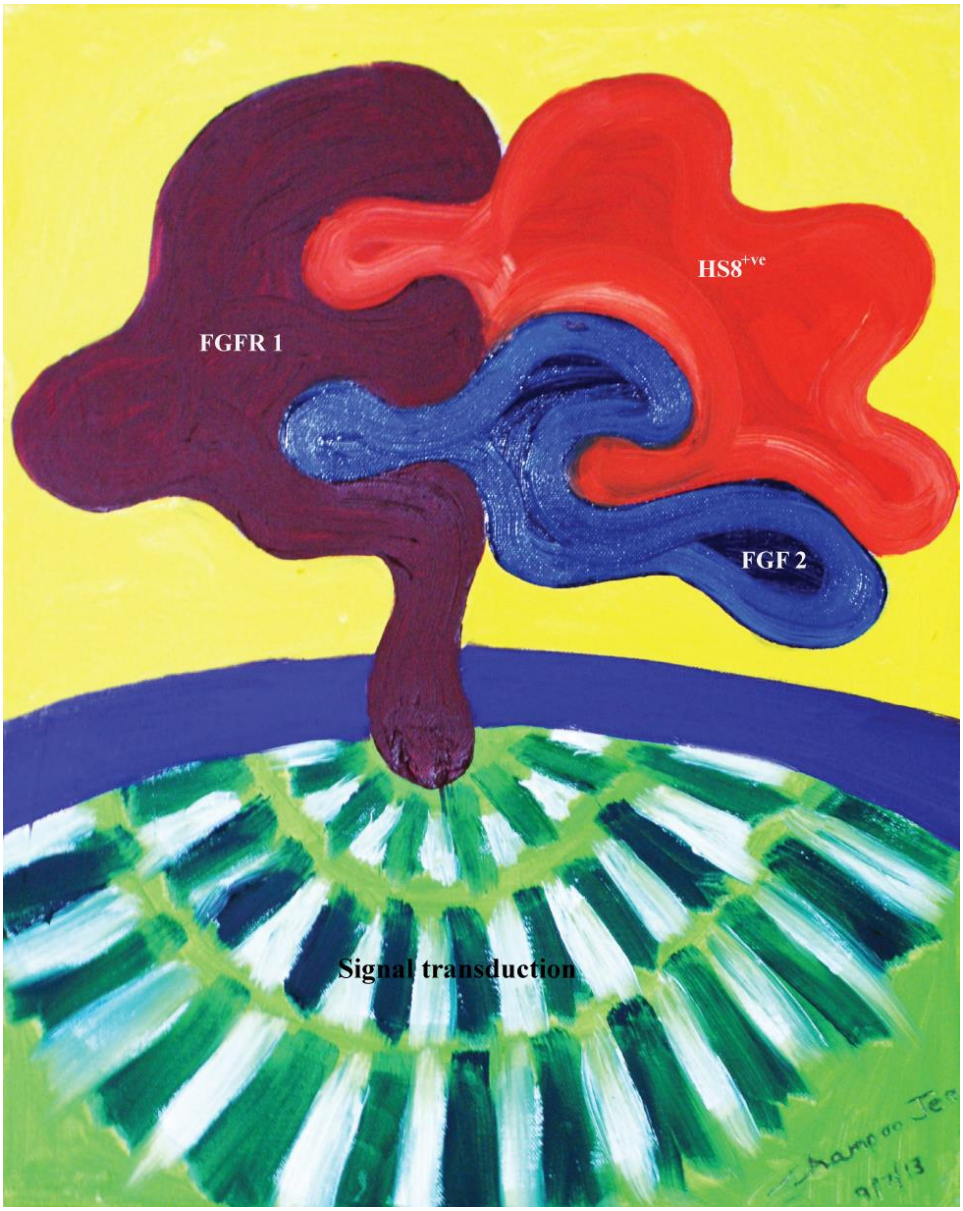

Figure 3.31. Abstract art depicting the proposed FGF-2-FGFR1-HS8^{+ve} trimeric structure and signal transduction

CHAPTER 4: LONG-TERM CELL CULTURE STUDIES ON HS8 VARIANTS

4.1 Introduction

Chapter 2 described the successful isolation by affinity of three $HS8^{+ve}$ variants with a relatively high binding preference for particular FGF-2-derived HBD peptides. Chapter 3 saw extensive biochemical assaying of the variants and revealed that $HS8^{+ve}$ binds FGF-2 with a higher propensity than other HS variants and heparin-binding growth factors. $HS8^{+ve}$ significantly increased cell proliferation compared to HS^{pm} and $HS8^{-ve}$. Moreover, $HS8^{+ve}$ had little anticoagulant activity, increased FGF-2 stability and enhanced FGF-2-mediated hMSC growth via FGF-2-FGFR1-HS ternary complex formation and subsequent signaling.

In this Chapter, I set out to observe the effects of HS variants on long-term hMSC proliferation. HS variants, particularly the robust, highly scalable, simple and cost-effective $HS8^{+ve}$ fraction, as well as the crude unfractionated HS^{pm} and flow through $HS8^{-ve}$ fractions were used as media supplements for the culture of both plastic-adherent and $STRO1^{+}$-isolated hMSCs. The cumulative growth (CG) of these cells was monitored and the cells assessed in the colony-forming unit fibroblastic assay (CFU-F), by flow cytometric analysis (FC) and by multilineage differentiation (MLD) assays.

Next, I investigated whether hMSCs isolated from bone marrow aspirates also responded positively to exogenous $HS8^{+ve}$ supplementation, with a view to determining its direct clinical utility. To examine this cryopreserved bone marrow mononuclear cells (Lonza) from three human donors were used in this part of the study. The isolation and expansion of hMSCs was carried out with media supplemented with the various HS variants. The cumulative growth (CG) of hMSCs was observed and the cells

assessed by colony-forming unit fibroblastic assay (CFU-F), flow cytometric analysis (FC), multilineage differentiation (MLD) as well as immunomodulatory analysis (IM) during their serial passaging.

4.2. Materials and Methods

4.2.1. Long term proliferation

HS variants (HS^{pm}, $HS8^{-ve}$ and $HS8^{+ve}$) were used as stand-alone media supplements (Fig. 4.1). Two types of isolated and expanded hMSCs, plastic adherent and STRO-1^{+} were used at passage 3, and culture-expanded over 4 passages in the presence of HS variants. The optimum concentration of each HS variant ($HS8^{+ve}$ at 2.5 µg/ml, HS^{pm} and $HS8^{-ve}$ at 1.25 µg/ml) were used as identified by short-term proliferation assays (Fig. 3.14). In addition, optimum concentrations of heparin (1.25 µg/ml) and FGF-2 (2.5 ng/ml) were used as positive controls (Fig. 3.23).

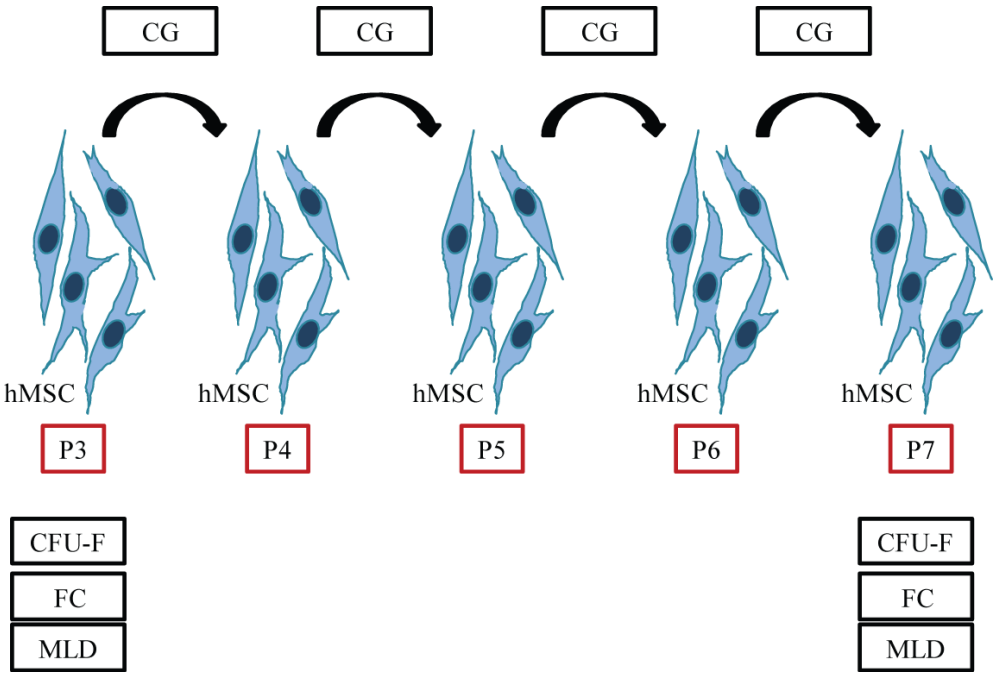

Figure 4.1. Experimental layout of long-term proliferation studies of plastic adherent and STRO-1$^+$ hMSCs. Plastic adherent and STRO-1$^+$ hMSCs were culture-expanded from passage 3 to 7 with the exogenous addition of HS variants into culture media. The cumulative growth (CG) of hMSCs was observed and the cells at the beginning and end of the study were assessed by colony forming unit fibroblastic assay (CFU-F), flow cytometry analysis (FC) and multilineage differentiation (MLD).

4.2.1.1. Cumulative growth (CG)

Plastic adherent and STRO-1$^+$ hMSCs at passage 3 were seeded at a density of 3000 cells per cm^2 in multidish 6-well tissue culture plates (Nunc) with 2 ml of culture media to evaluate their cumulative population doubling and growth over a period of 4 passages in a humidified atmosphere at 37 °C with 5% CO_2. Plastic adherent hMSCs were cultured in maintenance media containing DMEM-LG 1000 mg/l supplemented with 10 % FCS, 50 units/ml penicillin and 50 µg/ml streptomycin, while STRO-1$^+$ hMSCs were cultured with maintenance media containing α-MEM supplemented with 10 % FCS, 100 µM L-ascorbate-2-phosphate, 50 units/ml penicillin and 50 µg/ml streptomycin and 2 mM L-glutamine. Both maintenance medias were

supplemented with each of the HS variants or the positive controls and the media changed every 2nd day of expansion. Once the cells reached 70-80 % confluence, the cells were harvested with 0.125 % trypsin/Versene (pH 7.0±0.3). An aliquot of each of the triplicate wells was stained with Viacount flex reagent (1:200) to detect viable cells by the microcapillary flow cytometry platform of the EasyCyte™ Plus system and analyzed using the EasyCyte™ Plus software (Millipore). The rest of the cell suspension from the triplicate wells was pooled and reseeded at 3000 cells per cm^2 in triplicate wells. This process was repeated for four subsequent passages, with a media change performed once every two days and cumulative cell numbers calculated and plotted against passage number. Excess cells were cryopreseved in FCS (Hyclone, Thermo Scientific) containing 10 % (v/v) dimethyl sulfoxide (DMSO, Sigma Aldrich).

4.2.1.2. Colony forming unit fibroblastic assay (CFU-F)

CFU-F assays (Rider *et al*., 2008) were performed using hMSCs at 70-80 % confluency at the beginning and end of the expansion phase of the study as described in Chapter 3. Briefly, hMSCs were seeded (150 cells in 100 x 15 mm petri dishes (Nunc)) in triplicate in 10 ml of culture maintenance media and cultured for 14 days with a single medium change at day 7. Colonies were stained with crystal violet (Sigma-Aldrich), counted as described earlier (Chapter 3.2.3.1) and CFU-F efficiency was calculated as a percentage of colonies formed against the number of cells seeded.

4.2.1.3. Flow cytometry analysis (FC)

For the flow cytometry analysis, hMSCs were maintained in 140 x 20 mm tissue culture dishes (Nunc) in triplicate with maintenance media supplemented with either HS, heparin or FGF-2 as positive controls. The cells in three plates were pooled together after reaching 70-80 % confluence and the FC analysis of hMSCs (gated at 1% of the isotype control) was performed as described in Chapter 3.2.3.2. Briefly, hMSCs were tested for positive expression of the surface markers CD73, CD90, CD105, and negative expression of CD14, CD19, CD34, CD45, HLA-DR, using isotype matched controls IgG1, IgG1κ and IgG2bκ to determine whether they fulfilled the minimal criteria to define multipotent mesenchymal stem cells (Dominici *et al*., 2006). In addition, cells were also assayed for the expression of the surface markers STRO-1 (Gronthos *et al*., 1999), SSEA-4 (Gang *et al*., 2007) and CD49a (Rider *et al*., 2007) using isotype-matched controls IgM, IgG3k and IgG1k. All primary antibodies for flow cytometry were conjugated with either PE or FITC (BD Biosciences, eBioscience and Invitrogen) except for STRO-1 (Gronthos lab) where the secondary antibody was goat anti-mouse IgM (μ) conjugated with PE (Invitrogen). Full details of antibodies and their corresponding isotype are provided in Appendix B. Next, stained cells were analyzed on BD FACS Array^{TM} Bioanalyzer and gating and analysis performed using FlowJo software (Tree Star, Inc.).

4.2.1.4. Multilineage differentiation (MLD)

Human MSCs cultured in 140 x 20 mm tissue culture dishes (Nunc) with maintenance media supplemented with HS and positive controls (heparin

or FGF-2) were pooled together after reaching 70-80 % confluency and induced to differentiate along the osteogenic, adipogenic or chondrogenic lineages as previously reported by our research group (Rider *et al*., 2008) over 28 days, with a medium change every 3 days as previously described (Chapter 3.2.3.3). Osteogenic differentiaiton was assessed by Alizarin Red S (Sigma-Aldrich) staining for calcium and von Kossa (Sigma-Aldrich) staining for calcium phosphate. Whilst, adipogenic and chondrogenic differentiation was detected by Oil Red O (Sigma-Aldrich) (to visualize lipid droplets) and Alcian blue (Sigma-Aldrich) (to visualize chondrogenic glycosaminoglycans) stains respectively. The capacity for multilineage differentiation was then quantified by Quantity-One® 1-D analysis software (Bio-Rad Laboratories) based on stain density.

4.2.2. Long-term proliferation study of hMSC for direct clinical utility

To determine the effect of $HS8^{+ve}$ on hMSC proliferation during long-term serial passaging, naïve hMSCs were isolated from bone marrow mononuclear cells (Lonza) from three donors (Table 4.1) and cultured in media containing HS variants (HS^{pm}, $HS8^{-ve}$ and $HS8^{+ve}$) until passage 6 (Fig. 4.2). HS dose ($HS8^{+ve}$ at 2.5 µg/ml, and both HS^{pm} and $HS8^{-ve}$ dose at 1.25 µg/ml), was based on earlier screening assays in Chapter 3 (Fig. 3.14). In addition, heparin (1.25 µg/ml) and FGF-2 (2.5 ng/ml) were used as positive control supplements (Fig. 3.23). Cumulative growth (CG), clonegenic ability (colony forming unit fibroblastic (CFU-F)), biomarker expression by flow cytometry analysis (FC), multilineage differentiation (MLD) and immunomodulatory (IM) ability was also assessed during serial passaging in the various conditions (Fig. 4.2).

Table 4.1. Description of the bone marrow mononuclear cell donors used in the long-term proliferation study of hMSC for direct clinical utility.

Donor	Age	Sex	Race	Cat. and lot No.	Source
A	21Y	Male	Caucasian	2M-125A 1F3283B	Lonza, Walkersville Inc., MD
B	28Y	Male	Caucasian	2M-125A 1F3302	Lonza, Walkersville Inc., MD
C	22Y	Male	Black	2M-125A 1F3378B	Lonza, Walkersville Inc., MD

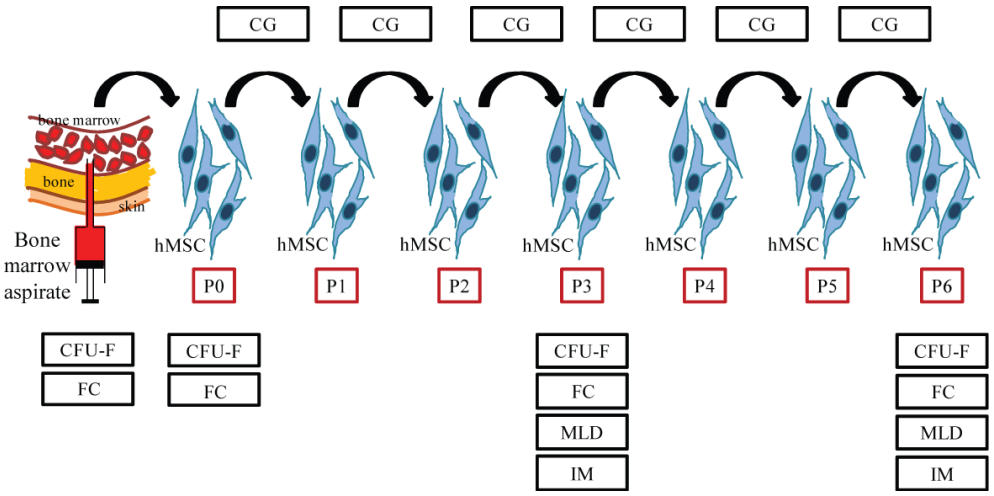

Figure 4.2. Experimental layout of long-term proliferation assay of hMSC for direct clinical utility. Human MSCs were continuously dosed with HS (HS^{pm}, $HS8^{-ve}$ and $HS8^{+ve}$) until passage 6. Assessment of cumulative growth (CG), colony forming ability (CFU-F), biomarker expression by flow cytometry analysis (FC), multilineage differentiation (MLD) and immunomodulatory (IM) potential at various passages during serial expansion was assessed.

4.2.2.1. Thawing and isolation of hMSCs by plastic adherence.

Bone marrow mononuclear cells (BMMNCs) from different donors (Table 4.1) were thawed in complete maintenance medium as per manufacturer's specifications (Lonza) as described in Chapter 3. Then the BMMNCs (1×10^7) were seeded in T175 flasks (Nunc) in 30 ml of basal

media (DMEM-LG 1000 mg/l, 10 % FCS, 50 units/ml penicillin and 50 µg/ml streptomycin) supplemented with HS variants or positive controls (heparin or FGF-2) in triplicate. Cells were allowed to adhere for 5 days before the first media change, thereupon media replacement was performed every 3 days. All cultures were maintained under humidified atmosphere at 37 °C with 5 % CO_2. Cells were detached with 0.125 % trypsin/versene (pH 7.0±0.3) upon reaching 75–80 % confluency and an aliquot used to determine the number of viable cells by the EasyCyte™ Plus system and analyzed by EasyCyte™ Plus software (Millipore). The remainder of the cells were pooled and used for cumulative growth assays, CFU-F assays, flow cytometry analysis or cryopreseved in FCS (Hyclone, Thermo Scientific) containing 10 % (v/v) dimethyl sulfoxide (DMSO, Sigma Aldrich).

4.2.2.2. Cumulative growth (CG)

Cumulative growth assays were conducted as described earlier from P0 to P6 using pooled cells isolated by plastic adherence (P0) or from cells at later passages. In addition to 6-well tissue culture plates (Nunc) cells were cultured in 140 x 20 mm tissue culture dishes (Nunc) at a density of 3,000 cells per cm^2 in 20 ml of culture media. Cells were cultured in maintenance media (DMEM-LG 1000 mg/l, 10 % FCS, 50 units/ml penicillin and 50 µg/ml streptomycin) supplemented with HS variants, or positive controls (heparin or FGF-2) in triplicate from Passage 0 to Passage 6 passages in a humidified atmosphere at 37 °C with 5 % CO_2. During serial passaging cells were harvested at 70-80% confluency, counted and replated as above and excess

cells cryopreseved in FCS (Hyclone, Thermo Scientific) containing 10 % (v/v) dimethyl sulfoxide (DMSO, Sigma Aldrich).

4.2.2.3. Colony forming unit fibroblastic assay (CFU-F)

CFU-F assays were performed at P0, P3 and P6 as described above and in Chapter 3.2.3.1. In addition, CFU-F assays were conducted on the bone marrow mononuclear cells (BMMNCs). Briefly, BMMNCs from different donors (Table 4.1) were thawed in complete maintenance medium as per manufacturer's specifications (Lonza) and plated in 0.5, 1 and 2 x 10^6 in 100 x 15 mm petri dishes (Nunc) with 10 ml of culture media supplemented HS and positive controls (heparin or FGF-2) in triplicate. Cells were then cultured for 14 days with a single medium change at day 7. Colonies were stained with crystal violet (Sigma-Aldrich), counted and CFU-F efficiency calculated.

4.2.2.4. Flow cytometry analysis (FC)

For flow cytometry analysis, cells were maintained in 140 x 20 mm tissue culture dish (Nunc) in triplicate with maintenance media supplemented with HS, heparin or FGF-2. Cells from the three plates were pooled together after reaching 70-80 % confluence and FC analysis performed at P0, P3 and P6 as described above and in Chapter 3.2.3.2. Expression of the biomarkers CD73, CD90, CD105, STRO-1, SSEA-4, CD49a (expressed by MSCs) and CD14, CD19, CD34, CD45, HLA-DR (not expressed by MSCs) was determined. For comparison, FC analysis was also performed on BMMNCs (from the 3 donors) prior to plastic adherent isolation of P0 hMSCs.

Expression analysis was performed on BD FACS Array™ Bioanalyzer and FlowJo software (Tree Star, Inc.).

In addition, flow cytometry assay was employed to detect levels of FGF receptors (1-4) on the cell surface of hMSCs. The hMSCs were harvested using TrypLE™ (Invitrogen) (6 ml for each 140 x 20 mm tissue culture dish) and neutralized with the same amount of media, centrifuged at 300 g for 5 min and the media aspirated. New media was added into the Falcon tube and the cell suspension was incubated for 30 min in humidified atmosphere at 37 °C, 5 % CO_2. The lid of the 15 ml tube was slightly loosened for air exchange and the tube on a rack was shaken every 10 min to prevent cells attaching to the tube. The FC analysis of hMSCs was performed at P3 and P6 as described. The IMBR1 antibody (Ling *et al.*, 2006) against FGFR1 and against FGFRs 2-4 (R & D Systems) were used with isotype-matched controls of IgG1 and IgG2ak. The FGFR 2-4 antibodies used for flow cytometry were primary antibodies conjugated with either PE except for IMBR1 where a secondary antibody goat anti rabbit IgG1 conjugated with AF (Invitrogen) was used. The details of the antibodies and their corresponding isotypes are provided in the Appendix. The stained cells were analyzed on BD FACS Array™ Bioanalyzer and FlowJo software (Tree Star, Inc.).

In addition, as described by Smith *et al.,* flow cytometry was used to analyze the cell sizes of the hMSCs at P0, P3 and P6 (Smith *et al.*, 2004). The hMSCs were categorized into small, fast-growing cells and large, slow-growing cells accordingly and comparisons made between the cells expanded with different HS variants.

4.2.2.5. Multilineage differentiation (MLD)

The hMSCs maintained in 140 x 20 mm tissue culture dishes (Nunc) with hMSC maintenance media supplemented with HS variants and positive controls were pooled together at 70-80 % confluence and used in osteogenic, adipogenic and chondrogenic differentiation assays (Rider *et al*., 2008) over 28 days, as previously described (Chapter 3.2.3.3). Quantification of multilineage differentiation was performed by measurements of the respective staining intensity using Quantity-One® 1-D analysis software (Bio-Rad Laboratories).

4.2.2.6. Immunomodulatory analysis (IM)

Immunomodulation ability was determined by two methods. The first examined the ability of hMSCs to suppress the proliferation of a mixture of stimulatory and reactionary human peripheral blood mononuclear cells (PBMCs) from two different, healthy, un-matched donors. Assessment of changes in the number of $CD3^+$ $Ki67^+$ T-cells was determined by flow cytometry as previously published by our group (Helledie *et al*., 2011; Rai *et al*., 2010). The second method determined the level of TNF-α receptor type 1 expression on hMSCs by ELISA assay (R & D systems) following the manufacture's recommendations.

4.2.2.6.1. Suppression of peripheral blood mononuclear cell (PBMCs) assay

The immunomodulatory analysis capacity of hMSCs is widely assessed as a function of their therapeutic potency. Briefly, hMSCs expanded

in media containing different HS variants and positive controls at P3 and P6 were seeded at 1 x 10^5 cells/well in 96-well plates (Nunc). A mixture of stimulatory and reactionary human peripheral blood mononuclear cells (PBMCs) from two different healthy un-matched donors (Singapore Cord Blood Bank) was added to the wells 24 h later at different PBMC: hMSC ratios (1:1 and 1:10) and the cells incubated for 7 days in a humidified atmosphere at 37 °C with 5 % CO_2. The expression of $CD3^+$ $Ki67^+$ cells was assessed by two colour FACS array as described below.

The pelleted cells were resuspended in hMSC maintenance media and the cell suspension centrifuged at 2000 rpm for 4 min. Then the media was aspirated and the cells resuspended in 100 µl of FACS buffer (0.05 % BSA, 2 mM EDTA in PBS). The cell suspension was added with 2 µl of CD3 antibody or isotype (BD Biosciences) and incubated for 30 min at 4 °C. The cells were spun down at 2000 rpm for 4 min and washed twice with PBS. Next, the cells were resuspended in 100 µl fix perm (eBioscience) in diluent (eBioscience) and incubated for 30 min at 4 ˚C. Afterwards the cells were neutralized with 100 µl of FACS buffer, spun down and the media aspirated. Then the cells were resuspended in 100 µl perm buffer (eBioscience) and incubated for 10 min at 4 °C. Another 100 µl perm buffer was added, spun down and the media was aspirated. Later cells were resuspended in 50 µl perm buffer and 5 µl of Ki-67 antibody or isotype (BD Biosciences) and incubated for 30 min at 4 °C. Then 100 µl perm buffer was added, spun down and the media was aspirated. The cells were washed twice with perm buffer. Then the sample was resuspended in 200 µl of FACS buffer and the stained cells were

analyzed on BD FACS Array™ Bioanalyzer and FlowJo software (Tree Star, Inc.).

4.2.2.6.1. TNF-α receptor type 1 quantitative ELISA assay

TNF-α receptors are expressed on the surface of mesenchymal stem cells (Tartaglia *et al*., 1991) and TNFR1 is the predominant type (Vancheri *et al*., 2000). Danilkovitch *et al* have described that that hMSCs expression of TNF-α receptors may be critical for immunosuppressive, immunomodulatory, anti-inflammatory, tissue-repairing, and wound-healing activities, as well as migration to sites of inflammation (Danilkovitch *et al*., 2012). Therefore, a quantikine ELISA kit for human sTNFRI (R&D Systems) was used for the detection of TNFRI in cell lysates of hMSCs as per the manufacturer's recommendations (Danilkovitch *et al*., 2012).

For the ELISA assay, 2.5 x 10^5 hMSCs were lysed using 250 µl of mammalian cell lysis/extraction reagent (Sigma-Aldrich) containing a complete protein inhibitor cocktail (Sigma-Aldrich). The cell lysates were centrifuged for 10 min at 12,000-14,000 rpm to remove any insoluble material from the lysis buffer solution. The cell lysates were collected in a new tube for use in the ELISA assay.

The sTNF RI Standard was reconstituted as recommended with Calibrator Diluent RD5-5 to produce a stock solution of 500 pg/ml. After the standard was mixed with gentle agitation for 15 min, 7.8, 15.6, 31.2, 62.5, 125, 250 and 500 pg/ml standard solutions were made through serial dilution. The Calibrator Diluent RD5-5 serves as the zero standard (0 pg/ml). All reagents and working standards were brought to room temperature and all

standards, samples and controls were assayed in duplicates. Firstly, each well of the microplate strips was added with 50 µl of Assay Diluent HD1-7. Afterwards, 200 µl of standard, control, or sample per well was added. Then the microplate was covered with the adhesive strip and incubated for 2 h at room temperature. Each well was aspirated and washed, repeating the process three times for a total of four washes by using 400 µl of wash buffer (dilute 20 ml of wash buffer concentrate in 500 ml of deionized or distilled water) per well. After the last wash the microplate was inverted and blot dried against clean paper towels to remove liquids completely. Then 200 µl of sTNF RI conjugate was added to each well, covered with a new adhesive strip and incubated for 2 h at room temperature. Wells were aspirated and washed as earlier. Then 200 µl of substrate solution (colour reagents A and B mixed in equal volumes) was added to each well and incubated for 20 min at room temperature while protecting from light. Next 50 µl of stop solution was added to each well. Finally the optical density was determined within 30 min, using a Bechmark Plus Spectophometer (Bio-Rad) set to 450 nm and a wavelength correction made by subtracting the readings at 540 nm. Optical density readings of the standards were used to plot the standard curve. The best-fit line was determined by regression analysis and the equation yielded used to determine the sTNF RI concentrations of the samples.

4.2.3. Statistical analysis

All data values are reported as the mean ± standard deviation (SD) taken from triplicate experiments. Where appropriate, mean differences between samples were analyzed using SPSS statistics software (IBM, USA)

by performing an exploratory data analysis and homogeneity of variance test, followed by ANOVA and Tukey's or Games–Howell posthoc testing. Statistical significance was defined at >0.05. Graphs were plotted and data transformed using Sigma plot software (Systat software Inc, USA) and Adobe illustrator (Adobe, USA).

4.3. Results

4.3.1. Long-term proliferation study

4.3.1.1. $HS8^{+ve}$ increases cumulative viable cell number in plastic adherent and STRO-1 hMSCs.

In chapter 3, a significant increase (~ 1.4 fold) in hMSC proliferation following $HS8^{+ve}$ supplementation was observed when cells were cultured over a 4 day period (Figs. 3.9, and 3.14). To determine the cumulative effect of HS supplementation during serial passaging, cells were cultured in media contain HS (HS^{pm}, $HS8^{-ve}$ and $HS8^{+ve}$) for 4 passages, with media changes every 2 days. Cells were harvested at 70-80 % confluence and cell number determined by Guava EasyCyte™ Plus System/CytoSoft™ software platform (Millipore™) and reseeded at the same cell density for the subsequent passage.

Overall, irrespective of the different media with or without any supplementation STRO-1^{+} hMSCs had a higher cumulative cell numbers compared to the plastic adherent hMSCs (Fig. 4.3). In both plastic adherent and STRO-1^{+} hMSCs expanded in media supplemented with $HS8^{+ve}$, significantly higher cumulative cell numbers were observed compared to the controls (Fig. 4.3). The increase in the sub-confluent hMSC number was evident from the first passage of expansion. Whereas, HS^{pm} and $HS8^{-ve}$ triggered cell expansion was very much similar for plastic adherent hMSCs, or only slightly elevated in STRO-1+ hMSCs compared to the control. HS^{pm} showed an intermediate level of cell growth with STRO-1 hMSCs. On the other hand, the positive control FGF-2 showed the greatest cumulative cell number increase while negatively charged heparin showed a similar trend in growth compared with $HS8^{+ve}$ (Fig. 4.3). These data revealed that $HS8^{+ve}$

increases cumulative viable cell number and the effect of the HS variants on growth was again in the order of their binding affinity for FGF-2.

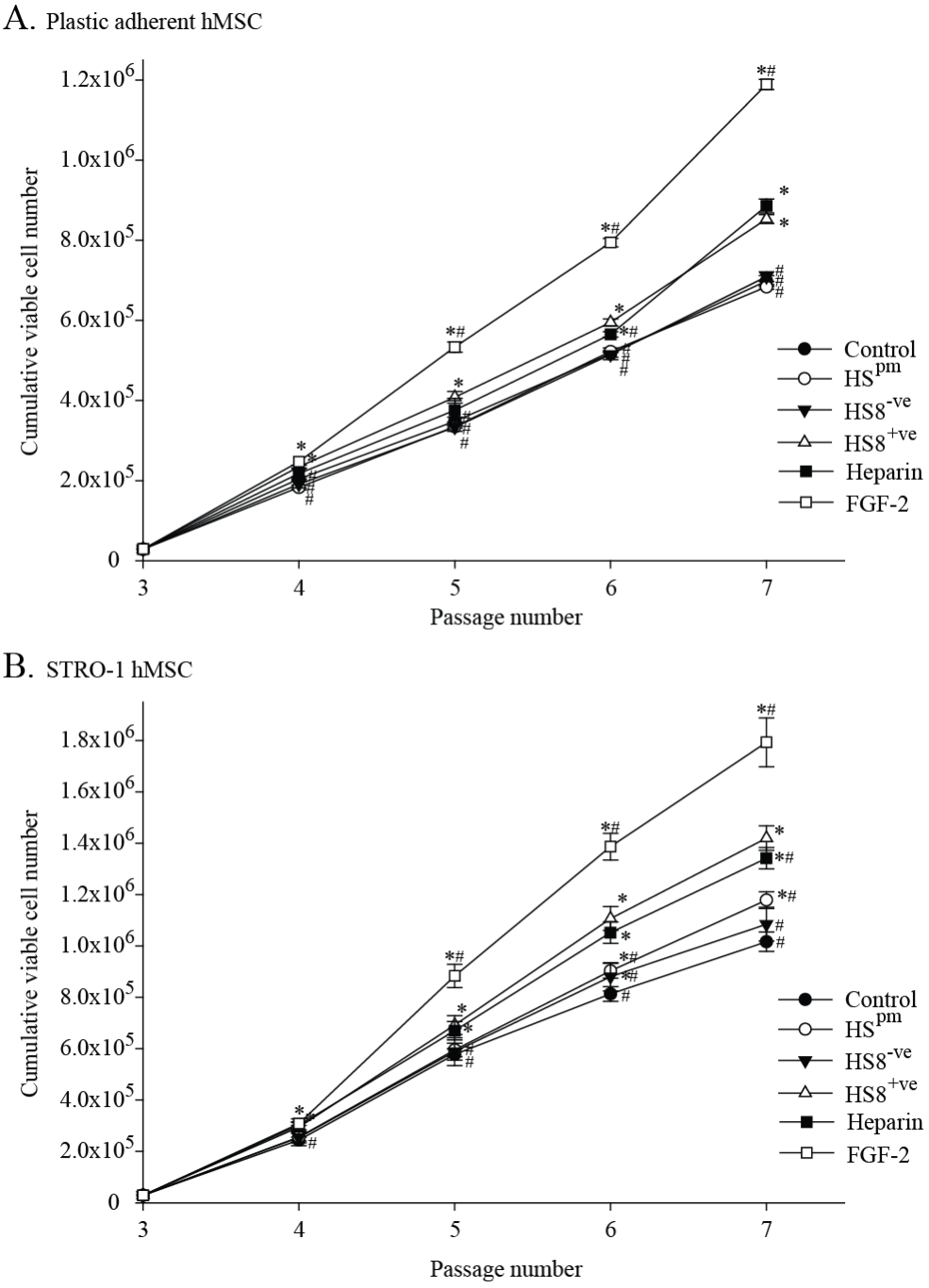

Figure 4.3. HS8^{+ve} increases cumulative viable cell number over 4 passages in (A) plastic adherent and (B) STRO-1+ hMSCs. Cells were seeded at 3000 cells per cm^2 in multidish 6-well tissue culture plates and cumulative viable cell number of hMSCs expanded in maintenance media (Control) and media supplemented with different HS variants (HS^{pm}, HS8^{-ve} and HS8^{+ve}) over 4 passages with media change at every 2 days, was plotted. Cells were harvested at 70-80 % confluence, analyzed by Guava and reseeded at same cell density for subsequent passage. Significant difference is denoted as * when compared to control and $^{\#}$ when compared to HS8^{+ve} at equivalent passage ($p<0.05$).

4.3.1.2. $HS8^{+ve}$ increases plastic adherent and STRO-1 hMSCs CFU-F efficiency.

Plastic adherence is a well described property of hMSCs; if cells are maintained and expanded in normal culture conditions they should adhere to the plastic surface and form mesenchymal stem cell colonies when plated at low densities (Friedenstein *et al*., 1976; Pochampally, 2008). In addition, hMSC cultures are known to contain a heterogeneous population of cells, especially in regards to the presence of naïve progenitor cells (Pochampally, 2008). Furthermore CFU-F assays highlight the relationship between clonegenicity and the proportion of early progenitors in a pool of hMSCs (Pochampally, 2008; Reger and Prockop, 2014). Therefore, to assess the ability of HS to preference the expansion of naïve MSCs in the heterogenous pool of cultured cells, CFU-F assays were repeatedly performed during the serial passaging of hMSCs under HS supplementation.

Irrespective of the HS variant and baseline media control cells, there was an increase in CFU-F efficiency after 4 passages (Fig. 4.4). In addition, irrespective of the different media used STRO-1 hMSCs had a better CFU-F efficiency than plastic adherent hMSCs. In both plastic adherent and STRO-1 hMSCs, those expanded in media supplemented with $HS8^{+ve}$ demonstrated significantly higher CFU-F efficiency when compared to the controls before and after 4 passages. In addition, the CFU-F efficiency of $HS8^{+ve}$ grown cells was significantly higher than the crude HS^{pm} and flow through $HS8^{-ve}$, whereas, HS^{pm} and $HS8^{-ve}$ showed an intermediate level and lower level of colony formation compared to $HS8^{+ve}$ grown cells. This trend again resembles the relative affinity of HS variants to FGF-2. On the other hand, the positive

controls of heparin and FGF-2 showed lower levels of colony formation compared to HS8^{+ve} (Fig. 4.4). Interestingly, cells grown with FGF-2 demonstrated significantly lower CFU-F efficiencies than the baseline control (Fig. 4.4).

The data suggests that HS8^{+ve} supplementation results in an increased CFU-F efficiency compared with the other HS variants and heparin. Whilst, supplementation with FGF-2 resulted in a decrease in CFU-F efficiency, that may reflect fewer naive progenitors in FGF-2 supplemented cultures.

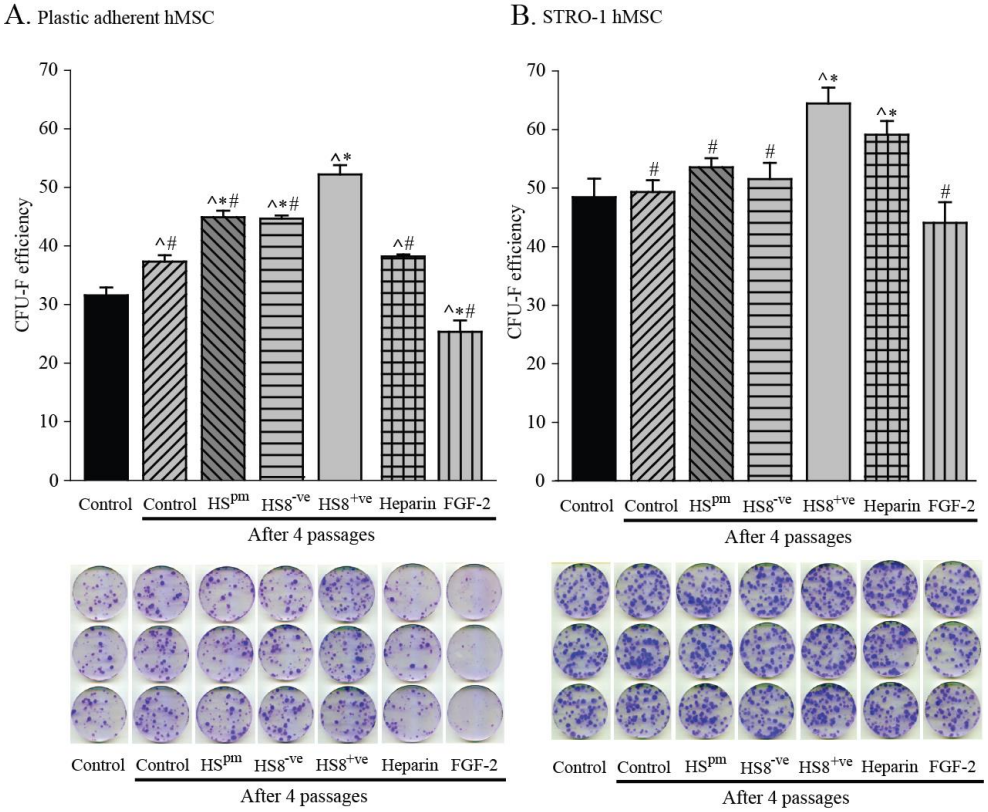

Figure 4.4. HS8^{+ve} increases (A) plastic adherent and (B) STRO-1+ hMSC CFU-F efficiency. The hMSCs were seeded at 150 cells per and cultured for 14 days. By day 14, cultures were terminated and stained with Crystal violet. Significant difference is represented as ^ when compared to starting control group, * when compared to control after 4 passages and $^{\#}$ when compared to HS8^{+ve} ($p<0.05$).

4.3.1.3. Immunophenotypic profile of plastic adherent and STRO-1 hMSCs.

Measures of ‘‘stemness’’ in hMSCs typically consist of the basis of adherence to tissue culture plastic, their immunophenotypic profile and their multi-lineage proliferation. Therefore I next looked at the Immunophenotypic profile of hMSCs after long-term HS expansion. Single-color flow cytometry analysis revealed that both types of hMSCs were positive for the MSC-related markers CD73, CD90, CD105 (> 99 % positive) but negative for haematopoeitic markers (< 2 % positive) of CD14, CD19, CD34, CD45 and HLA-DR (Table 4.2). Irrespective of media used to expand the hMSCs except in $HS8^{-ve}$ grown plastic adherent cells' CD14 haemotopoeitic marker (4.7±0.74). This was evident with cells grown with media supplemented with the positive controls, heparin and FGF-2, except for the effects of FGF-2 on the expression of CD90 (91±0.21) (Table 4.2).

In addition to the MSC-related biomarkers described by (Dominici *et al*., 2006)) expression of STRO-1, SSEA-4 and CD49a was also determined. These additional MSC biomarkers have also shown to identify multipotent MSCs (Gronthos *et al*., 1999, Gang *et al*., 2007, Rider *et al*., 2007). Serial passaging of cells had an effect on these additional biomarkers. Plastic adherent hMSCs after 4 passages showed a statistical increase in expression of STRO-1, SSEA4 and CD49a irrespective of the media supplemented with or without HS variants (including the positive control heparin) expect for few notable instances. No statistical significance was observed in STRO1 expression for HS^{pm} and CD49a expression for heparin while SSEA4 expression in $HS8^{-ve}$ was statistically lower than that of control cells at passage

3. On the other hand, FGF-2 grown cells had significantly lower expression of STRO1 and CD49a while SSEA4 was significantly higher than that of control cells at passage 3. In addition, after 4 passages, in the $STRO1^{+}$ isolated hMSCs showed statistically increased expression only in STRO-1 biomarker with cells expanded with $HS8^{+ve}$ and heparin.

After 4 serial passages plastic adherent hMSCs expanded in $HS8^{+ve}$ showed a statistically increased expression of STRO-1, SSEA-4 and CD49a when compared to cells expanded in HS^{pm} and $HS8^{-ve}$. In the $STRO\text{-}1^{+}$ isolated hMSCs, $HS8^{+ve}$ showed statistically increased levels of STRO-1 when compared to HS^{pm} and $HS8^{-ve}$, higher levels of SSEA-4 and CD49a when compared to cells expanded in HS^{pm} and similar levels of SSEA-4 and CD49a $HS8^{-ve}$. In comparison to the control cells of plastic adherent hMSCs, $HS8^{+ve}$ grown cells showed significantly increased levels of SSEA4, higher levels of CD49a and similar levels of STRO1. In $STRO\text{-}1^{+}$ isolated hMSCs, $HS8^{+ve}$ expanded cells showed significantly higher levels of STRO1, higher levels of SSEA4 and similar levels of CD49a. On the other hand, in both plastic adherent and STRO-1 hMSCs, HS^{pm} and $HS8^{-ve}$ grown cells showed variability in their expression of these three surface markers over the control. Although these cells in general showed an intermediary level of expression of stemness surface markers when compared to control and $HS8^{+ve,}$ it still indicated the trend in the relative affinity of these HS variants to FGF-2. The surface marker expression of STRO-1, SSEA-4 and CD49a in cells grown with positive control heparin showed essentially similar expression to that of $HS8^{+ve}$ (Table 4.2). In contrast, FGF-2-cultured cells showed a marked decline in STRO-1 and CD49a expression, even compared to control cells, and an

increase in SSEA-4 levels over control and all HS variant-maintained cells (Table 4.2). Therefore, it was evident that serial passaging of hMSCs supplemented with $HS8^{+ve}$ had a beneficial effect on the cells while FGF-2 supplementation had a detrimental effect on the expanded hMSCs. This further supports the idea that $HS8^{+ve}$ may target the expansion of early progenitors in heterogeneous hMSC culture, in contrast to exogenous FGF-2 supplementation, tends to expand fewer naive progenitors.

Table 4.2. Immunophenotypic profile of (A) plastic adherent and (B) STRO-1 hMSC. Single-color flow cytometry analysis of hMSCs was performed on P3 control cells and P7 expanded cells with or without HS variants for positivity markers, negativity markers and stemness markers. The level of positivity of relevant surface marker is depicted as below. Significant difference is represented as ^ when compared to starting control group, * when compared to control after 4 passages and # when compared to $HS8^{+ve}$ ($p<0.05$).

A. Plastic adherent hMSC

		Negative markers					Positive markers			Stemness		
		CD14	CD19	CD34	CD 45	HLA-DR	CD 73	CD90	CD105	STRO-1	SSEA-4	CD49a
P3	Control	0.8±0.13	0.1±0.21	1.0±0.21	0.9±0.05	1.0±0.02	99.9±0.07	99.6±0.42	99.9±0.07	24.1±3.68	33.7±3.32	34.0±16.97
P7	Control	0.9±0.25	0.9±0.33	0.9±0.40	1.0±0.40	1.2±0.28	99.9±0.00	99.9±0.07	99.9±0.07	34.5±1.06^	56.3±1.77^#	54.0±0.64^
	HS^{pm}	1.1±0.46	1.5±0.13	0.9±0.03	0.9±0.07	1.2±0.14	100.0±0.00	100.0±0.00	99.9±0.00	26.5±0.42*#	63.9±0.99^*#	83.7±0.64^*#
	$HS8^{-ve}$	4.7±0.74^*#	1.6±0.37	1.3±0.42	1.5±0.44	1.2±0.41	100.0±0.00	100.0±0.00	100.0±0.00	28.4±0.49^*#	13.9±1.41^*#	68.9±1.98^*
	$HS8^{+ve}$	1.1±0.35	1.1±0.45	0.9±0.43	1.2±0.58	1.5±0.31	99.9±0.00	100.0±0.00	99.9±0.00	35.3±0.57^	71.2±0.21^*	63.0±2.26^
	Heparin	0.7±0.34	1.3±0.46	1.3±0.55	1.1±0.54	1.2±0.32	99.8±0.00	99.6±0.07	99.5±0.00	34.6±0.07^	74.6±1.70^*	55.8±4.60
	FGF-2	1.2±0.38	1.1±0.45	1.3±0.32	1.3±0.30	1.6±0.45	99.8±0.07	91.0±0.21^*#	99.9±0.07	3.9±0.52^*#	84.3±0.85^*#	29.2±1.63^*#

B. STRO-1 hMSC

		Negative markers					Positive markers			Stemness		
		CD14	CD19	CD34	CD 45	HLA-DR	CD 73	CD90	CD105	STRO-1	SSEA-4	CD49a
P3	Control	1.4±0.20	1.3±0.23	1.5±0.71	1.2±0.25	1.0±0.37	99.1±0.00	99.9±0.00	99.4±0.21	3.4±0.33	3.9±1.34	8.9±6.70
P7	Control	1.3±0.04	1.3±0.24	1.2±0.19	1.1±0.06	0.9±0.02	99.0±0.49	99.9±0.00	99.2±0.64	3.4±0.49#	2.1±0.23	9.0±1.60
	HS^{pm}	1.1±0.29	0.9±0.05	1.2±0.23	1.3±0.11	1.1±0.17	99.4±0.14	99.9±0.00	99.4±0.00	3.5±0.69#	3.4±0.36	6.0±0.01
	$HS8^{-ve}$	1.2±0.19	1.0±0.13	1.1±0.04	1.2±0.03	1.0±0.04	99.5±0.64	99.9±0.14	99.5±0.14	2.6±0.29#	8.3±4.8	8.1±6.15
	$HS8^{+ve}$	1.0±0.10	1.4±0.23	0.9±0.02	1.1±0.06	1.0±0.10	98.8±0.49	99.9±0.13	98.9±0.21	4.7±0.37^*	6.6±0.88	7.6±6.24
	Heparin	1.0±0.39	1.2±0.04	1.3±0.25	0.9±0.49	0.9±0.27	98.4±0.85	99.8±0.00	99.2±0.07	4.8±0.23^*	4.9±2.94	3.5±0.58
	FGF-2	1.6±0.34	1.0±0.13	1.1±0.13	1.1±0.17	1.1±0.22	98.7±0.71	99.9±0.00	99.2±0.42	2.7±0.63#	7.3±8.57	5.5±0.04

4.3.1.4. Multi lineage differentiation of plastic adherent and STRO-1 hMSCs.

Finally I looked at the multilineage differentiation potential of cells expanded in the different HS variants compared to the control. Irrespective of media used to expand them, the plastic adherent and STRO-1^{+} hMSCs were able to differentiate down the osteogenic, adipogenic and chondrogenic lineages (Fig. 4.5). In addition, after 4 passages in plastic adherent hMSCs, $HS8^{+ve}$ showed statistically increased osteogenic differentiation as evident with calcium staining by Alizarin Red and calcium phosphate staining by von Kossa staining while heparin was significantly higher in von Kossa staining as compared to the control hMSCs at passage 3. The passage 7, control cells showed similar osteogenic, adipogenic and chondrogenic differentiation as compared to the different HS variants yielded from affinity chromatography. Similarity was shown in the plastic adherent hMSCs, heparin-grown cells (positive control), except; calcium staining by Alizarin Red, which were statistically lower than that of control and $HS8^{+ve}$. The FGF-2-grown plastic adherent hMSCs (positive control) were lacking osteogenic differentiation capacity in both calcium and calcium phosphate staining by Alizarin Red S and von Kossa respectively (Fig. 4.5). On the other hand, STRO-1^{+} hMSCs tri-lineage differentiation occurred in a similar manner among different cells (Fig. 4.5).

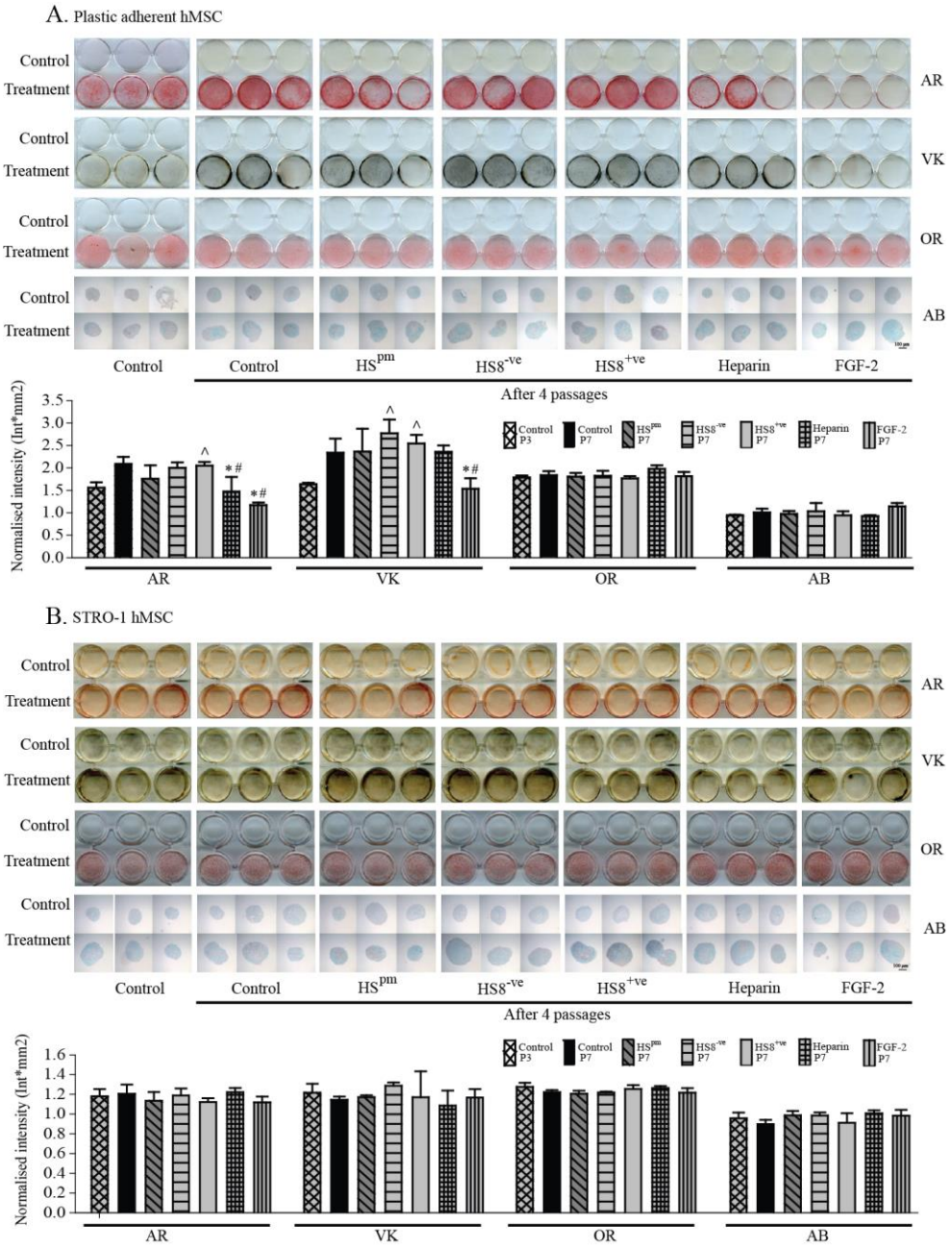

Figure 4.5. Multilineage differentiation of (A) plastic adherent and (B) STRO-1+ hMSCs before and after 4 passages. hMSCs were subjected to osteogenic, adipogenic, or chondrogenic *in vitro* differentiation for 28 days. Mineralization was examined in osteogenic cultures stained positively with Alizarin Red (AR) and von Kossa (VK). The lipid droplets in adipogenic cultures and glycosaminoglycans in sections of the chondrocyte pellets were detected by Oil Red O (OR) and Alcian blue (AB) staining respectively. Quantification of multilineage differentiation was performed by measurements of the respective staining intensity using Quantity-One® 1-D analysis software (Bio-Rad Laboratories). Significant difference is represented as ^ when compared to starting control group, * when compared to control after 4 passages and # when compared to $HS8^{+ve}$ ($p<0.05$).

4.3.2. Long-term proliferation study of hMSC for direct clinical utility

In the previous study I have successfully shown that the effectiveness of $HS8^{+ve}$ for the expansion of multipotent hMSCs, while maintaining or increasing the measures of ‘‘stemness’’, based on adherence to tissue culture plastic, immunophenotypic profile and multi-lineage proliferation. The effect of $HS8^{+ve}$ supplementation on hMSCs directly isolated from unfractionated bone marrow was investigated, with a view to determine the direct clinical utility of such a procedure. Therefore a long-term proliferation study using cryopreserved bone marrow mononuclear cells (Lonza) was conducted from three male donors aged between 20-30 yrs (Table 4.1). The cells, starting at the time of their isolation, were in contact with media with or without HS variants (HS^{pm}, $HS8^{-ve}$ and $HS8^{+ve}$) or the positive controls (heparin and FGF-2).

4.3.2.1. $HS8^{+ve}$ increases hMSC isolation from bone marrow aspirates

Irrespective of the HS variant that was supplementing in the media, there was a fold-increase in isolated viable cell counts compared to the controls for the cells derived from all three donor bone marrow preparations (Fig. 4.6). This was evident with the positive controls as well (Fig. 4.6). For all three donors, media supplemented with $HS8^{+ve}$ demonstrated significantly higher viable cell count when compared to controls. The isolated numbers of hMSCs with $HS8^{+ve}$ was greater than that of crude HS^{pm} and flow-through $HS8^{-ve}$. Moreover, HS^{pm} and $HS8^{-ve}$ showed only an intermediate level of cell recovery, between that of control and $HS8^{+ve}$. Positive controls heparin and

FGF-2 showed almost similar levels compared to $HS8^{+ve}$ grown cells except in donor A; FGF-2 had a higher fold increase in viable cell isolation.

Overall, the CFU-F efficiency (percentage number of colonies formed per 100,000 cells plated) of BMMNCs from donor A were the greatest, followed by donor C and the lowest by donor B. In addition, for all three donors, media supplemented with $HS8^{+ve}$ triggered similar CFU-F efficiency (percentage of number of colonies formed per 100,000 cells plated CFU-F efficiency) as compared to controls and the other HS variants (Fig. 4.7). The positive control heparin showed similar results to that of $HS8^{+ve}$ supplementation (Fig. 4.7). Although FGF-2 supplementation increased isolation of hMSCs, its CFU-F efficiency was lower than baseline control, heparin and the other HS variants tested (Fig. 4.7). The statistical testing revealed that the low levels of CFU-F efficiency of FGF-2 in all 3 donors were significant when compared to control and $HS8^{+ve}$. Thus indicating that, $HS8^{+ve}$ may target the expansion of early progenitors in heterogeneous hMSC culture, in contrast to exogenous FGF-2 supplementation, tends to expand fewer early progenitors.

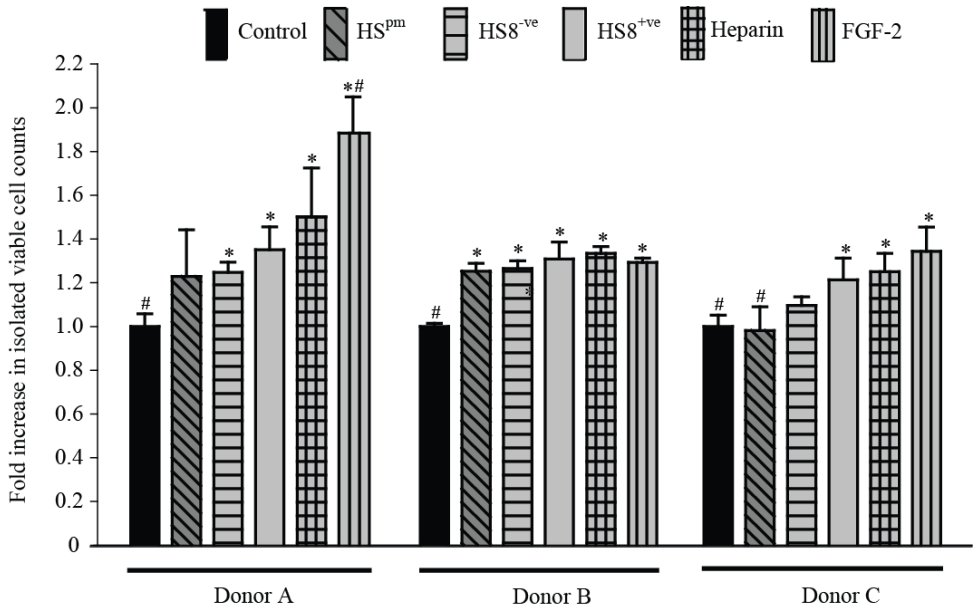

Figure 4.6. HS8^{+ve} increases hMSC isolation from bone marrow aspirates. BMMNCs were seeded in basal media supplemented with HS variants (HS^{pm}, HS8^{-ve} and HS8^{+ve}) and positive controls (Heparin and FGF-2). The cells were allowed to adhere for 5 days with media replacement every 3 days. Upon reaching confluence an aliquot was used to count the viable cells by the EasyCyte™ Plus System. Significant difference is represented as * when compared to the cells isolated with maintenance media and # when compared to the cells isolated with HS8^{+ve} ($p<0.05$).

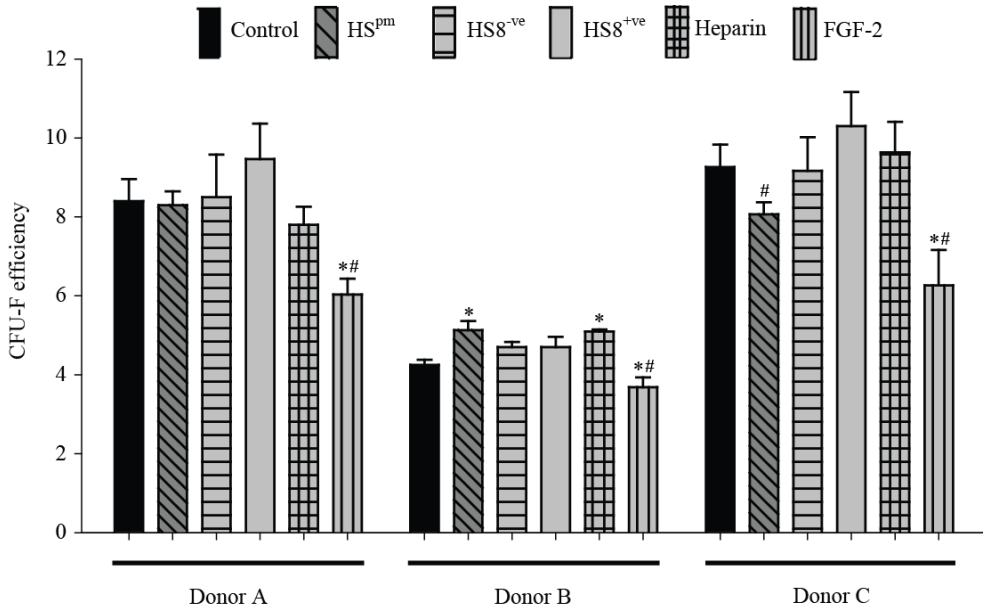

Figure 4.7. HS8^{+ve} increased the CFU-F efficiency of BMMNCs. The BMMNCs were plated in media supplemented with HS variants (HS^{pm}, HS8^{-ve} and HS8^{+ve}) and positive controls (Heparin and FGF-2). They were cultured for 14 days and stained with Crystal violet. Significant difference is represented as * when compared to the CFU-F efficiency of cells grown in maintenance media and # when compared to the CFU-F efficiency of cells grown in HS8^{+ve} ($p<0.05$).

4.3.2.2. $HS8^{+ve}$ robustly expands hMSCs isolated from bone marrow aspirates

$HS8^{+ve}$ gave rise to a significantly greater cumulative cell number compared to the control or the other HS variants in long-term proliferation assays. Next, I sought to determine the cumulative effect of the HS variants on hMSC expansion when I assayed the cells that had encountered the HS variants during their isolation from BMMNCs. Therefore, cells were expanded in media supplemented with the different HS variants, HS^{pm}, $HS8^{-ve}$ and $HS8^{+ve}$, and the positive controls (heparin and FGF-2) over 6 passages with media change at every 2 days. Cells were harvested at 70-80 % confluence, analyzed via the Guava EasyCyte™ Plus System/CytoSoft™ software platform and pooled cells from triplicate plates reseeded at the same cell density for subsequent passage. Cumulative viable hMSC number was plotted against the passage number when cultured in 140 x 20 mm tissue culture dishes in triplicate.

For all three donors, hMSCs expanded in media supplemented with $HS8^{+ve}$ demonstrated significantly greater cumulative cell number controls (Fig. 4.8). The increases in sub-confluent hMSC number were evident from P1 in donor C, P2 in donor A and P3 in donor B, indicating $HS8^{+ve}$ brings about greater cell proliferation within a few days of contact with the cells. The HS^{pm}- and $HS8^{-ve}$-expanded cells had almost similar cell counts to the control except in the cases of donor A and C where $HS8^{-ve}$ grown cells had an elevated cumulative growth over the control, although clearly lower than the $HS8^{+ve}$. The supplementation with FGF2 that served as the control positive showed the greatest cumulative cell number, while supplementation with

heparin triggered a similar extent of growth as $HS8^{+ve}$ except with donor A; heparin showed a greater cumulative cell number than that of $HS8^{+ve}$ (Fig. 4.8). Similar results were obtained when these cells cultured in multi-dish 6-well plates (Fig. 4.9), indicating that the effect of $HS8^{+ve}$ is constant irrespective of the surface area of the culture plate.

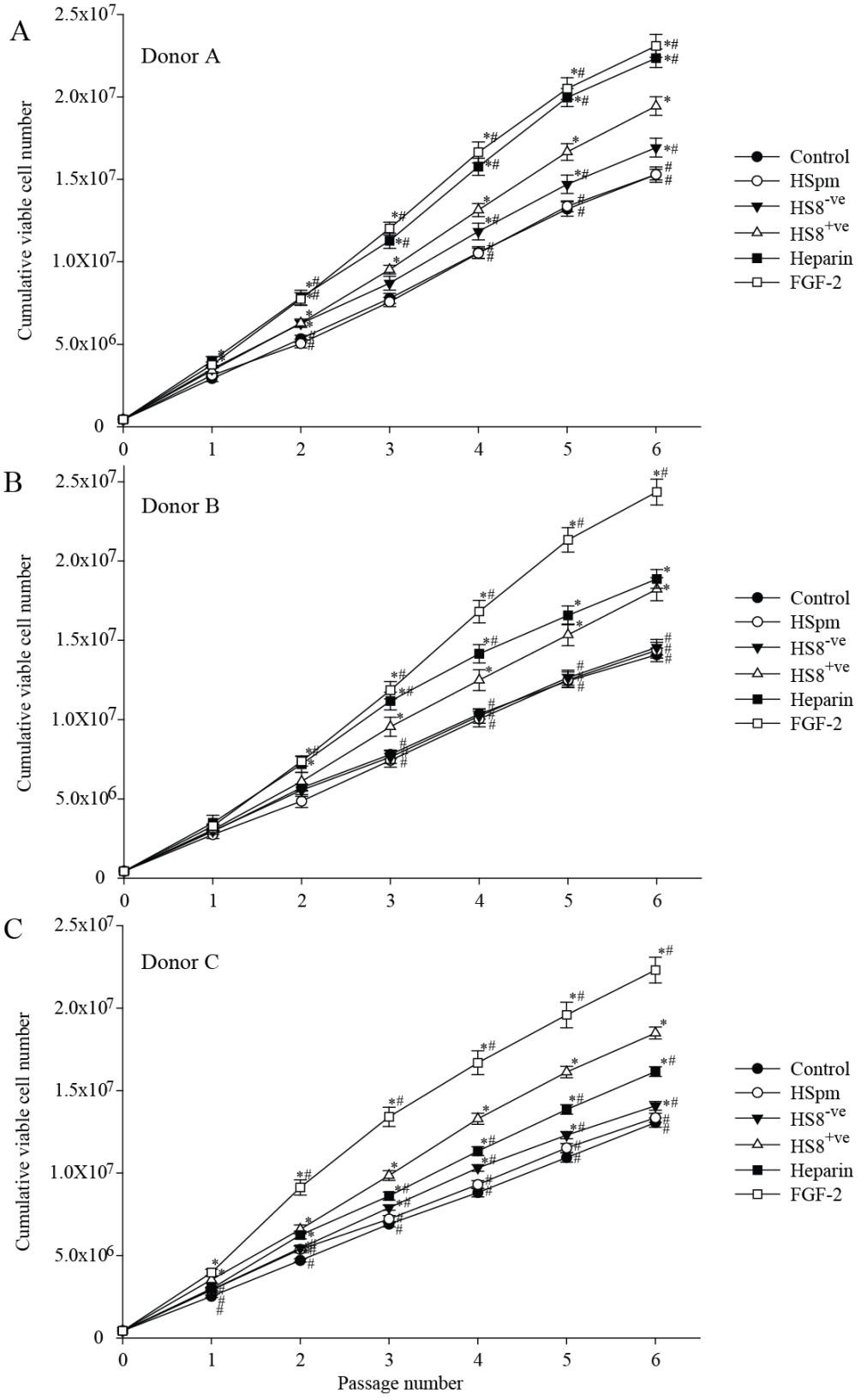

Figure 4.8. HS8^{+ve} robustly expands hMSCs isolated from bone marrow aspirates. Cells were seeded in either control media or media supplemented with different HS variants. Cells at 70-80 % confluence were analyzed and reseeded at the same cell density for cumulative viable cell numbers from P0 to P6. Significant difference is denoted as * when compared to control and $^{\#}$ when compared to HS8^{+ve} at equivalent passage ($p<0.05$).

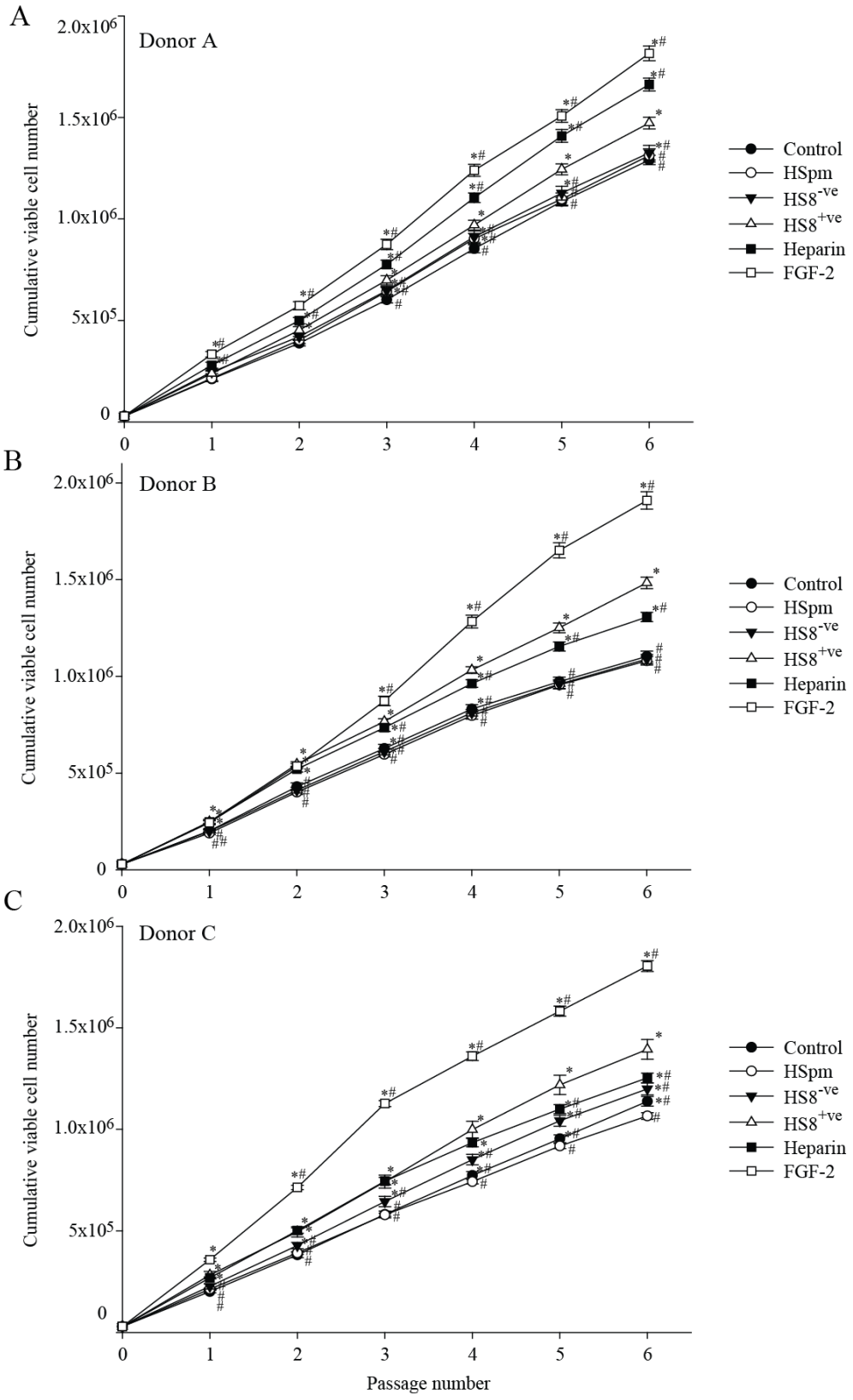

Figure 4.9. HS8^{+ve} robustly expands hMSCs isolated from bone marrow aspirates in multi-dish 6-well plates. Cells were seeded in either control media or media supplemented with different HS variants. Cells at 70-80 % confluence were analyzed and reseeded at the same cell density for cumulative viable cell numbers from P0 to P6. Significant difference is denoted as * when compared to control and $^{\#}$ when compared to HS8^{+ve} at equivalent passage ($p<0.05$).

4.3.2.3. $HS8^{+ve}$ increases hMSCs isolated from bone marrow aspirates CFU-F efficiency.

Similar to BMMNC CFU-F efficiency in established hMSCs, overall, the CFU-F efficiency of donor A was greatest, followed by donor C and then donor B. In addition, in all the donors, irrespective of the media used (including the positive controls) except $HS8^{+ve}$, CFU-F efficiency increased from passage 0 to passage 3 and afterwards started to decline as evident in passage 6. In case of $HS8^{+ve}$ in donor A and B the CFU-F efficiency was increasing even at the later passages (passage 6). Furthermore, irrespective of donor, $HS8^{+ve}$ grown cells had a greater CFU-F efficiency than either the control, HS^{pm} or $HS8^{-ve}$ except in two instances; passage 0 of donor A, the CFU-F was lower than the control and at passage 0 of donor B, it was similar to the control (Fig. 4.10). In contrast, HS^{pm} and $HS8^{-ve}$ had CFU-F efficiencies greater or similar to the control at passages 0 and 3 with all the three donors, but by passage 6, their CFU-F efficiency was similar to the control. At passage 6 for all three donors, $HS8^{+ve}$ CFU-F efficiencies were significantly higher than the controls across all three donors. In addition, at passage 3, this was evident in donor A and C while at passage 0, it was evident in donor C. This further confirms that $HS8^{+ve}$ stimulates the robust expansion of a hMSC population with greater early progenitors, thus corroborating the results obtained with established hMSC cultures. The cells in the positive heparin control yielded CFU-F efficiencies greater than control but lower than $HS8^{+ve}$ except at passage 0 of donor A and donor B (Fig. 4.10). Positive FGF-2 control grown cells demonstrated a CFU-F efficiency lower than that of all GAGs and the control (Fig. 4.10). This reduction of FGF-2 CFU-F efficiencies were statistically significant in all the passages across all donors as compared

to HS8^{+ve}, except at donor A passage 0 and donor B passage 0 and passage 3. Therefore this further demonstrated that although FGF-2 can mediate a rapid expansion of cells in culture, these may consist of fewer naive progenitors.

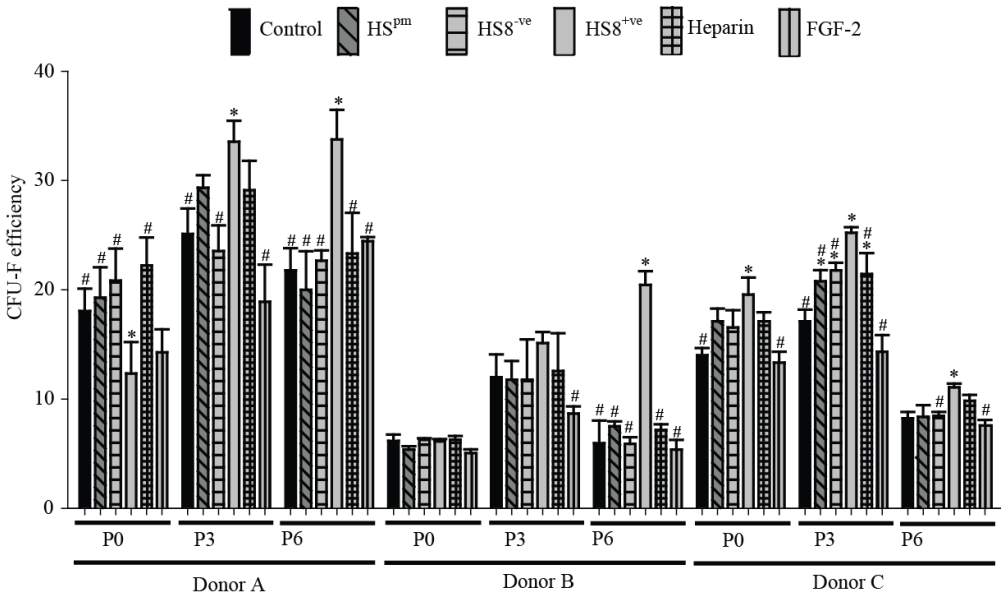

Figure 4.10. HS8^{+ve} increased the CFU-F efficiency of hMSCs isolated from Donor A, B and C. The hMSCs were cultured for 14 days in standard conditions. By day 14, cultures were terminated and stained with Crystal violet to visualize the colonies. Significant difference is represented as * when compared to the CFU-F efficiency of control and # when compared to the CFU-F efficiency of HS8^{+ve} at equivalent passage ($p<0.05$).

4.3.2.4. Immunophenotypic profile of hMSCs isolated from 3 donors

I have seen that HS8^{+ve} targets the robust expansion of purer hMSC population. I next examined the immunophenotypic profiles of hMSCs from the 3 donors (Tables 4.3, 4.4 and 4.5). As expected, the single-color flow cytometry analysis revealed that the bone marrow aspirates of the 3 donors were positive for haematopoeitic markers expression across all donors; the pan leukocyte marker CD45 was on ~ 86 % of the cells and the hematopoietic progenitor marker CD34 ranged from 4.0±0.67-8.3±0.70 %. The leukocyte marker HLA-DR ranged from 20.4±0.64-39.5±0.07 % and the CD19 (B

lymphocytes) ranged from 7.9±4.0-27.4±1.13 %. In addition the monocyte/macrophage marker CD14 ranged from 1.8±0.17-4.7±0.51 %. In contrast, the MSC-related markers CD73, CD90, CD105 which usually > 99 % positive in hMSCs, but were low in BMMNCs (ranged from 4.1±0.30-28±0.85 %). In addition, the stemness markers (STRO-1, SSEA-4 and CD49a) were overall less expressed in BMMNCs.

In contrast, hMSCs after isolation showed a distinctly different profile compared to the BMMNCs. On the membranes, the MSC-related markers CD73, CD90, CD105 showed > 99 % expression in passage 3 and 6 cells across all 3 donors irrespective of the HS variant and control media used to expand the hMSCs. At passage 0 they showed a slight deviation from normal (> 99 % positive) where CD73 > 98 %, CD90 > 98 % and CD105 > 99 %. The haematopoeitic marker expression was markedly reduced in hMSCs compared to the BMMNCs. The expression of CD19 and CD34 were extremely low (< 2 % positive) across all passages and donors. CD45 was essentially the same except at passage 0 (< 4 % positive). The expression of the monocyte/macrophage marker CD14 ranged from < 1-6 % at passage 0, but rose into the accepted range of < 2 % by passage 3 and 6 across all passages and donors. The leukocyte marker HLA-DR was in the normal range (> 2 % positive) across all passages of donor A. In donor B there was a slight elevation but all were in the range of > 2-4 %. In contrast, donor C had a bigger range (> 2.5±0.04-55.5±0.71 %). Passage 0 had the highest range amongst all the cells subjected to different media, but by passage 6 it had reduced to > 8 %. Interestingly, out of all the cells expanded, cells exposed to $HS8^{+ve}$ displayed the lowest levels of for HLA-DR expression, but by passage

6 (2.5±0.04 % positive) had almost reached the normal level. This further validates that in culture $HS8^{+ve}$ seems to increase hMSCs rather than the other progenitor cells. The positive heparin control showed similar positive and negative surface marker expression to that of $HS8^{+ve}$ albeit a significant difference with respect to HLA-DR. Although donor A HLA-DR expression was in the normal range, the other 2 donors were not: in donor B it was 6.4±1.21-10.2±0.53 % and in donor C it was 58.2±1.28-78.3±1.97 % (Tables 4.3, 4.4 and 4.5). The other positive control, FGF-2, caused the resultant expanded cells, for certain surface markers, to further deviate from accepted levels. The CD90 ranged from 78.2±0.62-96.0±0.21 % while HLA-DR expression ranged from 1.61±0.21-87.0±1.34 % on all donors, indicating FGF-2 was driving the rapid expansion of progenitor cells other than MSCs (Tables 4.3, 4.4 and 4.5).

Differences were observed when I looked at the surface marker expression set characteristic of stemness. The hMSCs grown in $HS8^{+ve}$ showed greater levels of STRO-1 at almost all passages for all donors. Similarly, at most passages, SSEA-4 and CD49a levels were higher in $HS8^{+ve}$ cells than that of controls. HS^{pm} and $HS8^{-ve}$ cells showed greater variability in the expression of these three surface markers over the control. The surface marker expression of STRO-1, SSEA-4 and CD49a in cells grown in heparin showed essentially similar expression to that of $HS8^{+ve}$ except few instances where significant differences were noted between them (Tables 4.3, 4.4 and 4.5). In contrast, cells grown in FGF-2 showed declines in STRO-1 and CD49a expression, and, on most occasions, an increase in SSEA-4 levels over control and all HS variant-grown cells (Tables 4.3, 4.4 and 4.5). This further

justifies our hypothesis that $HS8^{+ve}$ is better at targeting the expansion of hMSC rather than a mixed population of progenitors, and that the opposite is true with respect to exogenous FGF-2 supplementation.

Table 4.3. Immunophenotypic profile of Donor A. Single-color flow cytometry analysis of bone marrow aspirate (BMA) and hMSCs was performed for the stem cell positive markers CD73, CD90, CD105, the negative markers CD14, CD19, CD34, CD45, HLA-DR, and stemness markers STRO-1, SSEA-4, CD49a. The level of positivity of relevant surface marker is depicted as below. Significant difference is represented as * when compared to control after 4 passages and # when compared to $HS8^{+ve}$ ($p<0.05$).

Donor A

		Negative markers					Positive markers			Stemness		
		CD14	CD19	CD34	CD 45	HLA-DR	CD 73	CD90	CD105	STRO-1	SSEA-4	CD49a
	BMA	2.1±0.41	7.9±0.40	5.4±0.52	86.0±0.42	20.4±0.64	26.6±0.85	4.3±0.09	11.5±2.16	0.6±0.76	1.1±0.06	1.6±0.34
P0	Control	6.8±0.54$^{\#}$	1.3±0.08	1.0±0.08	1.2±0.02$^{\#}$	1.5±0.37	99.9±0.00	99.6±0.07$^{\#}$	99.9±0.00	4.6±0.40$^{\#}$	3.1±0.11	47.0±5.23
	HS^{pm}	1.3±0.18$^{*\#}$	0.9±0.24	1.2±0.26	1.5±0.07$^{\#}$	1.6±0.06	99.9±0.00	99.8±0.00$^{\#}$	99.9±0.07	2.6±0.08$^{*\#}$	2.0±0.36$^{\#}$	50.6±2.26$^{\#}$
	$HS8^{-ve}$	0.9±0.04$^{*\#}$	1.5±0.11	1.0±0.24	1.4±0.09	1.2±0.10	99.9±0.07$^{\#}$	99.9±0.00$^{*\#}$	99.9±0.00	8.1±1.18$^{*\#}$	4.7±1.66	38.2±5.30
	$HS8^{+ve}$	2.1±0.43*	1.1±0.11	0.8±0.07	1.4±0.03*	1.0±0.25	99.4±0.14	98.5±0.14*	99.9±0.07	6.2±0.06*	6.0±0.80	25.5±7.21*
	Heparin	0.8±0.06$^{*\#}$	1.0±0.08	0.7±0.16	1.0±0.14	1.7±0.05	99.8±0.14	98.8±0.14*	99.9±0.07	3.2±0.18$^{*\#}$	2.6±0.30$^{\#}$	30.9±1.63*
	FGF-2	1.4±0.32$^{*\#}$	1.2±0.07	1.0±0.24	14.5±2.12$^{*\#}$	12.5±1.20$^{*\#}$	99.9±0.00	96.3±0.35$^{*\#}$	99.9±0.00	4.6±0.16$^{*\#}$	12.2±0.42$^{*\#}$	38.3±9.90*
P3	Control	2.3±0.56	1.2±0.09	1.1±0.42	1.0±0.49	1.0±0.20	100.0±0.00	99.8±0.21	99.9±0.07	3.1±1.12	6.7±1.80	34.3±4.81
	HS^{pm}	0.8±0.07*	1.0±0.05	0.8±0.04	0.9±0.20	0.9±0.30	99.9±0.00	99.8±0.14	99.9±0.00	4.3±0.94$^{\#}$	0.6±0.00$^{*\#}$	27.9±7.92
	$HS8^{-ve}$	1.2±0.05*	1.0±0.46	1.0±0.03	0.9±0.25	1.1±0.17	99.9±0.07	99.7±0.21	99.9±0.07	1.8±0.98*	4.4±4.86	28.4±7.42
	$HS8^{+ve}$	1.2±0.41*	1.2±0.01	1.0±0.10	1.2±0.02	0.9±0.23	99.9±0.00	99.9±0.07	99.9±0.07	2.3±0.21	2.9±0.30	41.0±12.0
	Heparin	0.5±0.03$^{*\#}$	1.6±0.40$^{*\#}$	1.0±0.09	1.0±0.28	0.7±0.24	99.5±0.64	99.9±0.00	99.9±0.00	3.9±0.16$^{\#}$	5.4±0.88	32.1±8.63
	FGF-2	1.1±0.01*	1.1±0.05	1.3±0.29	1.4±0.10	10.1±2.31$^{*\#}$	100.0±0.00	94.1±1.06$^{*\#}$	99.9±0.07	1.6±0.04*	13.8±4.17$^{*\#}$	38.6±11.8
P6	Control	1.5±0.18	0.9±0.28	1.2±0.10	1.0±0.07$^{\#}$	0.9±0.29	99.9±0.00	99.9±0.07	99.9±0.00	5.1±0.54	4.2±0.03*	40.7±8.27
	HS^{pm}	0.0±0.01$^{*\#}$	1.2±0.41	0.9±0.09	0.7±0.40	0.8±0.34	99.9±0.00	99.9±0.00	99.9±0.00	1.6±0.18$^{*\#}$	6.8±0.69	40.1±4.31
	$HS8^{-ve}$	3.7±0.40$^{*\#}$	0.9±0.73	1.1±0.24	1.0±0.35	0.8±0.03	100.0±0.00	100.0±0.00	99.9±0.00	2.4±0.07$^{*\#}$	15.9±0.64$^{*\#}$	50.7±1.06
	$HS8^{+ve}$	2.1±0.42	0.9±0.30	0.9±0.04	1.3±0.06*	0.9±0.31	99.9±0.07	99.9±0.00	99.9±0.07	4.9±0.30	6.5±0.01	46.1±9.19
	Heparin	1.3±0.05$^{\#}$	1.1±0.02	1.2±0.01	1.4±0.22	1.0±0.16	99.9±0.00	100.0±0.00	99.9±0.00	3.7±0.40$^{*\#}$	4.4±0.35$^{\#}$	36.9±9.33
	FGF-2	0.9±0.10$^{*\#}$	1.2±0.03	1.1±0.43	1.1±0.51	1.6±0.21	99.9±0.00	99.0±0.21*	99.7±0.00	4.5±0.54	30.4±4.03$^{*\#}$	31.2±2.69

Table 4.4. Immunophenotypic profile of Donor B. Single-color flow cytometry analysis of bone marrow aspirate (BMA) and hMSCs was performed for the stem cell positive markers CD73, CD90, CD105, the negative markers CD14, CD19, CD34, CD45, HLA-DR, and stemness markers STRO-1, SSEA-4, CD49a. The level of positivity of relevant surface marker is depicted as below. Significant difference is represented as * when compared to control after 4 passages and # when compared to $HS8^{+ve}$ ($p<0.05$).

Donor B

		Negative markers					Positive markers			Stemness		
		CD14	CD19	CD34	CD 45	HLA-DR	CD 73	CD90	CD105	STRO-1	SSEA-4	CD49a
	BMA	4.7±0.51	18.6±0.42	4.0±0.67	86.8±0.99	36.5±0.71	28.3±0.85	4.1±0.30	6.3±0.54	2.3±0.28	0.9±0.27	4.0±3.20
P0	Control	1.4±0.29	1.5±0.09#	1.0±0.18	1.6±0.85	2.9±0.15	99.5±0.57	98.4±0.99	99.9±0.07	3.9±0.08	1.2±0.12#	26.7±11.17
	HS^{pm}	2.0±0.68	1.0±0.22	1.0±0.14	1.7±0.62	3.9±0.28	99.5±0.57	98.5±0.64	99.9±0.00	4.4±0.58	11.3±14.88	41.45±1.20*#
	$HS8^{-ve}$	1.6±0.50	1.0±0.43	1.2±0.51	1.8±0.30	3.3±0.36	99.5±0/28	98.5±0.21	99.9±0.07	4.4±0.27	6.3±7.43	38.5±10.82#
	$HS8^{+ve}$	2.3±0.70	0.9±0.19	0.9±0.14	2.1±0.75	3.7±0.00	98.5±0.28	97.5±0.21	99.9±0.07	8.8±2.45	30.5±1.06*	23.3±4.67
	Heparin	2.7±0.97*	2.2±0.40*#	0.5±0.02	2.7±1.77	6.4±1.42*#	99.4±0.49	98.2±0.14	99.9±0.00	7.2±0.89	11.6±1.20*#	18.4±3.46
	FGF-2	1.2±0.31#	1.0±0.06	1.1±0.11	1.4±0.23	22.2±2.55*#	99.9±0.07	91.5±3.61*#	99.9±0.00	4.8±0.02	20.7±7.42	29.6±9.76
P3	Control	0.8±0.15	0.8±0.19	1.0±0.21	0.8±0.21	1.7±0.03	99.9±0.07	99.9±0.07	99.9±0.07	5.0±0.40	12.1±0.49#	24.0±5.23#
	HS^{pm}	0.9±0.03	1.0±0.01	1.3±0.12	1.3±0.08#	1.2±0.23#	99.9±0.00	99.8±0.00	99.9±0.07	3.4±0.28*#	11.1±0.92	30.2±6.93#
	$HS8^{-ve}$	1.8±0.39	1.0±0.07	0.9±0.07	1.1±0.18	1.3±0.15	99.9±0.00	99.7±0.00	99.9±0.07	3.4±0.23*#	6.2±0.96*#	27.5±5.44#
	$HS8^{+ve}$	1.2±0.06	1.2±0.32	1.0±0.10	1.0±0.06	3.2±0.06	99.9±0.07	99.7±0.00	99.9±0.07	4.7±0.12	22.9±1.20*	54.4±9.40*
	Heparin	1.8±0.49*	1.0±0.05	1.1±0.10	1.2±0.16	8.0±1.15*#	100.0±0.00	99.9±0.00	99.9±0.00	4.1±0.25	27.1±1.77*	66.5±8.63*
	FGF-2	1.2±0.01	1.1±0.05	9.4±11.31	1.0±0.16	30.8±1.41*#	99.9±0.00	78.2±0.42*#	99.9±0.00	3.0±0.09*#	40.0±8.27	22.6±7.28#
P6	Control	1.3±0.27	1.5±0.31	1.0±0.05	0.9±0.28	1.7±0.07	99.9±0.07	99.8±0.00	99.9±0.07	3.6±0.35	7.7±1.63	32.6±2.97
	HS^{pm}	1.1±0.22	1.0±0.12	1.4±0.18	0.7±0.12	1.2±0.06	100.0±0.00	99.9±0.00	99.9±0.00	2.5±1.50	8.9±0.01#	44.3±7.14
	$HS8^{-ve}$	1.1±0.01	0.9±0.09*	0.5±0.02	0.4±0.01	1.8±0.31	99.9±0.07	99.8±0.00	99.9±0.07	3.4±0.30	10.7±1.56	29.8±1.63
	$HS8^{+ve}$	1.6±0.71	1.2±0.36	1.2±0.33	0.9±0.11	2.0±0.28	99.9±0.00	99.9±0.07	99.9±0.00	4.5±0.81	11.6±0.14	42.8±3.61
	Heparin	1.3±0.28	1.2±0.11	1.0±0.10	0.8±0.14	10.2±0.53*#	99.9±0.00	99.7±0.14	99.9±0.07	3.6±1.58	12.3±1.13	30.0±7.78
	FGF-2	1.1±0.18	1.2±0.28	1.2±0.06	1.1±0.21	34.6±0.14*#	99.9±0.00	81.4±1.48*#	99.40.42	5.7±0.25*	66.9±1.91*#	50.1±1,20

Table 4.5. Immunophenotypic profile of Donor C. Single-color flow cytometry analysis of bone marrow aspirate (BMA) and hMSCs was performed for the stem cell positive markers CD73, CD90, CD105, the negative markers CD14, CD19, CD34, CD45, HLA-DR, and stemness markers STRO-1, SSEA-4, CD49a. The level of positivity of relevant surface marker is depicted as below. Significant difference is represented as * when compared to control after 4 passages and $^{\#}$ when compared to $HS8^{+ve}$ ($p<0.05$).

Donor C

		Negative markers					Positive markers			Stemness		
		CD14	CD19	CD34	CD 45	HLA-DR	CD 73	CD90	CD105	STRO-1	SSEA-4	CD49a
	BMA	1.8±0.17	27.4±1.13	8.3±0.70	86.6±1.77	39.5±0.07	13.1±1.41	23.9±0.14	19.5±1.27	3.4±1.29	1.7±0.60	3.0±0.64
P0	Control	2.6±0.09	1.3±0.08	0.9±0.12	2.3±0.00	43.4±0.49$^{\#}$	99.3±0.00	99.3±0.07	99.9±0.07	4.3±0.15$^{\#}$	14.1±3.68$^{\#}$	67.0±5.66
	HS^{pm}	3.5±0.81*	1.3±0.33	1.1±0.06	1.9±0.33	53.5±0.21$^{*\#}$	99.7±0.14	99.6±0.14	99.9±0.07	5.8±0.30*	17.5±1.48$^{\#}$	87.5±1.91
	$HS8^{-ve}$	2.6±0.22	1.1±0.05	1.0±0.10	1.9±0.30	55.3±0.71$^{*\#}$	99.6±0.07	99.2±0.07	100.0±0.00	6.0±0.71*	22.9±2.26$^{*\#}$	71.1±4.17
	$HS8^{+ve}$	3.2±0.11	1.0±0.04	1.0±0.08	3.3±0.55	28.6±0.85*	98.4±0.64	98.6±0.28	99.8±0.07	6.7±0.66*	43.7±3.61*	70.3±5.30
	Heparin	3.1±0.32	1.2±0.13	1.3±0.21	2.3±0.16	76.2±3.75$^{*\#}$	99.7±0.14	99.9±0.07	99.9±0.07	8.4±0.92$^{*\#}$	29.6±5.09$^{*\#}$	90.1±1.48$^{*\#}$
	FGF-2	2.2±0.14*	1.2±0.16	1.0±0.18	1.9±0.33	78.3±1.91$^{*\#}$	99.8±0.21	96.4±1.20$^{*\#}$	99.9±0.00	3.4±0.50$^{\#}$	31.8±2.12$^{*\#}$	62.4±3.46
P3	Control	1.0±0.25	1.1±0.21	1.0±0.17	0.9±0.16	10.8±0.28	100.0±0.00	100.0±0.00	100.0±0.00	4.3±0.06	21.4±0.78$^{\#}$	85.1±1.98
	HS^{pm}	1.4±0.12	1.0±0.07	1.3±0.18	1.1±0.07	13.1±1.48	100.0±0.00	99.9±0.00	99.9±0.07	4.5±0.95	18.0±0.64$^{\#}$	87.6±4.60
	$HS8^{-ve}$	1.2±0.16	1.3±0.03	1.0±0.22	1.0±0.11	8.0±0.40	100.0±0.00	99.9±0.07	99.9±0.07	1.3±0.37$^{*\#}$	16.4±0.71$^{\#}$	80.4±3.25
	$HS8^{+ve}$	1.3±0.04	1.2±0.15	1.7±0.72	1.2±0.11	9.3±1.12	100.0±0.00	100.0±0.00	99.9±0.07	4.5±0.35	51.9±5.80*	72.0±5.30
	Heparin	0.7±0.60	1.3±0.06	0.8±0.17	0.8±0.64	37.4±1.13$^{*\#}$	99.9±0.07	99.9±0.00	99.9±0.07	6.3±0.81$^{*\#}$	23.1±1.48$^{\#}$	77.9±8.06
	FGF-2	1.3±0.28	1.0±0.12	1.3±0.04	1.3±0.30	87.0±1.34$^{*\#}$	99.9±0.07	91.4±0.21$^{*\#}$	99.9±0.00	3.5±0.26	43.0±1.41$^{*\#}$	47.7±6.29
P6	Control	1.2±0.46	1.1±0.41	1.2±0.34	1.4±0.14	3.7±0.52	100.0±0.00	100.0±0.00	99.9±0.00	3.4±0.37$^{\#}$	7.4±0.03	71.4±12.23$^{\#}$
	HS^{pm}	1.0±0.10	1.2±0.60	1.5±0.52	1.3±0.52	3.2±0.04	99.9±0.14	99.9±0.07	99.8±0.14	4.6±0.69$^{\#}$	13.5±2.33$^{\#}$	57.3±2.90
	$HS8^{-ve}$	1.1±0.15	1.1±0.03	1.2±0.07	1.2±0.16	6.8±1.62	99.9±0.07	99.9±0.07	99.9±0.07	6.4±1.11*	13.9±2.26*	69.6±15.27$^{\#}$
	$HS8^{+ve}$	0.7±0.14	1.1±0.15	1.1±0.48	1.0±0.64	2.5±0.04	99.9±0.00	99.9±0.00	99.7±0.14	6.7±0.24*	20.3±1.06*	47.7±13.36*
	Heparin	2.5±0.55$^{*\#}$	1.1±0.13	1.1±0.16	0.9±0.43	19.9±1.91$^{*\#}$	99.9±0.07	99.9±0.07	99.7±0.00	4.1±0.69$^{\#}$	16.1±0.42*	67.0±11.31$^{\#}$
	FGF-2	1.1±0.06	1.0±0.04	1.3±0.02	1.2±0.17	58.2±12.80$^{*\#}$	99.8±0.14	80.3±2.40$^{*\#}$	99.5±0.14	3.0±0.20$^{\#}$	54.6±7.35$^{*\#}$	33.5±15.20*

4.3.2.5. Multi-lineage differentiation of hMSCs isolated from 3 donors.

Finally I looked at the multi-lineage differentiation capacity of cells, at passages 3 and 6, expanded in different HS variants. Irrespective of the media used to expand them, and at both passages, the hMSCs were able to differentiate down osteogenic, adipogenic and chondrogenic lineages (Figs. 4.11, 4.12 and 4.13) comparable to each other except for few notable instances. The cells of donor B grown with $HS8^{+ve}$ at passage 6 realized the greatest tri-lineage differentiation potential. This evidence suggests that $HS8^{+ve}$-grown cells retain their multipotentiality and may even show increased capacity. Cells grown in the positive control heparin and FGF-2 acted in same manner while FGF-2-grown cells showed marked increases in chondrogenic differentiation compared to the others (Figs. 4.11, 4.12 and 4.13). Here FGF-2-grown cells differentiate down the osteogenic lineage, whereas there was a lack of osteogenic differentiation of plastic adherent hMSCs Long term proliferation in the previous study (Fig. 4.5).

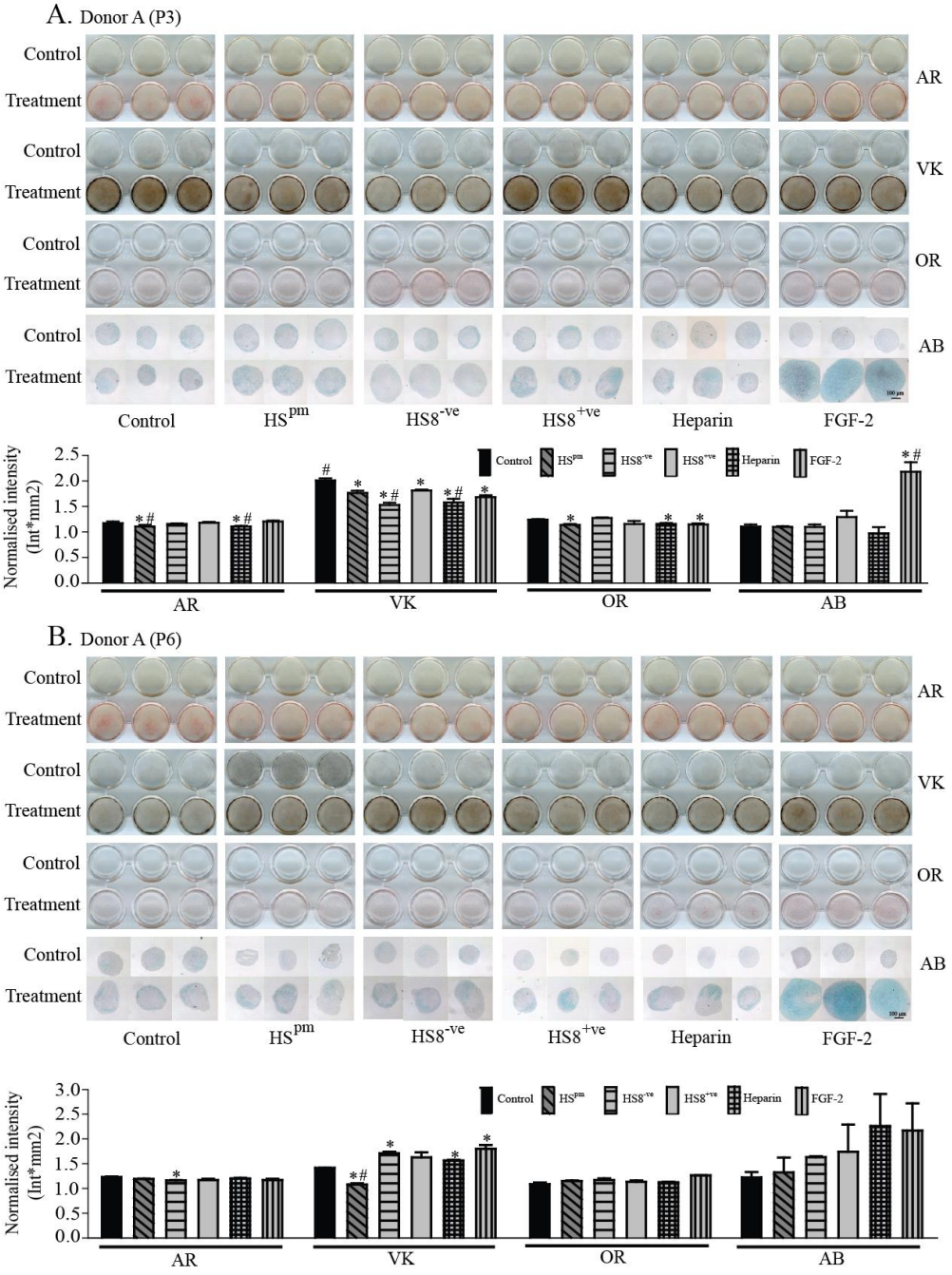

Figure 4.11. Donor A multi lineage differentiation at (A) P3 and (B) P6. The hMSCs were subjected to osteogenic, adipogenic, or chondrogenic *in vitro* differentiation for 28 days. Mineralization in osteogenic cultures stained positively with Alizarin Red (AR) and von Kossa (VK). The lipid droplets in adipogenic cultures and glycosaminoglycans in sections of the chondrocyte pellets were detected by Oil Red O (OR) and Alcian blue (AB) staining respectively. Quantification of multilineage differentiation was performed by measurements of the respective staining intensity using Quantity-One® 1-D analysis software (Bio-Rad Laboratories). Significant difference is represented as * when compared to control after 4 passages and # when compared to $HS8^{+ve}$ ($p<0.05$).

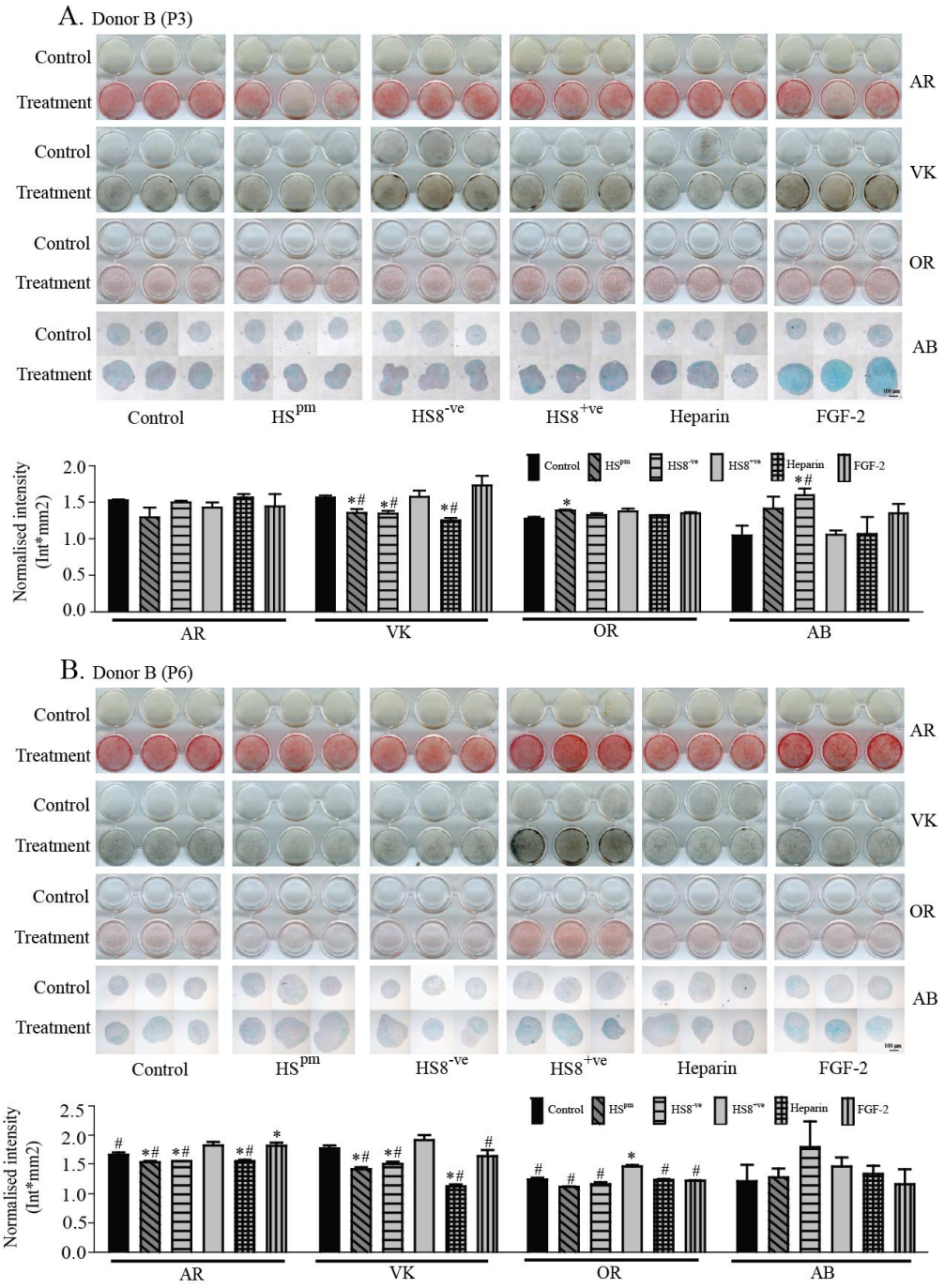

Figure 4.12. Donor B multi lineage differentiation at (A) P3 and (B) P6. The hMSCs were subjected to osteogenic, adipogenic, or chondrogenic *in vitro* differentiation for 28 days. Mineralization in osteogenic cultures stained positively with Alizarin Red (AR) and von Kossa (VK). The lipid droplets in adipogenic cultures and glycosaminoglycans in sections of the chondrocyte pellets were detected by Oil Red O (OR) and Alcian blue (AB) staining respectively. Quantification of multilineage differentiation was performed by measurements of the respective staining intensity using Quantity-One® 1-D analysis software (Bio-Rad Laboratories). Significant difference is represented as * when compared to control after 4 passages and # when compared to $HS8^{+ve}$ ($p<0.05$).

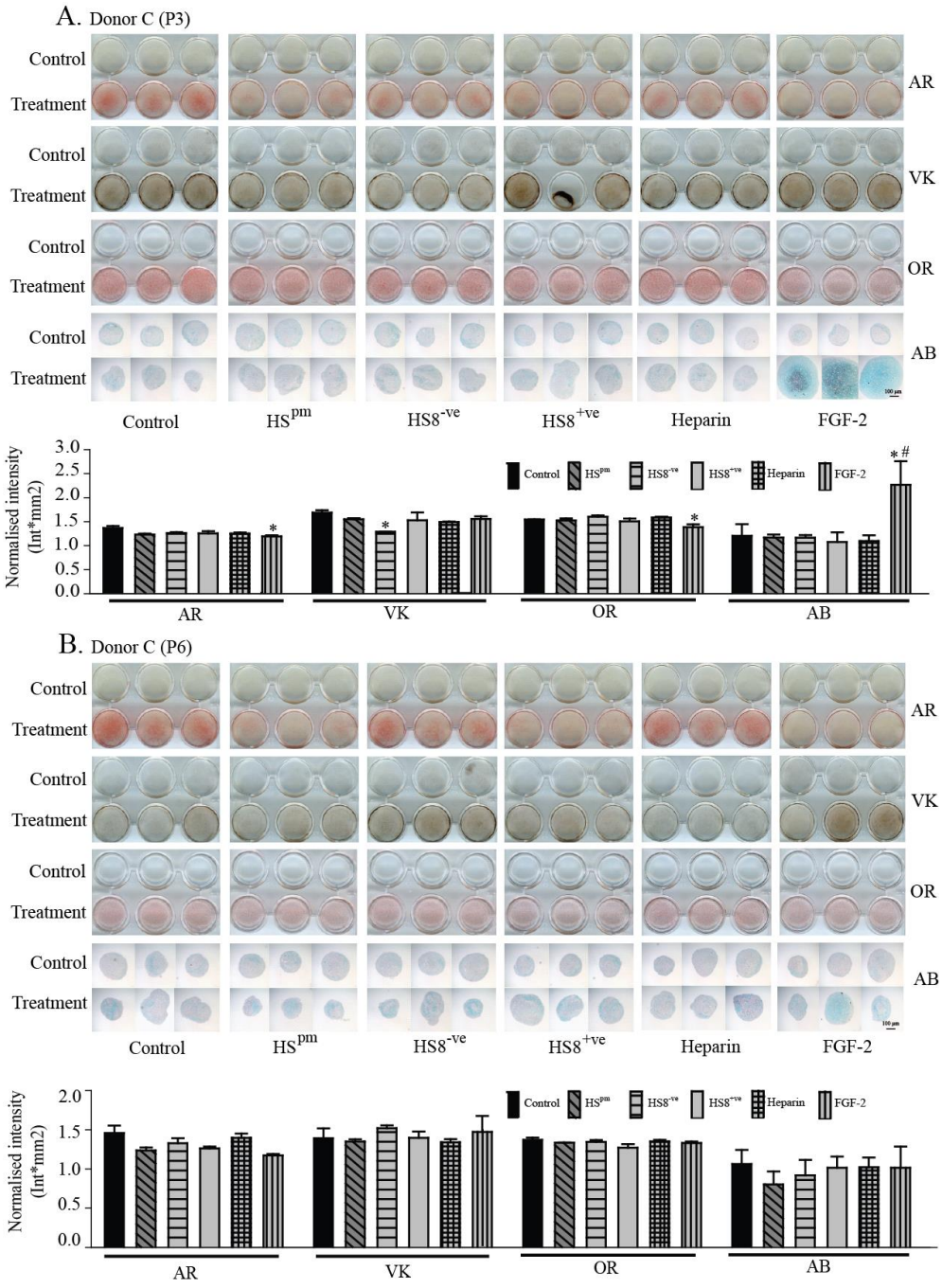

Figure 4.13. Donor C multi lineage differentiation at (A) P3 and (B) P6. The hMSCs were subjected to osteogenic, adipogenic, or chondrogenic *in vitro* differentiation for 28 days. Mineralization in osteogenic cultures stained positively with Alizarin Red (AR) and von Kossa (VK). The lipid droplets in adipogenic cultures and glycosaminoglycans in sections of the chondrocyte pellets were detected by Oil Red O (OR) and Alcian blue (AB) staining respectively. Quantification of multilineage differentiation was performed by measurements of the respective staining intensity using Quantity-One® 1-D analysis software (Bio-Rad Laboratories). Significant difference is represented as * when compared to control after 4 passages and $^{\#}$ when compared to $HS8^{+ve}$ ($p<0.05$).

4.3.2.6. hMSCs expanded in HS8^{+ve} are immunosuppressive

After proving HS8^{+ve} expansion-without-differentiation properties, I sought to further examine whether continuous expansion in the presence of each of the HS variants had an adverse effect on cells. Immunosuppressive capacity was monitored by two means. For both I used cells expanded in media containing different HS variants (HS^{pm}, HS8^{-ve} and HS8^{+ve}) or positive controls (heparin and FGF-2) at passage 3 and 6. In the first assay I checked the ability of hMSCs to suppress the proliferation of a mixture of stimulatory and reactionary human peripheral blood mononuclear cells (PBMCs) from two different healthy un-matched donors via CD3^{+} Ki67^{+} cell assessment in a two-colour FACS array, as I have previously utilised (Helledie *et al*., 2011; Rai *et al*., 2010). Hence a reduction in % CD3^{+} Ki67^{+} indicates a greater immunomodulatory capacity (Fig. 4.14).

Irrespective of the cells expanded in different media and passage, all showed a potent immunosuppressive effect at a PBMC: hMSC ratio of 1:10 compared to that of hPBMC donor A: hPBMC donor B. But, at a lower ratio (PBMC: hMSC ratio of 1:1) different cells showed variable immunosuppressive effects as compared to that of hPBMC donor A: hPBMC donor B. In donor A at passage 3, with the PBMC: hMSC ratio of 1:1, all the cell types revealed a decreased immunomodulatory effect, but by passage 6, the HS8^{+ve}-expanded cells were showing an increased immunomodulatory capacity when compared to the control and the other HS variants. A similar effect from HS8^{+ve}-grown cells was seen at both passages of donor C. The only instance of a decrease in immunomodulatory effect of HS8^{+ve} grown cells at the lower ratio was observed at passage 3 of donor B, while at passage 6

almost similar levels were observed. The heparin- and FGF-2-expanded cells also displayed a potent immunosuppressive effect at the PBMC: hMSC ratio of 1:10, while a variable effect was seen at a PBMC: hMSC ratio of 1:1 (Fig. 4.14). Therefore, overall, $HS8^{+ve}$ did not impair the immunosuppressive effects of the hMSCs, but in most instances actually enhanced the effect, despite their greatly accelerated growth rate.

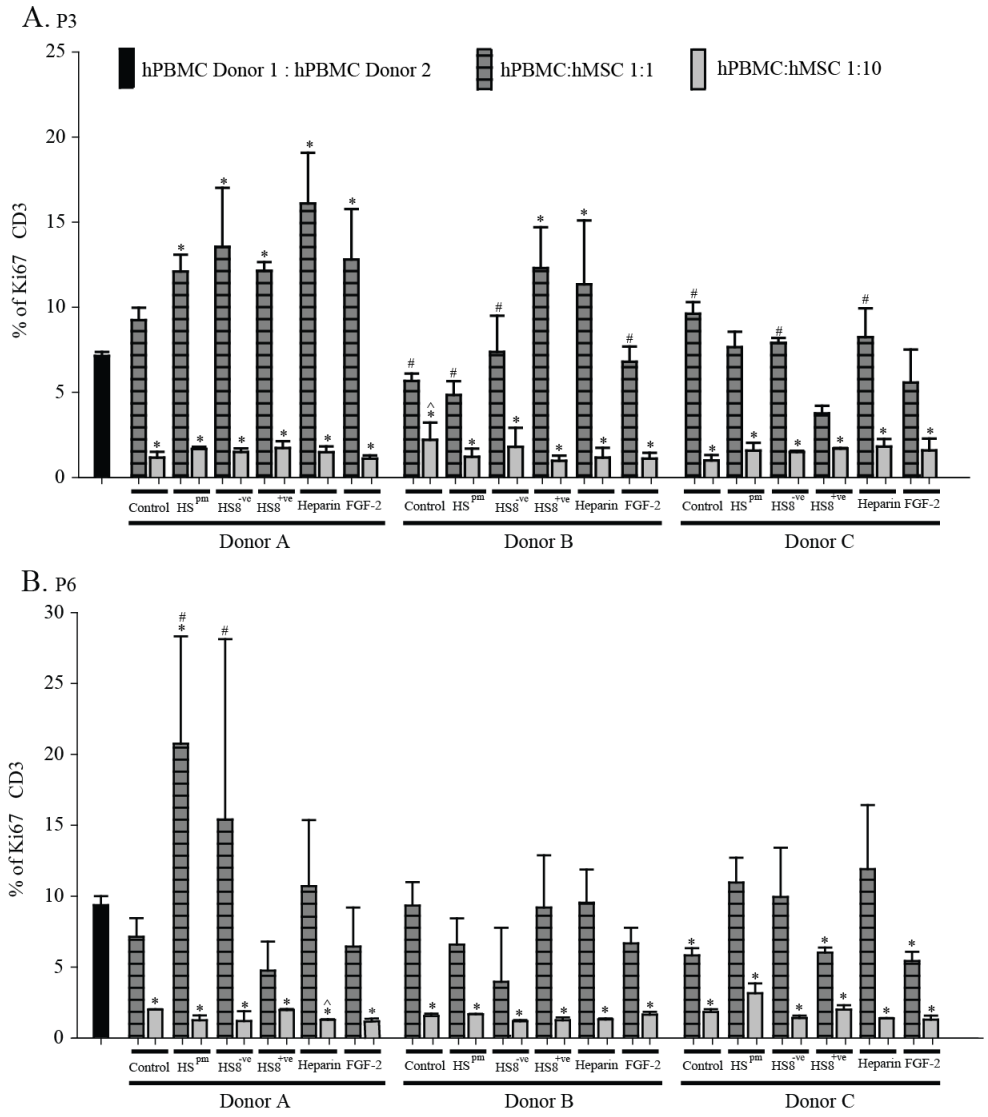

Figure 4.14. Immunomodulatory activity of hMSCs expanded with HS variants. The hMSCs at P3 (A) and P6 (B) were seeded and a mixture of stimulatory and reactionary human peripheral blood mononuclear cells (PBMCs) from two different healthy un-matched donors (Singapore Cord Blood Bank) was added to the wells 24 h later at different PBMC: hMSC ratios (1:1 and 1:10). The expression of $CD3^+$ $Ki67^+$ cells was assessed by two colour BD FACSArray. The hPBMC mixed at equal amounts served as a positive control represents the where the % of $CD3^+$ $Ki67^+$ cells obtained in the absence of Hs variant- or control-expanded hMSCs. Significant difference is represented as * when compared to hPBMC donor A: hPBMC donor B, # when compared to $HS8^{+ve}$ PBMC: hMSC ratio 1:1 and ^ when compared to $HS8^{+ve}$ PBMC: hMSC ratio 1:10 ($p<0.05$).

Secondly, I investigated the amount of TNF-α receptor type 1 expressed on hMSC surfaces by means of a quantitative ELISA assay (Fig. 4.15). TNF-α receptors are expressed on the surface of mesenchymal stem

cells (Tartaglia *et al*., 1991) with TNFR1 being the predominant type (Vancheri *et al*., 2000). Danilkovitch *et al.* have described how the hMSC expression of TNF-α receptors is critical for their immunosuppressive, immunomodulatory, anti-inflammatory, tissue-repairing, and wound-healing activities, as well as for migration to sites of inflammation (Danilkovitch *et al*., 2012). Therefore, a greater TNFR1 level, as measured by ELISA, indicates a greater potential for immunomodulatory activity (Danilkovitch *et al*., 2012).

Cells from all 3 donors grown in $HS8^{+ve}$ at passage 3 had increased TNFR1 levels (ranging 110 - 140 pg/ml) compared to the controls (ranging 60 - 120 pg/ml). The statistical analysis revealed that this was significant in donor B and donor C. By passage 6, the levels of TNFR1 of $HS8^{+ve}$ cells from donors A and C were comparable to controls, although donor B showed the significant greatest level, of ~ 180 pg/ml. The HS^{pm}- and $HS8^{-ve}$-expanded cells expressed TNFR1 levels similar to control media-expanded cells, except for the passage 3, $HS8^{-ve}$ cells of donor B, which was greater than the control. The heparin-expanded cells also showed similar levels to that of controls (Fig. 4.15). The FGF-2-expanded cells displayed significant lower levels of TNFR1 at passage 3 of donor A and donor B compared to the controls. Although by passage 6 FGF-2 cells showed significant higher levels especially of donor A and donor C (Fig. 4.15). These results further demonstrate that $HS8^{+ve}$ does not impair the immunosuppressive effects of the hMSCs, but in most instances actually enhanced the capability.

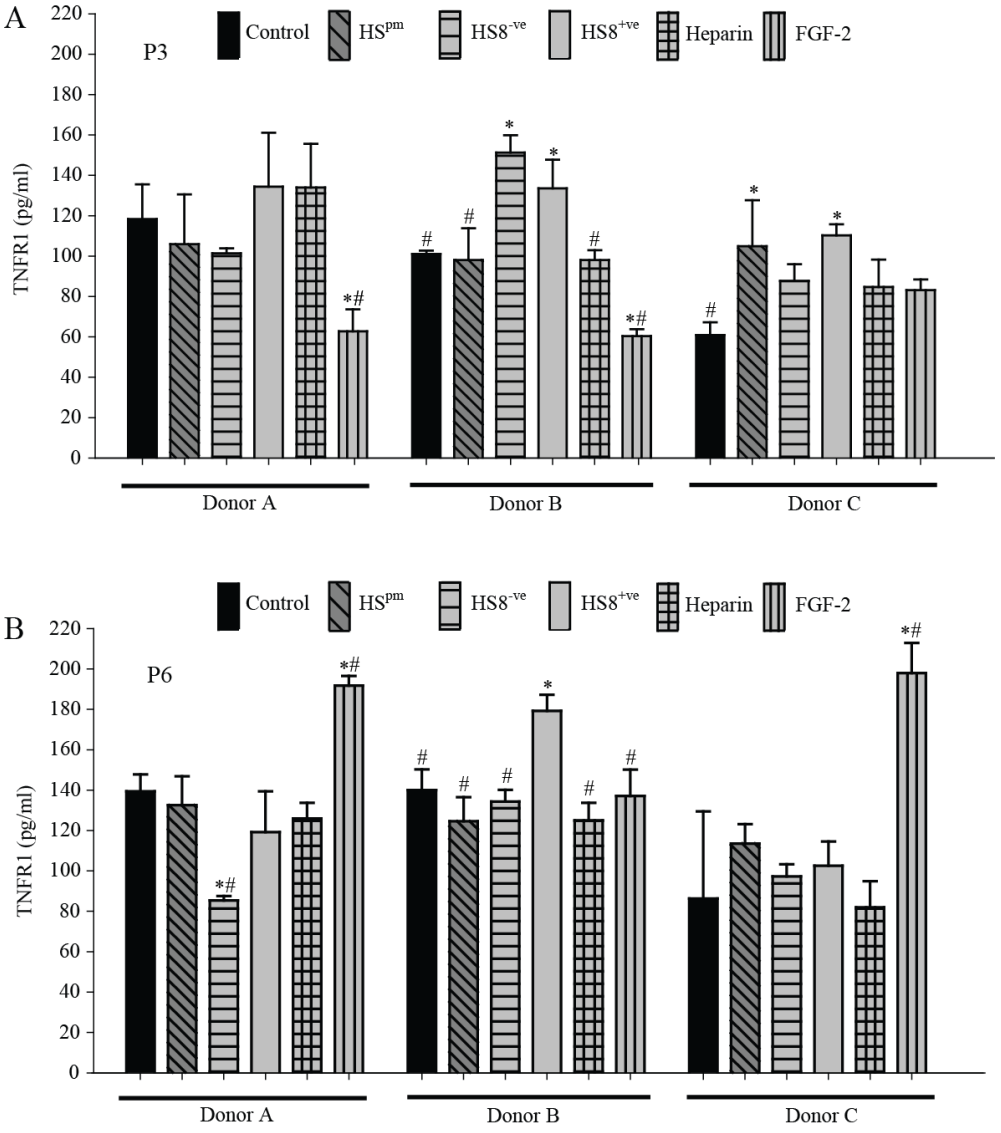

Figure 4.15. TNFR1 expression of hMSCs expanded with HS variants. The hMSCs cell lysates were used to detect TNFRI levels of hMSCs by quantikine ELISA at passage 3 (A) and passage 6 (B). Significant difference is represented as * when compared to control and # when compared to $HS8^{+ve}$ ($p<0.05$).

4.3.2.7. Cells expanded in $HS8^{+ve}$ are small, fast growing cells.

The single-cell-derived colonies of marrow stromal cells contain two distinct cell types, namely spindle-shaped and large flat cells (Colter *et al.*, 2001). Smith and colleagues have described a light scattering assay for the measurement of rapidly self-renewing cells (RS cells) within preparations of

MSCs (Smith *et al*., 2004). In addition, Lee *et al.* have examined this subset of rapidly self-renewing human marrow stromal cells after their preferential engraftment into mice (Lee *et al*., 2006). Therefore I have used this assay to measure the cell sizes and morphology of hMSCs expanded in the different HS variants and positive controls (heparin and FGF-2) at passages 3 and 6 (Fig. 4.16). The hMSCs were categorized as small fast growing cells, rapidly self-renewing cells (RS cells) or large slow growing cells accordingly, and compared (Figs. 4.16 A and B).

Irrespective of passage and donor, addition of HS variants in to media tends to increase the proportion of RS cells. $HS8^{+ve}$-expanded cells had higher percentages of RS cells than the controls except few occurrences. The $HS8^{+ve}$ proportion of RS cells were similar with that of controls at passage 6 of donor A and donor C. In addition, the $HS8^{+ve}$ and $HS8^{-ve}$ proportion of RS cells at passage 3 of donor B were significantly lower than that of respective controls. When consider the large slow growing cells of HS variants, they were lower in most instances and similar in few instances compared to the controls. Positive control heparin yielded similar results to $HS8^{+ve}$ except for few instances; the proportion of RS cells of $HS8^{+ve}$ was significantly higher in passage 0 and passage 6 of donor B, and passage 0 of donor C (Fig. 4.16). In addition, it was significantly lower in passage 3 of donor A and B as compared with heparin. The FGF-2 grown cells showed much higher proportions of RS cells compared to $HS8^{+ve}$ and controls (Fig. 4.16). These results were supported by the phase contrast photomicrographs taken of the cells (Fig. 4.16C). They revealed that the controls have more large flat cells, while FGF-2-grown cells consist mainly of small spindle-shaped cells. In contrast, the $HS8^{+ve}$ cells

appeared as intermediate sized and spindle-shaped, with a resemblance to the small spindle-shaped FGF-2 cells.

A

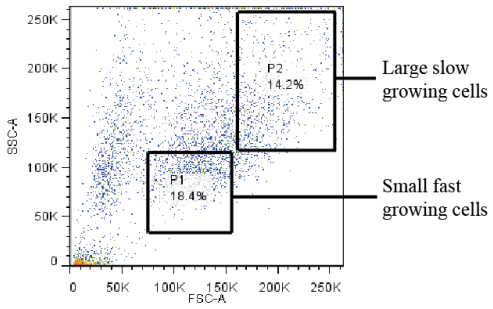

B

		Control		HS^{pm}		$HS8^{-ve}$		$HS8^{+ve}$		Heparin		FGF-2	
Donor	**Passage**	**P1**	**P2**	**P1**	**P2**	**P1**	**P2**	**P1**	**P2**	**P1**	**P2**	**P1**	**P2**
A	**P0**	10.2±0.36$^{\#}$	19.8±2.05	12.2±0.42$^{*\#}$	21.3±1.84	15.4±0.49*	20.8±4.88	16.0±0.64*	13.4±2.33	16.4±1.84	20.1±0.64	28.2±0.07$^{*\#}$	16.2±0.28
	P3	15.6±0.92	27.4±0.71	21.3±1.63*	17.3±0.14	17.6±0.64	27.5±2.40	20.2±0.00*	16.0±4.24	26.4±1.20$^{*\#}$	19.6±1.06$^{\wedge}$	22.5±3.89$^{\#}$	26.3±3.46
	P6	4.0±0.45	16.1±0.21	10.3±2.48	14.5±8.19	11.5±0.07$^{*\#}$	17.8±0.78	4.2±0.25	16.4±0.49	4.8±0.06	18.7±1.91	5.3±0.17$^{\#}$	16.6±1.77
B	**P0**	9.7±0.81$^{\#}$	25.6±2.40$^{@}$	14.4±0.57$^{*\#}$	21.1±0.21$^{@}$	9.6±0.74$^{\#}$	28.2±0.78$^{@}$	27.5±1.41*	13.3±0.28$^{\wedge}$	21.2±0.57$^{*\#}$	18.5±0.21@	21.3±2.40$^{*\#}$	17.4±0.42$^{@}$
	P3	9.0±0.64$^{\#}$	31.4±5.16	8.1±0.32$^{\#}$	31.5±9.33	3.0±0.11*	32.1±4.17	3.2±0.22*	34.7±8.27	5.9±0.21$^{*\#}$	40.0±7.14	20.7±1.91$^{*\#}$	27.4±2.83
	P6	7.9±0.63	24.3±0.00	5.1±0.43$^{*\#}$	16.4±2.76	9.6±1.94	26.2±2.69$^{@}$	9.7±0.35	16.2±1.70$^{\wedge}$	6.7±0.57$^{\#}$	17.5±0.28$^{\wedge}$	14.8±0.28$^{*\#}$	16.8±0.28$^{\wedge}$
C	**P0**	11.9±1.70$^{\#}$	33.0±2.40$^{@}$	19.3±0.78$^{*\#}$	27.4±0.64$^{@}$	16.6±2.55$^{\#}$	25.4±0.14$^{@}$	31.4±0.49*	16.7±0.99$^{\wedge}$	24.5±0.92$^{*\#}$	26.8±0.35@	37.5±1.27$^{*\#}$	13.6±6.30
	P3	12.2±1.56$^{\#}$	27.4±0.92$^{@}$	15.1±6.36	18.4±0.42$^{\wedge@}$	16.7±2.55	25.9±0.71$^{@}$	20.7±1.56*	19.9±0.00$^{\wedge}$	13.9±0.28	20.2±3.89	39.4±4.38$^{*\#}$	13.1±0.99$^{\wedge}$
	P6	7.8±0.50	25.1±2.33	10.1±3.39	17.6±2.55	9.1±0.42$^{\#}$	22.9±5.16	7.4±0.26	19.9±1.06	5.5±0.79	19.6±1.70	5.6±0.35$^{*\#}$	13.4±0.07$^{\wedge@}$

C

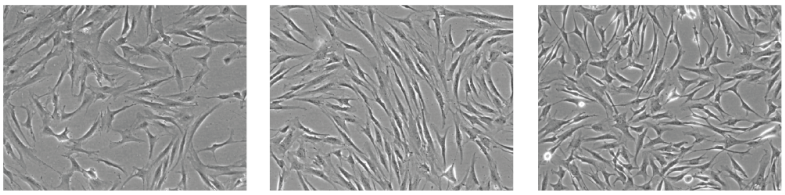

Figure 4.16. $HS8^{+ve}$-expanded cells are small fast growing cells. A light scattering assay by flow cytometry was used to analyze cell size of the hMSCs at P0, P3 and P6. (A) The hMSCs were categorized in-to small fast growing cells and large slow growing cells, and (B) the cells expanded with different HS variants compared. P1 = small rapidly growing cells and P2 = large slow growing cells. (C) Phase-contrast photomicrographs of hMSCs expanded in control media, $HS8^{+ve}$ and FGF-2 supplemented media. Significant difference is represented as * when compared to proportion of RS cells in control, $^{\#}$ when compared to proportion of RS cells in $HS8^{+ve}$, $^{\wedge}$ when compared to proportion of slow growing cells in control and $^{@}$ when compared to proportion of slow growing cells in $HS8^{+ve}$ ($p<0.05$).

4.3.2.8. HS8^{+ve} expanded cells express more FGFR1 receptors.

In chapter 3, I demonstrated that the HS8^{+ve} variant possesses strong binding to FGF-2, as well as to FGFR1 protein, by GAG-ELISA. Also, HS8^{+ve} activity is mediated by FGFR1 signaling (data from FGFR1 inhibition assays). I can thus posit that HS8^{+ve} has binding sites for both FGF-2 and FGFR1 that is important for effective FGF signaling and hMSC proliferation. Therefore I sought to determine the relative levels of FGFRs 1-4 on hMSC cell surfaces. For this purpose single-colour flow cytometry analysis was employed. The hMSCs were grown in control media or media supplemented with HS8^{+ve} and FGF-2 to passages 6. Cells were harvested using TrypLE^{TM} (Invitrogen), and stained with specific antibodies, including IMBR1(Ling *et al*., 2006) against FGFR1 and against FGFRs 2-4 (R & D Systems).

The results indicate that out of the 4 receptors, the predominant receptor in hMSCs is FGFR1 (Fig. 4.16). Cells grown in HS8^{+ve} and FGF-2 also revealed that FGFR1 is the receptor most elevated during cell proliferation. In addition, HS8^{+ve} cells showed similar or greater expression of FGFR1 compared to the controls (passages 3 and 6 of donor B and C). At passage 6 in all donors HS8^{+ve} cells showed greater levels of FGFR1 compared to that of FGF-2 grown cells.

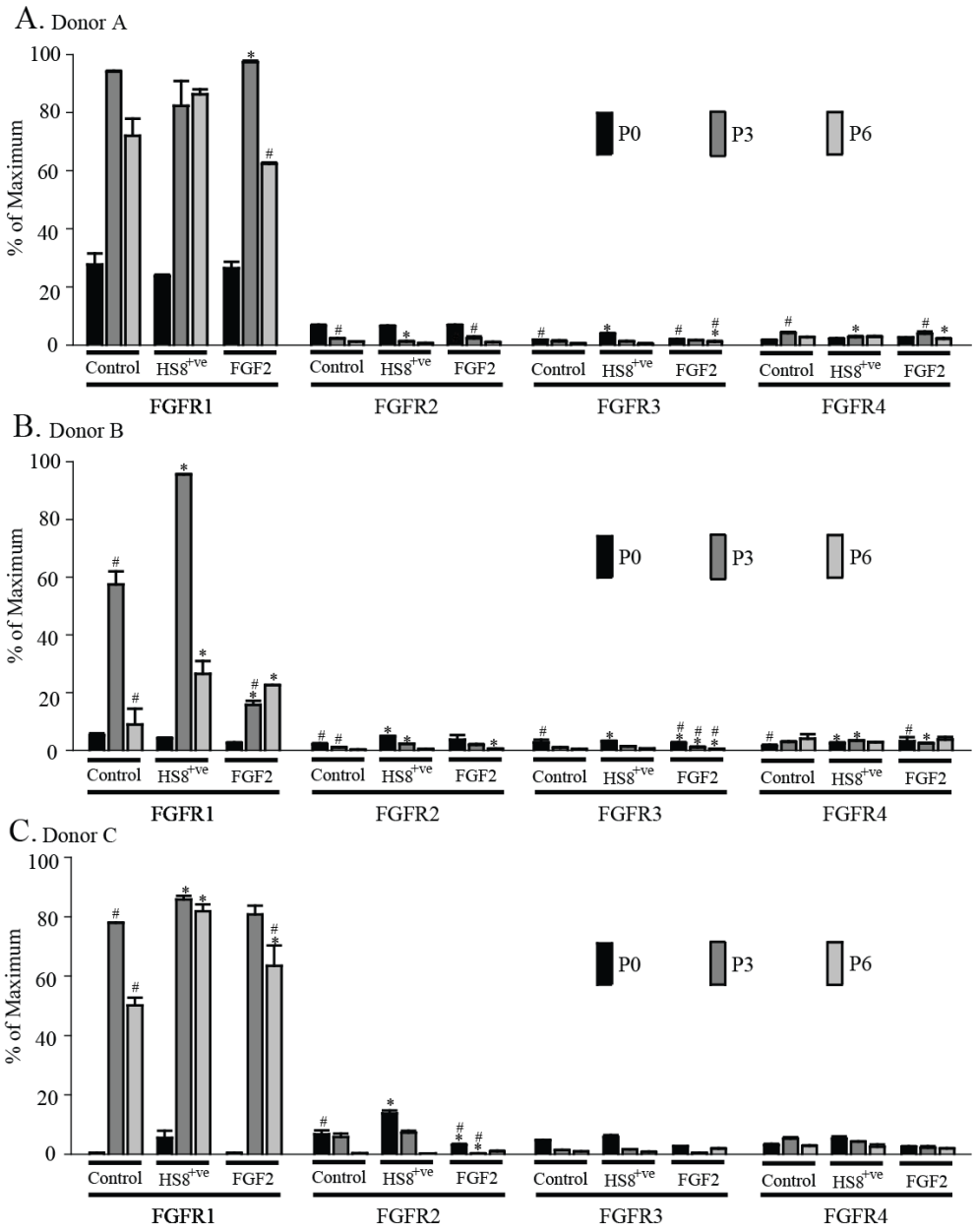

Figure 4.17. Immunophenotypic profile of FGFR 1-4 expression in multiple donors. Single-color flow cytometry analysis of FGF receptors (1-4) on the cell surface of hMSCs was employed. The hMSCs were grown in control media and media supplemented with $HS8^{+ve}$ and FGF-2 for up to 6 passages. Cells were harvested using Triple E (Invitrogen), stained with specific antibodies against the FGFRs. Finally stained cells were analyzed on BD FACS Array™ Bioanalyzer. Significant difference is represented as * when compared to control and # when compared to $HS8^{+ve}$ ($p<0.05$).

4.4. Discussion

Mesenchymal stem cells (MSCs) have been posited to have significant therapeutic potential, and have already been trialed clinically for tissue regeneration and to accelerate bone marrow transplant integration (Wagner *et al*., 2009) . Caplan and Correa described the now standard view of MSCs: the potential they offer because of their multipotentiality, their means of tissue homing and integration, as well as the evolving view of their role as "cellular modulators" (Caplan and Correa, 2011). Most notably, they highlighted the trophic and immunomodulatory activities of MSCs as constituting an "injury drugstore".

The major drawback retarding the wider exploitation of hMSCs for cell-based therapies is the difficulty in generating sufficient cell numbers to meet the clinical demand, both now and in to the future. In order to address this major question (hMSC market supply), the *in vitro* mimicking of the bone marrow microenvironment is now a major research direction. It can be achieved in two broad ways: either growing hMSCs on properly re-constituted ECM substrates, or exogenous growth factor supplementation. Certain ECM substrates have been shown to increase both hMSC attachment and cumulative cell number (Grünert *et al*., 2007; Matsubara *et al*., 2004) but the resulting expanded cells appear to lose the requisite level of "stemness" for clinical usefulness (Cool and Nurcombe, 2005). The potent mitogen FGF-2 is commonly used for exogenous growth factor supplementation, as it clearly drives the proliferation of these cells (Dombrowski *et al*., 2009; Ling *et al*., 2006; Sotiropoulou *et al*., 2006). However, as observed for the MSCs grown on artificial ECM substrates, MSCs cultured in the presence of exogenous

FGF-2 go on to generate greater and greater proportions of differentiated progenitors as compared to unstimulated hMSCs in control cultures (Gronthos *et al*., 1999; Walsh *et al*., 2000). Others have claimed that MSCs grown with FGF-2 supplementation resulted in cells that do maintain their multipotency, as well as other characteristics (Auletta *et al*., 2011; Sotiropoulou *et al*., 2006). Supporting this, autocrine FGF-2 has also been shown to increase the multipotentiality of human adipose-derived MSCs (Rider *et al*., 2008). Therefore not surprisingly, endogenous growth factor activity also seems to modulate hMSC behaviour (Hudalla *et al*., 2011).

The question then becomes: is there a way of presenting hMSCs with the FGF-2 they need for expansion without simultaneously deviating from their multilineage potential, and hence having "drugstore" like qualities? In this thesis I sought to augment the endogenous FGF-2 already secreted by MSCs in order to increase proliferation while retaining its hMSC qualities through targeted HS fractions. This justification appeared reasonable as HS clearly regulates FGF signaling by direct molecular trimeric association with both FGFRs and FGFs (Pellegrini, 2001). In addition, Dombrowski *et al.* from our group has shown that embryonic HS can mediate the proliferation and differentiation of rat MSCs (Dombrowski *et al*., 2009).

The work builds on the original data of Nurcombe *et al.* (1993) who demonstrated that the activity of particular FGF isoforms for murine neural precursor cells was tightly regulated by HS and that this interaction is a requirement for the binding of FGF-2 to their receptors (Nurcombe *et al*., 1993). In addition, unique HS forms mediated the binding of FGF-2 to specific receptors via an interaction with specific cell-surface receptors on the neural

precursor cells (Brickman *et al*., 1995). In 1998, Brickman *et al.* provided further structural support for these physiological findings by isolating and characterizing two separate HS pools that preferentially bind and activate either FGF1 or FGF-2 from immortalized embryonic day 10 and 12 mouse neuroepithelial cells, and proving they had quite distinct binding preferences (Brickman *et al*., 1998). This led to the isolation and characterization of the embryonic HS preparation named HS2, which in turn was shown to be able to accelerate hMSC growth without significant loss of multipotentiality; cells grown in this HS could in turn trigger increased bone formation in mice when they were transplanted *in vivo* (Helledie *et al*., 2011). As a direct development of this work, Murali *et al.* extracted HS from the livers of mice which also increased the rates of hMSC expansion and osteogenic differentiation (Murali *et al*., 2011). These data suggested HS isolated from tissue components could selectively improve the growth of the hMSCs exposed to FGF-2 without adversely affecting their multipotentiality, notwithstanding that although liver is a better source of HS than embryonic mouse brain, the problem of scalability was not resolved.

In chapter 2, I examined the possibility of fine tuning and enhancing the endogenous FGF-2 activity of MSCs through judicious use of targeted HS. The successful isolation of a highly scalable HS fraction variant with higher binding affinity for BMP-2, as our group has previously published (Murali *et al*., 2013; Wang *et al*., 2014) made this a possibility. Chapter 3 saw extensive biochemical assaying of the variants and revealed that $HS8^{+ve}$ binds FGF-2 with higher capacity than other HS variants and heparin-binding growth factors. $HS8^{+ve}$ significantly increased cell proliferation compared to HS^{pm}

and $HS8^{-ve}$. Furthermore, the additive effect of $HS8^{+ve}$ and FGF-2 were monitored by proliferation assays and cell signaling studies, which revealed its enhanced effects on FGF-2-mediated hMSC growth. Moreover, $HS8^{+ve}$ was non-anticoagulant, increased FGF-2 stability and enhanced FGF-2-mediated hMSC growth via FGF-2-FGFR1-HS ternary complex formation and subsequent signaling. Thus I have developed a robust, scalable, simple and cost-effective process to identify a ligand that can bind to both endogenous FGF-2 and FGFR1 and thereby better control FGF-2-mediated hMSC proliferation.

In this chapter, I explored the effectiveness of this ligand ($HS8^{+ve}$) by first determining its effect on long-term hMSC proliferation and then investigated whether hMSCs directly isolated from unfractionated bone marrow also positively responded to $HS8^{+ve}$ supplementation, with a view to determining its direct clinical utility.

In the long-term proliferation of hMSC (Chapter 4.3.1) I used two types of isolated hMSCs; plastic adherent (Friedenstein *et al*., 1976) and STRO-1 (Friedenstein *et al*., 1976; Gronthos and Zannettino, 2008; Gronthos *et al*., 1999; Gronthos *et al*., 2003). In this study irrespective of the different media used $STRO\text{-}1^{+}$ hMSCs had a better cumulative cell numbers compared to the plastic adherent hMSCs. These results were comparable to published results as described by Psaltis *et al* where STRO-1 cells achieved approximately 20 % more population doublings than plastic adherent hMSCs resulting in higher cumulative population expansion (Psaltis *et al*., 2010). In both plastic adherent and $STRO\text{-}1^{+}$ hMSCs expanded in media supplemented with $HS8^{+ve}$, significantly higher cumulative cell numbers were observed

compared to the controls (Fig. 4.3). The increase in the sub-confluent hMSC number was evident from the first passage of expansion in this study (Fig. 4.3). These data were comparable to the data published by Helledie *et al* where they described the embryonic form of heparan sulfate (HS2) supplemented cultures resulted in significantly more cells than controls in 21 days and the effect of HS2 was evident from the second passage (Helledie *et al*., 2011). Whereas, HS^{pm} and $HS8^{-ve}$ triggered cell expansion was very much similar or only slightly elevated compared to the control. These data revealed that $HS8^{+ve}$ increases cumulative viable cell number and the effect of the HS variants on growth was again in the order of their binding affinity for FGF-2.

As previously mentioned growth factors are known to influence cell proliferation. Ng and colleagues have shown that FGF-2, TGFβ and PDGF signaling pathways are essential in hMSC proliferation (Ng *et al*., 2008). They have shown that in the presence of FGF-2, TGFβ1 and PDGF BB in serum-free medium maintained hMSCs for 5 passages while in their absence hMSCs showed a more flattened morphology. In addition, Rodrigues and colleagues in their review paper have also highlighted the importance of several growth factors including TGFβ, FGF-2, FGF-4, VEGFA, PDGF BB, HGF, EGF and Wnt3a as mitogenic factors for MSC proliferation (Rodrigues *et al*., 2010). Furthermore, Gharibi and Hughes have used several growth factors including FGF-2, PDGF BB, Wnt3a, IL-6 and EGF as medium supplements for MSC self-renewal and differentiation potential (Gharibi and Hughes, 2012). They observed that out of all supplements FGF-2 has given the highest increase in MSC proliferation over passage 3 to 10. These data justified the usage of FGF-2 as a positive control in my long term proliferation

studies in a traditional monolayer system. In addition, I have used highly sulfated heparan sulfate in the form of heparin as another positive control. In the long term proliferation study with plastic adherent and STRO-1 hMSCs, the positive control FGF-2 showed the greatest cumulative cell number similar to published results (Auletta *et al*., 2011; Gharibi and Hughes, 2012; Hagmann *et al*., 2013; Sotiropoulou *et al*., 2006) while negatively charged heparin showed a similar trend in growth compared with $HS8^{+ve}$ (Fig. 4.3).

In the long term proliferation study aimed at direct clinical utility, the numbers of recoverable hMSCs from BMMNCs were assayed by GUAVA, while their clonability was assessed by CFU-efficiency. Plastic adherence is a well described property of hMSCs: if cells are maintained and expanded in normal culture conditions they should adhere to plastic surface, and form mesenchymal stem cell colonies when plated at low densities (Friedenstein *et al*., 1976; Pochampally, 2008). Hence I performed CFU-F assays (Rider *et al*., 2008) on HS variant-expanded hMSCs to rigorously demonstrate that $HS8^{+ve}$ supplementation is indeed capable of targeting the isolation and expansion of early progenitors in heterogeneous hMSC culture, over the long-term in culture. For all three donors, media supplemented with $HS8^{+ve}$ demonstrated significantly greater isolation of viable cell counts compared to the controls. In addition, $HS8^{+ve}$ cells demonstrated triggered similar CFU-F efficiency as with the control. The greater isolation of hMSCs with $HS8^{+ve}$ was comparable with the results of embryonic form of heparan sulfate (HS2) when used to isolate hMSCs from unfractionated bone marrow (Helledie *et al*., 2011). They have shown that bone marrow aspirates from three healthy donors strongly responded to HS2, both in terms of their proliferative capacity and their

colony forming ability. In my study, the positive control heparin showed similar results to that of $HS8^{+ve}$ supplementation. Although FGF-2 supplementation increased cell numbers, its lack of CFU-F efficiency was clearly evident. Supplementation of $HS8^{+ve}$ increased hMSC isolation similar to FGF-2 except in one donor where FGF-2 supplementation had significant higher hMSC isolation (Fig. 4.6). Sotiropoulou and colleagues have isolated hMSCs with media supplemented with FGF-2 (Sotiropoulou *et al*., 2006). They also claimed that FGF-2 supplementation clearly affects isolation which resulted in vast numbers of cells, but the colony-forming ability of such cells does not differ significantly among the groups. Although similar to my results, Martin and colleagues have reported that FGF-2 supplementation in isolation of hMSCs from BMMNCs significantly reduced the CFU-F efficiency compared to unsupplemented media (Martin *et al*., 1997). In addition, Fresciline *et al* claimed that rat MSC isolation from BMMNCs with FGF-2 supplemented media had decreased amounts of CFU-F efficiencies (Frescaline *et al*., 2012). The low proportion of hMSCs within bone marrow (0.01 - 0.0001 %) (Caplan, 2009) and the plastic adherence requirement (Friedenstein *et al*., 1970) create major limitations, primarily the yielding of low frequencies of colonies (Colter *et al*., 2001), which the platform technology I am exploring here seems to help rectify.

In my long term proliferation study directly aimed at clinical utility, irrespective of the donor, hMSCs generated with the tuned HS variants had a significantly greater cumulative cell number compared to other methods. The significance of increase in the sub-confluent hMSC number was evident within 4-12 days of contact with the cells (chapter 4.3.2.2). These results

corroborate with the results obtained with HS2, where hMSCs from the 3 donors were continuously cultured in the presence or absence of HS2 (Helledie *et al*., 2011). They have shown that in all 3 donors, HS2 greatly accelerated the cumulative increase in cell numbers and this growth advantage was visible as early as 8 days in culture. Furthermore in my study, supplementation with positive control heparin triggered a similar extent of growth as $HS8^{+ve}$ except with one donor where heparin showed a greater cumulative cell number than that of $HS8^{+ve}$. On the other hand, FGF-2 showed the highest cumulative cell number thus corroborating with the results with other researchers' evidence on FGF-2 supplementation on long term proliferation of hMSC (Auletta *et al*., 2011; Gharibi and Hughes, 2012; Hagmann *et al*., 2013; Sotiropoulou *et al*., 2006).

In the long term proliferation assay (Fig. 4.4) STRO-1hMSCs had a better CFU-F efficiency compared to the plastic adherent hMSCs irrespective of the different media used, thus comparable to the results of Psaltis and colleagues (Psaltis *et al*., 2010). In addition, in both plastic adherent and STRO-1 hMSCs, those expanded in media supplemented with $HS8^{+ve}$ demonstrated significantly higher CFU-F efficiency (1.3 – 1.4 fold) when compared to that of control (Fig. 4.4). In addition, $HS8^{+ve}$ CFU-F efficiency was higher than that of crude HS^{pm} and flow through $HS8^{-ve}$, while resembling the trend of the relative affinity of HS variants to FGF-2. Similar results were obtained when hMSCs were expanded in HS-2 showed higher rates of colony formation (1.4-fold) than cells in control media (Helledie *et al*., 2011). In addition, in the study when I looked at direct clinical utility, irrespective of the media used (including the positive controls) except $HS8^{+ve}$ in all donors, CFU-

F efficiency increased from passage 0 to passage 3 and afterwards started to decline as evident in passage 6. Usually, CFU-F decrease with increasing passage (Gothard *et al*., 2013; Hoch and Leach, 2014; Schellenberg *et al*., 2013; Schellenberg *et al*., 2012). In case of $HS8^{+ve}$ in two donors the CFU-F efficiency was increasing even in the later passages (passage 6). In addition, similar to CFU-F efficiency in established hMSCs, $HS8^{+ve}$ grown cells had a greater CFU-F efficiency than either the control, HS^{pm} or $HS8^{-ve}$ especially at later passages (Fig. 4.10). On the other hand, in both my long term proliferation studies the positive controls (heparin and FGF-2) showed lower levels of colony formation compared to $HS8^{+ve}$ (Figs. 4.4 and 4.10). Interestingly, cells grown with FGF-2 demonstrated significantly lower CFU-F efficiencies than the baseline control. This further confirms that $HS8^{+ve}$ stimulates the robust expansion of a hMSC population with greater early progenitors, over the other HS variants and heparin. In contrast, exogenous FGF-2 supplementation mediates a rapid expansion of cells in culture, with fewer naïve progenitors.

Measures of ‘‘stemness’’ in hMSCs are assessed on the basis of adherence to tissue culture plastic, immunophenotypic profile and multi-lineage proliferation (Dominici *et al*., 2006). In the long term proliferation study immunophenotypic profiling revealed that both types of hMSCs were positive for the MSC-related markers CD73, CD90, CD105 (> 99 % positive) but negative for haematopoeitic markers (< 2 % positive) of CD14, CD19, CD34, CD45 and HLA-DR (Table 4.2) irrespective of media used to expand the hMSCs except in $HS8^{-ve}$ grown plastic adherent cells’ CD14 haemotopoeitic marker (4.7±0.74). This was evident with cells grown with

media supplemented with positive controls, heparin and FGF-2 except for the effects of FGF-2 on the expression of CD90 (91±0.21) (Table 4.2). In addition, differences were observed when I looked at the "stemness" surface marker expression. In plastic adherent hMSCs grown in $HS8^{+ve}$ showed statistically greater levels of STRO-1, SSEA-4 and CD49a when compared to cells grown in HS^{pm} and $HS8^{-ve}$; the exceptions were, statistically higher CD49a levels in the cells grown in HS^{pm} and statistically insignificant levels of CD49a grown in $HS8^{-ve}$. When compared with the control hMSCs grown with $HS8^{+ve}$ showed statistically greater levels of SSEA-4 and higher levels of STRO-1 and CD49a. In the $STRO\text{-}1^{+}$ hMSCs $HS8^{+ve}$ showed statistically greater levels of STRO-1 and higher levels of SSEA-4 and CD49a when compared to cells grown in HS^{pm} and $HS8^{-ve}$. Helleide *et al* have shown that the expression of STRO-1 and CD49a was significantly increased in the presence of embryonic heparan sulfate, HS2 (Helledie *et al*., 2011). Gronthos *et al* have mentioned that STRO-1 antibody can be used as a single reagent to isolate hMSCs (Gronthos *et al*., 1999; Gronthos *et al*., 2003) while Rider and colleagues have shown that CD49a selection can be used for the enrichment of mesenchymal stem cells (Rider *et al*., 2007). In addition, Gang *et al* have reported that SSEA-4, an early embryonic glycolipid antigen, commonly used marker for undifferentiated pluripotent human embryonic stem cells, can be used to identify adult mesenchymal stem cell population (Gang *et al*., 2007). Therefore higher expression of these surface markers can be related to purer hMSCs and thereby I can interpret that $HS8^{+ve}$ expanded hMSCs cultures have more hMSCs compared in the heterogeneous culture compared to the controls.

In the same study, the surface marker expression of STRO-1, SSEA-4 and CD49a in cells grown in positive control heparin showed essentially similar expression that of $HS8^{+ve}$ (Table 4.2). In contrast, FGF-2-cultured cells showed a marked decline in STRO-1 and CD49a expression, even compared to the control cells, and an increase in SSEA-4 levels over control and all HS variant-maintained cells (Table 4.2). The reduction in CD49, STRO-1 and CD90 in FGF-2 expanded cells as compared to controls were recently reported (Hagmann *et al*., 2013). This further supports the idea that $HS8^{+ve}$ may target the expansion of early progenitors in heterogeneous hMSC culture, in contrast to exogenous FGF-2 supplementation, that tends to expand fewer naive progenitors.

In the long term proliferation for direct clinical utility study, the isolated hMSCs from 3 donors revealed that $HS8^{+ve}$ supplementation reduces haematopoeitic marker expression in early passages, indicating the initial contamination of hMSCs cultures with other cells diminished with exposure to $HS8^{+ve}$ (Chapter 4.3.2.4). The presence of significant numbers of contaminating cells was a major concern after the plastic adherence step for hMSCs from bone marrow (Colter *et al*., 2001). Similar to the results with established hMSCs long-term proliferation assay, the hMSCs grown in $HS8^{+ve}$ in this study showed a higher level of STRO-1 and other stemness markers. On the other hand, the positive heparin control showed similar positive and negative surface marker expression to that of $HS8^{+ve}$ albeit a significant difference with respect to HLA-DR expression which deviated from the accepted norm. The other positive control, FGF-2, caused the resultant expanded cells expression of CD90 and HLA-DR to further deviate from

accepted levels (Table 4.3, 4.4 and 4.5). The surface marker expression of STRO-1, SSEA-4 and CD49a in cells grown in heparin showed essentially similar expression to that of $HS8^{+ve}$ except few instances where significant differences were noted between them (Table 4.3, 4.4 and 4.5). In contrast, cells grown in FGF-2 showed declines in STRO-1 and CD49a expression, and, on most occasions, an increase in SSEA-4 levels over control and all HS variant-grown cells (Table 4.3, 4.4 and 4.5). Recently Hagmann *et al* reported the reduction in CD49, STRO-1, CD90 and HLA-DR in FGF-2 expanded cells as compared to controls (Hagmann *et al*., 2013). In addition, Gharibi *et al* also supported the reduction in CD90 in FGF-2 expanded cells (Gharibi and Hughes, 2012). Although FGF-2 expanded cells in my study were in the accepted range, others have documented that FGF-2 expanded hMSCs' CD105 expression was deviated from the accepted levels (Gharibi and Hughes, 2012; Hagmann *et al*., 2013). All in all, this further justifies my idea that $HS8^{+ve}$ may target the expansion of early progenitors in heterogeneous hMSC culture, in contrast to exogenous FGF-2 supplementation, that tends to expand fewer early progenitors.

The multi-lineage differentiation potential of cells expanded in different HS variants compared to the control revealed that $HS8^{+ve}$ grown cells retain their multipotentiality and may even increase it. Helledie *et al.* have shown similar results where, with an embryonic heparan sulfate, which enhanced the self-renewal and therapeutic potential of hMSCs from bone marrow (Helledie *et al*., 2011). Murali *et al.* have extracted HSs from the livers of mice which also increased rates of hMSC expansion and osteogenic differentiation (Murali *et al*., 2011). The hMSCs grown in the positive control

heparin differentiated in to the three lineages similar to that of $HS8^{+ve}$. In both long term proliferation assays, cells grown in the positive control FGF-2 acted similarly in adipogenic differentiation. In contrast FGF-2-grown cells showed marked increase in chondrogenic differentiation compared to the others (Figs. 4.11, 4.12 and 4.13). Others have also reported that FGF-2 expanded cells have increased chondrogenic potential (Hagmann *et al*., 2013; Tsutsumi *et al*., 2001). With regard to osteogenesis in the long term proliferation assay FGF-2 expanded hMSCs were lacking osteogenic differentiation (Fig. 4.5) while the other; long term proliferation for clinical utility study, revealed that FGF-2-grown cells differentiate down the osteogenic lineage. FGF-2 generated greater proportions of differentiated progenitors as compared to the unstimulated hMSCs in the control cultures (Gronthos *et al*., 1999; Walsh *et al*., 2000). In addition, Ling *et al.* have shown that the longer osteogenic cells are in contact with FGF-2, the less potential they have for osteogenic development (Ling *et al*., 2006). It needs to be kept in mind that others have claimed that MSCs grown with FGF-2 supplementation results in cells that do maintain their multipotency, as well as other characteristics (Auletta *et al*., 2011; Gharibi and Hughes, 2012; Sotiropoulou *et al*., 2006). As such, there remains a conflict in this area.

Next I wanted to examine whether continuous expansion in the HS variants had an adverse effect on hMSC properties; therefore, their immunosuppressive capacities (Abdi *et al*., 2008; Caplan, 2009; Caplan and Correa, 2011; Gebler *et al*., 2012; Weil *et al*., 2011) were measured by two means. First I checked the ability of hMSCs to suppress the proliferation of a mixture of stimulatory and reactionary human peripheral blood mononuclear

cells (PBMCs); there was a reduction in the percentage of $CD3^{+}$ $Ki67^{+}$, which resembled an increased immunomodulatory property. Therefore, $HS8^{+ve}$ does not appear to impair the immunosuppressive effects of the hMSCs, but in most instances seemed to enhance the effect, despite the accelerated growth rate. Helledie *et al.* have shown similar results where an embryonic heparan sulfate enhanced the self-renewal and therapeutic potential of hMSCs from bone marrow (Helledie *et al*., 2011). In addition, FGF-2 cells also showed a potent immunosuppressive effect generally consistent with other published literature (Auletta *et al*., 2011; Sotiropoulou *et al*., 2006).

Secondly, I investigated the amount of TNF-α receptor type 1 expressed by hMSCs (Tartaglia *et al*., 1991), as TNFR1 is known to be the predominant receptor type (Vancheri *et al*., 2000). Danilkovitch *et al.* have suggested that hMSC expression of TNF-α receptors may be critical for their immunosuppressive and immunomodulatory activities, and TNFR1-expressing hMSCs can inhibit the proliferation of lymphocytes, indicating a possible usefulness for such conditions as GvHD (Danilkovitch *et al*., 2012). The results revealed that $HS8^{+ve}$ expanded cells have much higher TNFR1 levels than controls, comparable to the levels seen by Danilkovitch *et al* (Danilkovitch *et al*., 2012*).* The heparin-expanded cells also showed similar levels to the controls except in two instances (Fig. 4.15). The FGF-2-expanded cells displayed significant lower levels of TNFR1 at two donors (passage 3) while by passage 6, FGF-2 cells showed significant higher levels in two donors (Fig. 4.15). The increase of TNFR1 receptors in FGF-2 grown cells can be related to their potent immunosuppressive effect as described by others (Auletta *et al*., 2011; Sotiropoulou *et al*., 2006). Altogether these results

further demonstrate that HS8^{+ve} does not impair the immunosuppressive effects of the hMSCs, but in most instances actually enhanced the capability.

Next, I looked at the size and morphology of our HS8^{+ve} expanded cells with a light scattering assay to measure rapidly self-renewing cells (RS cells) (Smith *et al*., 2004). The single-cell-derived colonies of marrow stromal cells contain two distinct cell types, namely spindle-shaped and large flat cells (Colter *et al.*, 2001); the subset of spindle-shaped, rapidly self-renewing marrow stromal cells are known to preferentially engraft in mice (Lee *et al*., 2006). In general, irrespective of passage and donor, exposure to HS8^{+ve} increased the proportions of RS cells. FGF-2 cells showed even higher percentages of RS cells compared to HS8^{+ve}. These results were supported by the phase contrast photomicrographs, which revealed that controls had more large flat cells, and FGF-2 had more small and intermediate spindle-shaped cells. This further supports the idea that HS8^{+ve} expands cells via the fine-tuning of endogenous FGF-2.

In the previous chapter I demonstrated that HS8^{+ve} can bind strongly to FGF-2. I posited that HS8^{+ve} has binding sites for both FGF-2 and FGFR1; the mechanism involved in triggering the proliferation by HS8^{+ve} was consistent with FGF-2-FGFR1 signaling (as revealed by FGFR1 inhibition studies). Therefore I also sought out to find the expression of FGFRs 1-4 on the cell surfaces of the expanded hMSCs. The results indicated the receptor most abundant in proliferating hMSCs was FGFR1. HS8^{+ve} cells showed continued high expression of FGFR1 over the other receptors even at late passages. The HS isolated from mouse embryonic neuroepithelial tissue also regulate the expression of the FGF receptors, by promoting the expression of the

proliferative receptor (FGFR1) while simultaneously down regulating FGFR2 and R3 (Dombrowski *et al*., 2009). Coutu *et al*. have shown that FGFR1 and 2 are expressed by rare mesenchymal progenitors in MSC niches such as perichondrium, periosteum and trabecular marrow (Coutu *et al*., 2011). These $FGFR^{+ve}$ cells displayed MSC phenotype *in vitro* when expanded with FGF-2. They further demonstrate that these MSCs maintain the stemness by inhibiting cellular senescence through a PI3K/AKT-MDM2 pathway and thus promoting proliferation. Therefore they posit that FGFRs may thus be involved in self-renewal of MSC and are important to maintain stemness of MSC. In addition, Dombrowski and colleagues have shown that FGFR1 signaling activity is rate limiting for self-renewal of hMSCs and thereby stimulates proliferation of hMSCs (Dombrowski *et al*., 2013). This is achieved by several mechanisms by inhibiting the cyclin-dependent kinase inhibitors $p21^{Waf1}$ and $p27^{Kip1}$. Thus the relative abundance and activity of FGFR1 might be a useful means of diagnosing healthy, more stem-like MSCs. Thus the relative abundance and activity of FGFR1 as shown by my study is a useful means of diagnosing healthy, more stem-like MSCs.

4.5. Summary

The aim of this chapter was to utilize $HS8^{+ve}$ for selection and expansion of hMSCs from bone marrow. The long term proliferation studies revealed that $HS8^{+ve}$ robustly increased hMSC proliferation. They preserved or improved their multilineage differentiation and immunophenotypic profiling while ensuring normal or augmented immunosuppressive characteristics. In addition, with the increase in CFU-F efficiencies and the reduction of contaminant haematopoeitic cells, $HS8^{+ve}$ may target early progenitor cells in the heterogeneous hMSC cultures. Finally, the proportion of active FGFR1 appears to be a useful marker for an optimal hMSC phenotype.

CHAPTER 5: CONCLUSIONS AND RECOMMENDATIONS

5.1. Conclusions

The major aim of the thesis was to engineer a scalable heparan sulfate that was capable of binding to FGF-2 in such a way that it maintained the naiveté of human bone marrow-derived mesenchymal stem cells while at the same time greatly enhancing their expansion. Consideration was given to certain key factors such as simplicity, safety, scalability and efficacy. Based on this study, the following conclusions were formed:

1. An HS sub-fraction ($HS8^{+ve}$) was successfully produced using FGF-2 peptide-affinity chromatography from commercially available unfractionated porcine intestinal mucosa HS in a manner that was simple, reproducible and readily scalable.
2. $HS8^{+ve}$ mediates the activity of FGF-2 based on its increased FGF-2 binding affinity and specific disaccharide composition.
3. $HS8^{+ve}$ has little anticoagulant activity and thus may be used in regenerative settings where normal blood clotting is particularly beneficial.
4. $HS8^{+ve}$ increases the efficiency of hMSCs isolation from bone marrow mononuclear cells by plastic adherence and increases their proliferation through a mechanism that may involve improving the stability of endogenous FGF-2, and fine-tuning the formation of an FGF-2-FGFR1 signaling cascade. These expanded hMSCs are consisting with higher CFU-F efficiencies and preserved or augmented

multilineage differentiation, immunophenotypic profiling and immunosuppressive characteristics.

Overall, this thesis concludes that serially passaging hMSCs in standard culture conditions results in the expansion of a pool of multipotent cells, and that continual supplementation with the FGF-2 binding HS variant, $HS8^{+ve}$, increases the total number of hMSCs whilst simultaneously preserving their immunomodulatory ability, clonegenicity and multipotentiality. The same cannot be said for the potent mitogen FGF-2, a protein growth factor routinely used to grow and expand many types of stem and progenitor cells. Serial passaging with FGF-2 supplementation, whilst strongly mitogenic, resulted in a significant decrease in cell homogeneity (near loss of STRO-1 expression) and a subsequent loss of osteogenic potential, highlighting their overall decrease in multipoteniality.

Because obtaining sufficient numbers of highly potent hMSCs from a bone marrow aspirate has always been a seen as the bottleneck to their therapeutic application. This study mainly focused on addressing this unmet medical need. The data in this thesis helps to advance MSCs manufacturing using a compound that acts to mediate the activity of endogenous growth factors like FGF-2 naturally present in the culture milieu.

5.2. Possible future research

5.2.1. In vivo efficacy of HS8^{+ve} expanded hMSCs

Robustly-expanded, but still plastic adherent hMSCs should have a major advantage for regenerative medicine. They should thus be trialled in preclinical animal models of ectopic bone formation, a relatively circumscribed *in vivo* situation (Scott *et al*., 2011). Composite scaffolds containing HS8^{+ve}, or HS8^{+ve}-expanded cells, could also be tested as previously described by our group (Rai *et al*., 2010). We could also use these expanded cells in mouse bone regeneration models (Zannettino *et al*., 2010) as well as the rat femoral defect model (Rai *et al*., 2010). To test their immunomodulatory properties *in vivo*, HS8^{+ve} expanded cells could be subjected to the xenogenic human NOD-SCID mice model of GvHD (Tisato *et al*., 2007; Toubai *et al*., 2009).

5.2.2. Further fine-tuning of HS8^{+ve} variants, and eventual synthetic forms

We also envisage a "second generation" HS8^{+ve} variant, with an increased binding avidity for FGF-2. The delay in HS8^{+ve} variant elution in high salt buffer suggested that a mixture of binding HSs are present in the HS8^{+ve} variant fraction that could be sub-fractionated yet again. Hence, during affinity chromatography, if we use a gradual, step-wise NaCl series of washes, instead of the single 1.5 M NaCl wash, we could generate several sub-fractions of HS8^{+ve}. This would enable us to effectively remove the weaker binding HS8^{+ve} variants, and leave the stronger binding (more avid) HS bound to the peptide. As FGF-2 mediates its proliferation action on hMSCs via the FGFR1 receptor, and HS spans both species, we could use an FGFR1-HBD

peptide to further sub-fractionate a bifunctional HS fraction with affinity for both the FGF-2 and the FGFR1. As the HS becomes more homogenous, compositional analysis coupled with strict separation on the basis of chain length, should generate candidates that, when further broken down with heparanases and nitrous acid, could be sequenced. As organic synthesis methods improve, it can be envisaged that completely synthetic versions of HS8 could be generated.

5.2.3. The 3-dimensional (3-D) culturing of hMSCs

The major drawback retarding the wider exploitation of hMSCs for cell-based therapies is the difficulty in generating sufficient cell numbers to meet the clinical demand. The use of stirred microcarrier (MC) culture has been suggested as another method for supplying large volumes of hMSCs for clinics (Chen *et al*., 2013; Goh *et al*., 2013; Rafiq *et al*., 2013; Santos *et al*., 2011). Goh *et al.* have shown that a 12- to 16-fold enhancement in expansion of fetal MSCs can be effected by three-dimensional (3D) scaffold culturing as compared to the 4- to 6-fold expansion with traditional monolayer (MNL) cultures (Goh *et al*., 2013). Similar to these finding Rafiq *et al*. have shown that hMSCs cultured at the litre-scale on microcarriers in a stirred-tank of 5 l bioreactor had a 6-fold increase with traditional monolayer (MNL) cultures while cells retained their multipotentiality (Rafiq *et al*., 2013). In addition, Santos *et al.* have shown hMSC expansion in a microcarrier-based culture system under xeno-free conditions (Santos *et al*., 2011). Therefore, it would be interesting to see the expansion of hMSCs in either xeno-free culture media or normal culture media supplemented with $HS8^{+ve}$ in 3-D culture systems.

5.2.4. Synergistic effect of HS8^{+ve} and FGF-2 used on hMSCs proliferation

I was able to reach the maximum fold-increase in hMSC proliferation with 16-times less FGF-2 (from 2.5 to 0.156 ng/ml) combined with 8-times less HS8^{+ve} (from 2.5 to 0.3125 µg/ml). In addition, HS8^{+ve} was also able to bind and increase the stability of FGF-2 under normal culture conditions. I believe it would therefore be worth observing cells expanded with the combination of HS8^{+ve} and FGF-2 in long-term proliferation studies, and examining their properties.

REFERENCES

Abdelrazik, H., Spaggiari, G.M., Chiossone, L., and Moretta, L. (2011). Mesenchymal stem cells expanded in human platelet lysate display a decreased inhibitory capacity on T-and NK-cell proliferation and function. European Journal of Immunology *41*, 3281-3290.

Abdi, R., Fiorina, P., Adra, C.N., Atkinson, M., and Sayegh, M.H. (2008). Immunomodulation by mesenchymal stem cells a potential therapeutic strategy for type 1 diabetes. Diabetes *57*, 1759-1767.

Adams, J.C., and Watt, F.M. (1993). Regulation of development and differentiation by the extracellular matrix. Development-Cambridge- *117*, 1183-1183.

Alós, J., Arlinghaus, R., Palmer, M., March, D., and Álvarez, I. (2009). The influence of type of natural bait on fish catches and hooking location in a mixed-species marine recreational fishery, with implications for management. Fisheries research *97*, 270-277.

Ampofo, S., Wang, H., and Linhardt, R. (1991). Disaccharide compositional analysis of heparin and heparan sulfate using capillary zone electrophoresis. Analytical biochemistry *199*, 249-255.

Ang, X.M., Lee, M.H., Blocki, A., Chen, C., Ong, L.S., Asada, H.H., Sheppard, A., and Raghunath, M. (2013). Macromolecular Crowding Amplifies Adipogenesis of Human Bone Marrow-Derived Mesenchymal Stem Cells by Enhancing the Pro-Adipogenic Microenvironment. Tissue Engineering Part A *20*, 966-981.

Ashikari-Hada, S., Habuchi, H., Kariya, Y., Itoh, N., Reddi, A.H., and Kimata, K. (2004). Characterization of growth factor-binding structures in heparin/heparan sulfate using an octasaccharide library. Journal of Biological Chemistry *279*, 12346-12354.

Ashikari-Hada, S., Habuchi, H., Sugaya, N., Kobayashi, T., and Kimata, K. (2009). Specific inhibition of FGF-2 signaling with 2-O-sulfated octasaccharides of heparan sulfate. Glycobiology *19*, 644-654.

Auletta, J.J., Zale, E.A., Welter, J.F., and Solchaga, L.A. (2011). Fibroblast growth factor-2 enhances expansion of human bone marrow-derived mesenchymal stromal cells without diminishing their immunosuppressive potential. Stem cells international *2011*. DOI: 10.4061/2011/235176

Aumailley, M., and Gayraud, B. (1998). Structure and biological activity of the extracellular matrix. Journal of Molecular Medicine *76*, 253-265.

Baird, A. (1986). Molecular characterization of fibroblast growth factor. Distribution and biological activities in various tissues. Rec Prog Horm Res *42*, 143.

Baird, A., Schubert, D., Ling, N., and Guillemin, R. (1988). Receptor-and heparin-binding domains of basic fibroblast growth factor. Proceedings of the National Academy of Sciences *85*, 2324-2328.

Bârzu, T., Lormeau, J.C., Petitou, M., Michelson, S., and Choay, J. (1989). Heparin-derived oligosaccharides: Affinity for acidic fibroblast growth factor and effect on its growth-promoting activity for human endothelial cells. Journal of cellular physiology *140*, 538-548.

Beenken, A., and Mohammadi, M. (2009). The FGF family: biology, pathophysiology and therapy. Nature reviews Drug discovery *8*, 235-253.

Bienkowski, M., and Conrad, H.E. (1984). Kinetics of proteoheparan sulfate synthesis, secretion, endocytosis, and catabolism by a hepatocyte cell line. Journal of Biological Chemistry *259*, 12989-12996.

Bishop, J.R., Schuksz, M., and Esko, J.D. (2007). Heparan sulphate proteoglycans fine-tune mammalian physiology. Nature *446*, 1030-1037.

Boido, M., Garbossa, D., Fontanella, M., Ducati, A., and Vercelli, A. (2012). Mesenchymal stem cell transplantation reduces glial cyst and improves functional outcome following spinal cord compression. World neurosurgery.

Bossé, Y., and Rola-Pleszczynski, M. (2008). FGF2 in asthmatic airway-smooth-muscle-cell hyperplasia. Trends in molecular medicine *14*, 3-11.

Bramono, D.S., Murali, S., Rai, B., Ling, L., Poh, W.T., Lim, Z.X., Stein, G.S., Nurcombe, V., Van Wijnen, A.J., and Cool, S.M. (2012). Bone marrow-derived heparan sulfate potentiates the osteogenic activity of bone morphogenetic protein-2 (BMP-2). Bone *50*, 954-964.

Brickman, Y.G., Ford, M.D., Small, D.H., Bartlett, P.F., and Nurcombe, V. (1995). Heparan sulfates mediate the binding of basic fibroblast growth factor to a specific receptor on neural precursor cells. Journal of Biological Chemistry *270*, 24941-24948.

Brickman, Y.G., Nurcombe, V., Ford, M.D., Gallagher, J.T., Bartlett, P.F., and Turnbull, J.E. (1998). Structural comparison of fibroblast growth factor-specific heparan sulfates derived from a growing or differentiating neuroepithelial cell line. Glycobiology *8*, 463-471.

Bueno, E.M., and Glowacki, J. (2009). Cell-free and cell-based approaches for bone regeneration. Nature reviews rheumatology *5*, 685-697.

Burns, J.S., Abdallah, B.M., Guldberg, P., Rygaard, J., Schrøder, H.D., and Kassem, M. (2005). Tumorigenic heterogeneity in cancer stem cells evolved from long-term cultures of telomerase-immortalized human mesenchymal stem cells. Cancer research *65*, 3126-3135.

Bush, M.A., Samara, E., Whitehouse, M., Yoshizawa, C., Novicki, D.L., Pike, M., Laham, R.J., Simons, M., and Chronos, N.A. (2001). Pharmacokinetics and Pharmacodynamics of Recombinant FGF-2 in a Phase I Trial in Coronary Artery Disease. The Journal of Clinical Pharmacology *41*, 378-385.

Cain, S.A., McGovern, A., Small, E., Ward, L.J., Baldock, C., Shuttleworth, A., and Kielty, C.M. (2009). Defining Elastic Fiber Interactions by Molecular Fishing AN Affinity Purification And Mass Spectrometry Approach. Molecular & Cellular Proteomics *8*, 2715-2732.

Caldwell, M.A., Garcion, E., terborg, M.G., He, X., and Svendsen, C.N. (2004). Heparin stabilizes FGF-2 and modulates striatal precursor cell behavior in response to EGF. Experimental neurology *188*, 408-420.

Campagnoli, C., Roberts, I.A., Kumar, S., Bennett, P.R., Bellantuono, I., and Fisk, N.M. (2001). Identification of mesenchymal stem/progenitor cells in human first-trimester fetal blood, liver, and bone marrow. Blood *98*, 2396-2402.

Caplan, A. (2009). Why are MSCs therapeutic? New data: new insight. The Journal of pathology *217*, 318-324.

Caplan, A.I. (2007). Adult mesenchymal stem cells for tissue engineering versus regenerative medicine. Journal of cellular physiology *213*, 341-347.

Caplan, A.I., and Correa, D. (2011). The MSC: an injury drugstore. Cell Stem Cell *9*, 11-15.

Cardin, A.D., and Weintraub, H. (1989). Molecular modeling of protein-glycosaminoglycan interactions. Arteriosclerosis, Thrombosis, and Vascular Biology *9*, 21-32.

Castelo-Branco, M.T., Soares, I.D., Lopes, D.V., Buongusto, F., Martinusso, C.A., do Rosario Jr, A., Souza, S.A., Gutfilen, B., Fonseca, L.M.B., and Elia, C. (2012). Intraperitoneal but not intravenous cryopreserved mesenchymal stromal cells home to the inflamed colon and ameliorate experimental colitis. PloS one *7*, e33360.

Chatterjea, A., Meijer, G., van Blitterswijk, C., and de Boer, J. (2010). Clinical application of human mesenchymal stromal cells for bone tissue engineering. Stem cells international *2010*. Article ID 215625, 12 pages

Chellaiah, A., Yuan, W., Chellaiah, M., and Ornitz, D.M. (1999). Mapping Ligand Binding Domains in Chimeric Fibroblast Growth Factor Receptor Molecules Multiple Regions Determine Ligand Binding Specificity. Journal of Biological Chemistry *274*, 34785-34794.

Chen, A., Reuveny, S., and Oh, S. (2013). Application of Human Mesenchymal and Pluripotent Stem Cell Microcarrier Cultures in Cellular Therapy: Achievements and Future Direction. Biotechnology advances.

Chen, F.H., and Tuan, R.S. (2008). Mesenchymal stem cells in arthritic diseases. Arthritis Res Ther *10*, 223.

Chen, G., Gulbranson, D.R., Yu, P., Hou, Z., and Thomson, J.A. (2012). Thermal Stability of Fibroblast Growth Factor Protein Is a Determinant Factor in Regulating Self-Renewal, Differentiation, and Reprogramming in Human Pluripotent Stem Cells. Stem cells *30*, 623-630.

Chen, L., Tredget, E.E., Wu, P.Y., and Wu, Y. (2008). Paracrine factors of mesenchymal stem cells recruit macrophages and endothelial lineage cells and enhance wound healing. PloS one *3*, e1886.

Clegg, D.O., Reda, D.J., Harris, C.L., Klein, M.A., O'Dell, J.R., Hooper, M.M., Bradley, J.D., Bingham III, C.O., Weisman, M.H., and Jackson, C.G. (2006). Glucosamine, chondroitin sulfate, and the two in combination for painful knee osteoarthritis. New England Journal of Medicine *354*, 795-808.

Colter, D.C., Class, R., DiGirolamo, C.M., and Prockop, D.J. (2000). Rapid expansion of recycling stem cells in cultures of plastic-adherent cells from human bone marrow. Proceedings of the National Academy of Sciences *97*, 3213-3218.

Colter, D.C., Sekiya, I., and Prockop, D.J. (2001). Identification of a subpopulation of rapidly self-renewing and multipotential adult stem cells in colonies of human marrow stromal cells. Proceedings of the National Academy of Sciences *98*, 7841-7845.

Cool, S., and Nurcombe, V. (2009). Methods for proliferating stem cells (Google Patents).

Cool, S.M., and Nurcombe, V. (2005). Substrate induction of osteogenesis from marrow-derived mesenchymal precursors. Stem cells and development *14*, 632-642.

Cool, S.M.K., and Nurcombe, V. (2012). Methods of culturing mesenchymal stem cells (Google Patents).

Coutu, D.L., François, M., and Galipeau, J. (2011). Inhibition of cellular senescence by developmentally regulated FGF receptors in mesenchymal stem cells. Blood *117*, 6801-6812.

Cummings, R.D., and Etzler, M. (2009). Essentials of glycobiology. Varki, A, 633-648.

Danilkovitch, A., Carter, D., Tyrell, A., Bubnic, S., Marcelino, M., and Monroy, R. (2012). Mesenchymal Stem Cells Expressing TNF-alpha Receptors (US Patent 20,120,214,178).

Davidson, J.M., Klagsbrun, M., Hill, K.E., Buckley, A., Sullivan, R., Brewer, P.S., and Woodward, S.C. (1985). Accelerated wound repair, cell proliferation, and collagen accumulation are produced by a cartilage-derived growth factor. The Journal of cell biology *100*, 1219-1227.

De Bari, C., Dell'Accio, F., Tylzanowski, P., and Luyten, F.P. (2001). Multipotent mesenchymal stem cells from adult human synovial membrane. Arthritis & Rheumatism *44*, 1928-1942.

Delehedde, M., Lyon, M., Gallagher, J., Rudland, P., and FERNIG, D. (2002). Fibroblast growth factor-2 binds to small heparin-derived oligosaccharides and stimulates a sustained phosphorylation of p42/44 mitogen-activated protein kinase and proliferation of rat mammary fibroblasts. Biochem J *366*, 235-244.

Delpech, B., and Halavent, C. (1981). Characterization and Purification from Human Brain of a Hyaluronic Acid-Binding Glycoprotein, Hyaluronectin. Journal of neurochemistry *36*, 855-859.

Delpech, B., Maingonnat, C., Delpech, A., Maes, P., Girard, N., and Bertrand, P. (1991). Characterization of a hyaluronic acid-binding protein from sheep brain comparison with human brain hyaluronectin. International journal of biochemistry *23*, 329-337.

Desai, U.R., Wang, H.M., and Linhardt, R.J. (1993). Specificity studies on the heparin lyases from Flavobacterium heparinum. Biochemistry *32*, 8140-8145.

Dombrowski, C., Helledie, T., Ling, L., Grünert, M., Canning, C.A., Jones, C.M., Hui, J.H., Nurcombe, V., van Wijnen, A.J., and Cool, S.M. (2013). FGFR1 Signaling Stimulates Proliferation of Human Mesenchymal Stem Cells by Inhibiting the Cyclin-Dependent Kinase Inhibitors p21Waf1 and p27Kip1. Stem Cells *31*, 2724-2736.

Dombrowski, C., Song, S.J., Chuan, P., Lim, X., Susanto, E., Sawyer, A.A., Woodruff, M.A., Hutmacher, D.W., Nurcombe, V., and Cool, S.M. (2009). Heparan sulfate mediates the proliferation and differentiation of rat mesenchymal stem cells. Stem cells and development *18*, 661-670.

Dominici, M., Le Blanc, K., Mueller, I., Slaper-Cortenbach, I., Marini, F., Krause, D., Deans, R., Keating, A., Prockop, D., and Horwitz, E. (2006). Minimal criteria for defining multipotent mesenchymal stromal cells. The International Society for Cellular Therapy position statement. Cytotherapy *8*, 315-317.

Dong, X.-J., Zhang, H., Pan, R.-L., Xiang, L.-X., and Shao, J.-Z. (2010). Identification of cytokines involved in hepatic differentiation of mBM-MSCs under liver-injury conditions. World journal of gastroenterology: WJG *16*, 3267.

Duchesne, L., Octeau, V., Bearon, R.N., Beckett, A., Prior, I.A., Lounis, B., and Fernig, D.G. (2012). Transport of fibroblast growth factor 2 in the pericellular matrix is controlled by the spatial distribution of its binding sites in heparan sulfate. PLoS biology *10*, e1001361.

Dutta, R.C., and Dutta, A.K. (2010). Comprehension of ECM-cell dynamics: a prerequisite for tissue regeneration. Biotechnology advances *28*, 764-769.

Erices, A., Conget, P., and Minguell, J.J. (2000). Mesenchymal progenitor cells in human umbilical cord blood. British journal of haematology *109*, 235-242.

Esch, F., Baird, A., Ling, N., Ueno, N., Hill, F., Denoroy, L., Klepper, R., Gospodarowicz, D., Böhlen, P., and Guillemin, R. (1985). Primary structure of bovine pituitary basic fibroblast growth factor (FGF) and comparison with the amino-terminal sequence of bovine brain acidic FGF. Proceedings of the National Academy of Sciences *82*, 6507-6511.

Evseenko, D., Schenke-Layland, K., Dravid, G., Zhu, Y., Hao, Q.-L., Scholes, J., Wang, X.C., MacLellan, W.R., and Crooks, G.M. (2009). Identification of the critical extracellular matrix proteins that promote human embryonic stem cell assembly. Stem cells and development *18*, 919-928.

Faham, S., Hileman, R., Fromm, J., Linhardt, R., and Rees, D. (1996a). Heparin structure and interactions with basic fibroblast growth factor. Science *271*, 1116-1120.

Faham, S., Hileman, R., Fromm, J., Linhardt, R., and Rees, D. (1996b). Heparin structure and interactions with basic fibroblast growth factor. Science-New York Then Washington-, 1116-1119.

Falcone, D.J., and Salisbury, B. (1988). Fibronectin stimulates macrophage uptake of low density lipoprotein-heparin-collagen complexes. Arteriosclerosis, Thrombosis, and Vascular Biology *8*, 263-273.

Fan, C.G., Tang, F.W., Zhang, Q.J., Lu, S.H., Liu, H.Y., Zhao, Z.M., Liu, B., Han, Z.B., and Han, Z.C. (2005). Characterization and neural differentiation of fetal lung mesenchymal stem cells. Cell transplantation *14*, 311-321.

Fernaud-Espinosa, I., Nieto-Sampedro, M., and Bovolenta, P. (1994). Differential effects of glycosaminoglycans on neurite outgrowth from hippocampal and thalamic neurones. Journal of cell science *107*, 1437-1448.

Ferrara, J.L., Levine, J.E., Reddy, P., and Holler, E. (2009). Graft-versus-host disease. The Lancet *373*, 1550-1561.

Folkman, J., and Klagsbrun, M. (1987). Angiogenic factors. Science *235*, 442-447.

Frescaline, G., Bouderlique, T., Huynh, M.B., Papy-Garcia, D., Courty, J., and Albanese, P. (2012). Glycosaminoglycans mimetics potentiate the clonogenicity, proliferation, migration and differentiation properties of rat mesenchymal stem cells. Stem cell research *8*, 180-192.

Friedenstein, A., Chailakhjan, R., and Lalykina, K. (1970). The development of fibroblast colonies in monolayer cultures of guinea-pig bone marrow and spleen cells. Cell Proliferation *3*, 393-403.

Friedenstein, A.J., Gorskaja, J., and Kulagina, N. (1976). Fibroblast precursors in normal and irradiated mouse hematopoietic organs. Experimental hematology *4*, 267-274.

Fromm, J., Hileman, R., Caldwell, E., Weiler, J., and Linhardt, R. (1997a). Pattern and spacing of basic amino acids in heparin binding sites. Archives of biochemistry and biophysics *343*, 92-100.

Fromm, J.R., Hileman, R.E., Weiler, J.M., and Linhardt, R.J. (1997b). Interaction of fibroblast growth factor-1 and related peptides with heparan sulfate and its oligosaccharides. Archives of biochemistry and biophysics *346*, 252-262.

Gandhi, N.S., and Mancera, R.L. (2008). The structure of glycosaminoglycans and their interactions with proteins. Chemical biology & drug design *72*, 455-482.

Gang, E.J., Bosnakovski, D., Figueiredo, C.A., Visser, J.W., and Perlingeiro, R.C. (2007). SSEA-4 identifies mesenchymal stem cells from bone marrow. Blood *109*, 1743-1751.

Gattazzo, F., Urciuolo, A., and Bonaldo, P. (2014). Extracellular matrix: A dynamic microenvironment for stem cell niche. Biochimica et Biophysica Acta (BBA)-General Subjects. *1840 (8)*,2506-2519

Gebler, A., Zabel, O., and Seliger, B. (2012). The immunomodulatory capacity of mesenchymal stem cells. Trends in molecular medicine *18*, 128-134.

Gharibi, B., and Hughes, F.J. (2012). Effects of medium supplements on proliferation, differentiation potential, and in vitro expansion of mesenchymal stem cells. Stem cells translational medicine, sctm. 2010-0031.

Goh, T.K.-P., Zhang, Z.-Y., Chen, A.K.-L., Reuveny, S., Choolani, M., Chan, J.K.Y., and Oh, S.K.-W. (2013). Microcarrier Culture for Efficient Expansion and Osteogenic Differentiation of Human Fetal Mesenchymal Stem Cells. BioResearch open access *2*, 84-97.

Gospodarowicz, D. (1974). Localisation of a fibroblast growth factor and its effect alone and with hydrocortisone on 3T3 cell growth. Nature *249*, 123-127.

Gospodarowicz, D., and Cheng, J. (1986). Heparin protects basic and acidic FGF from inactivation. Journal of cellular physiology *128*, 475-484.

Gospodarowicz, D., Ferrara, N., Schweigerer, L., and Neufeld, G. (1987). Structural characterization and biological functions of fibroblast growth factor. Endocrine reviews *8*, 95-114.

Gothard, D., Dawson, J., and Oreffo, R. (2013). Assessing the potential of colony morphology for dissecting the CFU-F population from human bone marrow stromal cells. Cell and tissue research *352*, 237-247.

Gottipamula, S., Muttigi, M.S., Chaansa, S., Ashwin, K., Priya, N., Kolkundkar, U., Sundar Raj, S., Majumdar, A.S., and Seetharam, R.N. (2013). Large-scale expansion of pre-isolated bone marrow mesenchymal stromal cells in serum-free conditions. Journal of tissue engineering and regenerative medicine, DOI:10.1002/term/1713

Gronthos, S., Mankani, M., Brahim, J., Robey, P.G., and Shi, S. (2000). Postnatal human dental pulp stem cells (DPSCs) in vitro and in vivo. Proceedings of the National Academy of Sciences *97*, 13625-13630.

Gronthos, S., and Zannettino, A.C. (2008). A method to isolate and purify human bone marrow stromal stem cells. In Mesenchymal Stem Cells (Springer), pp. 45-57.

Gronthos, S., Zannettino, A.C., Graves, S.E., Ohta, S., Hay, S.J., and Simmons, P.J. (1999). Differential cell surface expression of the STRO-1 and alkaline phosphatase antigens on discrete developmental stages in primary cultures of human bone cells. Journal of Bone and Mineral Research *14*, 47-56.

Gronthos, S., Zannettino, A.C., Hay, S.J., Shi, S., Graves, S.E., Kortesidis, A., and Simmons, P.J. (2003). Molecular and cellular characterisation of highly purified stromal stem cells derived from human bone marrow. Journal of cell science *116*, 1827-1835.

Grünert, M., Dombrowski, C., Sadasivam, M., Manton, K., Cool, S.M., and Nurcombe, V. (2007). Isolation of a native osteoblast matrix with a specific affinity for BMP2. Journal of molecular histology *38*, 393-404.

Guglieri, S., Hricovíni, M., Raman, R., Polito, L., Torri, G., Casu, B., Sasisekharan, R., and Guerrini, M. (2008). Minimum FGF2 Binding Structural Requirements of Heparin and Heparan Sulfate Oligosaccharides As Determined by NMR Spectroscopy†. Biochemistry *47*, 13862-13869.

Guimond, S., Maccarana, M., Olwin, B., Lindahl, U., and Rapraeger, A. (1993). Activating and inhibitory heparin sequences for FGF-2 (basic FGF). Distinct requirements for FGF-1, FGF-2, and FGF-4. Journal of Biological Chemistry *268*, 23906-23914.

Hagmann, S., Moradi, B., Frank, S., Dreher, T., Kämmerer, P., Richter, W., and Gotterbarm, T. (2013). FGF-2 addition during expansion of human bone marrow-derived stromal cells alters MSC surface marker distribution and chondrogenic differentiation potential. Cell proliferation *46*, 396-407.

Hakala, H., Rajala, K., Ojala, M., Panula, S., Areva, S., Kellomäki, M., Suuronen, R., and Skottman, H. (2009). Comparison of biomaterials and extracellular matrices as a culture platform for multiple, independently derived human embryonic stem cell lines. Tissue Engineering Part A *15*, 1775-1785.

Hanson, S.E., Bentz, M.L., and Hematti, P. (2010). Mesenchymal stem cell therapy for nonhealing cutaneous wounds. Plastic and reconstructive surgery *125*, 510-516.

Hay, E.D. (1991). Cell biology of extracellular matrix (Springer).

Hayek, A., Culler, F., Beattie, G., Lopez, A., Cuevas, P., and Baird, A. (1987). An in vivo model for study of the angiogenic effects of basic fibroblast growth factor. Biochemical and biophysical research communications *147*, 876-880.

Helledie, T., Dombrowski, C., Rai, B., Lim, Z.X., Hin, I.L.H., Rider, D.A., Stein, G.S., Hong, W., Van Wijnen, A.J., and Hui, J.H. (2011). Heparan sulfate enhances the self-renewal and therapeutic potential of mesenchymal stem cells from human adult bone marrow. Stem cells and development *21*, 1897-1910.

Hileman, R.E., Fromm, J.R., Weiler, J.M., and Linhardt, R.J. (1998). Glycosaminoglycan-protein interactions: definition of consensus sites in glycosaminoglycan binding proteins. Bioessays *20*, 156-167.

Hoch, A.I., and Leach, J.K. (2014). Concise Review: Optimizing Expansion of Bone Marrow Mesenchymal Stem/Stromal Cells for Clinical Applications. Stem cells translational medicine, sctm. 2013-0196.

Höök, M., Björk, I., Hopwood, J., and Lindahl, U. (1976). Anticoagulant activity of heparin: separation of high-activity and low-activity heparin species by affinity chromatography on immobilized antithrombin. FEBS letters *66*, 90-93.

Hudalla, G.A., Kouris, N.A., Koepsel, J.T., Ogle, B.M., and Murphy, W.L. (2011). Harnessing endogenous growth factor activity modulates stem cell behavior. Integrative Biology *3*, 832-842.

Hudson, J.E., Mills, R.J., Frith, J.E., Brooke, G., Jaramillo-Ferrada, P., Wolvetang, E.J., and Cooper-White, J.J. (2010). A defined medium and substrate for expansion of human mesenchymal stromal cell progenitors that enriches for osteo-and chondrogenic precursors. Stem cells and development *20*, 77-87.

Humphreys, B.D., and Bonventre, J.V. (2008). Mesenchymal stem cells in acute kidney injury. Annu Rev Med *59*, 311-325.

Hynes, R.O. (2009). The extracellular matrix: not just pretty fibrils. Science *326*, 1216-1219.

Ikehara, S. (2013). Bone-Marrow-Derived Mesenchymal Stem Cells for Organ Repair. Stem cells international *2013*, Article ID 132642, 8 pages.

Ishihara, M. (1994). Structural requirements in heparin for binding and activation of FGF-1 and FGF-4 are different from that for FGF-2. Glycobiology *4*, 817-824.

Itano, N. (2008). Simple primary structure, complex turnover regulation and multiple roles of hyaluronan. Journal of biochemistry *144*, 131-137.

Jackson, W.M., Nesti, L.J., and Tuan, R.S. (2012). Concise review: clinical translation of wound healing therapies based on mesenchymal stem cells. Stem cells translational medicine *1*, 44-50.

Jandik, K.A., Gu, K., and Linhardt, R.J. (1994). Action pattern of polysaccharide lyases on glycosaminoglycans. Glycobiology *4*, 289-296.

Jorpes, J.E. (1959). Heparin: a mucopolysaccharide and an active antithrombotic drug. Circulation *19*, 87-91.

Jorpes, J.E., and Gardell, S. (1948). On heparin monosulfuric acid. Journal of Biological Chemistry *176*, 267-276.

Karamanos, N.K., Vanky, P., Tzanakakis, G.N., and Hjerpe, A. (1996). High performance capillary electrophoresis method to characterize heparin and heparan sulfate disaccharides. Electrophoresis *17*, 391-395.

Kim, Y., and Linhardt, R. (1989). Structural features of heparin and their effect on heparin cofactor II mediated inhibition of thrombin. Thrombosis research *53*, 55-71.

Kinsella, L., Chen, H.L., Smith, J.A., Rudland, P.S., and Fernig, D.G. (1998). Interactions of putative heparin-binding domains of basic fibroblast growth factor and its receptor, FGFR-1, with heparin using synthetic peptides. Glycoconjugate journal *15*, 419-422.

Kreuger, J., and Kjellén, L. (2012). Heparan Sulfate Biosynthesis Regulation and Variability. Journal of Histochemistry & Cytochemistry *60*, 898-907.

Kuznetsov, S.A., Mankani, M.H., Gronthos, S., Satomura, K., Bianco, P., and Robey, P.G. (2001). Circulating skeletal stem cells. The Journal of cell biology *153*, 1133-1140.

Lamanna, W.C., Kalus, I., Padva, M., Baldwin, R.J., Merry, C.L., and Dierks, T. (2007). The heparanome—the enigma of encoding and decoding heparan sulfate sulfation. Journal of biotechnology *129*, 290-307.

Lamari, F., Militsopoulou, M., Gioldassi, X., and Karamanos, N.K. (2001). Capillary electrophoresis: a superior miniaturized tool for analysis of the mono-, di-, and oligosaccharide constituents of glycan moieties in proteoglycans. Fresenius' journal of analytical chemistry *371*, 157-167.

Lange, C., Cakiroglu, F., Spiess, A.N., Cappallo-Obermann, H., Dierlamm, J., and Zander, A.R. (2007). Accelerated and safe expansion of human mesenchymal stromal cells in animal serum-free medium for transplantation and regenerative medicine. Journal of cellular physiology *213*, 18-26.

Lazebnik, L., Trubitsyna, I., Agafonov, M., Kniazev, O., and Liundup, A. (2011). Mesenchymal stromal cells transplantation in acute and chronic pancreatitis in rats. Experimental & clinical gastroenterology, 7, 28-31.

Le Blanc, K., Frassoni, F., Ball, L., Locatelli, F., Roelofs, H., Lewis, I., Lanino, E., Sundberg, B., Bernardo, M.E., and Remberger, M. (2008). Mesenchymal stem cells for treatment of steroid-resistant, severe, acute graft-versus-host disease: a phase II study. The Lancet *371*, 1579-1586.

Lee, J., and Blaber, M. (2013). Increased Functional Half-life of Fibroblast Growth Factor-1 by Recovering a Vestigial Disulfide Bond. Journal of Proteins & Proteomics *1*, *2*, 37-42

Lee, J.Y., Choo, J.E., Choi, Y.S., Lee, K.Y., Min, D.S., Pi, S.H., Seol, Y.J., Lee, S.J., Jo, I.H., and Chung, C.P. (2007). Characterization of the surface immobilized synthetic heparin binding domain derived from human fibroblast growth factor-2 and its effect on osteoblast differentiation. Journal of Biomedical Materials Research Part A *83*, 970-979.

Lee, R.H., Hsu, S.C., Munoz, J., Jung, J.S., Lee, N.R., Pochampally, R., and Prockop, D.J. (2006). A subset of human rapidly self-renewing marrow stromal cells preferentially engraft in mice. Blood *107*, 2153-2161.

Lemmon, M.A., and Schlessinger, J. (2010). Cell signaling by receptor tyrosine kinases. Cell *141*, 1117-1134.

Lindahl, U., Bäckström, G., Thunberg, L., and Leder, I.G. (1980). Evidence for a 3-O-sulfated D-glucosamine residue in the antithrombin-binding sequence of heparin. Proceedings of the National Academy of Sciences *77*, 6551-6555.

Lindahl, U., Feingold, D.S., and Rodén, L. (1986). Biosynthesis of heparin. Trends in biochemical sciences *11*, 221-225.

Lindner, V., and Reidy, M. (1991). Proliferation of smooth muscle cells after vascular injury is inhibited by an antibody against basic fibroblast growth factor. Proceedings of the National Academy of Sciences *88*, 3739-3743.

Ling, L., Murali, S., Dombrowski, C., Haupt, L.M., Stein, G.S., Van Wijnen, A.J., Nurcombe, V., and Cool, S.M. (2006). Sulfated glycosaminoglycans mediate the effects of FGF2 on the osteogenic potential of rat calvarial osteoprogenitor cells. Journal of cellular physiology *209*, 811-825.

Lu, P., Takai, K., Weaver, V.M., and Werb, Z. (2011). Extracellular matrix degradation and remodeling in development and disease. Cold Spring Harbor perspectives in biology *3*, a005058.

Lundin, L., Larsson, H., Kreuger, J., Kanda, S., Lindahl, U., Salmivirta, M., and Claesson-Welsh, L. (2000). Selectively desulfated heparin inhibits fibroblast growth factor-induced mitogenicity and angiogenesis. Journal of Biological Chemistry *275*, 24653-24660.

Maccarana, M., Casu, B., and Lindahl, U. (1993). Minimal sequence in heparin/heparan sulfate required for binding of basic fibroblast growth factor. Journal of Biological Chemistry *268*, 23898-23905.

Mahoney, D.J., Whittle, J.D., Milner, C.M., Clark, S.J., Mulloy, B., Buttle, D.J., Jones, G.C., Day, A.J., and Short, R.D. (2004). A method for the non-covalent immobilization of heparin to surfaces. Analytical biochemistry *330*, 123-129.

Maquart, F., and Monboisse, J. (2014). Extracellular matrix and wound healing. Pathologie Biologie *62*, 91-95.

Marson, A., Robinson, D.E., Brookes, P.N., Mulloy, B., Wiles, M., Clark, S.J., Fielder, H.L., Collinson, L.J., Cain, S.A., and Kielty, C.M. (2009). Development of a microtiter plate-based glycosaminoglycan array for the investigation of glycosaminoglycan–protein interactions. Glycobiology *19*, 1537-1546.

Martin, I., Muraglia, A., Campanile, G., Cancedda, R., and Quarto, R. (1997). Fibroblast Growth Factor-2 Supports ex Vivo Expansion and Maintenance of Osteogenic Precursors from Human Bone Marrow 1. Endocrinology *138*, 4456-4462.

Matsubara, T., Tsutsumi, S., Pan, H., Hiraoka, H., Oda, R., Nishimura, M., Kawaguchi, H., Nakamura, K., and Kato, Y. (2004). A new technique to expand human mesenchymal stem cells using basement membrane extracellular matrix. Biochemical and biophysical research communications *313*, 503-508.

Maxson, S., Lopez, E.A., Yoo, D., Danilkovitch-Miagkova, A., and LeRoux, M.A. (2012). Concise review: role of mesenchymal stem cells in wound repair. Stem cells translational medicine *1*, 142-149.

McCaffrey, T.A., Falcone, D.J., and Du, B. (1992). Transforming growth factor-β1 is a heparin-binding protein: Identification of putative heparin-binding regions and isolation of heparins with varying affinity for TGF-β1. Journal of cellular physiology *152*, 430-440.

McLean, J. (1916). The thromboplastic action of cephalin. Am J Physiol *41*, 57.

Meuleman, N., Tondreau, T., Ahmad, I., Kwan, J., Crokaert, F., Delforge, A., Dorval, C., Martiat, P., Lewalle, P., and Lagneaux, L. (2009). Infusion of mesenchymal stromal cells can aid hematopoietic recovery following allogeneic hematopoietic stem cell myeloablative transplant: a pilot study. Stem cells and development *18*, 1247-1252.

Miyamoto, M., Naruo, K., Seko, C., Matsumoto, S., Kondo, T., and Kurokawa, T. (1993). Molecular cloning of a novel cytokine cDNA encoding the ninth member of the fibroblast growth factor family, which has a unique secretion property. Molecular and cellular biology *13*, 4251-4259.

Morigi, M., Imberti, B., Zoja, C., Corna, D., Tomasoni, S., Abbate, M., Rottoli, D., Angioletti, S., Benigni, A., and Perico, N. (2004). Mesenchymal stem cells are renotropic, helping to repair the kidney and improve function in acute renal failure. Journal of the American Society of Nephrology *15*, 1794-1804.

Motomura, K., Hagiwara, A., Komi-Kuramochi, A., Hanyu, Y., Honda, E., Suzuki, M., Kimura, M., Oki, J., Asada, M., and Sakaguchi, N. (2008). An FGF1: FGF2 chimeric growth factor exhibits universal FGF receptor specificity, enhanced stability and augmented activity useful for epithelial proliferation and radioprotection. Biochimica et Biophysica Acta (BBA)-General Subjects *1780*, 1432-1440.

Murali, S., Leong, D.F., Lee, J.J., Cool, S.M., and Nurcombe, V. (2011). Comparative assessment of the effects of gender-specific heparan sulfates on mesenchymal stem cells. Journal of Biological Chemistry *286*, 17755-17765.

Murali, S., Rai, B., Dombrowski, C., Lee, J., Lim, Z., Bramono, D., Ling, L., Bell, T., Hinkley, S., and Nathan, S. (2013). Affinity-selected heparan sulfate for bone repair. Biomaterials. *34(22)* 5594-5605

Mustoe, T.A., O'Shaughnessy, K., and Kloeters, O. (2006). Chronic wound pathogenesis and current treatment strategies: a unifying hypothesis. Plastic and reconstructive surgery *117*, 35S-41S.

Ng, F., Boucher, S., Koh, S., Sastry, K.S., Chase, L., Lakshmipathy, U., Choong, C., Yang, Z., Vemuri, M.C., and Rao, M.S. (2008). PDGF, TGF-β, and FGF signaling is important for differentiation and growth of mesenchymal stem cells (MSCs): transcriptional profiling can identify markers and signaling pathways important in differentiation of MSCs into adipogenic, chondrogenic, and osteogenic lineages. Blood *112*, 295-307.

Niesen, F.H., Berglund, H., and Vedadi, M. (2007). The use of differential scanning fluorimetry to detect ligand interactions that promote protein stability. Nature protocols *2*, 2212-2221.

Noort, W.A., Kruisselbrink, A.B., Kruger, M., van Bezooijen, R.L., de Paus, R.A., Heemskerk, M.H., Löwik, C.W., Falkenburg, J., Willemze, R., and Fibbe, W.E. (2002). Mesenchymal stem cells promote engraftment of human umbilical cord blood–derived CD34 cells in NOD/SCID mice. Experimental hematology *30*, 870-878.

Nurcombe, V., Ford, M.D., Wildschut, J.A., and Bartlett, P.F. (1993). Developmental regulation of neural response to FGF-1 and FGF-2 by heparan sulfate proteoglycan. Science *260*, 103-106.

Nurcombe, V., Goh, F.J., Haupt, L.M., Murali, S., and Cool, S.M. (2007). Temporal and functional changes in glycosaminoglycan expression during osteogenesis. Journal of molecular histology *38*, 469-481.

Ono, K., Hattori, H., Takeshita, S., Kurita, A., and Ishihara, M. (1999). Structural features in heparin that interact with VEGF165 and modulate its biological activity. Glycobiology *9*, 705-711.

Ori, A., Free, P., Courty, J., Wilkinson, M.C., and Fernig, D.G. (2009). Identification of heparin-binding sites in proteins by selective labeling. Molecular & Cellular Proteomics *8*, 2256-2265.

Ori, A., Wilkinson, M.C., and Fernig, D.G. (2008). The heparanome and regulation of cell function: structures, functions and challenges. Frontiers in bioscience: a journal and virtual library *13*, 4309.

Ornitz, D.M., and Itoh, N. (2001). Fibroblast growth factors. Genome Biol *2*, 3005.3001-3005.3012.

Page-McCaw, A., Ewald, A.J., and Werb, Z. (2007). Matrix metalloproteinases and the regulation of tissue remodelling. Nature reviews Molecular cell biology *8*, 221-233.

Pellegrini, L. (2001). Role of heparan sulfate in fibroblast growth factor signalling: a structural view. Current opinion in structural biology *11*, 629-634.

Pellegrini, L., Burke, D.F., von Delft, F., Mulloy, B., and Blundell, T.L. (2000). Crystal structure of fibroblast growth factor receptor ectodomain bound to ligand and heparin. Nature *407*, 1029-1034.

Philippe, B., Luc, S., Valérie, P.-B., Jérôme, R., Alessandra, B.-R., and Louis, C. (2010). Culture and use of mesenchymal stromal cells in phase I and II clinical trials. Stem cells international *2010*.

Plum, S.M., Holaday, J.W., Ruiz, A., Madsen, J.W., Fogler, W.E., and Fortier, A.H. (2000). Administration of a liposomal FGF-2 peptide vaccine leads to abrogation of FGF-2-mediated angiogenesis and tumor development. Vaccine *19*, 1294-1303.

Pochampally, R. (2008). Colony forming unit assays for MSCs. In Mesenchymal Stem Cells (Springer), pp. 83-91.

Powers, C., McLeskey, S., and Wellstein, A. (2000). Fibroblast growth factors, their receptors and signaling. Endocrine-related cancer *7*, 165-197.

Prestrelski, S.J., Fox, G.M., and Arakawa, T. (1992). Binding of heparin to basic fibroblast growth factor induces a conformational change. Archives of biochemistry and biophysics *293*, 314-319.

Price, R.D., Myers, S., Leigh, I.M., and Navsaria, H.A. (2005). The role of hyaluronic acid in wound healing. American journal of clinical dermatology *6*, 393-402.

Psaltis, P.J., Paton, S., See, F., Arthur, A., Martin, S., Itescu, S., Worthley, S.G., Gronthos, S., and Zannettino, A.C.W. (2010). Enrichment for STRO-1 expression enhances the cardiovascular paracrine activity of human bone marrow-derived mesenchymal cell populations. Journal of cellular physiology *223*, 530-540.

Pye, D.A., Vives, R.R., Turnbull, J.E., Hyde, P., and Gallagher, J.T. (1998). Heparan sulfate oligosaccharides require 6-O-sulfation for promotion of basic fibroblast growth factor mitogenic activity. Journal of Biological Chemistry *273*, 22936-22942.

Rafiq, Q.A., Brosnan, K.M., Coopman, K., Nienow, A.W., and Hewitt, C.J. (2013). Culture of human mesenchymal stem cells on microcarriers in a 5 l stirred-tank bioreactor. Biotechnology letters, 1-13.

Rai, B., Lin, J.L., Lim, Z.X., Guldberg, R.E., Hutmacher, D.W., and Cool, S.M. (2010). Differences between in vitro viability and differentiation and in vivo bone-forming efficacy of human mesenchymal stem cells cultured on PCL-TCP scaffolds. Biomaterials *31*, 7960-7970.

Rayment, E.A., and Williams, D.J. (2010). Concise Review: Mind the Gap: Challenges in Characterizing and Quantifying Cell-and Tissue-Based Therapies for Clinical Translation. Stem cells *28*, 996-1004.

Reger, R.L., and Prockop, D.J. (2014). Should Publications on Mesenchymal Stem/Progenitor Cells Include In-Process Data on the Preparation of the Cells? Stem cells translational medicine *3*, 632-635.

Ren, G., Su, J., Zhang, L., Zhao, X., Ling, W., L'huillie, A., Zhang, J., Lu, Y., Roberts, A.I., and Ji, W. (2009). Species Variation in the Mechanisms of Mesenchymal Stem Cell-Mediated Immunosuppression. Stem cells *27*, 1954-1962.

Rider, D.A., Dombrowski, C., Sawyer, A.A., Ng, G.H., Leong, D., Hutmacher, D.W., Nurcombe, V., and Cool, S.M. (2008). Autocrine Fibroblast Growth Factor 2 Increases the Multipotentiality of Human Adipose-Derived Mesenchymal Stem Cells. Stem cells *26*, 1598-1608.

Rider, D.A., Nalathamby, T., Nurcombe, V., and Cool, S.M. (2007). Selection using the alpha-1 integrin (CD49a) enhances the multipotentiality of the mesenchymal stem cell population from heterogeneous bone marrow stromal cells. Journal of molecular histology *38*, 449-458.

Ringdén, O., Uzunel, M., Rasmusson, I., Remberger, M., Sundberg, B., Lönnies, H., Marschall, H.-U., Dlugosz, A., Szakos, A., and Hassan, Z. (2006). Mesenchymal stem cells for treatment of therapy-resistant graft-versus-host disease. Transplantation *81*, 1390-1397.

Rodrigues, M., Griffith, L.G., and Wells, A. (2010). Growth factor regulation of proliferation and survival of multipotential stromal cells. Stem Cell Res Ther *1*, 32.

Ruiz-Calero, V., Puignou, L., and Galceran, M. (1998). Use of reversed polarity and a pressure gradient in the analysis of disaccharide composition of heparin by capillary electrophoresis. Journal of Chromatography A *828*, 497-508.

Salgado, A.J., Coutinho, O.P., and Reis, R.L. (2004). Bone tissue engineering: state of the art and future trends. Macromolecular bioscience *4*, 743-765.

Santiago, J.A., Pogemiller, R., and Ogle, B.M. (2009). Heterogeneous differentiation of human mesenchymal stem cells in response to extended culture in extracellular matrices. Tissue Engineering Part A *15*, 3911-3922.

Santos, F.d., Andrade, P.Z., Abecasis, M.M., Gimble, J.M., Chase, L.G., Campbell, A.M., Boucher, S., Vemuri, M.C., Silva, C.L.d., and Cabral, J.M. (2011). Toward a clinical-grade expansion of mesenchymal stem cells from human sources: a microcarrier-based culture system under xeno-free conditions. Tissue Engineering Part C: Methods *17*, 1201-1210.

Scapol, L., Marchi, E., and Viscomi, G. (1996). Capillary electrophoresis of heparin and dermatan sulfate unsaturated disaccharides with triethylamine and acetonitrile as electrolyte additives. Journal of Chromatography A *735*, 367-374.

Schäfer, T., Zentgraf, H., Zehe, C., Brügger, B., Bernhagen, J., and Nickel, W. (2004). Unconventional secretion of fibroblast growth factor 2 is mediated by direct translocation across the plasma membrane of mammalian cells. Journal of Biological Chemistry *279*, 6244-6251.

Schellenberg, A., Hemeda, H., and Wagner, W. (2013). Tracking of replicative senescence in mesenchymal stem cells by colony-forming unit frequency. In Stem Cells and Aging (Springer), pp. 143-154.

Schellenberg, A., Stiehl, T., Horn, P., Joussen, S., Pallua, N., Ho, A.D., and Wagner, W. (2012). Population dynamics of mesenchymal stromal cells during culture expansion. Cytotherapy *14*, 401-411.

Scherjon, S.A., Kleijburg-van der Keur, C., Noort, W.A., Claas, F.H., Willemze, R., Fibbe, W.E., and Kanhai, H.H. (2003). Amniotic fluid as a novel source of mesenchymal stem cells for therapeutic transplantation. Blood *102*, 1548-1549.

Schlessinger, J. (2000). Cell signaling by receptor tyrosine kinases. Cell *103*, 211-225.

Schlessinger, J., Plotnikov, A.N., Ibrahimi, O.A., Eliseenkova, A.V., Yeh, B.K., Yayon, A., Linhardt, R.J., and Mohammadi, M. (2000). Crystal structure of a ternary FGF-FGFR-heparin complex reveals a dual role for heparin in FGFR binding and dimerization. Molecular cell *6*, 743-750.

Schmidt, A., Ladage, D., Schinköthe, T., Klausmann, U., Ulrichs, C., Klinz, F.J., Brixius, K., Arnhold, S., Desai, B., and Mehlhorn, U. (2006). Basic fibroblast growth factor controls migration in human mesenchymal stem cells. Stem cells *24*, 1750-1758.

Scott, M.A., Levi, B., Askarinam, A., Nguyen, A., Rackohn, T., Ting, K., Soo, C., and James, A.W. (2011). Brief review of models of ectopic bone formation. Stem cells and development *21*, 655-667.

Scully, M.F., Ellis, V., and Kakkar, V.V. (1988). Heparan sulphate with no affinity for antithrombin III and the control of haemostasis. FEBS letters *241*, 11-14.

Shabbir, A., Zisa, D., Suzuki, G., and Lee, T. (2009). Heart failure therapy mediated by the trophic activities of bone marrow mesenchymal stem cells: a noninvasive therapeutic regimen. American Journal of Physiology-Heart and Circulatory Physiology *296*, H1888-H1897.

Shi, Y., Hu, G., Su, J., Li, W., Chen, Q., Shou, P., Xu, C., Chen, X., Huang, Y., and Zhu, Z. (2010). Mesenchymal stem cells: a new strategy for immunosuppression and tissue repair. Cell research *20*, 510-518.

Shin, L., and Peterson, D.A. (2013). Human mesenchymal stem cell grafts enhance normal and impaired wound healing by recruiting existing endogenous tissue stem/progenitor cells. Stem cells translational medicine *2*, 33-42.

Shing, Y., Folkman, J., Haudenschild, C., Lund, D., Crum, R., and Klagsbrun, M. (1985). Angiogenesis is stimulated by a tumor-derived endothelial cell growth factor. Journal of cellular biochemistry *29*, 275-287.

Si, Y.-L., Zhao, Y.-L., Hao, H.-J., Fu, X.-B., and Han, W.-D. (2011). MSCs: biological characteristics, clinical applications and their outstanding concerns. Ageing research reviews *10*, 93-103.

Simonsen, J.L., Rosada, C., Serakinci, N., Justesen, J., Stenderup, K., Rattan, S.I., Jensen, T.G., and Kassem, M. (2002). Telomerase expression extends the proliferative life-span and maintains the osteogenic potential of human bone marrow stromal cells. Nature biotechnology *20*, 592-596.

Sinniger, V., Tapon-Bretaudiere, J., Millien, C., Muller, D., Jozefonvicz, J., and Fischer, A. (1993). Affinity chromatography of sulphated polysaccharides separately fractionated on antithrombin III and heparin cofactor II immobilized on concanavalin A—Sepharose. Journal of Chromatography B: Biomedical Sciences and Applications *615*, 215-223.

Smith, J.R., Pochampally, R., Perry, A., Hsu, S.C., and Prockop, D.J. (2004). Isolation of a highly clonogenic and multipotential subfraction of adult stem cells from bone marrow stroma. Stem cells *22*, 823-831.

Sommer, A., Brewer, M.T., Thompson, R.C., Moscatelli, D., Presta, M., and Rifkin, D.B. (1987). A form of human basic fibroblast growth factor with an extended amino terminus. Biochemical and biophysical research communications *144*, 543-550.

Sotiropoulou, P.A., Perez, S.A., Salagianni, M., Baxevanis, C.N., and Papamichail, M. (2006). Characterization of the optimal culture conditions for clinical scale production of human mesenchymal stem cells. Stem cells *24*, 462-471.

Stauber, D.J., DiGabriele, A.D., and Hendrickson, W.A. (2000). Structural interactions of fibroblast growth factor receptor with its ligands. Proceedings of the National Academy of Sciences *97*, 49-54.

Steiling, H., and Werner, S. (2003). Fibroblast growth factors: key players in epithelial morphogenesis, repair and cytoprotection. Current opinion in biotechnology *14*, 533-537.

Steringer, J.P., Müller, H.-M., and Nickel, W. (2014). Unconventional Secretion of Fibroblast Growth Factor 2—A Novel Type of Protein Translocation across Membranes? Journal of molecular biology. PMID:25051502

Syed, B.A., and Evans, J.B. (2013). Stem cell therapy market. Nature Reviews Drug Discovery *12*, 185-186.

Szlachcic, A., Zakrzewska, M., and Otlewski, J. (2011). Longer action means better drug: tuning up protein therapeutics. Biotechnology advances *29*, 436-441.

Tartaglia, L.A., Weber, R.F., Figari, I.S., Reynolds, C., Palladino, M.A., and Goeddel, D.V. (1991). The two different receptors for tumor necrosis factor mediate distinct cellular responses. Proceedings of the National Academy of Sciences *88*, 9292-9296.

Thompson, L.D., Pantoliano, M.W., and Springer, B.A. (1994). Energetic characterization of the basic fibroblast growth factor-heparin interaction: identification of the heparin binding domain. Biochemistry *33*, 3831-3840.

Timpl, R., and Brown, J.C. (1994). The laminins. Matrix biology *14*, 275-281.

Tisato, V., Naresh, K., Girdlestone, J., Navarrete, C., and Dazzi, F. (2007). Mesenchymal stem cells of cord blood origin are effective at preventing but not treating graft-versus-host disease. Leukemia *21*, 1992-1999.

Toubai, T., Paczesny, S., Shono, Y., Tanaka, J., Lowler, K.P., Malter, C.T., Kasai, M., and Imamura, M. (2009). Mesenchymal stem cells for treatment and prevention of graft-versus-host disease after allogeneic hematopoietic cell transplantation. Current Stem Cell Research & Therapy *4*, 252-259.

Trowbridge, J.M., and Gallo, R.L. (2002). Dermatan sulfate: new functions from an old glycosaminoglycan. Glycobiology *12*, 117R-125R.

Trowell, O.A., and Willmer, E.N. (1939). Growth Promoting Factors. Journal of Experimental Biology *16*, 60-67.

Tsutsumi, S., Shimazu, A., Miyazaki, K., Pan, H., Koike, C., Yoshida, E., Takagishi, K., and Kato, Y. (2001). Retention of multilineage differentiation potential of mesenchymal cells during proliferation in response to FGF. Biochemical and biophysical research communications *288*, 413-419.

Tu, X.H., Song, J.X., Xue, X.J., Guo, X.W., Ma, Y.X., Chen, Z.Y., Zou, Z.D., and Wang, L. (2012). Role of bone marrow-derived mesenchymal stem cells in a rat model of severe acute pancreatitis. World journal of gastroenterology: WJG *18*, 2270.

Turnbull, J.E., Fernig, D., Ke, Y., Wilkinson, M.C., and Gallagher, J.T. (1992). Identification of the basic fibroblast growth factor binding sequence in fibroblast heparan sulfate. Journal of Biological Chemistry *267*, 10337-10341.

Uccelli, A., Moretta, L., and Pistoia, V. (2008). Mesenchymal stem cells in health and disease. Nature Reviews Immunology *8*, 726-736.

Undale, A.H., Westendorf, J.J., Yaszemski, M.J., and Khosla, S. (2009). Mesenchymal stem cells for bone repair and metabolic bone diseases. Paper presented at: Mayo Clinic Proceedings (Elsevier).

Uniewicz, K.A., Ori, A., Xu, R., Ahmed, Y., Wilkinson, M.C., Fernig, D.G., and Yates, E.A. (2010). Differential scanning fluorimetry measurement of protein stability changes upon binding to glycosaminoglycans: a screening test for binding specificity. Analytical chemistry *82*, 3796-3802.

Urh, M., Simpson, D., and Zhao, K. (2009). Affinity chromatography: general methods. Methods in enzymology *463*, 417-438.

Vancheri, C., Sortino, M.A., Tomaselli, V., Mastruzzo, C., Condorelli, F., Bellistrí, G., Pistorio, M.P., Canonico, P.L., and Crimi, N. (2000). Different Expression of TNF-α Receptors and Prostaglandin E2Production in Normal and Fibrotic Lung Fibroblasts: Potential Implications for the Evolution of the Inflammatory Process. American journal of respiratory cell and molecular biology *22*, 628-634.

Varki, A., Cummings, R., Esko, J., Freeze, H., Hart, G., and Marth, J. (1998). Essentials of glycobiology, 1999. Cold Spring Harber Laboratory Press, New York.

Vemuri, S., Beylin, I., Sluzky, V., Stratton, P., Eberlein, G., and Wang, Y. (1994). The stability of bFGF against thermal denaturation. Journal of pharmacy and pharmacology *46*, 481-486.

Wagner, J., Kean, T., Young, R., Dennis, J.E., and Caplan, A.I. (2009). Optimizing mesenchymal stem cell-based therapeutics. Current opinion in biotechnology *20*, 531-536.

Walsh, S., Jefferiss, C., Stewart, K., Jordan, G., Screen, J., and Beresford, J. (2000). Expression of the developmental markers STRO-1 and alkaline phosphatase in cultures of human marrow stromal cells: regulation by fibroblast growth factor (FGF)-2 and relationship to the expression of FGF receptors 1–4. Bone *27*, 185-195.

Wang, C., Poon, S., Murali, S., Koo, C.Y., Bell, T.J., Hinkley, S.F., Yeong, H., Bhakoo, K., Nurcombe, V., and Cool, S.M. (2014). Engineering a vascular endothelial growth factor 165-binding heparan sulfate for vascular therapy. Biomaterials *35*, 6776-6786.

Ward, P., and Myers, R.A. (2007). Bait loss and its potential effects on fishing power in pelagic longline fisheries. Fisheries research *86*, 69-76.

Ware, J.A., and Simons, M. (1997). Angiogenesis in ischemic heart disease. Nature medicine *3*, 158-164.

Watt, F.M., and Driskell, R.R. (2010). The therapeutic potential of stem cells. Philosophical Transactions of the Royal Society B: Biological Sciences *365*, 155-163.

Watt, F.M., and Huck, W.T. (2013). Role of the extracellular matrix in regulating stem cell fate. Nature Reviews Molecular Cell Biology *14*, 467-473.

Weigel, P.H., Fuller, G.M., and LeBoeuf, R.D. (1986). A model for the role of hyaluronic acid and fibrin in the early events during the inflammatory response and wound healing. Journal of theoretical biology *119*, 219-234.

Weil, B.R., Manukyan, M.C., Herrmann, J.L., Abarbanell, A.M., Poynter, J.A., Wang, Y., and Meldrum, D.R. (2011). The immunomodulatory properties of mesenchymal stem cells: implications for surgical disease. Journal of Surgical Research *167*, 78-86.

Williams, J.T., Southerland, S.S., Souza, J., Calcutt, A.F., and Cartledge, R.G. (1999). Cells isolated from adult human skeletal muscle capable of differentiating into multiple mesodermal phenotypes. The American Surgeon *65*, 22-26.

Wu, Y., Huang, S., Enhe, J., Ma, K., Yang, S., Sun, T., and Fu, X. (2013). Bone marrow-derived mesenchymal stem cell attenuates skin fibrosis development in mice. International wound journal. *11(6)*, 701-710

Xu, R., Ori, A., Rudd, T.R., Uniewicz, K.A., Ahmed, Y.A., Guimond, S.E., Skidmore, M.A., Siligardi, G., Yates, E.A., and Fernig, D.G. (2012). Diversification of the Structural Determinants of Fibroblast Growth Factor-Heparin Interactions Implications for Binding Specificity. Journal of Biological Chemistry *287*, 40061-40073.

Zagris, N. (2000). Extracellular matrix in development of the early embryo. Micron *32*, 427-438.

Zakrzewska, M., Krowarsch, D., Wiedlocha, A., Olsnes, S., and Otlewski, J. (2005). Highly stable mutants of human fibroblast growth factor-1 exhibit prolonged biological action. Journal of molecular biology *352*, 860-875.

Zannettino, A.C., Paton, S., Itescu, S., and Gronthos, S. (2010). Comparative assessment of the osteoconductive properties of different biomaterials in vivo seeded with human or ovine mesenchymal stem/stromal cells. Tissue Engineering Part A *16*, 3579-3587.

Zuk, P.A., Zhu, M., Mizuno, H., Huang, J., Futrell, J.W., Katz, A.J., Benhaim, P., Lorenz, H.P., and Hedrick, M.H. (2001). Multilineage cells from human adipose tissue: implications for cell-based therapies. Tissue engineering *7*, 211-228.

Zulma, G., Pelled, G., Sheyn, D., Kimelman, N., and Gazit, N. (2011). Mesenchymal Stem Cells. In Principles of Regenerative Medicine, pp. 285-304.

APPENDIX A: SUPPLEMENTARY FIGURES AND TABLES

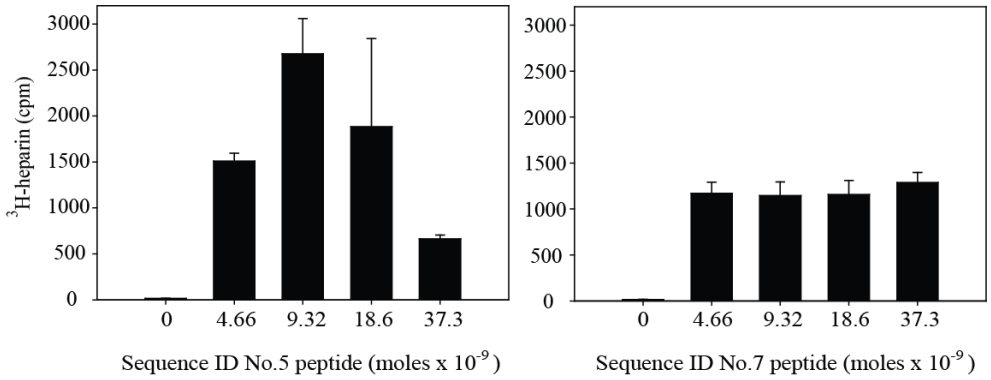

Figure A1: Binding capacity of FGF-2-HBD for ^{3}H-heparin. FGF-2-HBD peptides Sequence ID No. 5 and 7 were spotted onto nitrocellulose membranes, air-dried and incubated with ^{3}H-heparin. Bound ^{3}H-heparin was determined by liquid scintillation.

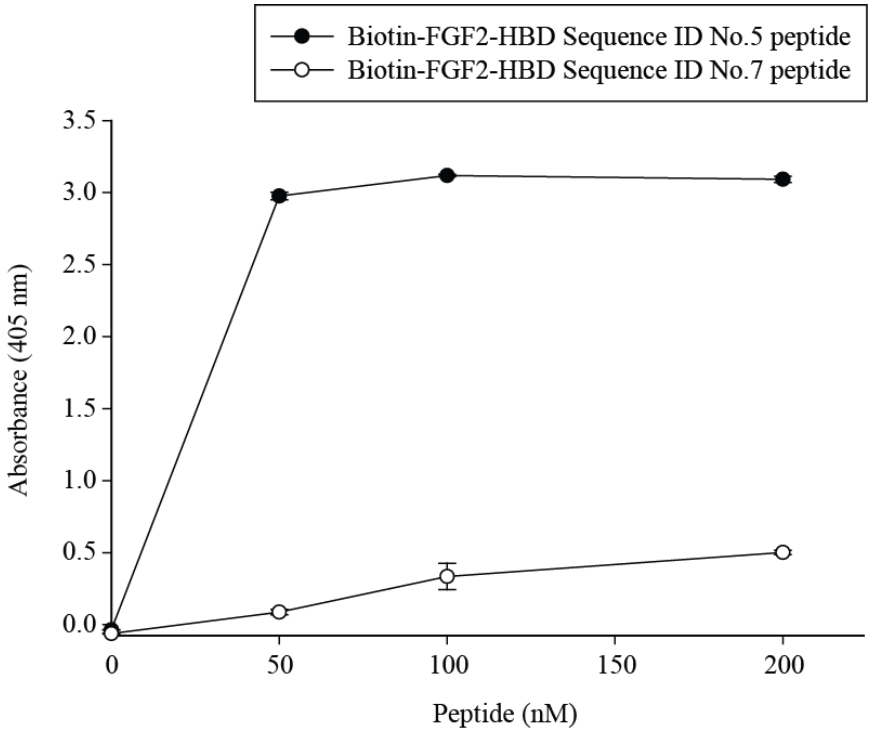

Figure A2: Binding capacities of FGF-2-HBDs for heparin. Heparin was immobilized onto the GAG-binding 96-well plates (Iduron) by electrostatic interaction, which did not affect protein binding capability. The Sequence ID No. 5 and 7 FGF-2-HBD peptides had their binding ability for immobilized heparin assessed by dint of their biotinylated portion yielding a colourimetric reaction.

APPENDIX B: SUPPLEMENTARY INFORMATION FOR MATERIAL AND METHODS

General chemicals and reagents

3,3′,5,5′-Tetramethylbenzidine (TMB) substrate (Cat No. 34021, Thermo Fisher Scientific Inc, IL, USA)

Acetic acid (Cat. No.1.00063.2500, Merck Millipore, Darmstadt, Germany)

Agarose powder (Cat. No. 10975-035, Invitrogen, Life Technologies Corporation, CA, USA)

Bio-Gel® P-10 Gel (Cat No. 150-4144, Biorad Laboratories, Hercules, USA)

Bovine serum albumin (BSA) (Cat No. A7906, Sigma Aldrich, MO, USA)

Crystal violet powder (Cat. No. C3886, Sigma Aldrich, MO, USA)

Dimethyl sulfoxide (DMSO) (Cat.No. D2438 , Sigma Aldrich, MO, USA)

Ethanol (Cat. No. 1.00983.2500, Merck Millipore, Darmstadt, Germany)

ExtrAvidin® - Alkaline phosphatase (Cat No. E2636, Sigma Aldrich, MO, USA)

Fish gelatin powder (Cat. No. G7041, Sigma Aldrich, MO, USA)

Heparan sulfate sodium salt from porcine intestinal mucosa (HSpm) (Cat No. HO-03103, Celsus Laboratories Inc, Ohio, USA)

Heparin Sepharose beads (Cat. No. H6508, Sigma Aldrich, MO, USA)

Heparin sodium salt from porcine intestinal mucosa (Cat. No. H3149, Sigma Aldrich, MO, USA)

HPLC grade water (Cat. No. 95304, Sigma Aldrich, MO, USA)

Laemmli buffer (Cat. No. S3401, Sigma Aldrich, MO, USA)

LumiGLO chemiluminescent substrate (Cat. No. 54-61-01, Kirkegaard & Perry Laboratories, Gaithersburg, USA))

Methanol (Cat. No. 1.06009.2500, Merck Millipore, Darmstadt, Germany)

MilliQ water (MilliQ Integral water purification system, Merck Millipore, Darmstadt, MO, USA)

MOPS SDS running buffer (20 X) (Cat No. NP 0001-02, Invitrogen)

Paraformaldehyde (Cat. No. P6148, Sigma Aldrich, MO, USA)

Ponceau S staining solution (Cat. No. P7170, Sigma Aldrich, MO, USA)

Precision Plus protein standards (Cat No. 161-0373, Biorad Laboratories, Hercules, USA)

SIGMAFAST™ p-Nitrophenyl phosphate tablets (Cat. No. N2770, Sigma Aldrich, MO, USA)

Sodium acetate (NaAc) (Cat No. 71185, Sigma Aldrich, MO, USA)

Sodium chloride (NaCl) (Cat No. 73575, Sigma Aldrich, MO, USA)

Sodium dodecyl sulfate (SDS) powder (Cat. No. 1.13760.1000, Merck Millipore, Darmstadt, Germany)

Sodium hydroxide (NaOH) (Cat. No. S8045, Sigma Aldrich, MO, USA)

Streptavidin-HRP (Cat No. 21324, Thermo Fisher Scientific Inc, IL, USA)

Sulfuric acid (H2SO4) (Cat No. 87003 – 234, VWR, USA)

Triton X100 (Cat No. 161-0407, Biorad Laboratories, Hercules, USA)

Trizma® base minimum 99.9 % (Cat No. T1503, Sigma Aldrich, MO, USA)

Tween 20 (Cat. No. P1379, Sigma Aldrich, MO, USA)

Ultima Gold scintillation cocktail (Cat. No. 6013321, Perkin Elmer, Massachusetts, USA.)

Other materials

0.2 μM nitroceullose membrane (Cat No. 162-0112, Biorad Laboratories, Hercules, USA)

20 ml glass scintillation vials (Cat No. 6000128, Perkin Elmer, Massachusetts, USA.)

COATEST®Heparin (Cat No.25 5539 63, Chromogenix, USA)

DNAse 1 (Cat No. 04716728001, Roche, USA)

FGF2 quantikine assay (R& D Systems) (Cat No. DFB50, R & D Systems, USA)

Glycosaminoglycan 96-well binding plates (Cat No. H/G Plates, Iduron Ltd, Manchester, UK)

HiPrep 26/10 Desalting, 53 ml (Cat No. 17-5087-01, GE Healthcare,UK)

HiTrap Streptavidin HP, 1 ml (Cat No. 17-5112-01, GE Healthcare,UK)

LumiGLO Chemiluminescent substrate (Cat No. 54-61-00, KPL, USA)
Manchester, UK)

NUPAGE® 4-12% Bis-Tris gel SDS-PAGE gel (Cat No. NP0335PK2, Invitrogen, Life Technologies Corporation, CA, USA)

SYPRO® Orange Protein Gel Stain (5000X Concentrate in DMSO) (Cat No.S-6650, Invitrogen, USA)

X-ray film (Cat No. 28906844, GE Healthcare)

Radiochemicals

^{3}H-heparin (0.35 mCi/mg) (Cat. No. NET476, Perkin Elmer, Massachusetts, USA)

Antibodies for inhibitory studies

Human FGF basic antibody Antigen Affinity-purified Polyclonal Goat IgG (Cat No. AF-233-NA, R & D Systems, USA)

IMBR1 (Ling *et al*, 2006)

SU5402 (Cat No. 572631-500UG Calbiochem, Merck Millipore

Proteins and antibodies for GAG-ELISA assay

Anti-BMP2 (Cat No. BAM 3552, R & D Systems, USA)

Anti-FGF-1 (Cat No. BAF232, R & D Systems, USA)

Anti-FGF-2 (Cat No. BAM233, R & D Systems, USA)

Anti-FGF-7 (Cat No. BAF251, R & D Systems, USA)

Anti-PDGF-BB (Cat No. BAF220, R & D Systems, USA)

Anti-VEGF (Cat No. BAF 293293 VE, R & D Systems, USA)

BMP2 (Cat No. 355 BM, R & D Systems, USA)

FGF-1 (Cat No. 231 BC, R & D Systems, USA)

FGF-2 (Cat No. 233 FB, R & D Systems, USA)

FGF-7 (Cat No. 251 KG, R & D Systems, USA)

PDGF-BB (Cat No. 220 BB, R & D Systems, USA)

VEGF (Cat No. 293 VE, R & D Systems, USA)

Media, TCPS and solutions for cell culture

0.25 % Trypsin-EDTA (Cat No. 25200, Invitrogen, Life Technologies Corporation, CA, USA)

24-well TCPS plates (Cat No. 142475, NUNC, Denmark)

48-well TCPS plates (Cat No. 150687, NUNC, Denmark)

6-well TCPS plates (Cat No. 140675, NUNC, Denmark)

96-well TCPS plates (Cat No. 167008, NUNC, Denmark)

DMEM high glucose 4500 mg/l (Biopolis Shared Fascility, A*STAR, Singapore)

DMEM low glucose 1000 mg/l (Biopolis Shared Fascility, A*STAR, Singapore)

Fetal calf serum (FCS) (Cat No. AUD34653, HyClone, Thermo Scientific)

L-glutamine (Cat No. 25030-081, Invitrogen, Life Technologies Corporation, CA, USA)

Penicillin-Streptomycin (Cat. No. 15140, Invitrogen, Life Technologies Corporation, CA, USA)

Phosphate buffered saline 1 X (1XPBS) (Biopolis Shared Fascility, A*STAR, Singapore)

TrypLETM express (Cat No.12604-021, Invitrogen, Life Technologies Corporation, CA, USA)

α-MEM (Biopolis Shared Fascility, A*STAR, Singapore)

Preparation of media and solutions

FACS blocking buffer

PBS, 5% FCS, 1% BSA and 10% human serum (NHS)

FACS staining buffer

PBS, 2% FCS, 0.02% sodium azide (NaN_3)

FACS Buffer for immunomodulation

0.05% BSA, 2mM EDTA in PBS

Low salt affinity chromatography buffer

20 mM phosphate buffer, 150 mM NaCl, pH 7.2

High salt affinity chromatography buffer

20 mM phosphate buffer, 1.5 M NaCl, pH 7.2

0.1 M MES buffer

Weigh 1.952 g MES powder and dissolve in 100 ml MilliQ water.

PBST

30 ml 5 M NaCl, 66 ml 1.5 M Tris, 1ml Tween 20 and 990 ml MilliQ water

1 x Transfer buffer

For 1 L, add 24.22 g of Triza® base, 112.6 g glycine and top up with MilliQ water

Standard assay buffer (SAB)

100 mM NaCl, 50 mM NaAc, (v/v) 0.2 % Tween 20, pH 7.2 FACS

Flow cytometry Antibodies

FGFR1 (IMBR1) (Ling *et al*, 2006)

FITC Mouse Anti-human HLA-DR (Cat No. 555560, BD Diagnostics, USA)

FITC Mouse IgG1k Isotype control (Cat No. 555748, BD Diagnostics, USA)

FITC Mouse IgG2bk Isotype control (Cat No. 555742, BD Diagnostics, USA)

Goat anti mouse IgM(μ) PE (Cat No. M31504, Invitrogen, USA)

IgG1 PE (Cat No. 349043, R & D Systems , USA)

Mouse IgM (Cat No. MGM00, Invitrogen, USA)

PE Mouse Anti-human CD105 (Cat No. 550257, BD Diagnostics, USA)

PE Mouse Anti-human CD14 (Cat No. 340683, BD Diagnostics, USA)

PE Mouse Anti-human CD19 (Cat No. 555412, BD Diagnostics, USA)

PE Mouse Anti-human CD34 (Cat No. 555822, BD Diagnostics, USA)

PE Mouse Anti-human CD45 (Cat No. 555483, BD Diagnostics, USA)

PE Mouse Anti-human CD49a (Cat No. 559596, BD Diagnostics, USA)

PE Mouse Anti-human CD73 (Cat No. 550257, BD Diagnostics, USA)

PE Mouse Anti-human CD90 (Cat No. 555596, BD Diagnostics, USA)

PE Mouse Anti-human FGFR2 – PE (Cat No. FAB684P, R & D Systems , USA)

PE Mouse Anti-human FGFR3 – PE (Cat No. FAB766P, R & D Systems , USA)

PE Mouse Anti-human SSEA-4 (Cat No. 560128, BD Diagnostics, USA)

PE Mouse IgG1 Isotype control Cat No. 349043, BD Diagnostics, USA)

PE Mouse IgG1 k Isotype control (Cat No. 555749, BD Diagnostics, USA)

PE Mouse IgG2bk Isotype control (Cat No. 555743, BD Diagnostics, USA)

PE Mouse IgG3 k Isotype control (Cat No. 556659, BD Diagnostics, USA)

PE rat Anti-human FGFR4 – PE (Cat No. FAB6852P, R & D Systems, USA)

Rabbit IgG1 (Cat No. 02-6102, Invitrogen, USA)

Rabbit IgG1 AF (Cat No. A11008, Invitrogen, USA)

Rat IgG2ak PE (Cat No. MAB006, R & D Systems, USA)

STRO1 (From Stan Gronthos lab)

Immunomodulation assays

Diluent (Cat No. 00-5223-56, eBioscience , USA)

FITC-conjugated Mouse anti-Human CD3 (Cat No. 555332, BD Pharmingen, USA)

FITC-conjugated Mouse IgG1 k Isotype (Cat No. 555748, BD Pharmingen, USA)

Fix Perm (Cat No. 00-5123-43, eBioscience , USA)

Human cTNF R1/TNFRSF1A Quantikine ELISA Kit (Cat No. DRT100. R & D Systems, USA)

PE-conjugated Mouse anti-Human Ki-67 (Cat No. 51-36525X, BD Pharmingen, USA)

PE-conjugated Mouse IgG1 Isotype (Cat No. 51-35405X, BD Pharmingen, USA)

Perm Buffer (Cat No. 00-8333-56, eBioscience , USA)

Western blot antibodies

phospho-FRS2a (Cat No. 3861, Cell Signaling, USA)

actin (Cat No. MAB1501R, Millipore Chemicon, USA)

HRP-conjugated goat anti-mouse Ig G (H+L) antibody (Cat No. 115-035-062, Jackson Immunoresearch laboratories Inc, PA, USA)

HRP-conjugated goat anti-rabbit Ig G (H+L) antibody (Cat No. 111-035-045, Jackson Immunoresearch laboratories Inc, PA, USA)

Restore* Western Blot Stripping Buffer (Cat No. 21509, Thermo Scientific, USA)

Ponceau S staining solution (Cat. No. P7170, Sigma Aldrich, MO, USA)

LumiGLO chemiluminescent substrate (Cat. No. 54-61-01, Kirkegaard & PerryLaboratories, Gaithersburg, USA)

phospho-ERK1/2 (Cat No. 9106L, Cell Signaling, USA)

total ERK1/2 (Cat No. 9102L, Cell Signaling, USA)

Novex 4-12% Bis-Tris SDS PAGE gel, 10 well (Cat No. NP0335BOX, Invitrogen, Life Technologies Corporation, CA, USA)

Multilineage differentiation reagents

3-isobutyl-1-methylxanthine (Cat No. 15879, Sigma Aldrich, USA)

Alcian blue (Cat No. A5268, Sigma Aldrich, USA)

Alezarin red (Cat No. A5533, Sigma Aldrich, USA)

Dexamethasone (Cat No. D4902, Sigma Aldrich, USA)

hMSC Chondro Bullet kit (Cat No.PT3003, Cambrex, Lonza, USA)

Indomethacin (Cat No. 17378, Sigma Aldrich, USA)

Insulin (Cat No. 16634, Sigma Aldrich, USA)

L-ascorbate-2-phosphate (Cat No. A8960, Sigma Aldrich, USA)

Oil-red-O (Cat No. O0625, Sigma Aldrich, USA)

Silver nitrate (Cat No. S8157, Sigma Aldrich, USA)

Sodium thio sulfate (Cat No. S7026, Sigma Aldrich, USA)

TGF-β3 (Cat No. 243-B3, R & D Systems, USA)

β-glycerol-phosphate (Cat No. G9422, Sigma Aldrich, USA)